5-2024

Essays on spatial economics and international trade

Naiyuan HU
Singapore Management University, nyhu@smu.edu.sg

ESSAYS ON SPATIAL ECONOMICS AND INTERNATIONAL TRADE

By

NAIYUAN HU

A DISSERTATION

In

ECONOMICS

Presented to the Singapore Management University in Partial Fulfilment

of the Requirements for the Degree of PhD in Economics

2023

_____

Supervisor of Dissertation

_____

PhD in Economics, Programme Director

ESSAYS ON SPATIAL ECONOMICS AND INTERNATIONAL TRADE

by
Naiyuan Hu

Submitted to the School of Economics in Partial Fulfilment of the
Requirements for the Degree of Doctor of Philosophy in Economics

Dissertation Committee:

Yuan Mei (Supervisor/Chair)
Assistant Professor of Economics
Singapore Management University

Lin Ma (Supervisor/Co-Chair)
Assistant Professor of Economics
Singapore Management University

Jing Li
Associate Professor of Economics
Singapore Management University

Kohei Takeda
Assistant Professor of Economics
National University of Singapore

2024

Abstract

This dissertation consists of three papers on spatial economics and international trade. The first paper focuses on spatial inequalities. Educational resources are distributed unevenly and contribute to spatial inequality. A dynamic spatial model with life-cycle elements studies the impacts of location-specific educational resources. Individuals determine where to attend college, weighing distance, expected value of education, and available resources. Locations with more colleges attract more students. As mobility costs increase with age, many graduates stay in the city where they studied, affecting skill composition. Applied to China, it finds that the 2005-2015 college expansion had minimal welfare impacts and suggests better resource distribution could reduce inequality. The second paper considers the U.S.–China trade war. U.S. President Joe Biden has maintained Trump tariffs on Chinese imports, despite the promise to remove them before the 2020 presidential election. The hypothesis that these tariffs can serve as leverage in future tariff negotiations with China is investigated using a quantitative model that incorporates U.S. regions and international trade linkages. After estimating the bargaining power of the U.S. and China, their cooperative tariffs starting from the 2017 baseline and 2019 trade-war equilibrium are computed separately. Simulation results show that, regardless of the relative bargaining power of the U.S., the trade war always improves U.S. welfare in the post-negotiation cooperative equilibrium. With an estimated Nash bargaining weight between 0.47 and 0.70, the trade war with China yields a post-negotiation welfare improvement of 0.04The third paper focuses on trade policy and sanctions against Russia. It examines the most cost-efficient ways to impose sanctions. A quantitative model of international trade is employed. It finds that for countries with low willingness to pay, a uniform 20% tariff on all Russian products is optimal. For countries willing to pay at least $0.70 for each $1 drop in Russian welfare,

an embargo on Russia's mining and energy products, with tariffs above 50% on other products, is most efficient. If countries target politically relevant sectors, an embargo on Russia's mining and energy sector remains cost-efficient, even with low willingness to pay for sanctions.

Table of Contents

Acknowledgement

This dissertation marks the culmination of a journey that has been both challenging and rewarding. I am deeply grateful to the many individuals who have supported and guided me throughout this process.

First and foremost, I would like to express my deepest gratitude to my supervisors, Dr. Yuan Mei and Dr. Lin Ma. Their expertise, encouragement, and patience have been invaluable throughout this journey. Their guidance and constructive feedback have significantly shaped this work and my development as a researcher. I am profoundly thankful for the unwavering support. I hope to become a researcher of their caliber, contributing to the field with the same passion and excellence. I also extend my sincere thanks to my dissertation committee members, Dr. Jing Li and Dr. Kohei Takeda, for their insightful comments and suggestions, which have greatly improved the quality of this dissertation.

I am also grateful to my colleagues at SMU. The intellectual discussions, and moral support have made this journey more enjoyable and less daunting. Special thanks to Qiyuan Li and Yuexuan Ren for the friendship and encouragement.

A heartfelt thank you to my friends outside of academia: Xudong Wu, Kefan Jin, Yuxin Mao, Zheng Luo and Denys Lim. The constant encouragement, understanding, and the occasional distractions provided much-needed relief and balance throughout this process.

I would also like to thank my family. To my parents, their belief in me and their constant support have been my greatest source of strength. To my partner, Jiajin Cen, his patience, love, and understanding have been my anchor through this journey. Lastly, I want to extend a special thank you to my cat, Coco, for providing companionship and comfort during the stressful times.

Chapter 1

Educational Migration*

1.1 Introduction

The spatial distribution of colleges is highly uneven within a country. For example, in the context of China, educational hubs such as Beijing could host as many as 77 universities, while the average prefecture only has 6. Even worse, around a quarter of the cities, many with millions of population, have no more than a single college. The uneven distribution of educational resources could lead to dire consequences for both individuals and society. Access to colleges shapes the fate of young people: those born in unlucky locations with scarce resources must endure the ordeal of long-distance migration at a young age to seek a higher education; deterred by such costs, many talented students forgo the opportunities and remain as unskilled workers throughout their lifetime. The impacts of colleges do not stop at the student population either. Seeking higher education is one of the main motivations for migration (see, e.g., Dustmann and Glitz 2011). In fact, it is the *only* migration spell for many college graduates in their lifetime: they settle in the city of their alma mater. As a result, access to educational resources could influence one's lifetime location choices. At the aggregate level, the forces mentioned above affect the skill composition of a location in the long run, exerting their impacts on skill premium, population, and economic prosperity for many years to come. To what extent is the uneven distribution of educational resources responsible for the observed spatial inequality? What is the optimal distribution of colleges across space? The answers to

*This is a joint work with Lin Ma.

these questions not only arouse academic interests but also carry long-lasting policy implications. Answering these questions, however, requires careful modeling of individuals' educational and location choices over one's life cycle. Such a model is currently lacking in the literature, and we seek to fill the gap with this paper.

We developed a multi-sector general equilibrium dynamic spatial model with life-cycle elements to analyze the geography of educational resources. The model consists of overlapping generations of individuals that live for many periods. Upon entry into the model, individuals endogenously choose education levels, weighing the expected return to higher education against the costs of doing so. Conditional on seeking higher education, they then determine where to attend college. The locational choice of students depends on the distance to home, the option value of being a skilled worker in the destination, the opportunity costs of obtaining a degree, and non-monetary location characteristics such as the abundance of college resources. Upon graduation, individuals enter the labor market as skilled workers. The young workers who forgo higher education directly enter the labor market as unskilled workers. In each period, skilled and unskilled workers supply labor, consume, and move to other labor markets, subject to age-specific migration frictions throughout their life cycle until retirement and exit from the model.

Educational resources exert their long-run spatial impacts through several channels in the model. First, locations well-endowed with educational resources increase the appeal of higher education, encouraging more skill upgrading among local students. Moreover, the abundance of colleges also attracts potential students from all over the country, particularly individuals in nearby locations with relatively low migration costs. The implications of educational resources are also long-lasting. Given the considerable migration costs, many college students choose to stay in the location of their alma mater throughout their lifetime, pushing up the skill ratio of these locations persistently and contributing to local productivity through agglomeration forces. Lastly, the distribution of colleges also affects unskilled workers through general equilibrium effects: a relative abundance of skilled workers in one area pushes up the demand for unskilled workers, indirectly benefiting them.

We quantify and estimate the model in the context of China, a country with highly concentrated educational resources. The large spatial variations in educa-

tional resources are particularly valuable econometrically, as they allow us to structurally estimate the locations' attractiveness as educational migration destinations through the lens of our model. Moreover, China also offered an interesting policy experiment. Along with rapid economic development and urbanization, China initiated a large-scale college expansion program rarely seen worldwide. Between 2005 and 2015, the spending on college education increased by 466 percent, and the number of college teachers expanded by 84 percent. As a result, college enrollment increased from 5 million to around 14 million during a short period. We use our model to evaluate the aggregate and distributional impacts of the policy change; we also carry out counterfactual simulations to study if better aggregate and distributional results could be achieved with alternative distribution of educational resources.

To understand the spatial impacts of college distribution, the core empirical question is how the distribution of colleges affects educational migration — the destination choices of potential students. Our model offers a useful lens through which we can structurally map the observed educational resources, such as the number of college teachers and the quality of colleges, to the observed educational migration patterns. In particular, the predicted migration probability matrix of the students summarizes the attractiveness of a location to college seekers, which depends on the underlying geography, migration policy, expected option value, and educational resources. Controlling all the other elements shaping the migration probability, our model then provides a natural mapping from location-specific educational resources to the observed educational migration patterns. With some functional form assumptions, we can then infer a location's attractiveness for potential college students, which we call the "education appeals" of a location. We assume that the education appeals as a function of the quantity and quality of colleges, as well as natural amenities such as climate and terrain, and estimate these parameters using nonlinear least squares. The estimated education attractiveness suggests diminishing returns to college concentration. In the city with a median level of college teachers, a 10 percent increase in teachers leads to a 2.87 percent increase in education appeals. However, the return to more colleges quickly recedes in better-endowed locations. For example, in the 90th percentile of cities, a 10 percent increase in

teachers only increases its attractiveness by one-eighth of the same increment at the 10th percentile.

We find that college expansion between 2005 and 2015 led to a mild increase in the welfare and skill ratios at the aggregate level. To evaluate the effects of college expansion, we compare the baseline simulation of a transition path with the observed expansion to a counterfactual one without the college expansion. The comparison suggests that aggregate welfare increased by 0.52 percent and the aggregate skill ratio by 0.56 percent by 2015. Both skilled and unskilled workers benefited from the college expansion, while the average welfare gain among the skilled workers (0.82 percent) is substantially larger than that among the unskilled ones (0.24 percent). The college expansion increased the skilled ratio in most locations, leading to higher productivity, thus benefiting the unskilled workers. The gain in productivity is particularly rewarding to skilled workers through productivity-skill complementarity in the model. Eventually, it outweighs the negative impacts of an increased supply of college-educated workers on welfare, leading to considerable gains for college-educated workers. The mild response to college expansion comes as no surprise. The expansion program favored locations already well-endowed with educational resources while leaving the initially poorly-endowed locations behind. Given the high curvature of the education appeal function, the accessibility to higher education, especially in poor and remote locations, barely changed.

How can we better allocate educational resources across space? We answer this question in several ways. We first compute the welfare elasticity of college expansion prefecture-by-prefecture and find that the return to college investment is substantially higher in poorly endowed locations. The aggregate return to a 10% increase in college teachers is 2.6 times higher at the bottom 10% of the prefectures than those at the top 10%. We then simulate another counterfactual in which we allocate all the additional educational resources observed in the actual expansion program *equally* among all the prefectures. In this case, all prefectures receive an additional 2600 college teachers. We find that the aggregate welfare effects of this simple "equal growth" scheme are roughly 1.8 times larger, and the impacts on skill ratio more than 1.94 times higher than the observed expansion at 1.01%.

Lastly, we show that the unequal distribution of educational resources is re-

sponsible for up to 14% of the observed spatial inequality in skill composition. Moreover, equalizing educational resources is roughly 14% as effective as equalizing fundamental productivity in reducing spatial inequality in the short run. To understand the impact of college distribution on the observed spatial inequality, we first simulate one counterfactual called "equal college", in which we eliminate all spatial variation in educational resources and redistribute the existing stock equally across locations. Compared to the baseline result, the skill ratio dispersion across locations drops by around 3.74% to 0.47% along the transition path towards the long-run steady state. To benchmark the effect of equalization of educational access, we compute another counterfactual in which the location fundamental productivity, the usual culprit of spatial inequality (and structural residual that absorbs locational differences) in the quantitative models, is equalized across locations. In the productivity-equalizing world, the dispersion of skill ratio declines by 26.33% to 84.8% along the transition path to the steady state, as compared to the baseline model. In this sense, an evenly distributed educational resource is 14% as effective in reducing spatial inequality as an evenly distributed productivity in the short run, however, in the long run the skill ration inequality will be largely driven by the inequality in the productivity.

This paper is related to several strands of the literature. Firstly, our study is closely related to a broad literature on quantitative spatial and dynamic discrete choice models, such as Artuç et al. (2010); Allen and Arkolakis (2014); Ahlfeldt et al. (2015); Caliendo et al. (2019, 2021); Kleinman et al. (2023), as surveyed in Redding and Rossi-Hansberg (2017). We contribute to this literature in several ways. We are the first to introduce educational choice into the dynamic spatial framework to highlight the interlinkages between educational resources, transportation infrastructure, and geographical fundamentals. We show that the distribution of colleges not only directly affects student distribution but also shapes long-term skill composition in general equilibrium. We also introduce a structural interpretation to map the observed student distribution to the educational resources; through our estimation, we highlight the curvature of the education cost function, which could inform policy-making and researchers interested in educational issues.

Our research relates to the recent dynamic models with life-cycle assumptions,

including Allen and Donaldson (2022), Eckert and Peters (2022), Takeda (2022), Komissarova (2022), and Suzuki (2023). We contribute to this literature by modeling and examining the impact of inter-generational linkages on decisions made over one's lifespan, specifically focusing on education attainment. We are also the first to estimate age-specific migration costs using these models, and our results, as discussed later, reveal a shape increase in migration costs as people age.

Our work is also broadly related to the quantitative spatial works that focus on China, such as Tombe and Zhu (2019), Fan (2019), Ma and Tang (2020). While this strand of work focuses on elements specific to the context of China, such as the hukou restrictions, we are among the first to introduce a dynamic structure to study the migration decisions over one's lifetime. In contrast to Fan (2019), where skill type is taken as given, and migration is primarily driven by wage incentives and amenities, our approach introduces a nuanced perspective.

Finally, a few works have studied the impact of college expansion, including the impacts on innovation and trade (Ma 2023), the impacts on knowledge spillovers (Li et al. 2020), and the impact on human capital on productivity (Che and Zhang 2018). This paper contributes to the literature on the impacts of college expansion by estimating the education cost in each location and simulating the counterfactual college expansion scenarios and their economic impacts. Specifically, we estimate the education cost of China in all prefectures using a detailed migration matrix and uncover the highly uneven educational costs that lead to a suppression of the talents who can otherwise become skilled workers.

The remainder of this paper proceeds as follows. In Section 2.2, we present the quantitative spatial model. In Section 1.3, we calibrate the model parameters. In particular, we estimate the education cost base on the endogenous education migration model. In Section 1.4, we present the counterfactual simulations. In Section 1.5, we conclude.

1.2 Model

We develop a dynamic spatial life-cycle model emphasizing individuals' endogenous education choices. The model allows us to examine how the spatial distribution of educational resources affects individuals' migration choices, the com-

position of the labor market in each region, and its overall impact on inequality over time. Our model extends the quantitative model introduced by Caliendo et al. (2019) to cover heterogeneous cohorts and endogenous education choices.

1.2.1 Life-Cycle and Individual Decisions

The economy has $n = 1, 2, \cdots, N$ locations, $s = 1, 2, \cdots, S$ sectors, inhabited by overlapping generations of individuals that live up to J periods. Each cohort comprises $\tilde{L}$ individuals, and the total population in this economy equals $J\tilde{L}$. Each period t, individual in location n derive flow utility from consuming a composite good from all locations:

$$U_t(n) = \log\left[C_t(n)\right], \quad \text{where: } C_t(n) = \left(\sum_{i=1}^{N}\left[\prod_{s=1}^{S}\left(c_t^s(n,i)\right)^{\zeta^s}\right]^{\frac{\sigma-1}{\sigma}}\right)^{\frac{\sigma}{\sigma-1}}, \quad \sigma > 1, \tag{1.1}$$

where $C_t(n)$ is the consumption consumption, which is a nested composite good across all locations and sectors. The variable $c_t^s(n,i)$ denotes the goods from sector s produced in location i and consumed at location n. The parameter σ captures the elasticity of substitution of goods across locations, and $\zeta^s > 0$ and $\sum_{s=1}^{S}\zeta^s = 1$ captures the weight of sector s in the consumption bundle.

Timeline and Decisions $\tilde{L}$ newborn individuals enter the model every period. The spatial distribution of the newborn is the same as the old cohort exiting the model to ensure the stability of population distribution in a steady state. At the start of one's lifetime, an individual first observes an idiosyncratic education preference shock, z, and, based on which, decides whether to pursue higher education and become a skilled worker. Individuals maximize the expected lifetime utility at the birthplace n by choosing their skill type, $e = \{l, h\}$, where "l" stands for unskilled ,and "h" for skilled workers:

$$V_t^0(n) = \max_{\{e\}}\{V_t^0(n,e) + \psi z\}. \tag{1.2}$$

In this expression above, $V_t^0(0)$ is the unconditional lifetime utility of a newborn in location n at time t, and $V_t^0(n,e)$ is the lifetime utility conditional on skill type e. The education preference shock, z, can be equally interpreted as heterogeneity in

one's ability to learn — individuals with a higher z are innately better at learning and, therefore, have higher probabilities of attending college. We assume z follows a standard GEV-I distribution with zero mean and use ψ to capture the (inverse) elasticity of education choice that will be estimated later. Individuals can only choose education levels at the beginning of their lifetime, and those who forgo higher education will stay as unskilled workers for their entire lifetime.[1]

Conditional on pursuing higher education ($e = h$), the individual chooses the optimal location n' for college. For an individual born in location n, the decision is summarized as:

$$V_t^0(n,h) = E_{\varepsilon_n} \max_{\{n'\}} \{V_t^1(n',h) - D^1_{n'n,t} + F_{n',t} + \kappa\varepsilon_{n'}\}. \tag{1.3}$$

The location choice hinges on four factors. The first factor is the distance between their home location and the destination, $D^1_{n'n,t}$, which captures the roles of geography and transportation networks in education choice. The second factor is the option value of being a skilled worker in n', $V_t^1(n',h)$. The option value, which we will discuss in detail later, reflects two forces: the current wage for skilled workers in the destination and, recursively, the value of moving to other high-paying locations in the future. Everything else being equal, the potential students prefer to attend colleges in or close to locations with high-paying jobs for skilled workers to save on post-graduation migration costs. The third factor that affects one's location choice is the destination-specific "education appeals", denoted as $F_{n',t}$. We use this term to capture the non-monetary and unobserved appeals of a location for higher education. Conditional on a home location, two destinations with the same distance and option value might still differ in their attractiveness to students due to the abundance of college resources, the prestige of their colleges, and natural amenities such as temperature and precipitation. Lastly, as usual in the dynamic discrete choice literature, the location choice also depends on a vector of i.i.d idiosyncratic shocks, $\{\varepsilon'_n\}_{n'=1}^N$ that follows a Type-I GEV shock with zero mean, and κ is the inverse of the migration elasticity.

The option value of a skilled worker in location n' at age $j = 1,2,\cdots,J$, is

[1] In the data, continuing education plays a minor role in China. According to the 2015 Annual Report of the Ministry of Education, only 292 out of 2,852 colleges in China offer continuing education. The number further declined to 265 in 2020.

defined recursively as:

$$V_t^j(n,h) = U_t^j(n,h) + E_{\varepsilon_{n'}} \max_{n'} \left\{ \beta V_{t+1}^{j+1}(n',h) - D_{n'n,t+1}^{j+1} + \kappa \varepsilon_{n'} \right\}, \tag{1.4}$$

The above formulation is the same as a standard dynamic migration model: individual workers migrate every period to maximize the expected lifetime utility, considering distance, future payoff, and idiosyncratic location shocks.

We highlight two new features in our model. First, we directly model the opportunity cost of attending college. At $j = 1$, a college student cannot supply labor and relies on "home production" for consumption. The "home production" can be broadly interpreted as part-time and substance-level jobs that do not interfere significantly with the labor market clearing conditions or financial transfers from the government or family that we abstract away from the model. After graduation at $j > 1$, the educated worker earns the skilled wage rate. In summary, the flow indirect utility function for a skilled individual is as follows:

$$U_t^j(n,h) = \begin{cases} b_{nt} & \text{if } j = 1 \\ \ln w_{nt}^h - \ln P_{nt}, & \text{otherwise} \end{cases}, \tag{1.5}$$

where b_{nt} is the utility derived from home production, w_{nt}^h is the skilled wage, and P_{nt} is the ideal price index at location n, time t. The second new feature is directly linked to the life-cycle elements of the model. In the last period of an individual's life cycle at $j = J$, their value functions no longer include any future option and, therefore, simplify to:

$$V_t^J(n,h) = U_t^J(n,h). \tag{1.6}$$

The recursive problem of the unskilled workers ($e = l$) adopts a similar and simplified recursive structure following equations (1.4), (1.5) and (1.6), with three changes: 1) the skill type is no longer h but l, and 2) equation (1.4) applies to $j = 0, 1, \cdots, J$, due to the absence of college choice in equation (1.3), and 3) the unskilled workers start supplying labor at age $j = 1$ (when the skilled workers at the same age attend college), and therefore their flow utility is:

$$U_t^j(n,l) = \ln w_{nt}^l - \ln P_{nt}, \forall j \tag{1.7}$$

where w_{nt}^l is the wage for unskilled workers.

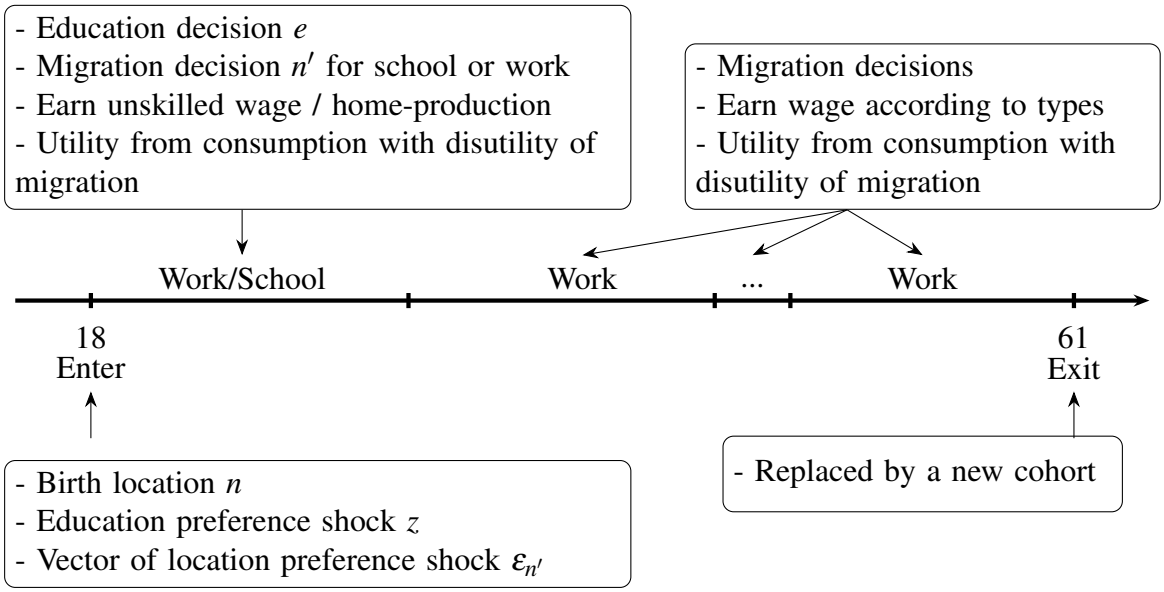

Figure 1.1: Decision Timeline

Note: This figure shows the timeline of individual decisions. A detailed description can be found in the text.

Figure 1.1 summarizes the timeline for individuals in the model. Individuals enter the model at age 18 and exit at age 61, spanning 11 periods with 4-year intervals. In the first period, an agent born in location n draws a preference for education and chooses whether to become a skilled worker. Conditional on education, the agent draws preference shocks for all locations and selects a place to attend college. Those who opt out of college become unskilled workers. After $j = 1$, skilled and unskilled workers make similar recursive migration decisions until they exit the model at $j = J$.

Solving the Individual Decisions Under the assumption that both the idiosyncratic shocks of the location taste $\varepsilon \geq 0$ and education taste $z \geq 0$ coming from type-I extreme distributions, we can solve the aggregate migration flow and the probability of educational choice.The expected lifetime value for worker with skill $e \in \{l,h\}$ being in location n, in period j, and $1 < j < J$, is given by,

$$V_t^j(n,e) = U_t^j(n,e) + \kappa \log \sum_{n'=1}^{N} \exp\left(\beta V_{t+1}^{j+1}(n',e) - D_{n'n,t+1}^{j+1}\right)^{1/\kappa}. \tag{1.8}$$

Therefore, the probability of the migration decisions for individuals at period j, with education level e, live in location n, moving to location n' is given by,

$$\pi_t^j(n'|n,e) = \frac{\exp(\beta V_{t+1}^{j+1}(n',e) - D_{n'n,t+1}^{j+1})^{1/\kappa}}{\sum_{n''=1}^{N} \exp(\beta V_{t+1}^{j+1}(n'',e) - D_{n''n,t+1}^{j+1})^{1/\kappa}}, \tag{1.9}$$

At the very beginning of one's lifetime, the probability of an individual's migration and educational choice can be written as

$$\pi_t^0(n',e|n) = (1) \times (2) \tag{1.10}$$
$$(1) = \frac{\exp(V_t^1(n',e) - D^1_{n'n,t} - 1_{e=h}F_{n't})^{1/\kappa}}{\sum_{n''=1}^{N} \exp\left(V_t^1(n'',e) - D^1_{n''n,t} - 1_{e=h}F_{n''t}\right)^{1/\kappa}}$$
$$(2) = \frac{\exp(V_t^0(n,e))^{1/\psi}}{\sum_{e'} \exp\left(V_t^0(n,e')\right)^{1/\psi}}.$$

The first part is the location choice conditional on education decision, e. The second part summarizes the decision to study and become a skilled laborer later in life, given the birthplace n.

Lastly, migration probabilities and the initial distribution summarize the population movement and its composition. Formally, the migration flows are expressed as:

$$\begin{aligned}
L^0_{nt} &= L^J_{nt-1} \\
L^1_t(n',e) &= \sum_n L^0_{nt}\pi^0_t(n',e|n) \\
L^j_t(n',e) &= \sum_n L^{j-1}_{t-1}(n,e)\pi^{j-1}_{t-1}(n'|e,n) \quad j = 2,...,J \\
\mathbb{L}_t(n,e) &= \sum_{j=2}^{J} L^j_t(n,e) + \mathbb{1}_{e=l}L^1_t(n,e).
\end{aligned}$$

In the set of equations above, the first one means that the newborn population in each location equals the retiring population in the previous period at the same location. The second equation describes the educational migration flows, and the third one describes the worker's movement. The last equation computes the total population across ages by location and education level.

1.2.2 Production, Aggregation, and Closing the Model

Production The production side in the model follows the Armington (1969) framework. We assume that each location specializes in producing goods in S sectors. Consumers demand all varieties of goods from all locations and sectors. In each location and sector, a perfectly competitive market prevails. Production technology is assumed to have a constant elasticity of substitution and requires both skilled and

unskilled workers. The output in location n, sector s is given by:

$$y_{nt}^{s} = A_{n}^{s}\left\{\chi^{s\frac{1}{\eta}}\left[(A_{n}^{s})^{-\omega}\,l^{l}{}_{nt}\right]^{\frac{\eta-1}{\eta}} + (1-\chi^{s})^{\frac{1}{\eta}}\left[(A_{n}^{s})^{\omega}\,l_{nt}^{h}\right]^{\frac{\eta-1}{\eta}}\right\}^{\frac{\eta}{\eta-1}},$$

where l_{nt}^{l} and l_{nt}^{h} are unskilled and skilled labor inputs respectively, to produce y_{nt}^{s} units of good. The parameter $A_{n}^{s} = \bar{A}_{n}^{s}\mathbb{L}_{t}(n,h)^{\phi}$ denotes the endogenous productivity in location n for sector s, where $\bar{A}_{n}^{s}$ is the fundamental productivity, $\mathbb{L}_{t}(n,h)$ is the total number of working skilled labor, and the parameter ϕ governs the agglomeration forces. We allow productivity-skill complementarity in the production process, denoted by ω, as introduced by Burstein and Vogel (2017). Productivity-skill complementarity implies that high-skilled labor is more effective in high-productivity locations.[2] The parameter χ^{s} is the share of input from skilled in production. The parameter η is the elasticity of substitution of skilled and unskilled worker in the production process. Workers can freely move across sectors. Wage in each location for each skill level, denoted as w_{nt}^{e}, is determined endogenously through local labor market clearing.

Market Clearing Conditions From the utility function, it is straightforward to see that the ideal price index can be expressed as

$$P_{nt} = \prod_{s=1}^{S}\left(\frac{\left(\sum_{i=1}^{N} p_{nit}^{1-\sigma}\right)^{\frac{1}{1-\sigma}}}{\zeta^{s}}\right)^{\zeta^{s}}$$

where p_{nit}^{s} is the price of goods in sector s purchased from location i for consumption in location n at time t. The Armington assumptions directly imply that p_{nit}^{s} equals the marginal cost of producing times the iceberg transportation cost τ_{ni} at time t,

$$p_{nit}^{s} = \tau_{ni}\frac{1}{A_{i}^{s}}\left[(A_{i}^{s})^{-\omega(\eta-1)}\chi^{s}\left(w_{it}^{l}\right)^{1-\eta} + (A_{i}^{s})^{\omega(\eta-1)}(1-\chi^{s})\left(w_{it}^{h}\right)^{1-\eta}\right]^{\frac{1}{1-\eta}}.$$

Subsequently, conditional on sector s, the share of income at location n spent on goods supplied by location i at time t is given by:

$$\alpha_{nit}^{s} \equiv \frac{(p_{nit}^{s})^{1-\sigma}}{\sum_{o=1}^{N}(p_{not}^{s})^{1-\sigma}}.$$

The market clearing condition in the labor market implies that the sum of labor income earned by both skilled and unskilled labor at all ages in location n at time t

[2] As we abstract away from physical capital formation, the coefficient governing this productivity-skill complementarity serves as a proxy for capital-skill complementarity in the model.

is the same as the total income spent on goods from all locations:

$$\sum_j \sum_e \mathbb{1}_{\{j\neq 1,\ e\neq h\}} L_t^j(n,e) w_{nt}^e = \sum_j \sum_e \sum_{n'} \mathbb{1}_{\{j\neq 1,\ e\neq h\}} \alpha_{n'nt}^1 \zeta L_t^j(n',e) w_{n't}^e + \sum_j \sum_e \sum_{n'} \mathbb{1}_{\{j\neq 1,\ e\neq h\}} \alpha_{n'nt}^2 (1-\zeta) L_t^j(n',e) w_{n't}^e.$$

Rearranging the terms and denote the working labor for each location, skill-type as $\mathbb{L}_t(n,e)$, the market clearing condition can also be written as:

$$\sum_e \mathbb{L}_t(n,e) w_{nt}^e = \sum_s \sum_{n'} \sum_e \alpha_{n'nt}^s \mathbb{L}_t(n',e) w_{n't}^e. \tag{1.11}$$

Sequential Equilibrium Given the path of exogenous parameters, including location-specific productivities A_n^s, and an initial distribution of workers $L(n,e;0)$, the recursive competitive equilibrium is defined by the paths of:

i. individuals' migration and educational choices for each location, education level, and age group: $\{\pi_t(n',e'|n)$ and $\pi_t^j(n'|n,e)\}_{t=0}^{\infty}$
ii. value functions for each location, education type, and age group $\{V_t^j(n,e)\}_{t=0}^{\infty}$
iii. the distribution of workers across location, educational type, and ages $\{L_t^j(n,e)\}_{t=0}^{\infty}$, and
iv. wages $\{w_{nt}^e\}_{t=0}^{\infty}$,

such that the value function (1.8), the population flow condition (1.9), the educational level condition (1.10) and the goods market clearing condition (1.11) are satisfied.

Steady State of the Equilibrium A steady state in this economy suggests no aggregate variables change over time. The labor composition in all locations stays unchanged; the individual migration still exists, while the net inflows by cohorts and skill types are equal to zero.

We solve the model in levels[3], the equations that characterize the steady state are in the Appendix.

[3]The model can be solved using hat algebra, but due to the lack of available data on internal trade flows at the prefecture-pair level in China, we have to solve the model in levels.

1.3 Parameterization

We conducted the quantitative exercise on 273 prefecture cities in China. The sample of cities in the paper is the intersection between the cities with available educational resource data (number of teachers in higher education) and the cities with available estimates of bilateral transportation cost from Ma and Tang (2024).

We model two broadly defined sectors $S = 2$ to distinguish the skill intensity in the production function. We first rank all the sectors from the industrial classification for national economic activities by their payment share to skilled workers observed in the *2005 One Percent Population Survey*, and classify the sectors above the median level as the "skilled-intensive sector", and those below the median as the "unskilled-intensive sector".

1.3.1 Data Description

We solve the model in levels and therefore require the following data: the initial distribution of labor by age, skill type, and location; wages and employment of skilled and unskilled workers in all regions; to calibrate share of high-skilled labor input in the production function, we need to calculate the share of the aggregate labor income earned by skilled labor; we need the bilateral trade costs and migration costs to address the bilateral frictions in the model; to calibrate the magnitude of the migration cost, we need the migration probability cognitional on age, skill-type, origin, and destination in 2015; to estimate parameters describing individual's education choice, we need the overall skill-ratio of individuals who are currently in higher education institutes in 2015.

The primary source of our data is the 2005 One Percent Population Survey (also known as the mini-census). The Survey was conducted by the National Bureau of Statistics of China, covering 1.31% of China's total population. This survey provides a comprehensive view of the population's demographic and socioeconomic characteristics. We use the 2005 One Percent Population Survey as our starting point to construct the initial labor distribution in the model. However, the 2005 One Percent Population Survey lacks a proportional representation of observations for the population size in each prefecture. To address this issue, we use only the educational level and age distribution data from each prefecture and scale the pre-

fecture's total population using the prefecture-level population data from the 2005 statistical yearbook. This approach allows us to establish a population distribution by age, education level, and location that closely represents the Chinese demography. We further standardize the distribution by creating an age and educational level grid. We only include individuals aged between 18 and 61, evenly spaced into 11 cohorts. We assume that individuals with an education level at or below high school are unskilled workers, and the other are skilled workers. To maintain a stable labor supply, we simplify the distribution of each age group within the population by assuming that each cohort has an equal total population. At this point, we have obtained comprehensive information on the labor distribution within 273 prefecture cities, broken down into 11 cohorts and two skill types.

In our analysis, we specifically utilize GDP data from 2005 and information on the number of teachers in higher educational institutions for the years 2005 and 2015.China City Statistical Yearbook (Yearbook hereafter) is a valuable resource for accessing detailed location-specific data. Published annually by the National Bureau of Statistics of China, it provides essential information on the prefecture level.

The geographic linkages in the model are summarized by bilateral trade costs and migration costs, which are from Ma and Tang (2024). They comprehensively document the quality of transportation infrastructure in China over time and estimate trade costs and migration costs from a spatial model.

Finally, we utilize data from the 2015 mini-census to gather detailed information on migration probabilities. This mini-census covers 1.55% of the population in mainland China. Survey participants were asked about their previous residential locations 5 years ago if they did not currently reside at the surveyed address. By combining this information with their current residential data and individual characteristics such as age and educational level, we can create a bilateral migration flow between cities in China that represents a snapshot of labor movement within the economy.

1.3.2 Estimation Procedure

In Table 1.1, we show two sets of parameters: The upper panel includes parameters that are either taken from the literature or calibrated directly without solving the model. The lower panel includes parameters calibrated by inverting the model.

Table 1.1: Parameters

Symbol	Description	Value	Source	Step
β	Discount rate	0.85	Yearly interest rate of 4%	
σ	Elasticity of substitution	4		
κ	Inverse elsaticity of migration	2.55	Kleinman et al. (2023)	
ω	Productivity skill complementarity	0.5	Burstein and Vogel (2017)	
η	Elasticity of substitution in production	1.4		
$\{\tau_{mn}\}_{m,n=1}^{N,N}$	Bilateral transportation cost		Ma and Tang (2024)	
$\{D_{mn}\}_{m,n=1}^{N,N}$	Bilateral migration cost		Ma and Tang (2024)	
β	Parameters map observed educational resources to educational appeals		2015 Migration probability	1
D^j	Magnitude of migration cost by cohort		2015 Migration matrix	1
χ	Weight of input share for low skilled labor	0.93	2005 Wage bill	2
$\{A_n\}_{n=1}^{N}$	Productivity in each location		2005 GDP share	2
ψ	Inverse elasticity of educational migration	2.72	2015 College share	3
$\bar{D}$	Magnitude of migration cost	0.93	2015 Stay rate	3

Notes: This table displays the parameters' estimated values along with the source materials used in calibration or relevant literature. The first and second columns show the symbolic representations used in the model and their respective descriptions. The third column provides the parameter values when available, and the last column describes the source citation or the source of the target used during the calibration.

We directly assign the following parameters of the model: we use a four-yearly discount rate β of 0.85, implying a yearly interest rate of roughly 4 percent[4]. We assume an elasticity of substitution in the utility function, $\sigma = 4$, as in Tombe and Zhu (2019). We choose $\kappa = 3\beta = 2.55$, following Kleinman et al. (2023). The productivity skill complementarity of ω equals 0.5, as in Burstein and Vogel (2017).

[4]The discount rate is $0.96^4 \approx 0.85$

We use the estimated trade directly from Ma and Tang (2024). The migration costs in our model vary across ages, while those in Ma and Tang (2024) do not have an age dimension. We therefore assume the following functional form to map the migration frictions in our model to those in Ma and Tang (2024):

$$D^j_{n'nt} = \bar{D} \times \bar{D}^j \times D_{n'nt}. \tag{1.12}$$

In the expression above, $D_{n'nt}$ is the estimated migration cost from n to n' at time t in Ma and Tang (2024). $\{D^j\}$ is an age-specific shifter, and $\bar{D}$ is an overall shifter that governs the magnitude of the migration matrix. We will estimate $\{\bar{D}, \bar{D}^j\}$ together with the other parameters, as discussed in detail below.

We quantify the remaining parameters in the following three steps. The first group of parameters is estimated using the structural equations of the model without any simulation. Conditional on the first group, the second step estimates several parameters by solving the initial static equilibrium of the model. Lastly, the third step solves the dynamic model in the steady state to estimate the last group of parameters. In the rest of this section, we provide more details of the three-step estimation.

Step 1: Structural Estimation without Solving the Model

In the first step, we estimate two objects: 1) the age-specific migration costs, D^j, and 2) the parameters that map the location-specific education appeals, F_{nt}, to observables using structural equations from the model. This step does not require solving any part of the model.

Age-Specific Migration Costs We estimate the migration cost for each age group to account for the observed variations in migration probability as individuals age. To estimate $\bar{D}^j$, first recall the value function and migration flow for individual of cohort j, with skill type e, in location n.

$$V^j_t(n,e) = U^j_t(n,e) + \kappa \log \sum_{n'=1}^{N} \exp\left(\beta V^{j+1}_{t+1}(n',e) - D^{j+1}_{n'n,t+1}\right)^{1/\kappa}$$

$$\pi^j_t(n'|n,e) = \frac{\exp(\beta V^{j+1}_{t+1}(n',e) - D^{j+1}_{n'n,t+1})^{1/\kappa}}{\sum_{n''=1}^{N} \exp(\beta V^{j+1}_{t+1}(n'',e) - D^{j+1}_{n''n,t+1})^{1/\kappa}}.$$

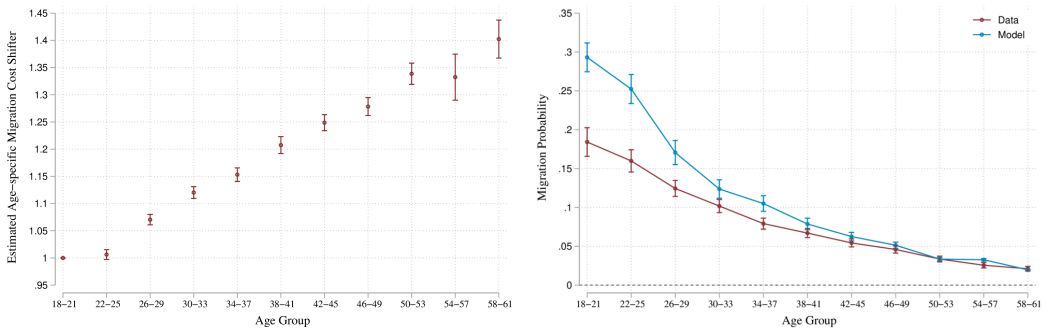

(a) Cost of Migration by Age Group **(b)** Probability of Migration by Cohort

Figure 1.2: Migration by Cohort

Note: Figure 1.2a shows estimated migration cost shifters by age group with 95% bootstrapped confidence interval. Figure 1.2b shows the migration probability by age group from both the model and the data. The migration probabilities from the data are plotted in red with confidence intervals computed by bootstrapping. The migration probabilities by cohort predicted by the model are plotted in blue, with confidence intervals calculated using weighted standard deviation.

Rearranging the terms, we can write the value function as a function of migration flow:

$$V_t^j(n,e) = U_t^j(n,e) - \kappa \log \pi_t^j(n'|n,e) + \beta V_{t+1}^{j+1}(n',e) - D_{n'n,t+1}^{j+1}. \tag{1.13}$$

We arrange Equation (1.13), and take the difference between the log probability of migrating to another location n' from n and the log probability of staying in location n given cohort j and skill type e.

$$\log\left(\frac{\pi_t^j(n'|n,e)}{\pi_t^j(n|n,e)}\right) = \frac{\beta}{\kappa}\left(V_{t+1}^{j+1}(n,e) - V_{t+1}^{j+1}(n',e)\right) - \frac{D_{n'n,t+1}^{j+1}}{\kappa},$$

Similar to estimating trade costs, double-differencing the migration flows leaves us with a simple equation linking migration probabilities to migration costs. We omit the t subscript for simplification:

$$\log\left(\frac{\pi^j(n'|n,e)}{\pi^j(n|n,e)}\right) + \log\left(\frac{\pi^j(n|n',e)}{\pi^j(n'|n',e)}\right) = -\frac{\bar{D}^{j+1}\left(D_{n'n} + D_{nn'}\right)}{\kappa}.$$

Lastly, the difference in the equation between each age group and the initial age group ($j = 1$) leads to the estimate of $\bar{D}^j$:

$$\underbrace{\frac{\log\left(\frac{\pi^j(n'|n,e)}{\pi^j(n|n,e)}\right) + \log\left(\frac{\pi^j(n|n',e)}{\pi^j(n'|n',e)}\right)}{\log\left(\frac{\pi^{j'}(n'|n,e)}{\pi^{j'}(n|n,e)}\right) + \log\left(\frac{\pi^{j'}(n|n',e)}{\pi^{j'}(n'|n',e)}\right)}}_{\text{data}} = \widetilde{D}^{j+1},$$

where $\widetilde{D}^{j+1} = \bar{D}^{j+1}/\bar{D}^1$ is the age-specific shifter, normalized by the first age group.

We observe the data on migration flows from the 2015 mini-census.

Figure 1.2 shows the estimated migration cost shifters by age group, where the first age group serves as a reference point and is normalized to 1.[5] We find that migration costs increase significantly as people age. For example, the migration costs among the oldest individuals are 1.4 times higher than those of the youngest cohort. The increasing migration costs by age comes from the pattern in the data that younger individuals are much more likely to migrate than older ones. The right panel of Figure 1.2 shows the data and model-simulated migration probability by age group. Generally speaking, the model does well, particularly for cohorts of later ages.

The Education Appeals The education appeals at each location, F_n, capture a location's non-monetary attributes that appeal to students in their destination choices. The educational appeals are unobservable; therefore, we need to map them to observable characteristics at a location and then back out the mappings using the structure of the model. To be concrete, we first hypothesize that the abundance of college resources, the prestige and rank of colleges, and the natural amenities of a location could affect a student's choice, conditional on distance and future returns. Based on this logic, we first assume the following functional form for F_n

$$F_n = \beta_2 \times \exp(\beta_1 \times \text{Num.teacher}_n + X\beta) + \varepsilon_n. \tag{1.14}$$

In the expression above, we first map F_n to the number of teachers in each location, which is a proxy for the abundance of educational resources. The educational resource is also the key variable through which we will conduct counterfactual analyses later. In addition to the main dependent variable, we also include a wide range of control variables in the vector X. These control variables include the number of elite universities measured as those that fall under Project 985 in a location as a proxy for the prestige and ranking of colleges.[6]. Lastly, we also include a prefecture's average elevation, slope, temperature, and precipitation as proxies for natural amenities. ε_n is the error term that varies across locations. The parameters of interest are β_1, β_2, and the factor loadings in the vector β.

[5]The 95% confidence intervals are computed using bootstrapping.

[6]A total of 39 elite colleges was included in the sponsorship scheme initiated by the central government in May 1998. These colleges were widely regarded as the elite colleges in China.

Our model provides a structural relationship between the education migration flows and educational appeals, based on which we can estimate the parameters of interest. We derive this structural equation using the migration flows and value functions. We first denote the educational migration probability as:

$$\pi_t^{0(1)}(n'|n,e) = \frac{\exp\left(V_t^1(n',e) - D_{n'n}^1 - F_{n't}\right)^{1/\kappa}}{\sum_{n''=1}^{N}\exp\left(V_t^1(n'',e) - D_{n''n}^1 - F_{n''t}\right)^{1/\kappa}}.$$

Conditional on pursuing higher education, the log difference between the probability of students moving from location n to n' and the probability of them staying in n can be written as:

$$\log\left(\frac{\pi_t^{o(1)}(n',h|n)}{\pi_t^{o(1)}(n,h|n)}\right) = \frac{1}{\kappa}\left(V_t^1(n',h) - V_t^1(n,h) - \tilde{D}_{n'n} - \tilde{D}_{nn}\right),$$

$$\text{where } \tilde{D}_{n'n} = D_{n'n}^1 + F_{n't}.$$

Lastly, similar to the estimation of the migration cost, applying a double-differencing, we arrive at the structural equation based on which to back out the parameters of interest:

$$\log\left(\frac{\pi_t^{o(1)}(n',h|n)}{\pi_t^{o(1)}(n,h|n)}\right) + \log\left(\frac{\pi_t^{o(1)}(n,h|n')}{\pi_t^{o(1)}(n',h|n')}\right) = \frac{-1}{\kappa}\left(2F_{n't} + 2F_{nt} + D_{nn'} + D_{n'n}\right).$$

In the expression above, the dependent variable is a function of the observed educational migration probabilities, $\pi_t^{o(1)}(n',h|n)$. The independent variables on the right-hand side of the equation depend on the observed migration costs and the education appeals. Plugging in the functional form of F_n defined in Equation (1.14), the equation above is the structural relationship based on which to estimate $\{\beta_1, \beta_2, \beta\}$. Due to the non-linear nature of the equation, we use non-linear least squares to carry out the estimation.

The appeal function we estimated shows strong diminishing returns with respect to college concentration. Figure 1.3 illustrates the estimated educational appeals and the number of teachers in 2015. The estimated educational appeal increases drastically when the number of teachers is low, while as resources concentrate, the educational cost changes minimally. The median city, in terms of number of teachers hired in higher education institutes, has approximately 2,000 teachers, while the city in the top 10% has 7.4 times as many teachers as a median city. In a median city with 2,000 teachers, a 10 percent increase in teachers leads to a 2.87 percent

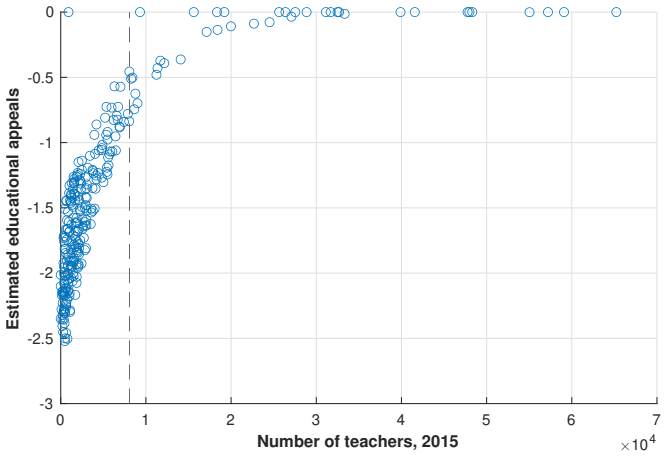

Figure 1.3: Estimated Education Costs

Note: This figure shows the estimated educational appeals and number of teachers in 2015. The estimated education appeals are plotted on the y-axis. The number of teachers hired in higher education institutes is plotted on the x-axis. Each dot represents a location in the model. The number of teachers in higher education institutes comes from China Statistical Yearbook. The dotted line indicates the cities in the 90th percentile regarding the number of teachers.

increase in education appeals. However, the return on investment in additional colleges quickly diminishes in better-endowed locations, as indicated by the curvature of the education appeal function. For example, at the 90th percentile of cities in terms of education resources, a 10 percent increase in teachers only increases costs by 0.13. In contrast, at the 10th percentile, the same increment leads to a increment of 8 times larger. This pattern strongly indicates the presence of a substantial number of potential students who would pursue higher education if resources were more accessible. Additionally, the data pattern suggests that in areas with a limited number of colleges, educational appeals are likely to be very low. The form of the cost function also anticipates several of our numerical findings: investing in education yields a greater benefit in areas with relatively fewer educational resources. Therefore, having an excessive concentration of colleges could have a notable negative impact. We elaborate on this point in a general equilibrium framework in the counterfactual exercise.

Step 2: Static Model Inversion at the Initial Equilibrium

In the second step, we invert the model at the initial static equilibrium to recover the location-specific fundamental productivity and the production function. The

initial equilibrium corresponds to the year 2005 ($t = 1$). Model inversion at the initial equilibrium only requires solving the static market clearing conditions using the initial population distribution but not the forward-looking migration decisions. As a result, static inversion has a clear advantage in computational load and data requirements as we do not need any information regarding the migration costs to compute the initial equilibrium.

To calibrate $\{\chi^s\}$, the parameter governing the weight of input share for low-skilled workers in sector s, we target the payment share to unskilled workers in each sector. The payment share data is inferred using the 2005 mini-census that recorded the industry of employment, education attainment, and income at the individual level. We target the prefecture-sector-level output share in the data to back out the location-sector-fundamental productivity, $\{A_n^s\}$. We combine the information from the *China City Statistical Yearbook* and the 2005 mini-census to compute the target data. The former source provided the total output of each prefecture in 2005, and the mini-census allows us to compute the within-prefecture share of output by sector. As we target output share by sector, we normalize $A_1^s = 1$.

To better suit our model, we assign a scalar, $\bar{D}$, uniformly to scale the migration costs. We estimate the migration cost scalar by matching the share of individuals choose to stay in their current location from the 2015 census and the model predicted value. Furthermore, to address the observed decreasing migration probability over ages, we utilize the migration flow by age group from the 2015 mini-census and calibrate the migration cost scalar, D^j, for different age groups. We discuss the detailed estimation process below.

Step 3: Dynamic Model Inversion at Steady State

In the last step, we have two more migration-related parameters to be calibrated. The first is ψ, the inverse elasticity of educational migration, and the second is $\bar{D}$, the overall magnitude of the migration cost matrix. Both parameters shape the individuals' migration behavior in the dynamic model; therefore, we need to invert the model to dynamic equilibrium to estimate these parameters. In particular, conditional on all the other parameters estimated in the previous steps, with a guess of $\{\psi, \bar{D}\}$, we solve the model's steady state and compute the target moments that are

used to calibrate these parameters.

We use a two-layer nested Nonlinear Least Squares procedure to perform the estimation. In the outer loop, we choose the overall migration cost shifter,$\bar{D}$, to match the overall stay rate to the 2015 stay rate in the data. To be specific, we compute the stay rate as:

$$\text{Stay Rate} = \frac{\sum_e \sum_{j=2}^{J} \sum_{n=1}^{N} (\pi^j(n|n,e) \times L_n^j) + \sum_e \sum_{n=1}^{N} (\pi^0(n,e|n) \times L_n^0)}{\text{Total Population}},$$

where $\pi^j(n|n,e)$ indicates the probability that an individual stays in location n with skill type e and age group j. We collect the 5-year stay rate from the One Percent Population Survey in 2015 and transform it into a 4-year stay rate[7] to align with our model period, assuming the same stay rate each year. The identification of the benchmark adjustment scalar, $\bar{D}$, relies on the stay rate of individuals. Migration costs can affect the value one can get from moving. Intuitively, the higher the migration cost, the higher the portion of individuals who choose to stay in their current location instead of pursuing higher wages elsewhere.

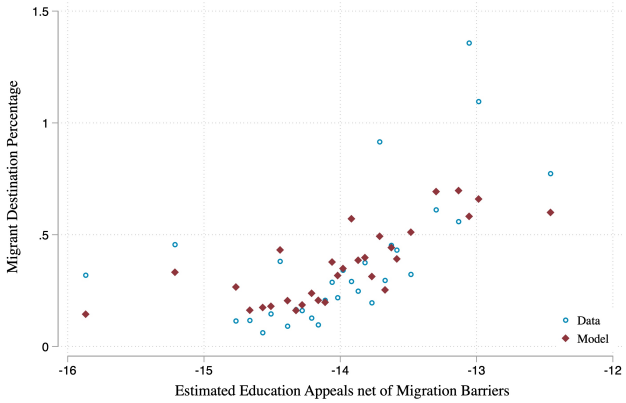

Figure 1.4: Migrants Destination Percentage

Note: This figure shows the binned scatter plot of the destination choice against the estimated education appeals net of the migration barrier costs for both data and model prediction. The number of bins is 30. The education cost plus the migration barrier is plotted on the x-axis, and the percentage of students who chose the place as the destination conditional on going to college in a place different from the home location is plotted on the y-axis. Each dot represents a group of observations with similar estimated destination-specific costs.

In the inner loop conditional on $\bar{D}$, we choose the inverse of education elasticity, ψ, to match the share of individuals who go to college when they are young in

[7]Five-year stay rate is 91%, we transform it by assuming the same one-year stay rate: Four-year stay rate = (Five-year stay rate)$^{4/5}$

2015. The identification of parameter ψ governs the education choices. Given the expected lifetime utility of being a skilled and unskilled worker, a larger ψ indicates the individual is less sensitive to the value difference between being a skilled worker and an unskilled worker. We match the model-predicted share of college students at the steady state to the ones we observed in the 2015 mini-census. The share of college students in the first cohort is given by

$$\frac{\sum_{n'=1}^{N}\sum_{n=1}^{N}(\pi_n^0(n',h|n)\times L_n^0)}{\sum_{n=1}^{N}L_n^0}.$$

The estimation strategy yields an estimate for the migration cost shifter, $\bar{D} = 0.93$, and education elasticity, $1/\psi = 0.38$[8]. Our estimation procedure fits the data fairly well. Figure 1.4 illustrates the destination choices of individuals. The estimated cost of obtaining an education is plotted on the x-axis, which includes $F_n + D_{n'n}$. We focus on the age group 18-21 who have chosen to attend college away from their hometown and compute the distribution of this group of people. The percentage of each location chosen as the migration destination is plotted on the y-axis. When the cost of education is lower, there is a greater likelihood that individuals will choose that location for college, given that they are part of the population pursuing higher education and moving. Our model can generate this pattern by only targeting the first moment of the distribution of migrant college students when estimating the model parameters.

1.4 Counterfactual Simulations

In this section, we evaluate the spatial impacts of educational resources. We carry out several counterfactual analyses with alternative distributions of higher education institutions and show how welfare and skill ratios respond to the changes in educational resources.

1.4.1 College Expansion

We first examine the impact of the factual expansion of the educational resources implemented by the central government between 2005 and 2015. Within a short span of time, the college expansion saw an 84 percent increase in the number of

[8] Appendix A.3 displays the objective function for estimating $\bar{D}$ and ψ with each parameter varying while keeping the other parameters at their estimated values.

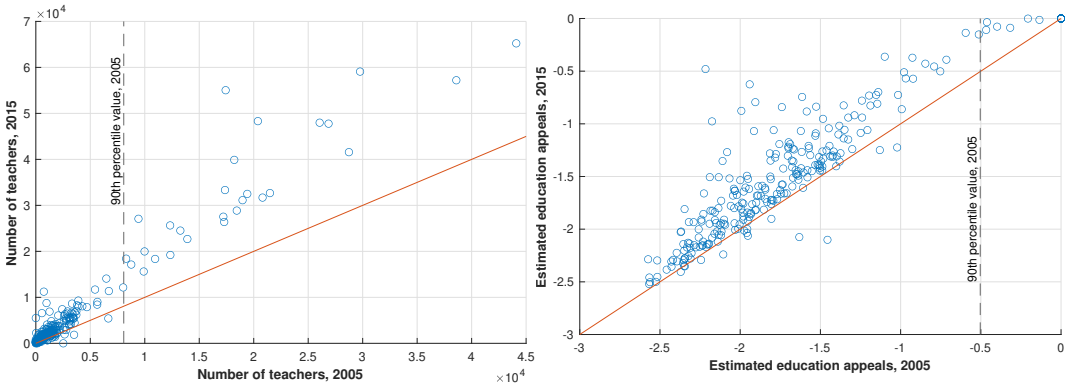

(a) Education Resources

(b) Estimated Education Appeals

Figure 1.5: Factual College Expansion

Note: Figure 1.4.1 shows the factual educational resources regarding the number of teachers hired in higher education institutes by location. Figure 1.5b shows estimated education appeals by location. The number of teachers hired in higher education institutes comes from the *China City Statistical Yearbook* in 2005 and 2015. The red line represents the 45-degree line.

college teachers hired in higher education institutes and a 466 percent increase in college enrollments.

Through the lens of our model, the college expansion affects the educational appeals of a location through Equation (1.14). Our baseline simulation incorporated the changes in educational resources over time, including the college expansion between 2005 and 2015. To evaluate the impact of the factual expansion, we conducted a “no expansion" counterfactual, in which the number of college teachers is fixed at the initial year of our analysis (2005). In this counterfactual analysis, the educational appeals of a location no longer evolve over time ($F_{nt} = F_n, \forall n, t$) because the number of teachers is the only location characteristics that change over time in Equation (1.14). Comparing the “no expansion” counterfactual with the baseline simulation uncovers the aggregated and distributional impact of college expansion.

The factual expansion of education resources is highly uneven across locations. Figure plots a location’s number of teachers in 2005 on the x-axis against that in 2015 on the y-axis, and the red solid line is the 45-degree line. As is evident in the figure, places with a high concentration of educational resources also received a disproportional allocation of additional resources. The additional resources allocated to the top 10 percent of prefectures in terms of number of teachers in 2005 is approximately 26 times higher than the additional resources allocated to the bottom 10 percent. The uneven distribution is partly due to cost considerations — expanding

existing colleges with more teachers is arguably cheaper than creating a new college with the same number of teachers. The pattern of concentration is partially reflected in the changes in educational appeals, as shown in Figure 1.5b. In locations already well endowed with colleges, such as Beijing, the additional college teachers do not significantly lead to higher appeals among the students. Furthermore, the curvature of the appeal function shown in Figure 1.3 suggests that an increase in areas with few resources could substantially increase their education appeals. However, in the factual expansion, these areas receive minimal new resources. The most significant increase in educational appeals occurs in locations with medium-level educational resources.

The college expansion between 2005 and 2015 led to moderate welfare improvements in all locations. Panel A of Table 1.2 reports the overall welfare and distributional impact of factual college expansion. By the year 2015, the aggregate welfare increased by 0.52% due to the expansion of education resources. Both skilled and unskilled workers experience welfare improvement on average, and the impact on skilled workers is substantially larger than on unskilled ones (0.82% v.s. 0.24%). The expansion of college also shifted the labor force towards skilled workers, leading to a 0.56% increase in the aggregate skill ratio. The aggregate impacts of college expansion are channeled through the educational decisions at the individual level in the model. The college expansion increases the educational appeal in most locations, leading to a higher expected lifelong welfare of the skilled worker and, thus, a higher skill ratio. The higher skill ratio increases location-specific productivity through agglomeration forces, resulting in overall welfare gains. Skilled workers receive the lion's share of the benefits associated with higher productivity due to the positive productivity-skill complementarity introduced through the parameter ω. The impact of the college expansion is also long-lasting, eventually leading to a 0.72% welfare improvement for the skilled worker and a 0.35% gain for unskilled workers when the economy transits to a steady state.

Locations that experienced a larger increase in educational appeals also see higher welfare impacts, mainly through its skilled workers. As shown in Figure 1.6a, the welfare changes are positively correlated with the changes in the educational appeals. The dispersion of welfare changes is also substantial: the 90th per-

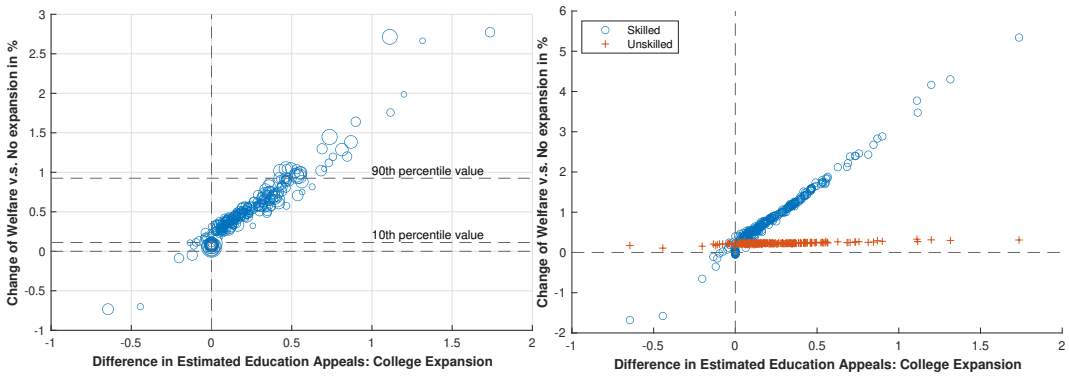

(a) Change in Welfare

(b) Change in Welfare by skill type

Figure 1.6: College Expansion Impacts

Note: Figure 1.6a shows the welfare change by locations. The size of the dot indicates the size of the population. Figure 1.6b shows the welfare change of skilled and unskilled by locations. All changes are compared against the scenario without college expansion. Each dot represents a location.

centile of the welfare change is around 0.9 percent, roughly nine times higher than those at the 10th percentile (0.1 percent). The spatial variation mainly comes from the welfare changes among the skilled workers, as shown in Figure 1.6b. The locations that benefited the most are often those with moderate resources initially. As a result, the spatial inequality, measured by the coefficient of variation of weighted welfare, also experienced a moderate decline due to the college expansion program. The mechanism at the prefecture level is the same as those at the aggregate level outlined above – higher educational resources lead to higher skill ratios, which benefit the local economy through agglomeration and the skilled workers through productivity-skill complementarity.

While the welfare impacts of the college expansion are non-trivial, the further concentration of educational resources in well-endowed locations could lead to suboptimal welfare impacts. For example, while Beijing received a considerable increase in educational resources during the expansion, the impacts of its educational attractiveness and subsequently, welfare, is limited. Thus, we seek alternative allocations to allocate educational resources across space better in the next subsection.

1.4.2 Alternative Allocations

The factual college expansion results suggest that the allocation of educational resources has varying effects on different locations. To analyze this, we calculate the welfare elasticity with respect to college expansion, examining each prefecture

Table 1.2: Summary of Counterfactual Exercises: Welfare Change and Skill Ratio

Panel A: Impacts of College Expansion					
		ΔWelfare	ΔDispersion	10^{th} percentile	90^{th} percentile
Overall	$T=3$	0.52%	-0.18%	0.11%	0.93%
	S.S.	0.44%	-0.11%	0.26%	0.65%
Skilled	$T=3$	0.82%	-0.03%	0.05%	1.66%
	S.S.	0.72%	0.01%	0.03%	1.62%
Unskilled	$T=3$	0.24%	-0.16%	0.2%	0.25%
	S.S.	0.35%	-0.26%	0.3%	0.38%
		ΔSkill Ratio	ΔDispersion	10^{th} percentile	90^{th} percentile
Overall	$T=3$	0.56%	-0.29%	-16.38%	113.83%
	S.S.	3.87%	0.61%	0.53%	7.79%
Panel B: Impacts of Equal Expansion					
		ΔWelfare	ΔDispersion	10^{th} percentile	90^{th} percentile
Overall	$T=3$	0.94%	-3.71%	0.51%	1.4%
	S.S.	0.83%	-2.16%	0.59%	1.06%
Skilled	$T=3$	1.38%	-7.08%	0.65%	2.47%
	S.S.	1.25%	-7.43%	0.6%	2.38%
Unskilled	$T=3$	0.52%	-0.39%	0.36%	0.44%
	S.S.	0.7%	-0.71%	0.6%	0.71%
		ΔSkill Ratio	ΔDispersion	10^{th} percentile	90^{th} percentile
Overall	$T=3$	1.01%	-1.35%	-14.71%	115.87%
	S.S.	6.4%	-1.41%	2.32%	10.59%
Panel C: Impacts of Proportionate to Population Expansion					
		ΔWelfare	ΔDispersion	10^{th} percentile	90^{th} percentile
Overall	$T=3$	0.98%	-2.88%	0.36%	1.49%
	S.S.	0.69%	-1.6%	0.46%	1%
Skilled	$T=3$	1.47%	-4.9%	0.36%	2.55%
	S.S.	1.08%	-4.99%	0.4%	2.52%
Unskilled	$T=3$	0.51%	-0.37%	0.36%	0.43%
	S.S.	0.58%	-0.57%	0.48%	0.59%
		ΔSkill Ratio	ΔDispersion	10^{th} percentile	90^{th} percentile
Overall	$T=3$	1.17%	-1.69%	-14.41%	113.3%
	S.S.	5.81%	-3.38%	1.96%	11.41%

Notes: This table illustrates the changes in the levels and dispersion of both welfare and labor composition in the model simulated 2015 and the steady state, compared to the no-expansion benchmark. In Panel A, we present scenarios reflecting factual college expansion, while Panel B depicts a situation where the additional educational resources between 2015 and 2005 are distributed equally in all locations. In Panel C, we reallocate the additional resources proportionate to the initial population. The changes are calculated in comparison to a scenario in which we maintain educational resources at the 2005 level. Welfare is weighted by the population, and we also present a dispersion measure using the coefficient of variation.

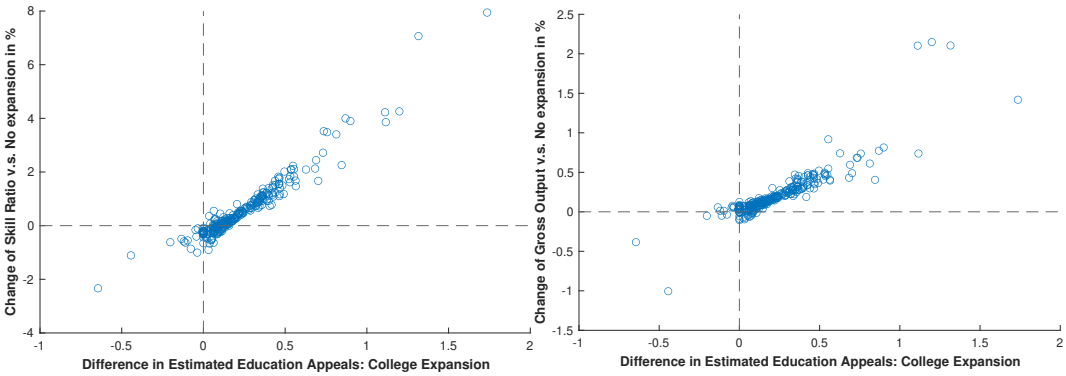

(a) Change in Skill Ratios **(b)** Change in Output

Figure 1.7: College Expansion Impacts

Note: Figure 1.7a shows the skill ratio change by locations. Figure 1.7b shows the gross output change by location. All changes are compared against the scenario without college expansion. Each dot represents a location.

individually. More specifically, we increase the actual number of college teachers by 10% in each location and then assess the change in local welfare compared to a scenario with no expansion. We categorize the prefectures based on their initial educational resources. Notably, the regional impact of a 10% increase in college teachers is 2.6 times greater in the bottom 10% of prefectures than in the top 10% when compared to the no expansion scenario.

We then conduct another simulation where we keep the total increment of education resources unchanged and distribute the additional teachers evenly across all locations. We call this counterfactual simulation *"equal expansion"*. In this case, all prefectures equally receive an additional 2600 college teachers. Figure 1.8 shows the counterfactual education appeals in this scenario. The evenly distributed resources keep the relative rank of education appeals untouched while substantially increasing the appeals of the prefectures with initially low appeals.

The *"equal expansion"* scheme leads to a substantially larger increase in welfare and skill ratio. Table 1.2 Panel B shows the equal expansion generates an aggregate welfare gain that is 1.8 times higher than the actual expansion program (0.94% v.s. 0.52%). The *"equal expansion"* scheme is also much more effective at increasing the overall skill ratio: the aggregate skill ratio in the counterfactual increased by 1.01%, as compared to the 0.56% increment in the baseline model. The abundance of educational resources is particularly effective in places where the initial number of teachers was low; subsequently, the welfare improvement for skilled

Table 1.3: Summary of Counterfactual Exercises: Skill Ratio

Panel A: Impacts of Education Equalization					
		ΔSkill Ratio	ΔDispersion	10^{th} percentile	90^{th} percentile
Overall	$T = 3$	1.53%	-3.72%	-1%	7.12%
	S.S.	4.36%	-0.47%	-1.74%	15.24%
Panel B: Impacts of Productivity Equalization					
		ΔSkill Ratio	ΔDispersion	10^{th} percentile	90^{th} percentile
Overall	$T = 3$	10.59%	-26.33%	0.39%	53.56%
	S.S.	30.72%	-84.8%	20.54%	112.81%

Notes: This table illustrates the changes in the levels and dispersion of labor composition in model simulated 2015 and the steady state, compared to the **college expansion** benchmark. In Panel F, we present scenarios reflecting educational resources equalization, while Panel G depicts a situation where fundamental productivities in both sectors are equalized to the average respectively in all location. The changes are calculated in comparison to a scenario in which we maintain the factual college expansion. We present a dispersion measure using the coefficient of variation.

workers from improved productivity is also more pronounced. The expansion of college programs also benefits unskilled workers through agglomeration. Figure 1.9 demonstrates this point by showing the welfare impact by skill type and location. On the x-axis, we show the estimated educational appeal under this "equal expansion" counterfactual. In this scenario, as shown in Figure 1.8, the locations with low initial education resources experienced the largest increase in education appeals and, subsequently, higher overall welfare.

We also conduct an expansion scheme, where we allocate the additional resources according to the population distribution. The impacts on education appeals for each location are shown in Figure 1.8. The *"population expansion"* yields a larger increase in educational appeal as compared to the factual expansion. The average educational costs decreased by 17.5% compared to the factual expansion. As a result, the overall welfare improvement is 0.98%, higher than both the factual expansion and *"equal expansion"*.

1.4.3 Equalization

The final counterfactual exercise we conduct involves equalizing all educational resources to examine the impact of this even distribution of resources on spatial inequality in skill composition.

In the 'Equal college' scenario, we demonstrate that the unequal distribution of educational resources contributes to as much as 14% of the observed spatial in-

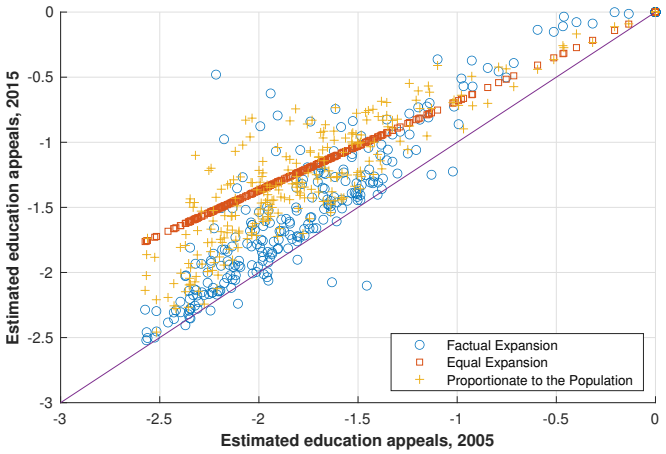

Figure 1.8: Factual College Expansion and Alternatives
Note: This figure shows the estimated education appeals for college expansion and alternative counterfactual in 2005 and 2015. Each dot represents a location.

equality in skill composition in the short run and persist. In this exercise, educational costs are standardized across all locations while keeping the overall resource level constant. Consequently, skill ratios are adjusted accordingly. As indicated in Table 1.3, the skill ratio dispersion decreases by approximately -3.72% to -0.47% compared to the baseline results along the transition path. Figure 1.10 illustrates the changes in skill ratios in various locations under this equalization scenario. In Figure 1.10a, the x-axis represents the skilled intensive sector productivity, while the y-axis depicts the change in skill ratios comparing to the factual expansion in the equalization scenario. The dashed vertical line indicates the 10th and 90th percentile productivity value. Meanwhile, Figure 1.10b displays the number of Teachers in 2015, plotted on the x-axis. Clearly apart from the educational resources, fundamental productivity also determines the labor compositions.

To assess the impact of this hypothetical resource equalization, we also standardize fundamental productivity across all locations. We set the fundamental productivity to the average estimated level across all locations. Table 1.3 demonstrates that equalizing productivity can significantly reduce skill ratio dispersion. The dispersion of skill ratio declines by 26.33% to 84.8% along the transition path to the steady state. An evenly distributed educational resource is 14% as effective at reducing spatial inequality as an evenly distributed productivity in the short run. However,in the long run, the skill ratio has a strong correlation with the sector productivity.

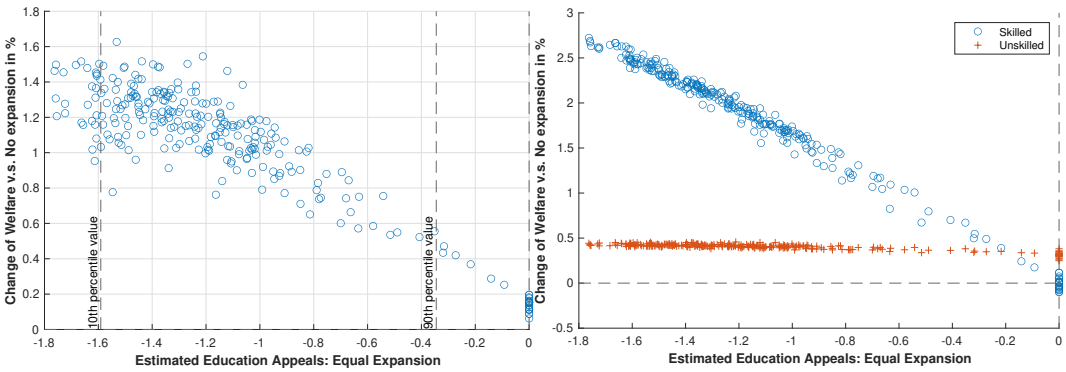

(a) Change in Welfare **(b)** Change in Welfare by skill type

Figure 1.9: Equal Expansion Impacts

Note: Figure 1.9a shows the welfare change by locations. Figure 1.9b shows the welfare change of skilled and unskilled by locations. All changes are compared against the scenario without college expansion. Each dot represents a location.

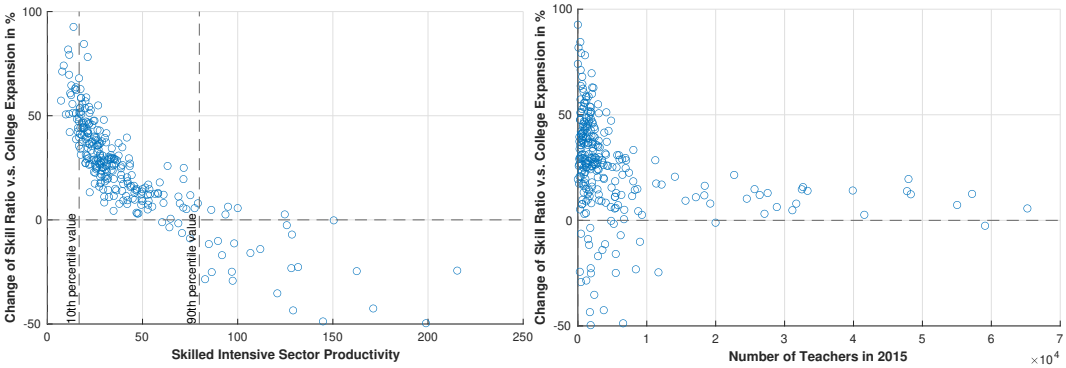

(a) Productivity **(b)** Resources

Figure 1.10: Education resources equalization

Note: Figure 1.10a plots the change of skill ratio against the productivity by locations. Figure 1.10b shows the change of skill ratio against factual educational resources in 2015. All changes are compared against the scenario with college expansion. Each dot represents a location.

1.5 Concluding Remarks

This paper integrates educational choices into a dynamic spatial model to examine how location-specific educational resources affect spatial inequality. We build a dynamic spatial model with overlapping generations. The individuals in the model make decisions on education, including, whether and where to attend college. We use the model to estimate the cost of higher education in each prefecture and perform counterfactual policy experiments to determine if more evenly distributed resources could lead to better outcomes. We quantify the model to mirror China and structurally estimate the cost of obtaining a college degree in each prefecture.

We find diminishing returns to college concentration in estimated education costs. Initially, educational costs decrease significantly with a small increase in resources. However, as resources continue to concentrate, the reduction in costs becomes less proportional compared to earlier stages. This suggests an over-concentration of colleges might carry a sizable negative consequences.

We also find that the real college expansion has a negligible effect on overall welfare and the skill ratio. This expansion disproportionately allocates resources to already well-endowed locations, with little impact on less-endowed areas. When we simulate a scenario in which additional resources are evenly distributed across regions, we observe a doubled increase in both the welfare impact and the impact on skill ratio comparing to the observed expansion.

Furthermore, we show that in the short run, equalizing educational resources is roughly 14% as effective as equalizing fundamental productivity. However in the long run, the labor distribution would be largely explained by productivity difference in skill-intensive and unskilled-intensive sectors.

Finally, this study abstracts government's decisions on investment in educational resources. Allowing local government optimizing investment in educational investment, the model could explore intriguing topics such as the competition among local governments and the evaluation of policies aimed at attracting skilled talent. An important direction for future work is to incorporate government's role into analyses. Furthermore, the spatial general equilibrium life-cycle model developed in this paper can be adapted to investigate other individual decisions such as marriage and

fertility.

Chapter 2

Tariffs as Bargaining Chips: A Quantitative Analysis of the U.S.–China Trade War[1]

2.1 Introduction

During the 2016 United States (U.S.) presidential campaign, Donald Trump denounced the U.S.–China trade relationship and repeatedly vowed to increase tariffs on Chinese imports. After winning the 2016 election, he kept his promise by imposing a series of wide-ranging increases in tariffs from 2018 through 2019. As documented in Bown (2021), the average U.S. tariff on China had risen to more than 19% by January 2021, up from 3% before the trade war. At the same time, China retaliated by increasing its average tariff on U.S. goods from 8% to more than 20%. During the next presidential campaign, Joe Biden attacked the trade war as reckless and irresponsible, and stated that he would remove the Trump tariffs.[1] However, Joe Biden has not kept his word since winning the 2020 election, and the existing Trump tariffs remain in place as of 2023.

[1]This is a joint work with Yuan Mei and Tong Ni. We thank Lorenzo Caliendo, Robert Staiger, Pao-Li Chang, and seminar participants at the CUHK Workshop on International Trade and Singapore Management University for their valuable comments.

[1]For example, on August 3, 2019, Joe Biden wrote on Twitter that "...Trump doesn't care about the farmers, workers, and consumers that are being crushed by his irresponsible trade war with China... I will reverse his senseless policies."

We explore one plausible hypothesis that explains the Biden administration's reluctance to remove the Trump-era tariffs: these tariffs can be used as bargaining chips in future trade negotiations with China.[2] In testimony before a U.S. Senate Appropriations subcommittee in June 2022, U.S. Trade Representative Katherine Tai stated, "The China tariffs are, in my view, a significant piece of leverage – and a trade negotiator never walks away from leverage". In this paper, we investigate this claim by quantitatively examining whether the trade war has improved the post-negotiation welfare outcomes of the U.S.

We start by developing a general equilibrium quantitative model that features both international trade and the U.S. economy disaggregated into eight regions and thirteen sectors. Firms in each U.S. region demand labor, local factors, and materials from all other markets in the economy, as in Caliendo et al. (2017). By incorporating intermediate goods, sectoral heterogeneity, and input-output linkages, our model features intersectoral trade, interregional trade, and international trade. The U.S. and China can engage in bilateral tariff negotiations, and the bargaining outcome depends on both the tariff levels before the negotiation and the relative bargaining power of the two countries.

We use the method of mathematical programming with equilibrium constraints (MPEC), popularized by Su and Judd (2012), to compute the outcomes of potential tariff negotiations between the U.S. and China in two scenarios. In the first scenario, the U.S. and China engage in Nash bargaining starting from the baseline equilibrium calibrated to the 2017 fundamentals before the trade war. In the second scenario, we first apply tariff changes observed during the trade war and then compute the cooperative tariffs starting from the trade-war equilibrium. If the combined U.S. welfare change relative to the 2017 baseline in the second scenario is larger than the U.S. welfare improvement in the first scenario, we consider it as supporting evidence of Katherine Tai's claim.

As analyzed in previous theoretical works on trade policy cooperation, tariff negotiations usually result in mutual tariff reductions. For example, Bagwell and Staiger (1999) show that, in a two-country, neo-classical trade model where non-

[2]Other theories include lobby pressure from firms that have benefited from the Trump tariffs, the concern about appearing weak on China, and campaign considerations for the 2024 presidential election.

cooperative tariffs can be imposed to improve terms of trade, both countries can benefit from a mutual reduction in tariffs. In addition, if political incentives are absent and governments simply use tariffs to maximize national income, the tariff negotiation will lead to an efficient equilibrium in which at least one country imposes zero tariffs. Ossa (2011) derives the same result in a Krugman (1980)-style environment in which tariffs can be used to improve welfare through production relocation. The results of our simulation, which uses the reasonably comprehensive general equilibrium model, are consistent with these predictions: the resulting cooperative equilibrium in both scenarios always involves one country imposing zero tariffs. However, since the total welfare change relative to the 2017 baseline in the second scenario also incorporates welfare change due to trade-war tariffs, existing theories cannot predict which scenario will lead to the greater welfare improvement for the U.S.

One key result from our simulation is that, regardless of the relative bargaining power between the U.S. and China, the U.S. always enjoys a larger welfare increase relative to the 2017 baseline in the second scenario. In other words, the trade-war tariffs always improve the U.S. post-negotiation welfare. This finding can be explained by the theoretical analysis of tariff bargaining in Bagwell and Staiger (1999) and Ossa (2011): the bilateral tariff negotiation between the U.S. and China involves reciprocal tariff reductions, and the U.S. welfare gain from the tariff negotiation starting from the 2017 baseline equilibrium is limited due to low U.S. tariff rates. For the same reason, tariff negotiation starting from high tariffs after the trade war can substantially improve the U.S. welfare. Our quantitative analysis shows that, even after taking the welfare effects of the trade war into consideration, the negotiation starting from trade-war tariffs leads to a larger U.S. welfare improvement relative to the negotiation starting from low tariffs before the trade war. This result is robust to incorporating political weights into the objective function of the U.S., allowing negative tariffs (import subsidies), fixing trade deficits between countries, and using alternative estimates of trade elasticities.

We estimate the bilateral bargaining power between the U.S. and China by examining China's accession to the World Trade Organization (WTO) in 2001. Our approach closely follows the simulated method of moments estimation introduced

in Bagwell et al. (2021). In particular, given the estimated parameters of the trade model and the outside options, we can predict cooperative tariffs between the U.S. and China with any bargaining power parameter. We then numerically search over the bargaining power parameter to minimize the distance between factual Chinese tariffs after China's accession to the WTO and the predicted bargaining tariff outcomes. The estimated Nash bargaining weight of the U.S. in the bilateral tariff negotiation with China ranges from 0.47 to 0.70. We obtain a range of the U.S. bargaining power because of the U.S. trade policy uncertainty before China's accession to the WTO. As documented in Handley and Limão (2017) and Alessandria et al. (2023), although the U.S. had already imposed low most favored nation (MFN) tariffs on Chinese imports before 2001, the U.S. Congress could vote to revoke China's MFN status and impose the non-cooperative "column 2" tariffs instead. These two possible outside options allow us to compute the two bounds of the U.S. bargaining power relative to China. Given this range of bargaining power, the trade war leads to an additional U.S. post-negotiation welfare gain of 0.04%–0.05% relative to its pre-trade-war welfare level. Meanwhile, China's post-negotiation welfare change decreases by 0.09%–0.10%.

Given the spatial features of our model, we can also analyze the heterogeneous impacts of trade negotiations with China on different U.S. regions. Since we assume free labor mobility within the country, as in Caliendo et al. (2017), the population change in each region is used to measure the impact of the U.S.–China tariff negotiation. Our simulation predicts that, given the estimated U.S. bargaining power, the tariff negotiation starting from the trade-war tariffs benefits the Southwest Region (Arizona, New Mexico, Oklahoma, and Texas) the most. By contrast, the New England region suffers the largest labor outflow.

By quantifying how the U.S.–China trade war affects potential negotiation outcomes, this paper contributes to the growing body of literature on quantitative trade policy. Ossa (2014) and Ossa (2016) initiated the study of non-cooperative and cooperative tariffs in multi-region quantitative trade models. Other papers in this strand of literature have analyzed the welfare effects of cooperative and non-cooperative trade policies either through numerical optimization (Mei 2020; Bagwell et al. 2021; de Souza et al. 2022; Beshkar et al. 2022; Ritel 2022; Mei ming) or through ana-

lytical characterization of optimal trade policy (Bartelme et al. 2021; Beshkar and Lashkaripour 2020; Lashkaripour 2021; Lashkaripour and Lugovskyy 2023). Most closely related to our work are Bown et al. (2023) and Beshkar et al. (2022), both of which focus on the reciprocal tariff reductions among WTO member countries. Our estimated Nash bargaining weight of the U.S. is also consistent with the finding in Bown et al. (2023) that China's tariff reductions after its accession to the WTO exceeded the norm of reciprocity.

Our work also complements the theoretical literature that analyzes the welfare outcomes of trade negotiations. In addition to Bagwell and Staiger (1999) and Ossa (2011), Bagwell and Staiger (2004), Bagwell and Staiger (2018), Bagwell et al. (2020), and Beshkar and Lee (2022) also study the implications of different institutional features for tariff bargaining outcomes. By contrast, we estimate the relative bargaining power between the U.S. and China, and quantify the potential welfare effects of the U.S.–China trade war on tariff bargaining. The numerical results computed from the comprehensive general equilibrium model also corroborate previous results derived theoretically from simpler trade models.

Finally, this paper contributes to a burgeoning body of literature that studies the impact of the trade war initiated by the Trump administration. Previous works have mainly focus on the impact on U.S. prices and welfare (Amiti et al. 2019; Waugh 2019; Fajgelbaum et al. 2020; Amiti et al. 2020; Handley et al. 2020; Bown 2021; Cavallo et al. 2021), responses from China (Chor and Li 2021; He et al. 2021; Ma et al. 2021; Benguria et al. 2022; Jiao et al. 2022; Jiang et al. 2023), and U.S. election outcomes (Blanchard et al. 2024; Che et al. 2022; Choi and Lim 2023).[3] Our paper is distinct from these works by considering the Trump tariffs as bargaining chips, thereby providing the first quantitative study of the potential negotiation outcomes between the U.S. and China.

The rest of the paper is structured as follows: we start by developing a general equilibrium quantitative model that features both international trade and spatial features within the U.S. in Section 2.2. After presenting data and calibrations in Section 2.3, we present simulation results of tariff negotiations in Section 2.4.

[3]See Fajgelbaum and Khandelwal (2022) for a comprehensive review of the literature on the impact of the U.S.–China trade war on aggregate welfare and distributional consequences for the U.S., China, and other countries.

Section 2.5 presents some extensions and robustness checks, and the last section concludes.

2.2 Model

To guide our analysis of cooperative tariffs, we follow Caliendo et al. (2017) and develop a quantitative model that features both international trade and the U.S. economy disaggregated by region and sector. The model incorporates intermediate goods, sectoral heterogeneity, and input-output linkages. We consider a total of $N+M$ locations, in which N is the number of regions in the U.S. and M is the number of other countries. The locations are indexed by i or $n \in \{1,\ldots,N,N+1,\ldots N+M\}$. The sectors are indexed by j or $k \in \{1,\ldots,J\}$. The U.S. economy has two factors: labor and a composite of land and structures. Labor can move freely across the regions and sectors in the U.S., but there is no international migration. The land and structures, H_n, are immobile and can be used by any sector. The total population of the U.S. is denoted by L_{US}, and the population in sector j, region n is denoted by L_n^j. For locations outside of the U.S., we abstract from the fixed factors and assume that labor is the only factor of production.

2.2.1 Consumers

Agents in location $n \in \{1,\ldots,N,N+1,\ldots,N+M\}$ have Cobb-Douglas preferences

$$U(C_n) = \prod_{j=1}^{J} \left(c_n^j\right)^{\alpha_n^j}, \quad \text{where} \quad \sum_{j=1}^{J} \alpha_n^j = 1,$$

with consumption share α_n^j for each sector $j \in \{1,\ldots,J\}$, over local final goods c_n^j from sector j bought at price index P_n^j. Income in each location, denoted by I_n, is derived from two sources: households supply labor L_n inelastically at wage w_n and receive transfers on a lump-sum basis (including both tariff revenues and transfers accounting for trade imbalances, which will be discussed in more detail later).

2.2.2 Technology

The production technology closely follows Eaton and Kortum (2002) and Caliendo and Parro (2015). Final goods can be used for consumption or as inputs for the pro-

duction of intermediate goods. In each sector, the final goods are produced using a continuum of intermediate goods in that sector. Intermediate goods are produced using labor and a fixed factor of land and structures in locations within the U.S., along with the final goods from all the sectors, while the production of intermediate goods from other countries uses only labor and final goods. The final goods used to produce intermediate goods are referred to as "materials".

The representative firms of sector j produce a continuum of varieties $\mu^j \in [0,1]$ in each region n. In each location n, sector j, each firm draws its productivity level z_n^j independently from a Fréchet distribution with shape parameter θ^j and location parameter T_n^j. The production of a variety within the U.S. associated with idiosyncratic productivity level z_n^j is given by

$$q_n^j(z_n^j) = z_n^j \left[\left[h_n^j(z_n^j) \right]^{\beta_n} \left[l_n^j(z_n^j) \right]^{(1-\beta_n)} \right]^{\gamma_n^j} \prod_{k=1}^{J} \left[M_n^{jk}(z_n^j) \right]^{\gamma_n^{jk}},$$

$$\text{for } n \in \{1,\ldots,N\},\ j \in \{1,..,J\},$$

where $h_n(\cdot)$ and $l_n(\cdot)$ denote demand for structures and labor, respectively. $M_n^{jk}(\cdot)$ denotes the demand for materials from sector k for the production of intermediate good in sector j in location n. $\gamma_n^{jk} \geq 0$ is the share of input from sector k in the production of goods in sector j in location n, and γ_n^j is the share of value added. The production function is constant return to scale; therefore $1-\gamma_n^j = \sum_{k=1}^{J} \gamma_n^{jk}$. Since the production of intermediate goods outside of the U.S. does not require a fixed factor, $\beta_n = 0$ for $n \in \{N+1,\ldots,N+M\}$, and the corresponding production function becomes

$$q_n^j(z_n^j) = z_n^j \left[l_n^j(z_n^j) \right]^{\gamma_n^j} \prod_{k=1}^{J} \left[M_n^{jk}(z_n^j) \right]^{\gamma_n^{jk}},$$

$$\text{for } n \in \{N+1,\ldots,N+M\},\ j \in \{1,\ldots,J\}.$$

Markets are competitive, so sector j firms in country n set the price at x_n^j/z_n^j. Taking x_n^j as the cost of the input bundle for intermediate goods in location n, sector j, we have

$$\begin{aligned} x_n^j =& B_n \left[r_n^{\beta_n} w_n^{1-\beta_n} \right]^{\gamma_n^j} \prod_{k=1}^{J} \left[P_n^k \right]^{\gamma_n^{jk}},\ \text{for } n \in \{1,\ldots,N\} \\ x_n^j =& B_n' w_n^{\gamma_n^j} \prod_{k=1}^{J} \left[P_n^k \right]^{\gamma_n^{jk}},\ \text{for } n \in \{N+1,\ldots,N+M\}, \end{aligned} \tag{2.1}$$

where $B_n = [\gamma_n^j(1-\beta_n)^{(1-\beta_n)}\beta_n^{\beta_n}]^{-\gamma_n^j}\prod_{k=1}^{J}[\gamma_n^{jk}]^{-\gamma_n^{jk}}$ and $B'_n = [\gamma_n^j]^{-\gamma_n^j}\prod_{k=1}^{J}[\gamma_n^{jk}]^{-\gamma_n^{jk}}$.

Final goods in each location are produced using intermediate goods from the lowest cost suppliers around the world. The production technology of Q_n^j is a constant elasticity of substitution (CES) aggregator given by

$$Q_n^j = \left[\int_{\mathscr{R}_+^{N+M}} \tilde{q}_n^j(z^j)^{1-1/\eta_n^j}\phi^j(z^j)dz^j\right]^{\eta_n^j/(\eta_n^j-1)},$$

where $\tilde{q}_n(z^j)$ is the demand for an intermediate good of a given variety such that the vector of productivity drawn from each location for that variety is $z^j = (z_1^j, z_2^j, \ldots, z_{N+M}^j)$. The joint density function for the vector z^j is denoted by $\phi^j(z^j) = \exp\{-\sum_{n=1}^{N+M} T_n^j (z_n^j)^{-\theta^j}\}$, with marginal densities given by $\phi_n^j(z_n^j) = \exp\{-T_n^j(z_n^j)^{-\theta^j}\}$, and the integral is over $\mathscr{R}_+^{N+M}$. For non-tradable sectors, the producers only use locally produced intermediates.

2.2.3 International trade costs and prices

We assume that trade in intermediate goods is costly. Trade costs occur due to iceberg trade costs and an ad valorem flat-rate tariff. In particular, $d_{ni}^j \geq 1$ units of tradable intermediate goods in sector j need to be shipped from location i to location n with $d_{nn}^j = 1$. Sector j goods imported by country n from country i have to pay an ad valorem flat-rate tariff τ_{ni}^j. For goods circulated within the U.S., only iceberg trade costs are applicable, so $\tau_{ni}^j = 1$ for $i,n \in \{1,\ldots,N\}$. Combining both the iceberg trade costs and the ad valorem tariff, we define $\kappa_{ni}^j = \tau_{ni}^j d_{ni}^j$, where $\tau_{ni}^j = 1 + t_{ni}^j$.[4] Non-tradable sectors have infinite trade costs, so $\kappa_{ni}^j = \infty$. After considering trade costs, the price of intermediate good μ^j in location n is given by

$$p_n^j(\mu^j) = \min_i \left\{\frac{x_i^j \kappa_{ni}^j}{z_i^j(\mu^j)}\right\}.$$

Following the probabilistic representation of technologies in Eaton and Kortum (2002), we can derive the price index for the composite of intermediate goods j in region n:

$$P_n^j = \Gamma\left(\frac{1-\eta_n^j}{\theta^j}+1\right)^{1/(1-\eta_n^j)}\left[\sum_{i=1}^{N} T_i^j\left(x_i^j\kappa_{ni}^j\right)^{-\theta^j}\right]^{-1/\theta^j}, \tag{2.2}$$

where $\Gamma(.)$ is the Gamma function. When j denotes a non-tradable sector, the price

[4] Triangular inequality also holds, hence $\kappa_{nh}^j\kappa_{hi}^j \geq \kappa_{ni}^j$ for all n,h,i.

index becomes

$$P_n^j = \Gamma\left(\frac{1-\eta_n^j}{\theta^j}+1\right)^{1/(1-\eta_n^j)}\left[T_n^j\left(x_n^j\right)^{-\theta^j}\right]^{-1/\theta^j}.$$

As consumers have Cobb-Douglas preferences, the aggregate consumption price index P_n is given by

$$P_n = \prod_{j=1}^{J}\left(\frac{P_n^j}{\alpha_n^j}\right)^{\alpha_n^j}.$$

We can also derive location n's expenditure on the intermediate goods of sector j purchased from location i. We use $X_n^j = P_n^j Q_n^j$ as the total expenditure on sector j goods in location n and X_{ni}^j as the expenditure of location n on sector j goods from location i. The expenditure share $\pi_{ni}^j = X_{ni}^j/X_n^j$ is given by

$$\pi_{ni}^j = \frac{T_i^j\left[x_i^j\kappa_{ni}^j\right]^{-\theta^j}}{\sum_{h=1}^{N+M}T_h^j\left[x_h^j\kappa_{nh}^j\right]^{-\theta^j}}. \tag{2.3}$$

2.2.4 Income

To address the regional trade imbalances within the U.S., we assume that the local factors are partly owned by local governments and the rents are redistributed to local residents. The rest of the rents are collected by central government, forming a national portfolio that is redistributed to all the agents within the U.S. However, trade imbalances still exist between countries and will be handled of through transfers.

We assume that a fraction of $\iota_n, n \in \{1,\ldots,N\}$ of the local factor rents is collected by the central government, forming the national portfolio. All residents within the U.S. hold an equal share of the national portfolio. The $(1-\iota_n)$ fraction of the return is redistributed to local residents equally. The difference between the remittances to the central government and the local factor income generates imbalances across regions within the U.S.:

$$\Upsilon_n \equiv \iota_n r_n H_n - \chi L_n, \text{ for } n \in \{1,\ldots,N\}. \tag{2.4}$$

The excess income generated by these imbalances in region n is spent by agents on local final goods. The magnitude of these across-region imbalances will change

in the model with the change of tariff, as it will affect the wages and the rental rates of land and structures. The tariff revenues are distributed as lump-sum payments to all residents in location $n \in \{1,\ldots,N,N+1,\ldots,N+M\}$, along with the unaddressed trade surplus across countries. The income for residents in location n within the U.S. is

$$I_n = w_n + \chi + (1-\iota_n) r_n H_n / L_n + \lambda_n - s_n, \text{ for } n \in \{1,\ldots,N\},$$

where w_n is the wage, r_n is the rental rate for the fixed factor, and $r_n H_n / L_n$ is per capita income of land and structure rents in location n. λ_n is the per capita tariff revenue received by agents in location n (which will be discussed later). s_n is the per capita trade surplus generated from the country-wide trade imbalances. Lastly, we define the share of national portfolio received by each resident in the U.S. as $\chi = \sum_{i=1}^{N} \iota_i r_i H_i / \sum_{i=1}^{N} L_i$. Similarly, the income for residents in other countries is given by $I_n = w_n + \lambda_n - s_n$ for $n \in \{N+1,\ldots,N+M\}$, since we abstract from the fixed factor for locations outside of the U.S.

2.2.5 Labor mobility and market clearing

We first focus on the U.S. economy. Regional labor market clearing for locations within the U.S. requires that

$$\sum_{j=1}^{J} \int_0^{\infty} l_n^j(z) \phi_n^j(z) dz = \sum_{j=1}^{J} L_n^j = L_n, \text{ for } n \in \{1,\ldots,N\},$$

where L_n^j is the number of workers in sector j in region n. In addition, the labor market clearing at the national level requires that $\sum_{n=1}^{N} L_n = L_{US}$. For any U.S. region, the market clearing condition for land and structures must satisfy

$$\sum_{j=1}^{J} \int_0^{\infty} h_n^j(z) \phi_n^j(z) dz = \sum_{j=1}^{J} H_n^j = H_n, \text{ for } n \in \{1,\ldots,N\},$$

where H_n^j denotes the land and structures used in sector j in region n. We abstract from labor mobility and fixed factor input for locations outside of the U.S.

Intermediate goods producers solve the profit maximization problem, along with the equilibrium condition between rental rates and wages $r_n H_n (1-\beta_n) = \beta_n w_n L_n$ for all $n \in \{1,\ldots,N\}$. Then, by defining $\omega_n \equiv [r_n/\beta_n]^{\beta_n} [w_n/(1-\beta_n)]^{(1-\beta_n)}$, free mobility along with the labor market clearing condition gives us an expression for

labor input in region n of the U.S.:

$$L_n = \frac{H_n \left[\frac{\omega_n}{P_n U + u_n - \lambda_n + s_n}\right]^{1/\beta_n}}{\sum_{i=1}^{N} H_i \left[\frac{\omega_i}{P_i U + u_i - \lambda_i + s_n}\right]^{1/\beta_n}} L, \tag{2.5}$$

where $u_n \equiv \Upsilon_n / L_n = \iota_n r_n H_n / L_n - \chi$. Since labor is perfectly mobile within the U.S., utility $U_n = U_{US}$ is equalized for $n \in \{1, \ldots, N\}$.

Total expenditure on final goods j in location n, X_n^j, is the sum of the expenditure on composite intermediate goods by firms and the expenditure on final consumption by households:

$$X_n^j = \sum_{k=1}^{J} \gamma_n^{j,k} \sum_{i=1}^{N+M} X_i^k \frac{\pi_{in}^k}{\tau_{in}^k} + \alpha_n^j I_n L_n, \tag{2.6}$$

where

$$I_n L_n = \omega_n (H_n)^{\beta_n} (L_n)^{1-\beta_n} - \Upsilon_n + \Lambda_n - S_n, \text{ for } n \in \{1, \ldots, N\},$$
$$I_n L_n = w_n L_n + \Lambda_n - S_n, \text{ for } n \in \{N+1, \ldots, N+M\}.$$

In particular, $\Lambda_n = \sum_{j=1}^{J} \sum_{i=1}^{N+M} t_{ni}^j X_n^j \frac{\pi_{ni}^j}{\tau_{ni}^j}$ refers to location n's tariff revenue on sector j goods from location i. The sum of international trade surplus is zero, $\sum_{n=1}^{N+M} S_n = 0$, and within the U.S. the sum of sectoral surpluses in location n is the national surplus, $\sum_{j=1}^{J} S_n^j = S_n$. Sectoral surplus is defined as $S_n^j = \sum_{i=1}^{N+M} \left(X_i^j \frac{\pi_{in}^j}{\tau_{in}^j} - X_n^j \frac{\pi_{ni}^j}{\tau_{ni}^j} \right)$. Note that although sectoral surpluses are endogenously determined, surpluses at the national level are exogenous.[5] Finally, using trade surplus and expenditure, we have the trade balance condition:

$$\sum_{j=1}^{J} \sum_{i=1}^{N+M} X_n^j \frac{\pi_{ni}^j}{\tau_{ni}^j} + \Upsilon_n + S_n = \sum_{j=1}^{J} \sum_{i=1}^{N+M} X_i^j \frac{\pi_{in}^j}{\tau_{in}^j}. \tag{2.7}$$

This equation suggests that the total expenditure net of tariff expenditure plus trade surpluses is equal to the sum of each country's expenditure.

2.2.6 Competitive equilibrium

Given factor supplies L and $\{H_n\}_{n=1}^N$, a competitive equilibrium under given tariff structure τ for this economy is a set of utility levels $\{U_{US}, U_n\}_{n=N+1}^{N+M}$, a set of factor prices in each region, $\{\omega_n\}_{n=1}^{N+M}$, a set of labor allocation within the U.S.

[5] Ossa (2016) discusses the implications of various approaches for managing trade deficits in counterfactual analysis. We set all national trade deficits to zero in our quantitative exercises, as in Bagwell et al. (2021).

$\{L_n\}_{n=1}^N$, regional transfers within the U.S. $\{\Upsilon_n\}_{n=1}^N$ and prices $\{P_n^j\}_{n=1,j=1}^{N+M,J}$, which satisfy equilibrium conditions 2.1, 2.2, 2.3, 2.4, 2.5, 2.6, and 2.7 for all sectors j and locations n. In practice, we solve the model using the exact hat algebra approach, as in Dekle et al. (2007), to avoid calibrating unchanged underlying parameters. We present the corresponding equilibrium conditions in Appendix Section A.1. In addition, as discussed in Ossa (2014), the presence of aggregate trade imbalances between countries can generate extreme general equilibrium adjustments in response to trade policy changes. Accordingly, we follow the exercise in Dekle et al. (2007) to construct a trade flow matrix of 2017 without trade imbalances. All later simulations of tariff negotiations in the main analysis will treat this purged trade flow data as the 2017 baseline equilibrium. Nevertheless, we also consider an alternative setup that fixes the 2017 factual imbalances in Section 2.5.4 as a robustness check.

2.2.7 Tariff negotiation

We assume that the U.S. and China can negotiate bilaterally over tariff vectors τ. In particular, the two countries select their bilateral tariffs to maximize the Nash product of their welfare:

$$\begin{aligned}\max_{\{\tau_{US,chn},\tau_{chn,US}\}} & \left[U_{US}\left(\tau_{US,chn},\tau_{chn,US}\right)-U_{US}\left(\tau^0_{US,chn},\tau^0_{chn,US}\right)\right]^{\psi} \\ & \left[U_{chn}\left(\tau_{chn,US},\tau_{US,chn}\right)-U_{chn}\left(\tau^0_{chn,US},\tau^0_{US,chn}\right)\right]^{1-\psi} \\ & \text{s.t. the competitive equilibrium conditions are satisfied, and} \\ & U_{US}\left(\tau_{US,chn},\tau_{chn,US}\right)\geq U_{US}\left(\tau^0_{US,chn},\tau^0_{chn,US}\right), \\ & U_{chn}\left(\tau_{chn,US},\tau_{US,chn}\right)\geq U_{chn}\left(\tau^0_{chn,US},\tau^0_{US,chn}\right),\end{aligned} \tag{2.8}$$

where the bargaining power of the U.S. against China is denoted by ψ. When $\psi=1$, the U.S. maximizes its own welfare while keeping China welfare non-decreasing. Throughout this paper, we refer to the solution to (2.8) as cooperative tariffs or post-negotiation tariffs. In particular, $\tau_{US,chn}$ refers to the predicted vector of cooperative tariffs imposed by the U.S. on Chinese goods and $\tau_{chn,US}$ is the vector of cooperative tariffs imposed by China on U.S. goods. $U_{US}\left(\tau^0_{US,chn},\tau^0_{chn,US}\right)$ and $U_{chn}\left(\tau^0_{chn,US},\tau^0_{US,chn}\right)$ denote the initial welfare levels of the U.S. and China under the pre-negotiation tariff profile $(\tau^0_{US,chn},\tau^0_{chn,US})$ that will prevail if the two coun-

tries fail to reach an agreement. In practice, we also adopt the exact hat algebra approach to solve the Nash bargaining problem, and the hat-algebra equilibrium details are presented in Appendix Section A.2.

2.3 Data, calibration, and some empirical facts

In this section, we first present the data and the calibration of parameters used in the quantitative exercise. We then discuss the estimation of two remaining key parameters: the bargaining power between the U.S. and China and the elasticity of substitution θ^j. In the last part of the section, we present some basic facts of the U.S.–China trade war.

2.3.1 Data

In our quantitative analysis, we consider two major economies: the U.S. and China. The remaining countries are grouped into one entity known as the Rest of the World (ROW). Following the classification in the Regional Economics Information System (REIS) of the U.S. Bureau of Economic Analysis (BEA), we disaggregate the U.S. into eight regions:*New England*, *Mideast*, *Great Lakes*, *Plains, Southeast*, *Southwest*, *Rocky Mountain*, and *Far West*. Each region represents a grouping of states with similar economic and social conditions. Twelve tradable sectors are organized as shown in the left column of Table 2.1. We combine non-tradable sectors into a single service sector.

We use the economy in 2017 as the pre-trade-war baseline to analyze the Nash bargaining over tariffs and the economy in 1997 to estimate the relative bargaining power between the U.S and China. Consequently, we need to calibrate two sets of parameters, those in 1997 and those in 2017, to accommodate different economic situations. The detailed data sources and the calibration process are formally stated as follows.

We obtain bilateral international trade flow data from the OECD Inter-Country Input-Output (ICIO) database for the years 1997 and 2017. Regional-sectoral trade flows within the U.S. are computed by using the standard Commodity Flow Survey (CFS). To disaggregate the trade flows between the U.S. and other trading countries to the regional level, we follow Caliendo et al. (2019) and allocate the aggregate

Table 2.1: Elasticity of Substitution and Political Economy Weight Estimates

Sector	θ_j	σ_{US}	σ_{CHN}
Chemical	2.43	0.91	1.12
Computer, electronic and electrical equipment	2.70	**1.32**	1.06
Food, beverages and tobacco	2.30	0.71	**1.28**
Machinery	2.56	**1.20**	1.02
Mineral	1.98	0.91	0.78
Miscellaneous	3.66	1.13	0.78
Petroleum	2.76	0.57	**1.15**
Primary and fabricated metal	2.82	1.03	**1.16**
Rubber	2.72	1.01	0.83
Service	3.31	1.00	1.00
Textiles	2.97	**1.35**	0.80
Transportation	2.98	1.08	1.12
Wood and paper	2.78	0.77	0.92
Mean	2.77	1.00	1.00

Note: The entries under θ_j are the estimates of elasticity of substitution. The entries under σ_{US} and σ_{CHN} are the estimates of political economy weights for the U.S. and China, respectively, which are scaled to have a mean of one. The bold entries highlight the sectors with the three highest values of political weights for each country. Parameter estimates are reported by sector in alphabetical order.

trade volume proportionally to the sectoral employment share in each region. The labor employment data at the region-sector level are obtained from BEA for the matching year or the nearest year available. In this way, we obtain a complete trade flow matrix that bilaterally links $8+2$ locations by 12 tradable sectors.

The OECD ICIO database also provides information regarding intermediate trade flows for any origin sector and destination sector, as well as the trade values used for final goods consumption. We directly back out value-added shares in gross production, γ_n^j, and input-output coefficients, γ_n^{jk}, from the database.

The consumption expenditure share in each location for each sector is computed as

$$\alpha_n^j = \frac{1}{I_n}\left(\sum_{i=1}^{N+M} X_n^j \pi_{ni}^j - \sum_{k=1}^{J}\sum_{i=1}^{N+M} \gamma_i^{kj}\frac{\pi_{in}^k}{\tau_{in}^k} X_i^k\right).$$

Because the implied intermediate good expenditures in some industries exceed gross expenditures, γ_n^{kj} and α_n^j are pinned down simultaneously à la Bagwell et al. (2021) to ensure that the calibrated α does not have a negative value.[6]

[6]Specifically, we adjust the values of γ_n^{kj} slightly to minimize the sum of the squared distance between the imputed input-output coefficients and the input-output coefficients from the OECD ICIO data, while ensuring that the final goods expenditure shares are all non-negative.

The shares of local rent allocated to the national portfolio, ι_n, are calibrated to eliminate trade imbalances between U.S. regions. Specifically, we compute the regional trade surplus for each location within the baseline model and then conduct a numerical search for a vector of ι that minimizes the sum of the squared regional surpluses within the U.S.

Lastly, we calibrate β_n, the input share of land and structures in intermediate goods production. We follow Caliendo et al. (2017) and calculate the value-added share of land and structures as

$$\beta_n = \left(\frac{Employment\ Compensation_n}{Value\ added_n} - 0.17 \right) / 0.83,$$

where the compensation data of the employees and the disaggregated value-added data are obtained from BEA. This adjustment process first teases out the value-added share of equipment (17%), and then renormalizes the remaining fraction in value added.

2.3.2 Estimation of bargaining power

We estimate the relative bargaining power between the U.S. and China by examining the episode of China's accession to the WTO in 2001. After joining the WTO, China significantly reduced its MFN tariff rates to other WTO member countries. In the meanwhile, the tariffs on China applied by the U.S. remained largely unchanged.[7] This is because the U.S. had already granted China normal trade relations (NTR) status and significantly reduced tariffs on Chinese products to MFN levels in 1980. The U.S. Congress voted annually throughout the 1990s on a bill to renew China's NTR status. If China's NTR status had been revoked, Chinese exports to the U.S. would have been subject to "column 2 tariffs", the non-cooperative tariffs applied to U.S. imports from non-WTO member countries (Ossa 2014). This trade policy uncertainty associated with U.S. tariffs on Chinese goods lasted until 2001 when China gained permanent NTR status after joining the WTO.[8]

[7] As documented in Dorsey (2003), "China will reduce tariffs on nonagricultural products (which account for 95% of its imports) to 8.9% by 2005, and tariffs on agricultural products to 15% by January 2004." In Figure B.1 of the Appendix, we plot the U.S. and China tariff rates at sector level in 1997 and 2005, respectively. The U.S. tariff rates on Chinese imports remained almost the same with only a slight decline. Meanwhile, China significantly lowered its tariffs on U.S. imports after joining the WTO.

[8] As discussed in Handley and Limão (2017), China never lost its NRT status, but it came close: "In the 1990s, after the Tiananmen Square protests, Congress voted on a bill to revoke MFN status

We estimate the bargaining power parameter ψ using a method of moments estimation that closely follows the approach introduced in Bagwell et al. (2021). In particular, given the estimated parameters of the trade model, we can predict post-negotiation tariffs with any bargaining weight and outside options by solving the Nash bargaining problem (2.8). We can then numerically search over ψ to minimize the distance between the post-negotiation tariffs predicted by our model and the factual bargaining outcomes that we discuss in more detail later. We use the world economy in 1997 and 2005 to approximate the equilibrium before and after China's accession to the WTO, respectively.

Given the institutional background of China's accession to the WTO, we introduce three institutional constraints when solving the Nash bargaining problem numerically to estimate the U.S. bargaining power ψ. The first constraint is about the outside option of the U.S.: since the U.S. already reduced tariffs on Chinese imports to MFN levels in 1980, setting $\tau^0_{US,chn}$ as the U.S. applied tariffs in 1997 as in Bagwell et al. (2021) may not accurately reflect the threat point of the U.S in the negotiation with China. In fact, since the U.S. tariffs remained largely unchanged, the computed U.S. bargaining power from this setup should be considered the upper bound ψ. As noted in Bagwell et al. (2021), a country tends to be assigned a larger bargaining power in a bilateral bargaining pair if tariff reductions of the country are smaller than those of its negotiating partner. The lower bound of ψ, meanwhile, is computed by setting $\tau^0_{US,chn}$ as the "column 2 tariffs" of the U.S, the outside option that would bring the largest tariff reductions on the U.S. side.

Second, because the applied MFN tariff rates imposed by the U.S. on most WTO members remained relatively stable between 1997 and 2005, we assume that China was fully aware of the U.S. post-negotiation tariff rates throughout the negotiation process. In other words, $\tau_{US,chn}$ in (2.8) is pinned down by the U.S. applied MFN tariff rates in 2005, and we only need to compute $\tau_{chn,US}$ to solve the Nash bargaining problem. We believe that this setup more accurately reflects the tariff bargaining environment during China's accession to the WTO. Nevertheless, we also consider the alternative setup in which $\tau_{US,chn}$ and $\tau_{chn,US}$ are both adjustable during the negotiation. The computed results are presented in Section 2.5.4 as a robustness

every year and the House passed it three times."

check.

Third, we treat the applied MFN tariffs in 2005 on ROW as given when estimating the relative bargaining power between the U.S. and China. Unlike the Uruguay Round, which involved a collection of inter-connected bilateral bargains (Bagwell et al. 2021), the U.S.–China bilateral agreement is generally regarded as the core of the negotiation on China's accession to the WTO (Dorsey 2003). Therefore, by focusing on the negotiation between the U.S. and China only, we do not need to consider the complications from the Nash-in-Nash approach adopted in Bagwell et al. (2021), which is substantially more computationally demanding than our current approach.

Given these assumptions, we estimate the bargaining power by searching for a value of ψ that minimizes the distance between the factual level of China's tariffs after joining the WTO and the solutions to China's cooperative tariffs given this ψ. Formally, the bargaining power of the U.S. relative China is backed out by solving

$$\min_{\psi} \left(\tau_{chn,US}(\psi) - \tau_{chn,US}^{2005} \right)' \left(\tau_{chn,US}(\psi) - \tau_{chn,US}^{2005} \right),$$

where $\tau_{chn,US}(\psi)$ is the vector of the predicted cooperative tariff of China on the U.S. exports given the bargaining power ψ from solving (2.8) and $\tau_{chn,US}^{2005}$ is the unilateral vector of the applied MFN tariff rates of China against the U.S. in the year 2005. Using the grid search method, we obtain the upper and lower bounds of the U.S. bargaining power relative to China: $\hat{\psi} = 0.47$ when setting $\tau_{US,chn}^{0}$ as "column 2 tariffs" and $\hat{\psi} = 0.70$ when setting $\tau_{US,chn}^{0}$ as the U.S. applied tariffs in 1997.

Our estimates of $\psi \in [0.47, 0.70]$ indicate that the U.S. had more bilateral bargaining power in the negotiation with China. Bown et al. (2023) also study the same event but focus on reciprocal tariff reductions that keep the terms of trade between the two countries unchanged (Bagwell and Staiger 1999). Bown et al. (2023) find that, contrary to recent accusations against China, the tariff reductions by China after its accession to the WTO actually exceeded the norm of reciprocity. This finding is consistent with our estimated value of the U.S. bargaining power: as noted in Bagwell et al. (2021), a country tends to be assigned a smaller bargaining power in bilateral bargaining if its tariff reductions will be larger than those of its negotiating

partner.

2.3.3 Elasticity of substitution

The elasticity of substitution, θ^j, is estimated using the well-known method first described by Feenstra (1994) and documented in Feenstra (2010). Data used for bilateral trade flow and quantity are from the CEPII's BACI database, covering the time period from 1996 to 2016. The estimated elasticities are reported in Table 2.1. The average of estimated elasticities of substitution is 2.77, which is similar to the estimated average of 2.80 in Mei (ming) and falls within the range of previous findings in the literature.[9] In Section 2.5.4, we also use estimates of elasticity of substitution from Caliendo and Parro (2015) as a robustness check.

2.3.4 Trade war tariffs

We obtain the tariff data from the World Integrated Trade Solution (WITS) at the country-product (HS 6-digit) level and aggregate it into sectors based on trade volume weight. As in Jiao et al. (2022), the bilateral trade war tariff data are calculated as the pre-trade war applied MFN tariff rates plus the changes in tariff rates caused by each round of the U.S–China tariff war until the end of 2019. Tariff changes in each round are obtained from the Peterson Institute for International Economics (PIIE). Following the approach in Fajgelbaum et al. (2021), the tariff changes are scaled by the total time in effect over the two-year window.

In Figure 2.1, we show the factual tariff rates before and after the trade war by sector. As can be seen from the left panel, the average U.S. tariffs on Chinese goods increased from 0.88% to 15.73%. At the same time, Chinese tariffs on U.S. goods increased from 1.66% to 16.45%.[10] The U.S. raised tariffs on Chinese goods in all sectors, whereas China did the same, with the exception of transportation. This is because China reduced the MFN tariffs on motor vehicles in July 2018. China later retaliated against the U.S. Section 301 Investigations by raising tariffs on the transportation industry, but the retaliation tariffs were suspended on January

[9] Ossa (2014) uses the GTAP database with trade data from 1994 to 2008, and the average of estimated elasticities is 3.42 with a range from 1.19 to 10.07. This is because the sectors in Ossa (2014) are more granular, and agricultural sectors such as wheat and rice exhibit greater elasticity of substitution.

[10] Despite using the same data source, the average tariff changes we calculate differ from those in Bown (2021) because we first aggregate tariffs at sector level before taking the simple average.

1, 2019. The reduction in MFN tariffs on motor vehicles also led to a slight decrease in Chinese tariffs on goods from ROW. Meanwhile, the U.S. tariffs applied to goods from other countries remained stable during the trade war.

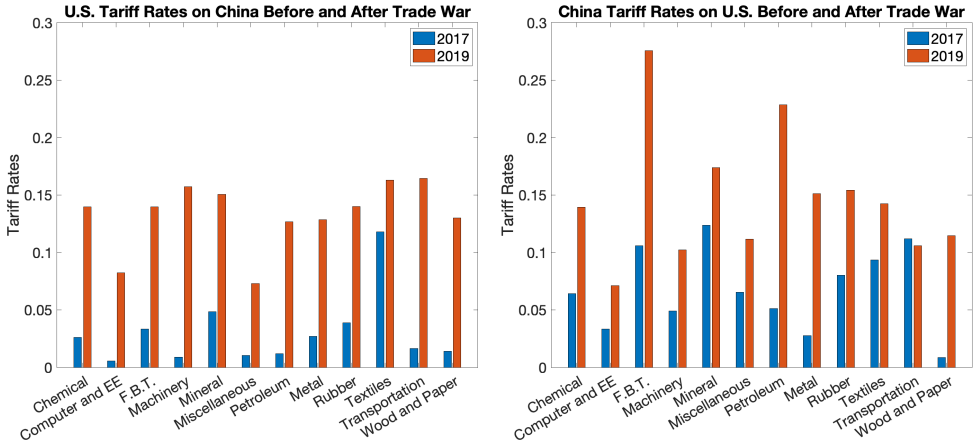

Figure 2.1: Tariff Rates Applied During the U.S.—China Trade War

Note: The figure plots the factual bilateral tariff rates between the U.S. and China in 2017 (before the trade war) and at the end of 2019 (after the trade war). Tariff data are aggregated into sectors based on trade volume. Sectors are arranged in alphabetical order.

2.4 Main results

In this section, we first describe the procedure used to examine the U.S. Trade Representative Katherine Tai's claim that the Trump-era tariffs can be used as a leverage in future tariff negotiations with China. Next, we present the computed cooperative tariffs as a result of negotiations and the corresponding welfare changes.

2.4.1 Procedure

We want to quantitatively analyze whether the trade war improves the U.S. post-negotiation welfare. To do so, we first calibrate the model constructed in Section 2.2 with the 2017 data. Next, we compute the cooperative tariffs between the U.S. and China given bargaining power ψ by solving (2.8) with the MPEC approach. $\tau^0_{US,chn}$ and $\tau^0_{chn,US}$ in the Nash bargaining problem are set to be the pre-trade-war tariffs of the two countries in 2017. We use $\hat{U}^{co-17}(\psi)$ to denote the corresponding the vector of welfare change from the 2017 baseline equilibrium when the computed cooperative tariffs were imposed, which incorporates each country's respective welfare change, $\hat{U}^{co-17}_{US}(\psi)$ and $\hat{U}^{co-17}_{chn}(\psi)$.

We then apply the trade-war tariffs rates observed in 2019 to the 2017 baseline equilibrium. Given the tariff changes, the resulting vector of welfare change of the trade war equilibrium relative to the 2017 baseline equilibrium is denoted by $\hat{U}^{war}$. Note that $\hat{U}^{war}$ does not depend on ψ as the computation of welfare changes does not involve tariff bargaining.

Starting from the equilibrium with trade-war tariffs, we can again use the MPEC approach to compute cooperative tariffs given ψ. In this scenario, $\tau^0_{US,chn}$ and $\tau^0_{chn,US}$ are set to be the trade-war tariffs of the two countries observed in 2019. The corresponding vector of welfare change from imposing cooperative tariffs relative to the trade-war equilibrium is denoted by $\hat{U}^{co-war}(\psi)$. Using $\hat{U}^{co-19}(\psi) \equiv \hat{U}^{war} \times \hat{U}^{co-war}(\psi)$ to denote the vector of welfare change relative to the 2017 baseline, we define $\hat{U}^{co-19}_{US}(\psi)$ as the corresponding relative welfare change of the U.S. By comparing $\hat{U}^{co-19}_{US}(\psi)$ with $\hat{U}^{co-17}_{US}(\psi)$, we can quantitatively evaluate Katherine Tai's claim about using the Trump tariffs as bargaining chips: if $\hat{U}^{co-19}_{US}(\psi) > \hat{U}^{co-17}_{US}(\psi)$, then the trade war improves the U.S. welfare from the tariff negotiation with China relative to the negotiation outcome using 2017 as the starting point.

2.4.2 Post-negotiation equilibrium

Figure 2.2 displays the average cooperative tariff rates of the U.S. and China in both pre- and post-war tariff negotiations given different bargaining powers. The two dashed lines on the left panel represent the simple average of bilateral cooperative tariff rates between the U.S. and China if the tariff negotiation starts from the 2017 equilibrium. It can be observed that, irrespective of the U.S. bargaining power, the average cooperative tariff of the U.S. is always zero if the negotiation starts from the 2017 equilibrium. At the same time, the computed cooperative tariff for China is always positive, although the level of tariffs decreases as the bargaining power of the U.S. increases. At our estimated range of $\psi = [0.47, 0.70]$, the average cooperative tariff of China ranges from 5.60% to 3.91%. Even when we set $\psi = 1$ and the U.S. gains all of the bargaining power against China, the average of China's predicted cooperative tariff rates is still 1.76%.

The solid lines on the right panel of Figure 2.2 refer to the average of bilateral

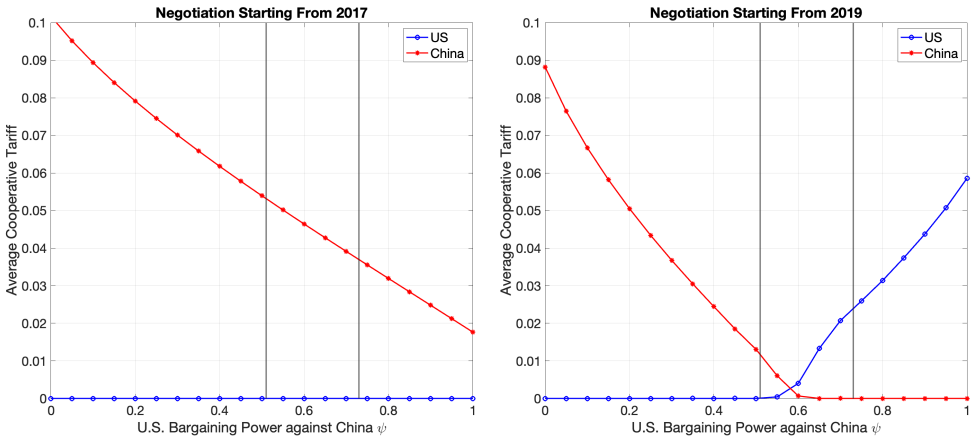

Figure 2.2: Average Post-Negotiation Tariffs for the U.S. and China

Note: This figure plots the simple average of post-negotiation tariffs across sectors for the U.S. and China. The left panel shows predicted tariffs when the negotiation starts from the 2017 baseline equilibrium, whereas the right panel shows predicted tariffs when the negotiation starts from the trade-war equilibrium. The two vertical lines indicate the lower bound (0.47) and upper bound (0.70) of the estimated bargaining power of the U.S. relative to China.

cooperative tariff rates for both countries if the tariff negotiation starts from the 2019 trade-war equilibrium. When $\psi < 0.6$, the U.S. cooperative tariff is zero and China's cooperative tariff is positive, just as with the negotiated tariffs starting from the 2017 equilibrium. However, when $\psi \geq 0.6$, the U.S. cooperative tariff becomes positive and that of China reaches zero. When $\psi = 0.47$, China's post-negotiation tariff rate is 1.61%, lower than 5.60% in the other scenario indicated by the red solid line. When $\psi = 0.70$, the average tariff rate for the U.S. is 2.07%.

Previous works on cooperative tariffs (Bagwell and Staiger 1999; Ossa 2011) have theorized that if political incentives are absent and governments simply use tariffs to maximize their own welfare, tariff negotiations will lead to an efficient equilibrium in which at least one country imposes zero tariffs.[11] The post-negotiation tariffs illustrated in Figure 2.2 are consistent with this theoretical prediction: the post-negotiation equilibrium always involves one country having zero tariffs, regardless of which tariff profile the negotiation starts from. However, previous theoretical studies cannot predict which of the two countries will impose zero tariffs. In fact, we can see from Figure 2.2 that the level of resulting cooperative

[11] In Section 2.5.4, we consider a setup that allows for negative tariffs or import subsidies. In this case, zero tariffs are no longer guaranteed in the cooperative equilibrium. However, the welfare outcomes discussed in the main text later still hold.

tariffs depends on both the bargaining power ψ and the pre-negotiation tariff profile $(\tau^0_{US,chn}, \tau^0_{chn,US})$.[12]

Comparing the cooperative tariffs in the two scenarios shown in Figure 2.2 also reflects the change in the U.S. bargaining position. Relative to the post-negotiation tariff starting from the 2017 equilibrium, the average U.S. post-negotiation tariff starting from the 2019 trade-war equilibrium is always equal or higher for any given ψ. Meanwhile, the average Chinese post-negotiation tariff starting from the 2019 trade-war equilibrium is always lower. This pattern can be explained by the improved bargaining position of the U.S. after the trade war. Prior to the trade war, the U.S. applied tariff rates are on average lower than the Chinese rates, as shown in Figure 2.1. Starting from this equilibrium, the U.S. does not have much room for mutual tariff reductions, and China is always able to impose positive tariffs in the post-negotiation equilibrium. However, the difference in pre-negotiation tariffs shrinks after the two countries raise tariffs amidst the trade war. Starting from the trade-war equilibrium, the U.S. has more room to reduce tariffs. China has to provide more tariff concessions in this case, which results in lower cooperative tariffs in the post-negotiation equilibrium.

2.4.3 Examining Katherine Tai's claim

It is worth noting that the improved bargaining position of the U.S. after the trade war does not automatically support Katherine Tai's claim about using the trade-war tariffs as bargaining chips. This is because in the second scenario, the U.S. needs to move from the 2017 equilibrium to the 2019 equilibrium in order to enjoy the improved bargaining position. If we simply compare $\hat{U}^{co-war}_{US}$ with $\hat{U}^{co-17}_{US}$, the U.S. welfare change in the trade war is excluded. In other words, the U.S. may enjoy a better bargaining position if the tariff negotiation starts from the trade-war equilibrium, but the cost of the trade war could be too large relative to the additional gain from the tariff negotiation. Therefore, we should compare $\hat{U}^{co-19}_{US}(\psi) \equiv \hat{U}^{war}_{US} \times \hat{U}^{co-war}_{US}(\psi)$ with $\hat{U}^{co-17}_{US}(\psi)$ when examining Katherine Tai's claim. In this way, the welfare change in both scenarios is relative to the 2017 baseline equilibrium.

[12]The role of initial tariff profile in trade policy cooperation has been emphasized by Ossa (2014) in the computation of world cooperative tariffs.

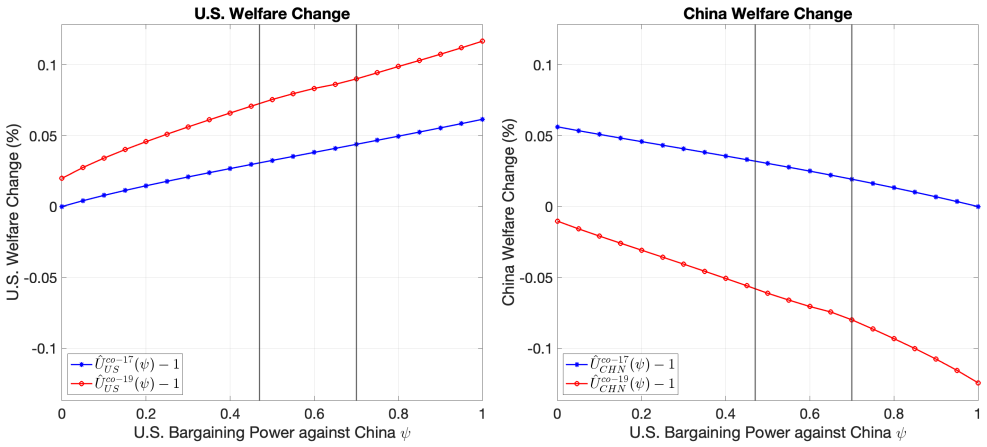

Figure 2.3: Post-Negotiation Welfare Change

Note: The blue lines refer to the welfare change of the tariff negotiation starting from the 2017 tariff profile. The red lines refer to the welfare change of the tariff negotiation starting from the 2019 tariff profile. The two vertical solid lines indicate the lower bound (0.47) and upper bound (0.70) of the estimated bargaining power of the U.S. relative to China.

Figure 2.3 illustrates the post-negotiation welfare change (relative to the 2017 baseline) of the two scenarios for the U.S. and China. In both panels, the blue lines represent $\hat{U}_{US}^{co-17}(\psi)$ and $\hat{U}_{chn}^{co-17}(\psi)$, the welfare change of the tariff negotiation starting from the 2017 equilibrium. The red lines represent $\hat{U}_{US}^{co-19}(\psi)$ and $\hat{U}_{chn}^{co-19}(\psi)$, the combined welfare change of the tariff negotiation starting from the trade-war equilibrium in 2019 and the welfare change from the 2017 baseline to the trade-war equilibrium. As expected, the U.S. post-negotiation welfare change is always increasing with the U.S. bargaining power ψ, and the opposite pattern is observed for China's post-negotiation welfare change.

One important result observed in Figure 2.3 is that, for any given ψ, it is always the case that $\hat{U}_{US}^{co-19}(\psi) > \hat{U}_{US}^{co-17}(\psi)$ and $\hat{U}_{chn}^{co-19}(\psi) < \hat{U}_{chn}^{co-17}(\psi)$. In other words, regardless of the relative bargaining power between the U.S. and China, the U.S. always enjoys greater welfare improvement by starting the tariff negotiation from the trade-war equilibrium. Given our estimated range of ψ, the difference in U.S. post-negotiation welfare improvement relative to the 2017 baseline is from 0.04% (when $\psi = 0.47$) to 0.05% (when $\psi = 0.70$). Meanwhile, China always experiences a smaller welfare improvement or even welfare loss when starting the negotiation from the trade-war equilibrium. For example, when $\psi = 0.70$, China enjoys a welfare improvement of 0.02% if the tariff negotiation starts from the 2017 baseline, but suffers a welfare loss of 0.08% by negotiating after engaging in the

trade war. In the second scenario, China incurs an overall welfare loss because the welfare improvement from the tariff negotiation $\hat{U}_{chn}^{co-war}(\psi)$ is not sufficient to cover the welfare loss from the trade war $\hat{U}_{chn}^{war}$.

We also observe the increasing welfare difference in the two scenarios for both the U.S. and China with larger U.S. bargaining power. Note that since $\hat{U}_{US}^{war}$ and $\hat{U}_{chn}^{war}$ do not depend on ψ, this pattern must be driven by the negotiation outcomes of the two scenarios. This is because the tariff negotiation starting from the 2017 baseline always results in zero U.S. cooperative tariffs due to the low U.S. tariff level prior to the negotiation. In this way, the potential welfare improvement from the tariff negotiation is constrained when ψ increases. By contrast, the room for mutual tariff reductions is greater when the tariff negotiation starts from the trade-war equilibrium. Consequently, the U.S. is able to reap more welfare improvement as ψ increases.

In sum, we compute the outcomes of potential tariff negotiations between the U.S. and China in two scenarios using the model constructed in Section 2.2. In the first scenario, the U.S. and China engage in Nash bargaining starting from the 2017 baseline equilibrium. In the second scenario, we first apply tariff changes observed during the trade war and then compute the cooperative tariffs starting from the trade-war equilibrium. Our simulation indicates that, regardless of the relative bargaining power between the U.S. and China, the U.S. always enjoys a larger welfare increase relative to the 2017 baseline in the second scenario. This result is consistent with Katherine Tai's claim that the tariffs on Chinese goods are a "significant piece of leverage".

2.5 Extensions

In this section, we complement the analysis in Section 2.4 with a few extensions. We first consider incorporating political incentives into the U.S. government's objective function in the tariff negotiation. Next, we show substantial heterogeneity in the changes to post-negotiation outcomes across U.S. states. We then discuss whether China can improve its post-negotiation outcomes by imposing a different set of retaliatory tariffs during the trade war. Lastly, we perform a series of checks to establish the robustness of our findings discussed in Section 2.4.

2.5.1 Political weights

Throughout the analysis presented in Section 2.4, we assume that the U.S. and China only care about welfare measured by real income in tariff negotiations. We now consider the possibility that each country's objective function incorporates political economy weights. In particular, the welfare in the Nash bargaining equation (2.8) now becomes

$$U^{pol} = \sum_{j=1}^{J} \sigma^j W^j, \tag{2.9}$$

where $W^j \equiv I^j/P$ is the welfare of sector j measured by real income, and $\sigma^j \geq 0$ is the political economy weight of sector j. Following Ossa (2014), we scale σ_j such that $\sum_{j=1}^{J} \sigma^j/J = 1$.[13]

The calibration of σ_j also closely follows the approach introduced in Ossa (2014). Specifically, we rely on a method of simulated moments to minimize the residual sum of squares between the model-predicted unilateral optimal tariffs and observed non-cooperative tariffs after controlling for their respective means. Since the trade-war tariffs between the U.S. and China are obviously non-cooperative and politically motivated, we use them as the matching targets in the calibration of political weights σ_j. The estimated political weights are reported in the last two columns of Table 2.1 where the highest three values of each country are highlighted by bold. We believe that these calibrated values are plausible: the three most favored sectors are textiles, machinery, and computer, electronic and electrical equipment in U.S., and food, beverage and tobacco, primary and fabricated metal, and petroleum in China. Similarly, Ossa (2014) also finds that textiles in the U.S. and beverage and tobacco products in China are the most protected sectors.

Figure 2.4 presents the corresponding welfare changes, and the results are similar to the situation without political weights. We can see that the mean message from Figure 2.3 still holds: regardless of the relative bargaining power between the U.S. and China, the U.S. always enjoys greater welfare improvement by starting the tariff negotiation from the trade-war equilibrium. We also re-calibrate the U.S. bargaining weight using the politically weighted objective function. The estimated range

[13] The equilibrium condition of U^{pol} in changes is reported in Section A.3 of the Appendix.

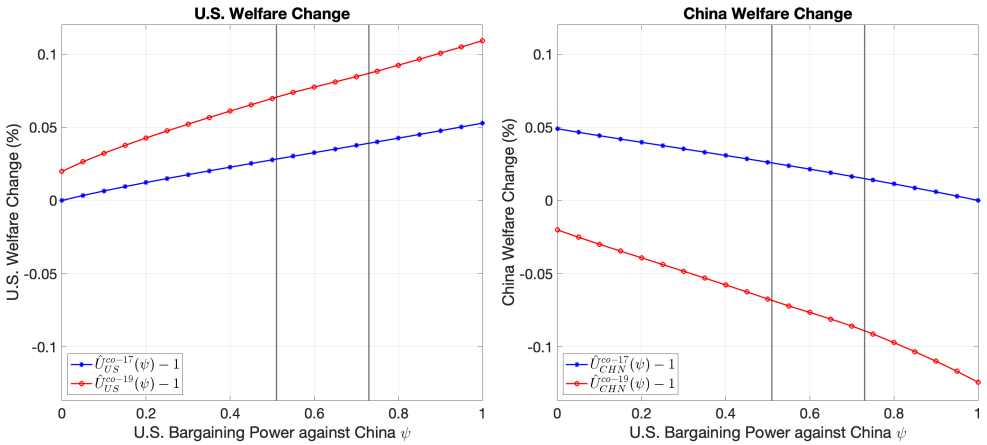

Figure 2.4: Post-Negotiation Welfare Change with Political Economy Weights

Note: The blue lines refer to the welfare change of the tariff negotiation starting from the 2017 tariff profile. The red lines refer to the welfare change of the tariff negotiation starting from the 2019 tariff profile. The two vertical solid lines indicate the lower bound (0.51) and upper bound (0.73) of the estimated bargaining power of the U.S. relative to China.

for ψ is $[0.51, 0.73]$, which is very close to the benchmark estimate. Given the new range of ψ, the difference in U.S. post-negotiation welfare improvement relative to the 2017 baseline is from 0.04% (when $\psi = 0.51$) to 0.05% (when $\psi = 0.73$).

2.5.2 Heterogeneity across U.S. regions

Since our model incorporates eight regions in the U.S. economy, we can analyze the heterogeneous impact of the U.S.–China tariff negotiation across regions. Because we assume free labor mobility within the U.S., the welfare level across U.S. regions is always equalized in equilibrium. For this reason, we use the population change to measure how the post-negotiation outcomes differ across regions. Figure 2.5 exhibits the change in population in different regions in the post-negotiation equilibrium when $\psi = 0.47$. Panel a depicts the outcomes of tariff negotiations from the 2017 baseline, whereas Panel b uses the trade-war equilibrium as the starting point. The colors for each region represent its population change relative to the 2017 baseline equilibrium.

From Figure 2.5, we can see that the spatial distribution of population changes in the two panels is very similar. Regardless of the starting point of the tariff negotiation, the Southwest Region (Arizona, New Mexico, Oklahoma, and Texas) always enjoys the largest labor inflow with a net labor influx of 1.38% and 1.30% in panel a and panel b, respectively. The New England region, on the contrary,

always suffers the largest labor outflow of 1.96% and 1.90% in the two scenarios, respectively. Overall, the negotiation starting from the 2017 baseline tariffs leads to slightly smaller change in the labor distribution than starting from the trade-war tariffs.

2.5.3 Can China do better?

Our results in Section 2.4 suggest that China's bargaining position deteriorated after the trade war. One natural question that follows is what could China have done to avoid this situation? To answer this question, we consider a counter-factual scenario in which China retaliates optimally during the trade war by maximizing its welfare. As shown in Figure 2.6, China's optimal retaliatory tariffs are in general higher than the observed tariffs with the exception of "Food, beverages and tobacco" and "Petroleum". This pattern is expected, as the higher tariffs on these two sectors probably aim to inflict a greater impact on Republican-leaning counties (Fajgelbaum et al. 2020).

Starting from the counter-factual equilibrium in which China retaliates optimally, we can simulate the tariff negotiation between the U.S. and China as in the main analysis. The green lines in Figure 2.7 show the welfare outcomes. We can see that, even when China retaliates optimally during the trade war, the U.S. post-negotiation welfare is only worse than negotiating from the 2017 baseline when $\psi \leq 0.10$. When $\psi \in [0.47, 0.70]$, the main results analyzed in Section 2.4 still hold. At the same time, China's post-negotiation welfare is still worse than ne-

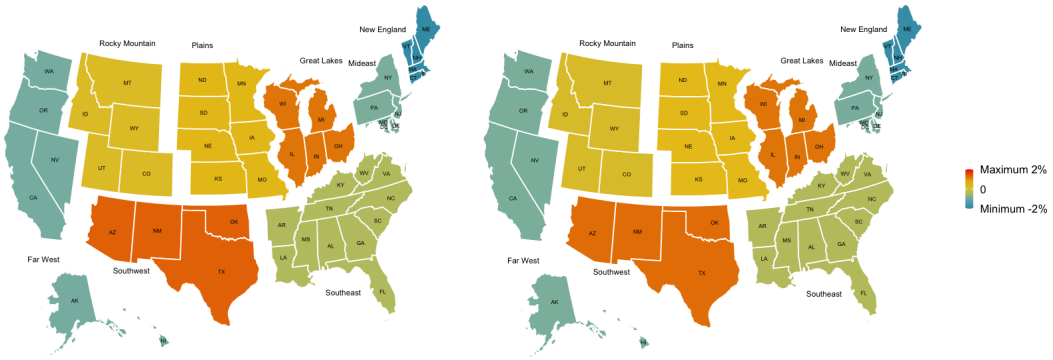

(a) Negotiation from 2017 Baseline **(b)** Negotiation from Trade War

Figure 2.5: Population Change across U.S. Regions

Note: For both panels, the population change of each region is relative to the 2017 baseline equilibrium.

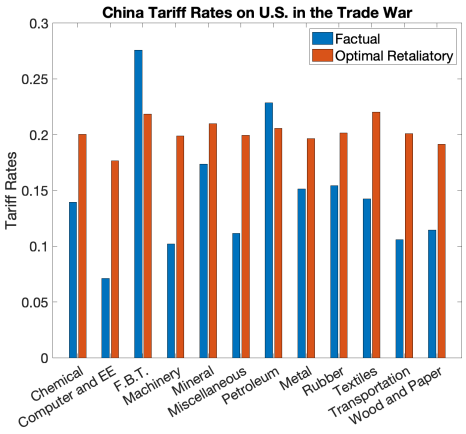

Figure 2.6: Optimal Retaliatory Tariffs from China

Note: The figure plots China's factual trade-war tariff rates and optimal retaliatory tariffs on the U.S. during the trade war. Sectors are arranged in alphabetical order.

gotiating from the 2017 baseline, regardless of the value of the bargaining power parameter ψ.

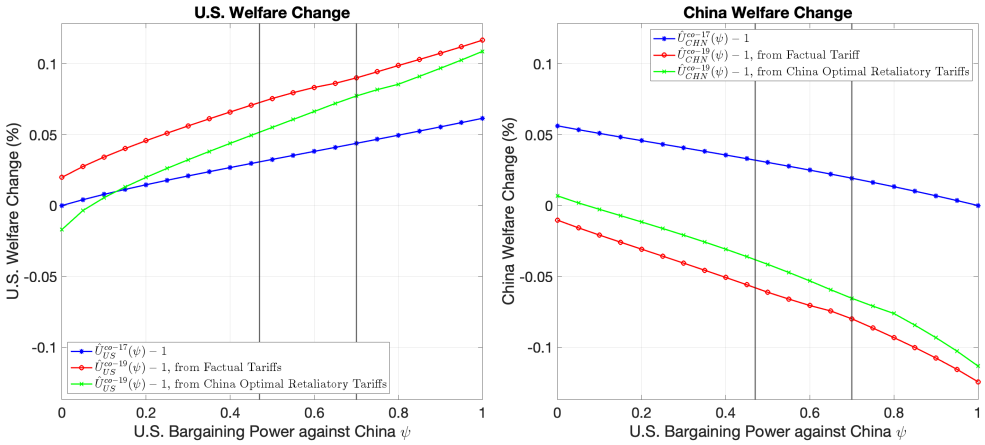

Figure 2.7: Post-Negotiation Welfare Change with Optimal Retaliatory Tariffs from China

Note: The blue lines refer to the welfare change of the tariff negotiation starting from the 2017 tariff profile. The red lines refer to the welfare change of the tariff negotiation starting from the 2019 factual trade-war tariff profile. The green lines refer to the welfare change of the tariff negotiation starting from China's optimal retaliatory tariffs. The two vertical lines indicate the lower bound (0.47) and upper bound (0.70) of the estimated bargaining power of the U.S. relative to China, respectively.

2.5.4 Robustness

Allowing for subsidies

In the baseline analysis in Section 2.4, we restrict the post-negotiation tariffs to be non-negative as in previous theoretical works. Figure B.3 displays the averages

of the predicted cooperative tariffs of the U.S. and China when we allow negative tariffs or import subsidies. When negative tariffs are allowed, it is no longer the case that at least one country imposes zero tariffs after the tariff negotiation. That being said, we can still infer from Figure B.3 that the U.S. bargaining position improves if the tariff negotiation starts from the trade-war equilibrium. Similar to the results in Ossa (2014), the restricted post-negotiation tariffs displayed in Figure 2.2 look like a truncated version of theunrestricted cooperative tariffs shown in Figure B.3.

Figure B.4 presents the corresponding welfare changes of the U.S. and China in the two negotiation scenarios. We can see that the welfare outcomes are very similar to the case without negative tariffs. Comparing this figure with Figure 2.3 reveals that allowing for negative tariffs makes very little difference from a welfare perspective.

ROW as fixed

In the main analysis, the applied tariff rates between the two countries and ROW change slightly from the 2017 baseline equilibrium to the trade-war equilibrium in 2019. To rule out the potential impact of this change, we now fix the U.S.–ROW and China–ROW bilateral tariffs at 2017 level and present the welfare outcomes in Figure B.5. In this way, the only exogenous changes from the 2017 baseline to the 2019 equilbrium are trade-war tariffs between the U.S. and China. The welfare outcomes displayed in Figure B.5 are very similar to those in Figure 2.3.

Fixed deficit

In the main analysis, we follow the approach of Ossa (2014) and treat the purged trade data without imbalances as the 2017 baseline. We also experiment with an alternative setup as a robustness check: instead of removing trade imbalances across countries, we now fix the international trade imbalances at the 2017 level when simulating the tariff negotiation from China. As can be seen in Figure B.6, the main welfare results from the main analysis in Section 2.4 still hold.

Elasticity of substitution from Caliendo and Parro (2015)

In the main analysis, we use the popular approach developed by Feenstra (1994) to estimate the elasticities of substitution. Caliendo and Parro (2015) estimate the same elasticities using the variation in tariffs and trade volumes before and after the North American Free Trade Agreement, and their estimates are on average larger than estimates using the Feenstra (1994) method. We repeat the simulation with the estimated elasticity of substitution from Caliendo and Parro (2015), and the corresponding welfare results are reported in Fig B.7. We can see that, for both countries, the welfare improvement from the tariff negotiation is greater than in Figure 2.3. A similar pattern is also observed in Ossa (2014) when computing the world cooperative tariffs with different elasticities of substitution. From Figure B.7, we still find that the U.S. always enjoys greater welfare improvement by starting the tariff negotiation from the trade-war equilibrium.

Estimation of bargaining power ψ

When we calibrate the U.S. bargaining weight ψ in Section 2.3, we assume that China is fully aware of the U.S. post-negotiation tariffs after China's accession to the WTO. We also estimate ψ without this assumption. That is, China and the U.S. simultaneously bargain over tariffs still using the same starting point as in Section 2.3.2. In this case, ψ is estimated by solving

$$\min_{\psi} \left[\left(\tau_{chn,US}(\psi) - \tau_{chn,US}^{2005} \right)' \left(\tau_{chn,US}(\psi) - \tau_{chn,US}^{2005} \right) + \left(\tau_{US,chn}(\psi) - \tau_{US,chn}^{2005} \right)' \left(\tau_{US,chn}(\psi) - \tau_{US,chn}^{2005} \right) \right].$$

When using 1997 applied tariffs as the threat point for the U.S., the estimated bargaining power of the U.S. relative to China is $\hat{\psi} = 0.03$. This result is consistent with the estimates in Bagwell et al. (2021), which also assume that both countries simultaneously bargain over tariffs. Focusing on the Uruguay Round of tariff bargaining, the estimated bargaining weights of the U.S. relative to the European Union, South Korea, and Japan are 0.01, 0.01, and 0.05, respectively. The small U.S. bargaining weight is again because of the negligible U.S. tariff changes after China's accession to the WTO. As argued in Bagwell et al. (2021), a country tends

to be assigned a smaller bargaining power in a bilateral bargaining pair if the tariffs of this country under negotiation are reduced to a greater degree than those of its negotiating partner. However, the very small estimate of U.S. bargaining power is inconsistent with the widely accepted perception that the U.S. had the upper hand in the bilateral negotiation with China.

In the main analysis, we provide the estimated upper and lower bounds of U.S. bargaining power ψ because the U.S. has two possible threat points in the WTO accession negotiation with China. Handley and Limão (2017) estimates a 0.13 probability of transition from China's temporary MFN status to "column 2" tariffs. Using this estimated probability, a back-of-envelop calculation generates an expected U.S. bargaining power of $\psi = 0.58$. However, we do not consider it to be the point estimate from our method of simulated moments because this back-of-envelop calculation may not be consistent with the solution of the Nash bargaining with two possible threat points.

2.6 Conclusion

This paper quantitatively analyzes the potential role of the Trump tariffs from 2018 through 2019 as bargaining chips for future trade negotiations with China. We develop a general equilibrium quantitative model that features both international trade and the U.S. economy disaggregated into eight regions and thirteen sectors. We find that, regardless of the relative bargaining power between the U.S. and China, the trade war always improves the U.S. post-negotiation welfare. We then estimate the bilateral bargaining power between the U.S. and China by examining China's accession to the WTO in 2001. The estimated U.S. bargaining power ranges from 0.47 to 0.70. With this estimated range, the trade war increases the U.S. post-negotiation welfare gain by 0.04%–0.05% relative to its pre-trade-war welfare level. Meanwhile, China's post-negotiation welfare change decreases 0.09%–0.10%. These results are consistent with U.S. Trade Representative Katherine Tai's claim that the Trump-era tariffs can be used as a leverage in future tariff negotiations with China.

By quantifying how the U.S.–China trade war affected the outcomes of tariff bargaining, this paper connects two separate but related fields in the literature. On

the one hand, previous works on cooperative tariffs have mostly focused on the reciprocal tariff reductions among WTO member countries. On the other hand, previous studies on the U.S.–China trade war have mostly emphasized the impact of higher tariffs on economic activities in the U.S. and China. By contrast, we consider the role of tariffs as bargaining chips, thereby providing the first quantitative study on the potential outcomes of negotiations between between the U.S. and China.

Chapter 3

(Trade) War and Peace: How to Impose International Trade Sanctions[1]

3.1 Introduction

Trade sanctions are a common instrument of diplomacy, with over 100 of them active in 2016. In the wake of Russia's invasion of Ukraine, trade sanctions have once again come into the public spotlight. Countries such as Canada, Japan, and the United Kingdom (UK) responded by imposing import tariffs on Russia, ranging from 8% to 35%. The Western countries jointly removed Russia's "Most Favored Nation (MFN)" status, enabling them to impose arbitrary tariffs against Russia without breaking World Trade Organization (WTO) regulations. Meanwhile, policymakers and politicians have advocated for an embargo on Russian oil and gas imports.

Ultimately, trade sanctions are meant to hurt the sanctioned country's economy. However, if they severely restrict trade, they also hurt the sanctioning countries.

[1]This is a joint work with Gustavo de Souza, Haishi Li and Yuan Mei. This paper benefited from valuable comments from Gadi Barlevy, Dominick Bartelme, Javier Bianchi, David DeRemer, Joakim Gullstrand, Thibault Fally, Gabriel Felbermayr, Justin Pierce, Marti Mestieri, Dávid Nagy, Bengt Söderlund, Robert Staiger, and Jing Zhang, as well as seminar participants at Aarhus University, Chicago Fed Brownbag, Kiel Institute, Lund University, University of Luxembourg, and WIFO. The views expressed herein are solely those of the authors and do not necessarily reflect the views of the Federal Reserve Bank of Chicago or the Federal Reserve System. All remaining errors are ours.

This trade-off raises the question: What is the most cost-efficient way to apply trade sanctions? How can a government reduce economic activity in the sanctioned country while minimizing local economic costs? When is an embargo cost-efficient?

We answer these questions using a quantitative model and empirical evidence. We build a model of tariff competition with international trade and input-output connections.[1] In the model, firms produce using labor, locally produced inputs, and inputs from other countries. To import inputs, firms have to pay an import tariff.

Tariffs are chosen by governments trading off two objectives. On the one hand, they want to maximize domestic real income, which is also a measure of household welfare. On the other hand, they want to minimize Russian welfare. If the government has a high willingness to pay for sanctions, it places a greater weight on hurting the Russian economy. As the government is trading off the cost of sanctioning Russia and its own welfare, we refer to these sanctions as cost-efficient sanctions.[2]

To construct reliable counterfactuals, we estimate the model to reproduce the effect of tariffs on Russia's international trade. Using the difference-in-differences estimation strategy introduced in de Souza and Li (2021), we find that a 10% ad-valorem tariff on Russia decreases imports of Russian products by 43% and total imports of the taxed goods by 15%, showing that both Russia and the sanctioning countries are negatively affected by tariffs. Using the method of de Souza and Li (2021) and tariff variation from all countries, we estimate sectoral trade elasticities to be 6 on average. These elasticities correlate with estimates by Caliendo and Parro (2015) and those that we recover using the Feenstra (1994) method.

We highlight five main findings. First, we show that for countries with low willingness to pay for sanctions, the best policy is to impose a small and similar tariff across all products. For instance, if the sanctioning countries are willing to pay US$0.10 for every US$1 of economic damage in Russia, import tariffs should

[1] The model builds on Ossa (2014) and Caliendo and Parro (2015).

[2] In practice, sanctions can take various forms, such as limiting the movement of capital, goods, or people between countries. To narrow down the scope of the problem, we focus on a specific type of trade sanctions: import tariffs, which also include embargoes as a special case. Due to the Lerner Symmetry (Lerner 1936; Costinot and Werning 2019), sanctions in the form of import tariffs are equivalent to export sanctions and there will be infinite combinations of optimal import and export tariffs resulting in the same welfare outcome when researchers simultaneously address both. Additionally, in the case of Russia, several countries, including the UK, Canada, Japan, United States (US), and the European Union (EU), have implemented sanctions in the form of import tariffs, making it the most relevant type of sanction for policy evaluation.

average 20%.[3]

Second, if the EU is willing to pay over US$0.70 for each US$1 of real income loss in Russia, an EU embargo on the mining and energy sectors with a 50% tariff on other sectors is cost-efficient.[4] For countries with high willingness to pay for sanctions, the main driver of cost-efficient tariffs is the import share; to cause more harm to Russia, sanctioning countries should target what Russia exports the most, i.e., mining and energy products.

Third, we show that the EU is the group of countries that can hurt the Russian economy the most – not the US or other sanctioning allies (OSA). Russia exports more to the EU than to the US or OSA.[5] Accordingly, tariffs imposed by the US or OSA can, at most, reduce Russian real income by only 0.07% or 0.22%, respectively. By contrast, the EU alone can reduce real income in Russia by as much as 0.8%. Therefore, the burden of trade sanctions against Russia has to be carried by the EU.

Fourth, if Russia retaliates, i.e., if it also chooses to impose tariffs to punish the sanctioning countries, the economic consequences of tariff sanctions against Russia would be more than double. Because the EU is an important importing origin for Russia but Russia is not an important exporting destination for the EU, Russia cannot decrease EU welfare by much through the imposition of high tariffs on the EU, but these tariffs cause a large decline in Russia's own welfare.

Finally, we show that if sanctions target sectors with larger political relevance in Russia, an embargo on Russian mining and energy sectors is cost-efficient even for countries with a low willingness to pay for sanctions. To calculate political relevance, we link each Russian individual sanctioned by the US, UK, or EU, whom

[3]For nations focused solely on maximizing their own welfare, there are two forces influencing their choice of tariffs. On one hand, governments impose high tariffs on sectors with low trade elasticity, i.e., on products for which trade flows are less affected by tariffs. On the other hand, they also impose high tariffs on products with lower import shares from Russia to minimize the impact on their domestic economy. Conversely, for nations whose primary objective is to punish their opponent, their governments would prefer to impose high tariffs on sectors with high trade elasticity to divert more trade away from Russia and on sectors with substantial import shares to reduce Russia's income further. For nations with a low willingness to pay for sanctions, these two motives counterbalance each other, resulting in similar tariffs across various sectors.

[4]The mining and energy sectors include the extraction of crude oil, natural gas, and other energy products (D05 and D06 in International Standard Industrial Classification (ISIC) Rev. 4) and the coke and refined petroleum sector (D19 in ISIC Rev. 4).

[5]More specifically, Russia's exports to the EU represent 4.85% of the country's total production; its exports to the US represent 0.55%; and its exports to the OSA represent 1.63%.

we call an oligarch, to the companies associated with that individual in Russia. Using the company's revenue, we calculate the revenue share of oligarch-owned companies by sector. If the sanctioning countries are willing to pay US$0.10 for each US$1 of consumption drop in Russian oligarch income, tariffs on the Russian mining and energy sectors should be above 80%, which would cause imports of mining and energy products to drop by almost 100%. Therefore, if the goal of sanctions is to target politically influential sectors, an embargo the optimal policy, even for nations with low willingness to pay for sanctions.

To confirm the robustness of our main findings, we test various calibration strategies and model assumptions. First, we examine if our results hold under alternative trade elasticity calibrations. We find that using the trade elasticity estimated by Caliendo and Parro (2015) or our estimates of the long-run trade elasticity does not qualitatively change the results. Second, we show that our results remain unchanged when we use alternative functional forms of the production function. Even when we use a constant elasticity of substitution (CES) production function with low elasticity of substitution across inputs or the elasticity of substitution estimated by de Souza and Li (2021), the results are qualitatively the same. In addition, assuming a very low elasticity of substitution across inputs, which is closer to a Leontief than empirically plausible, still delivers the same cost-efficient sanction patterns. Third, our results are not affected by the retaliation strategies implemented by Russia. Therefore, after this battery of tests, we conclude that our findings are robust and remain consistent under alternative calibration and modeling choices.

This paper contributes to the literature on tariff competition by studying the problem of a government trading-off welfare maximization and diplomatic objectives. The tariff competition literature has investigated optimal trade policy in different settings when countries maximize their own welfare. These settings include tariff cooperation (Ossa 2014), competition on non-tariff trade barriers (Mei 2021), MFN rules (Bagwell et al. 2021), export subsidies (Beshkar and Lashkaripour 2020), market access concessions (Beshkar et al. 2022), deep trade agreements (Lashkaripour and Lugovskyy 2023), and industrial policies (Bartelme et al. 2021). These studies have found that tariffs should be larger on sectors with lower trade elasticities and

that there are welfare gains from cooperation.[6]

We contribute to existing literature by examining countries' trade-offs between sanctions and welfare-maximizing trade policy, enabling us to calculate cost-efficient trade sanctions and contribute to policy debates. Unlike previous research on tariff competition, trade elasticity is not a crucial determinant of cost-efficient sanctions. As countries prioritize harming the Russian economy, optimal tariffs should increase in sectors with larger trade flows. If the willingness to pay exceeds US$0.70 for each US$1 drop in Russian welfare, tariffs should target major Russian export sectors irrespective of their trade elasticities.

Our work contributes to the literature on the economic impacts of sanctions. Sanctions and sanction threats are more effective if they impose more harm on the target and if the sender is more patient (Eaton and Engers 1992; Lacy and Niou 2004; Whang et al. 2013). Furthermore, sanctions should optimally trade off between the punishment of the target's leader and the negative impact on the general public (Baliga and Sjöström 2022). Empirical works have shown that the number of sanctions has risen over time(Elliott and Hufbauer 1999; Felbermayr et al. 2020a, 2021; van Bergeijk 2022). In the target country, sanctions exacerbate regional inequality (Lee 2018), induce firm exit (Ahn and Ludema 2020; Crozet et al. 2021), and lower stock market valuation (Draca et al. ming). In the sender country, sanctions also negatively impact firm business (Felbermayr et al. 2020b; Gullstrand 2020; Besedeš et al. 2021). Furthermore, sanctions disrupt international trade (Crozet and Hinz 2020; Miromanova 2021a,b; Kwon et al. 2022).

A few works have studied the impact of sanctions against Russia in response to its recent aggression in Ukraine, including how such sanctions have affected the ruble exchange rate (Lorenzoni and Werning 2022; Itskhoki and Mukhin 2022), the welfare implications of Western countries increasing the imposition of tariffs and non-tariff trade barriers on Russia (Evenett and Muendler 2022a,b), the consequences of banning Russian oil imports (Bachmann et al. 2022), and the effects on Russia's consumer prices of Russian retaliation in the form of import restrictions

[6]Another strand of this literature has developed theories on punitive tariffs. Punitive tariffs can sustain a cooperative equilibrium (Dixit and Bewley 1987) and thus lead to welfare gains (Mei 2020), should be higher when trade volume surges (Bagwell and Staiger 1990) and in small countries (Park 2000), can be more effective when implemented in a multilateral framework (Maggi 1999; Klimenko et al. 2008), and are easier to enforce than monetary fines (Limao and Saggi 2008).

(Hinz and Monastyrenko 2022). Sturm (2022) shows that the sanctioning countries can hurt the Russian economy while increasing their own welfare. Sturm (2023) and Sonali Chowdhry and Wanner (2022) study the effect of coalitions on the effectiveness of sanctions.

We contribute to the literature on the economic impacts of sanctions by estimating cost-efficient trade sanctions and their economic impact. To the best of our knowledge, this is the first paper to study optimal economic sanctions in a quantitative trade framework. As such, we differ from Eaton and Engers (1992), Lacy and Niou (2004), Whang et al. (2013), and Baliga and Sjöström (2022), taking the motivation for sanctions as a given and computing the set of tariffs that hurt the targeted country the most and cost the sanctioning countries the least. Inspired by Baliga and Sjöström (2022), we also calculate cost-efficient sanctions when the sanctioning countries target politically relevant sectors.

The rest of the paper proceeds as follows. In Section 3.2, we present empirical evidence on how a large increase in tariffs can disrupt international trade with Russia. In Section 3.3, we present the model and the governments' problems. In Section 3.4, we calibrate the model. In particular, we introduce the sectoral trade elasticities to our empirical estimates. In Section 3.5, we show our findings based on model simulations. In Section 3.6, we conclude.

3.2 Empirics

We take advantage of the difference-in-differences strategy introduced by de Souza and Li (2021) to investigate how an increase in tariffs disrupts trade with Russia. We compare Russian products which had an anti-dumping investigation that did not led to a tariff increase, the control group, to products which had an anti-dumping investigation that concluded with a tariff increase, the treatment group. According to WTO regulation, the decision to impose an anti-dumping tariff should be based on pre-determined characteristics of each product. Because of these characteristics are constant overtime, they can be teased out with a product level fixed effect.

This section is organized as follows. First, we discuss institutional details of anti-dumping tariff, which we will exploit to identify the causal effect of tariffs against Russia. Then we discuss the data and a series of validation exercises. Fi-

nally, we show our main specification and results. Section 3.2.3 discuss the main take-aways from the empirical section and Section 3.2.4 estimates sector level trade elasticities which will be used to calibrate the model.

3.2.1 Institutions

Dumping refers to an act of price discrimination in which an exporter charges a lower price in the destination market than in its home market adjusted for allowances, trade costs, and currencies in different markets.[7] The WTO allows the destination government to impose AD tariffs to correct for such price differences, but requires that they must follow certain procedures.[8] First, a sufficient number of firms in a domestic industry should submit a written request to the government. The request should provide evidence that import competition is doing harm to the domestic industry. It should also show that the foreign exporters are engaging in dumping. Second, upon receipt of the request, the government should establish a committee to investigate the case. Third, using the evidence collected during the investigation and following WTO rules, the committee calculates the normal value of the foreign product and the export price. If the committee finds that the foreign exporter is indeed charging a lower price in the export destination that in its home market, the government will conclude that the foreign exporter is dumping, and it will impose an AD tariff equal to the price difference.[9] If the committee finds otherwise, no AD tariff will be introduced. The committee should reassess the AD duty no later than five years after its imposition, occasionally resulting in the termination of the AD tariff.

Data

Our data source for AD investigations is the Global Anti-dumping Database (Bown 2005). The database contains all AD investigations conducted by 31 ma-

[7] Experts refer to the home market price, inclusive of these adjustments, as the "normal value". See Section "Fair comparison of normal value and export price" of WTO's technical note on AD (https://www.wto.org/english/tratop_e/adp_e/adp_info_e.htm).

[8] See WTO's AD rule (https://www.wto.org/english/docs_e/legal_e/19-adp_01_e.htm).

[9] Some investigations ended with the foreign exporter raising their price to avoid an AD tariff. See WTO Agreements on AD, subsidies, safeguards: contingencies, etc. (https://www.wto.org/english/thewto_e/whatis_e/tif_e/agrm8_e.htm) These observations are dropped from both the treatment and control groups.

jor economies on all trade partners. For each investigation, the database covers the investigated product and its Harmonized System (HS) code, the exporter and importer, the beginning and end dates of each investigation, and the measures taken. Our data source for international trade is the United Nations Comtrade Database, acquired through the BACI Database of CEPII (Gaulier and Zignago 2010). We merge the two datasets on the country–bilateral and HS 6-digit level.

In the Appendix, Table C.1 shows the summary statistics for AD investigations targeting Russia.[10] During the sample period (1995–2020), Russia faced 393 AD investigations, of which 298 (75%) concluded with an affirmative ruling. Figure C.1a shows the number of AD investigations and affirmative investigations by year. Figure C.1b shows the average tariff rate by sector conditional on an affirmative ruling. Table C.2 shows the summary statistics, by country, of the AD investigations targeting Russia. The US conducted the most AD investigations targeting Russia.

Table C.3 shows the summary statistics for AD investigations imposed by all countries on their trade partners. During the sample period, there was a total of 15,131 AD investigations, of which 10,370 (68%) concluded with an affirmative ruling. Figure C.2a shows the number of global AD investigations and affirmative investigations by year. Figure C.2b shows, at the world level, the average tariff rate by sector conditional on an affirmative ruling. Tables C.4 and C.5 show the summary statistics for global AD investigations by the investigating country and exporting country.

Discussion

Based on the WTO AD rules, two important lessons can be learned about how one should identify the impact of AD tariffs. First, one should not compare the products that are subject to an AD tariff to those that are not. To initiate the imposition of an AD tariff, an investigation committee has to be formed. As Staiger and Wolak (1994), Prusa (2001), Lu et al. (2013), and Besedeš and Prusa (2017), among others, have shown, these investigations can create trade policy uncertainty and disrupt trade even if the investigations do not conclude with tariff changes. Furthermore, as de Souza and Li (2021) show, the investigated products have a lower price, higher

[10] We discuss these summary statistics in further detail in Appendix Section A.1.

trade volume, decreasing price price trend, and increasing trade volume trend, compared to the products that are not investigated. Both the trade policy uncertainty and different trends can be confounding factors when comparing the tariffed products to the non-tariffed products without controlling for AD investigations. Therefore, the sample is composed of only the investigated products.

Second, conditional on an AD investigation, the WTO rules stipulate that whether a tariff should be imposed and, if so, the size of the tariff should depend on the difference in the prices set by the foreign exporter in the origin and destination countries in the pre-investigation period. We can use the product–country fixed effects to control for such a difference. Once we do so, the AD tariff should be exogenous to the potential trends of the treatment and control groups. To test that countries indeed follow the WTO rules, we employ an event study design showing parallel trends between the two groups before the treatment. In de Souza and Li (2021), we supplement it with additional evidence: (1) The AD tariff can be predicted by the exporting country's price that it charges and the AD tariff that it faces on the same product in a third country with a high R-squared. (2) The AD policy applied for a sector does not correlate with the sector's other benefits from the government, including political connections, public procurement, subsidies, and tax breaks. (3) Placebo tests show that if we replace the real treatment group with one that has similar trends or if we move the treatment time five years earlier, we do not identify any effect of AD tariffs.

3.2.2 Empirical Strategy

Impact of Import Restrictions on Russian Trade

Following de Souza and Li (2021), we study the impact of AD tariffs on Russian trade using:

$$\log(y_{p,c,t}) = \theta\tau_{p,c,t} + \beta\mathbb{I}_{p,c,t}\{\text{After AD}\} + \gamma\mathbb{N}_{p,c,t}\{\text{Committee}\} + \eta_{p,c} + \eta_{c,t} + \varepsilon_{p,c,t}, \tag{3.1}$$

where $y_{p,c,t}$ is imports of product p by country c from Russia in year t;[11] $\tau_{p,c,t}$ denotes the AD tariff that country c imposes on product p from Russia in year t

[11] A product refers to a Harmonized System (HS) 6-digit code.

(this variable equals zero for the control group); $\mathbb{I}_{p,c,t}\{\text{After AD}\}$ is a dummy after the beginning of the first AD investigation (it captures common trends between treatment and control leading to the investigation). The controls include the number of AD investigations conducted by country c on product p from Russia in year t, $\mathbb{N}_{p,c,t}\{\text{Committee}\}$, product–country fixed effect, $\eta_{p,c}$, and country–year fixed effect, $\eta_{c,t}$.[12] The sample consists of product–country pairs that have at least one AD investigation.

Our variable of interest is θ, which captures the average effect of AD tariffs on trade. As it is common in difference-in-differences, the identifying assumption is of parallel trends between treatment and control groups. To show supportive evidence for this assumption, we test for the existence of parallel trends (prior to the beginning of the investigation) using:

$$\log(y_{p,c,t}) = \sum_{u=-5}^{5} \theta_u \tau_{p,c,\text{first}} \mathbb{I}_{p,c,t}\{u \text{ Yrs. to AD}\} + \sum_{u=-5}^{5} \beta_u \mathbb{I}_{p,c,t}\{u \text{ Yrs. to AD}\} + \gamma \mathbb{N}_{p,c,t}\{\text{Committee}\} + \eta_{p,c} + \eta_{c,t} + \varepsilon_{p,c,t}, \tag{3.2}$$

where $y_{p,c,t}$ refers to imports of product p by country c from Russia in year t, and where $\tau_{p,c,\text{first}}$ denotes the first AD tariff that country c imposed on product p from Russia.[13] Moreover, in this equation, the dummy variable $\mathbb{I}_{p,c,t}\{u \text{ Yrs. to AD}\}$ takes 1 if year t is u years to the beginning of the first AD investigation; $\mathbb{N}_{p,c,t}\{\text{Committee}\}$ denotes the number of AD investigations conducted by country c on product p from Russia in year t; and $\eta_{p,c}$ and $\eta_{c,t}$ are the country–product fixed effects and country–year fixed effects, respectively.

We are interested in the coefficient θ_u, which captures the dynamic effect of AD tariffs in the uth year. Having no pre-trend is equivalent to $\theta_u = 0, \forall u < 0$.

3.2.3 Results

Figure 3.1 shows how AD tariffs against Russia affect a country's imports from Russia. AD tariffs cause a significant large drop in imports: A 10% increase in AD tariffs is associated with a nearly 40% decline in imports of the targeted products.

[12] We use the number of AD investigations to control the impact of trade policy uncertainties caused by such investigations and the formations of investigation committees.

[13] In this way, we ensure that there is no other investigation in the pre-period.

The figure also confirms the nonexistence of a pre-trend; that is, before the increase in tariffs, the treatment and control groups display similar import trends.

Figure 3.1: Impact of AD Tariffs on Imports

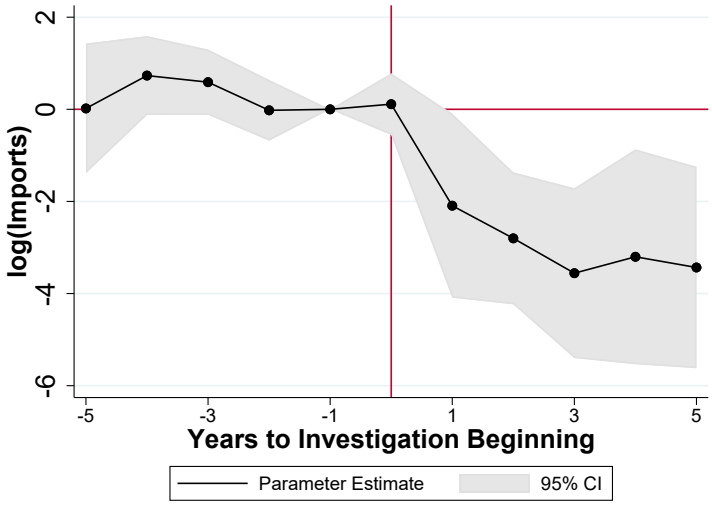

Description: This figure shows the dynamic impact of AD tariffs on imports using Model 3.2. The impact on yearly imports is plotted on the y-axis. The number of years to the beginning of the investigation is plotted on the x-axis. We study HS 6-digit level imports. Imports are measured in free on board (FOB), current dollar value terms. The import data are from the United Nations Comtrade Database, acquired through the BACI Database of CEPII (Gaulier and Zignago 2010). The AD data are from the Global Antidumping Database (Bown 2005). The sample runs from 1995 to 2020. The sample includes the product–origins that faced at least one AD investigation. The shaded area contains the 95% confidence interval. Standard errors are clustered at the product–country level.

In the Appendix, Figure C.3 shows the impact of AD tariffs on the quantity, pre-, and post-tariff price of the targeted product imported from Russia. Similar to the value of imports, AD tariffs significantly reduce the quantity of imports from Russia. Figure C.3a shows that, five years from the beginning of an AD investigation, a 10% increase in AD tariffs leads to about a 30% drop in the quantity of imports from Russia. Figure C.3b shows that it takes longer for the pre-tariff import price to respond to AD tariffs. A 10% increase in AD tariffs leads to about a 5% drop in pre-tariff import price, subsequently leading to a 5% increase in post-tariff import price (Figure C.3c). This suggests that Russian exporters have to lower prices to remain competitive, and there is about a 50% pass-through of AD tariffs to consumers in the destination country in year 5.

AD tariffs significantly reduce total exports (to all destinations) of the targeted Russian product, as shown in Figure 3.2a.[14] A 10% increase in tariffs leads to about a 15% decline in total exports five years after the AD investigation. This indicates

[14]Figure 3.2a is generated by estimating Equation 3.2, where the dependent variable represents Russia's total exports of product p and varies at the product-year level: $y_{p,t}$.

that the decline in Russian exports of a product to the destination that imposes import restrictions dominates the potential increase in Russian exports of the same product to other destinations. Indeed, Column 1 of Table C.8 shows that Russia can only weakly divert exports to other destinations.[15] These findings suggest that import sanctions by other countries on Russia will likely reduce Russian output and income, a hypothesis we build on in Section 3.3.

Similarly, Figure 3.2b shows that AD tariffs significantly reduce total imports (from all origins) of the targeted product to the country that imposes the import restriction: A 10% increase in tariffs leads to about a 20% decline in that country's total imports in the fifth year from the beginning of the AD investigation.[16] This demonstrates that the decline in imports of the targeted product from Russia dominates the potential increase in imports of the same product from other origins. This is further confirmed by Column 2 of Table C.8, the results of which show that AD tariffs also only weakly divert the sanctioning country's imports to other origins.[17] These findings suggest that import sanctions by other countries on Russia will likely also reduce the sanctioning country's consumption and income, a hypothesis we evaluate in Section 3.3.

Using variation from all AD tariffs imposed on Russia, we show in Table 3.1 that tariffs on Russia decrease imports, pre-tariff prices, and total exports of Russian products. A 10% increase in tariffs causes a 43% drop in imports of the targeted product from Russia (Column 1), with a 36% drop in quantity imported (Column 2) and a 7% drop in the price of imports (Column 3). Column 4 suggests that, in an average year after the tariff is imposed, 30% of the tariff is passed through to domestic consumers. Columns 5 and 6 show that a 10% increase in tariffs reduces total Russian exports of the targeted product by 16% and total imports of the targeted product by the tariffing country by 19%.

[15] This result is consistent with de Souza and Li (2021), who also find an insignificant trade diversion effect of the AD tariffs that the Brazilian government imposes on other countries.

[16] Figure 3.2b is generated by estimating Equation 3.2, where the dependent variable represents the sanctioning country c's total imports of product p and varies at the importing country-product-year level.

[17] Column 3 of C.8 also shows that tariffs do not significantly divert an importer's demand towards other Russian products within the same 4-digit product group.

Robustness: Alternative Specifications Tables C.9, C.10, and C.11 show that the effects of tariffs on imports from Russia, Russian total exports, and total imports are robust across various alternative specifications. Column 1 of these tables presents the baseline estimates. Column 2 clusters standard errors at the 4-digit product and importer level. Column 3 employs a dummy variable indicating whether an investigation committee is formed (as opposed to the number of committees) to control the impact of AD investigations. Column 4 includes separate product, importer, and year fixed effects. Column 5, building upon the baseline, further incorporates 4-digit product-time fixed effects. Column 6 of Tables C.9 and C.11 controls product-time fixed effects.[18] Column 7 of Tables C.9 and C.11 and Column 6 of Table C.10 apply the Poisson Pseudo Maximum Likelihood (PPML) estimator (Silva and Tenreyro 2006). Column 8 of Tables C.9 and C.11 estimates the PPML model with product-year fixed effects. Column 9 of Tables C.9 and C.11 and Column 7 of Table C.10 utilize the inverse hyperbolic sine of trade value as the outcome variable.[19]

Discussion Tariffs against Russia decrease the total imports of the taxed good and exports by Russia. This result implies that sanctions against Russia have two implications: one for domestic welfare and the other for Russian welfare.

First, the empirical results suggest that trade sanctions decrease domestic welfare. Because Russian products cannot be easily replaced, the domestic economy has to pay higher prices to either produce the product locally or import it from another country. Therefore, due to higher prices, domestic real income goes down.

Second, the empirical results also suggest that trade sanctions can decrease Russian welfare. Because Russia decreases its total exports of the tariffed good, it must be the case that it cannot supply it easily to other countries. The decrease in total Russian demand leads to a drop in income, output, and prices in Russia.

[18]The product-time fixed effects capture all variations in Russia's product-level total exports, so the result with product-time fixed effects is not reported in Table C.10. Additionally, it is important to note that the number of observations decreases substantially in Column 6 of Tables C.9 and C.11 when product-time fixed effects are included. Once these fixed effects are controlled for, the estimation of the tariff coefficient relies on variations across investigating countries. However, Figure C.4 indicates that approximately 80% of investigations against Russia are conducted by a unique country, leading to the exclusion of these observations when product-time fixed effects are considered. Furthermore, at most two countries investigate the same product from Russia in the same year.

[19]See Bellemare and Wichman (2020). The inverse hyperbolic sine of $y_{p,c,t}$ can be expressed as: $\text{Arsinh}(y_{p,c,t}) = \log(y_{p,c,t} + (y_{p,c,t}+1)^{1/2})$. This transformation offers an alternative method for estimating elasticities when the dependent variable contains zeros or small values.

Figure 3.2: Impact of AD Tariffs on Product-level Total Exports and Total Imports

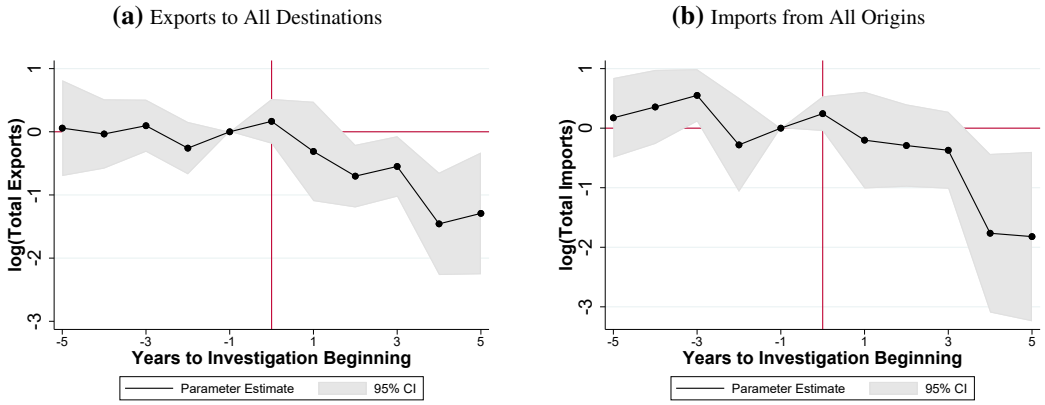

Description: This figure shows the dynamic impact of AD tariffs on total exports and total imports using Model 3.2. The impact on total imports and total exports is plotted on the y-axis. The number of years to the beginning of the investigation is plotted on the x-axis. Total exports refer to the total exports of the HS 6-digit level product by Russia to all destinations; these exports are of the same the same 6-digit product for which other countries initiated an AD investigation targeting Russia. Total imports refers to the imports of the HS 6-digit level product from all origins by the country that initiated an AD investigation targeting Russia; these imports are of the same 6-digit product on which the AD tariff has been imposed. The import data are from the United Nations Comtrade Database, acquired through the BACI Database of CEPII (Gaulier and Zignago 2010). The AD data are from the Global Antidumping Database (Bown 2005). The sample runs from 1995 to 2020. The sample includes the product–origins that faced at least one AD investigation. The shaded area contains the 95% confidence interval. Standard errors are clustered at the product–country level.

Therefore, the empirical results indicate that if countries want to sanction Russia, they will incur economic losses. Given the degree of willingness to pay for sanctions, how should countries impose tariffs to maximize their own welfare and punish Russia? To answer this question, we build a model of international sanctions with input-output connection. The model is described in Section 3.3.

Table 3.1: Effect of AD Tariffs on Russian Trade

	(1)	(2)	(3)	(4)	(5)	(6)
VARIABLES	Log Value	Log Quantity	Log Price	Log Post-tariff Price	Log Total Exports	Log Total Imports
AD Tariff	-4.306**	-3.605*	-0.701***	0.299	-1.577**	-1.867**
	(1.895)	(1.929)	(0.210)	(0.210)	(0.726)	(0.743)
Observations	1,534	1,534	1,534	1,534	1,534	1,534
R-squared	0.807	0.813	0.873	0.875	0.804	0.839
Fixed Effects	Product X Importer, Importer X Year, Number of AD committees, After AD investigation					
Cluster	Product X Importer					
Robust standard errors in parentheses						
*** p<0.01, ** p<0.05, * p<0.1						

Description: This table presents the impact of AD tariffs that other countries imposed on Russia on Russian trade, estimated with Model 3.1. *Log Value* denotes the log of HS 6-digit level FOB current dollar value imports from Russia. *Log Quantity* denotes the log of the quantity (in metric tons) imported by another country from Russia on the HS 6-digit level. *Log Price* and *Log Post-tariff Price* denote the log of pre- and post-tariff import price (measured with value per metric ton) by another country from Russia on HS 6-digit level. *Log Total Exports* denotes the log of HS 6-digit level total export value by Russia to all destinations for the same HS 6-digit product for which other countries initiated an AD investigation targeting Russia. *Log Total Imports* denotes the log of HS 6-digit level total imports from all origins by the country on which initiated an AD investigation targeting Russia for the same 6-digit product that the AD tariff is imposed. The import data are from the United Nations Comtrade Database, acquired through the BACI Database of CEPII (Gaulier and Zignago 2010). The AD data are from the Global Antidumping Database (Bown 2005). The sample runs from 1995 to 2020.

3.2.4 Estimation of Sector-level Trade Elasticity

We take advantage of the AD tariffs that all countries impose on all their trade partners to identify the trade elasticity at the sector level and in the short and long run. We estimate trade elasticity for each goods sector listed in the 2018 OECD Inter-country Input-Output Database (OECD ICIO 2018).[20] To this end, we use a specification similar to Equation 3.1:

$$\log(y_{p,d,o,t}) = \sum_{j=1}^{J} \theta^j \mathbf{1}(p \in j)\tau_{p,d,o,t} + \beta \mathbb{I}_{p,d,o,t}\{\text{After AD}\} + \gamma \mathbb{N}_{p,d,o,t}\{\text{Committee}\}$$
$$+ \eta_{p,t} + \eta_{p,d} + \eta_{p,o} + \eta_{d,t} + \eta_{o,t} + \varepsilon_{p,d,o,t}. \tag{3.3}$$

To identify all fixed effects and sectoral trade elasticities, we examine a pooled regression that includes all investigated products (p), all destinations (d), all origins (o), and all years (t). $y_{p,d,o,t}$ denotes the imports of product p from country o to country d in year t. $\tau_{p,d,o,t}$ denotes the AD tariff that d imposes on o in year t on the product p. $\mathbb{I}_{p,d,o,t}\{\text{After AD}\}$ takes 1 if year t is after the first AD investigation that country d conducts on product p from country o. $\mathbb{N}_{p,d,o,t}\{\text{Committee}\}$ controls for the number of investigation committees formed at the same product-country-bilateral-year level. $\eta_{p,t}$, $\eta_{p,d}$, $\eta_{p,o}$, $\eta_{d,t}$, and $\eta_{o,t}$ denote product-year, product–destination, product–origin, destination–year, and origin–year fixed effects, respectively.

We utilize within-sector, cross product-country-pair-time tariff variations to identify sectoral trade elasticities (by comparing affirmative and negative investigations). In the estimation equation, j represents a sector, and $\mathbf{1}(p \in j)$ is activated if product p belongs to sector j. The parameter θ^j captures the effect of tariffs on imports of products in sector j. As we average the effect of tariffs after their imposition, this parameter represents an average of long- and short-run trade elasticities, which we use to calibrate the baseline model. In Section 3.5.5, we calibrate the model using the long-run effect of tariffs on trade, i.e., the long-run trade elasticity. Table C.6 displays the summary statistics for the variables included in this regression. Table

[20] To ensure that there is sufficient cross-product variation to help us identify the trade elasticities by sector, we estimate the elasticities by pooling together the agriculture sector (D01-D02 of ISIC Rev. 4) and food sector (D10-D12 of ISIC Rev. 4), and pooling together all mining and energy sectors (D05-D09 and D19 of ISIC Rev. 4). We control for product–year, product–destination, product–origin, destination–year, and origin–year fixed effects separately to allow for sufficient variation in order to identify the elasticities by sector.

C.7 displays the correspondence between the sectors considered in this paper, the sectors included in the OECD Inter-Country Input-Output (OECD ICIO) Database, and ISIC Rev. 4 sectors.

Table 3.2 shows our estimated trade elasticities by sector. These elasticities range from 1.36 (other non-metallic mineral products) to 8.98 (mining and energy products). After all sectors are pooled together, the estimated average trade elasticity is 6.09.[21] Consistent with our intuition, sectors that are perceived as less substitutable across countries, for example, minerals and manufactured products, have lower trade elasticities than those that are perceived as more substitutable across countries, for example, energy and chemical products.

Figure C.7 shows that our estimated elasticities are correlated with the estimates of Caliendo and Parro (2015) and the values that we estimate using the Feenstra (1994) method.[22] On average, our estimates are lower than those found in Caliendo and Parro (2015) (in Figure C.7a more than half of the sectors are below the 45-degree line, and their average estimate across all sectors is 9.1).[23] Our estimates are higher than those that we estimate using the Feenstra (1994) method (in Figure C.7b, most sectors are above the 45-degree line).[24]

Robustness Tests

Alternative specifications Our trade elasticity estimates remain robust under alternative empirical specifications. Table C.12 displays the average trade elasticity across sectors estimated with different methods. Column 1 presents the baseline estimate (which is also reported in Table 3.2). Column 2 accounts for the exporter-

[21] To estimate the average trade elasticity across sectors with the baseline specification, we consider the following regression: $y_{p,d,o,t} = \theta\tau_{p,d,o,t} + \beta\mathbb{I}_{p,d,o,t}\{\text{After AD}\} + \gamma\mathbb{N}_{p,d,o,t}\{\text{Committee}\} + \eta_{p,t} + \eta_{p,d} + \eta_{p,o} + \eta_{d,t} + \eta_{o,t} + \varepsilon_{p,d,o,t}$.

[22] The method relies on time series variation in prices and market shares of imported varieties of goods. The identifying assumption is that shocks to import demand and export supply are uncorrelated, which serves as the moment condition. The trade value and quantity data are from the BACI Database of CEPII (Gaulier and Zignago 2010), covering the time period 1995–2019.

[23] The reason why our estimates are lower than those recovered in Caliendo and Parro (2015) is likely the role of trade policy uncertainty. de Souza and Li (2021) show that our treatment and control groups faced similar trade policy uncertainty before a tariff was imposed. However, Caliendo and Parro (2015) do not control for trade policy uncertainty in their regressions. As trade policy uncertainty is likely positively correlated with tariffs (Handley et al. 2020), this can exaggerate the estimates.

[24] Using the Feenstra (1994) method, the average elasticity across all sectors is 2.6. The reason why our estimates are higher than those estimated with the Feenstra (1994) method is likely that they rely on price changes rather than the larger time variations in tariffs.

Table 3.2: Estimated Sectoral Trade Elasticities, θ^j

Sector	Estimate	Standard Err	p-value	Sector	Estimate	Standard Err	p-value
Agriculture	5.18	1.17	0.000	Plastic	5.56	1.06	0.000
Fishing	6.96	1.34	0.000	Mineral	1.36	1.69	0.423
Mining energy	8.98	1.47	0.000	Basic metals	6.59	1.20	0.000
Mining non-energy	8.98	1.47	0.000	Fabricated metals	5.19	1.11	0.000
Mining support	8.98	1.47	0.000	Computer	4.97	1.11	0.000
Food	5.18	1.17	0.000	Electrical	5.44	1.29	0.000
Textiles	6.96	1.34	0.000	Machinery n.e.c.	5.22	1.05	0.000
Wood	6.01	1.48	0.000	Auto	5.98	1.46	0.000
Paper	4.44	1.71	0.010	Other transport	5.33	1.17	0.000
Petroleum	8.98	1.47	0.000	Manufacturing n.e.c.	4.55	1.09	0.000
Chemical	7.45	1.26	0.000	Service	4.17	1.27	0.001
Pharmaceuticals	5.80	1.27	0.000				
All	6.09	0.86	0.000				
Fixed Effects	Product X Time			Product X Exporter		Product X Importer	
Exporter X Time	Importer X Time			Number of AD committees		After AD Investigation	
Observations	269,950	**Cluster**		Product X Exporter X Importer			

Description: This table presents the sector-level trade elasticities that we estimate using the difference-in-differences method based on Model 3.3. The import data are from the United Nations Comtrade Database, acquired through the BACI Database of CEPII (Gaulier and Zignago 2010). The AD data are from the Global Antidumping Database (Bown 2005). The sample runs from 1995 to 2020. Standard errors are clustered at origin-destination-product level.

importer-year fixed effect. Column 3 incorporates both the exporter-importer-year fixed effect and the product-exporter-importer fixed effect. Column 4 presents the results using the PPML estimation method. Finally, Column 5 shows the outcome when employing the inverse hyperbolic sine of the trade flow values as the dependent variable.

Figure C.5 presents the sectoral trade elasticities estimated with alternative empirical specifications. Corresponding to the columns in Table C.12, we re-estimate Model 3.3 by incorporating origin-destination-year fixed effects, product-origin-destination fixed effects, and estimating the model using PPML as well as the inverse hyperbolic sine of the trade flow values as the dependent variable. Sectors with high trade elasticities in the baseline also exhibit high trade elasticities under alternative specifications.

Unique investigating country Our estimates remain robust even when the sample is limited to AD investigations involving a unique investigating country. Figure C.6 displays the distribution of the number of countries investigating the same product from the same country within the same year. Approximately 80% of AD investigations are conducted by only one country. Table C.13 presents the average trade elasticity across sectors for the sample containing only investigations conducted by a unique country, considering different fixed effect combinations, PPML, and using the inverse hyperbolic sine of the trade flow as the dependent variable. The

estimates continue to be robust.

Heterogeneity analysis Readers may be interested in whether the impact of tariffs is influenced not only by sectors, but also by country characteristics and tariff attributes. We examine this heterogeneity from two perspectives: pre-investigation trade flows and tariff sizes.

Table C.14 shows that the effect of tariffs decreases with pre-investigation trade flow values. We interact the tariff with the log of the trade flow value from the investigated country to the investigating country for the investigated product, one, five, and ten years before the investigation. Columns 1 to 3 show that tariffs have a smaller effect (in terms of elasticity) if countries traded more, suggesting that stronger trade linkages are more resilient to tariff shocks. Columns 4 to 6 demonstrate that these effects are robust when using the PPML estimation strategy.

Additionally, Table C.15 indicates that the effect of tariffs is larger for larger tariffs. We interact the tariff with a dummy variable denoting whether the tariff is among the top 5%, top 10%, and top 25% of all AD tariffs in Columns 1, 2, and 3, respectively. The interaction term is significant, negative, and greater in magnitude if the tariff is in more top percentiles. Columns 4 to 6 report the estimates using the PPML strategy, and these patterns remain robust.

3.3 Model

In this section, we present a multi-sector, multi-country quantitative trade model with input-output linkage. The exposition of the model has two sections. In the first section, tariffs are taken as given. In the second section, we present how governments choose tariffs.

3.3.1 Demographics

The global economy consists of N countries and J sectors. Each country has a mass L_n of households. The preference of country n's households is a Cobb-Douglas function of sector-level consumption goods, C_n^j. The labor supply of households is inelastic.

The household's problem is the following:

$$\max_{\left\{C_n^j\right\}_{j=1}^J} U_n = \prod_{j=1}^{J} \left(\frac{C_n^j}{\alpha_n^j} \right)^{\alpha_n^j}, \qquad \text{where} \sum_{j=1}^{J} \alpha_n^j = 1$$

$$\text{s.t.} \sum_{j=1}^{J} P_n^j C_n^j = I_n,$$

where P_n^j denotes the sector j composite goods price in country n. I_n denotes the country's total income. The consumer's problem implies that country n's households face the following consumer price index:

$$P_n^C = \prod_{j=1}^{J} \left(P_n^j \right)^{\alpha_n^j}. \tag{3.4}$$

3.3.2 Intermediate Goods Producer

We assume that all markets are competitive, in the same way as Caliendo and Parro (2015). Labor is freely mobile across sectors within a country, but immobile across countries. A representative firm in country n and sector j produces with labor and intermediate inputs from all sectors with a Cobb-Douglas technology:[25]

$$Y_n^j = A_n^j \left[\frac{L_n^j}{\gamma_n^j} \right]^{\gamma_n^j} \prod_{k=1}^{J} \left[\frac{M_n^{j,k}}{\gamma_n^{j,k}} \right]^{\gamma_n^{j,k}},$$

where A_n^j denotes the total factor productivity (TFP), L_n^j denotes sectoral employment, and $M_n^{j,k}$ denotes the quantity of sector k composite goods used by sector j as an input. γ_n^j and $\gamma_n^{j,k}$ are input-output coefficients with $\gamma_n^j + \sum_{k=1}^{J} \gamma_n^{j,k} = 1$.

Profit maximization implies that the output price equals the marginal cost:

$$p_n^j = \frac{1}{A_n^j} \left[w_n \right]^{\gamma_n^j} \prod_{k=1}^{J} \left[P_n^k \right]^{\gamma_n^{j,k}}, \tag{3.5}$$

where w_n denotes the wage of country n.

3.3.3 Composite Goods

A country's consumers and firms source their composite goods domestically and from other countries. Let Q_n^j be the quantity of composite goods of sector j used in

[25] In the robustness test section, Section 3.5.5, we relax the assumption of a Cobb-Douglas production function. Instead, we use a CES production function and test the sensitivity of the results to different elasticities of substitution between inputs.

country n:

$$Q_n^j = \left[\sum_{i=1}^{N} (q_{ni}^j)^{(\sigma^j-1)/\sigma^j}\right]^{\sigma^j/(\sigma^j-1)},$$

where q_{ni}^j denotes the quantity of sector j output that country n buys from country i and where σ^j is the elasticity of substitution between countries. Because composite goods are used as consumption and inputs, it must be the case that:

$$Q_n^j = C_n^j + \sum_{k=1}^{J} M_n^{k,j}.$$

3.3.4 Expenditure Share

To get a unit of sector j output from country i, consumers and firms in country n need to pay:

$$p_{ni}^j = t_{ni}^j k_{ni}^j p_n^j,$$

where $t_{ni}^j = 1 + \tau_{ni}^j$ is 1 plus the ad-valorem tariff that country n imposes on country i and where k_{ni}^j denotes the iceberg trade cost to ship one unit of sector j's output from country i to country n.

After country n chooses the quantity to source from each origin country i to minimize the cost of producing Q_n^j, country n's expenditure share on sector j's output from country i equals:

$$\pi_{ni}^j = \frac{(t_{ni}^j k_{ni}^j p_i^j)^{1-\sigma^j}}{\sum_{h=1}^{N} (t_{nh}^j k_{nh}^j p_h^j)^{1-\sigma^j}} \tag{3.6}$$

The composite goods price is thus given by:

$$P_n^j = \left[\sum_{i=1}^{N} (t_{ni}^j k_{ni}^j p_i^j)^{1-\sigma^j}\right]^{1/(1-\sigma^j)}. \tag{3.7}$$

From now on, we use $\theta^j = \sigma^j - 1$ to denote the trade elasticity.

3.3.5 Market Clearing

Let $X_n^j = P_n^j Q_n^j$ denote country n's total expenditure on sector j's composite goods. The market clearing condition for the composite goods implies that:

$$X_n^j = \sum_{k=1}^{J} \gamma_n^{k,j} \sum_{i=1}^{N} \frac{X_i^k \pi_{in}^k}{t_{in}^k} + \alpha_n^j I_n, \tag{3.8}$$

where the first term is country n's demand for inputs from sector j and the second term is the consumer's demand.

Household income, I_n, must be equal to labor income, tax revenue, and the trade deficit:

$$I_n = w_n L_n + R_n + D_n \tag{3.9}$$

where $w_n L_n$ is labor income, R_n is tariff revenue, and D_n is the trade deficit. Tariff revenue can be written as

$$R_n = \tau_{ni}^j \sum_{i=1}^{N} \frac{X_i^k \pi_{in}^k}{t_{in}^k}. \tag{3.10}$$

Using Equation 3.8 and the definition of the trade deficit, we can write the labor market clearing condition:

$$w_n L_n = \sum_{j=1}^{J} \gamma_n^j \sum_{i=1}^{N} \frac{X_i^j \pi_{in}^j}{t_{in}^j}. \tag{3.11}$$

With that, we are ready to define an equilibrium given tariffs.

Equilibrium given Tariffs *Given tariffs $\{\tau_{ni}^j\}_{j,n,i}$, an equilibrium is defined as a set of sectoral prices ,$\{P_n^j\}_{n,j}$, and wages, $\{w_n\}_n$, such that*

1. *firms maximize profit (Equation 3.5);*
2. *the price index satisfies Equations 3.6 and 3.7;*
3. *the goods markets clear, satisfying Equations 3.8 and 3.9;*
4. *the government budget constraint (Equation 3.10) holds;*
5. *the labor market clears, satisfying Equation 3.11.*

3.3.6 Tariff Competition

Import tariffs are chosen by governments. Countries are in three groups according to how they choose tariffs. There are sanctioning countries, the sanctioned country (Russia, in this case), and neutral countries (the rest of the world [ROW]). The sanctioning countries choose tariffs, trading off between two objectives. On the one hand, they want to maximize their domestic households' welfare. On the other

hand, they want to minimize Russian welfare. Russia also chooses tariffs to maximize its own welfare and reduce the sanctioning countries' welfare. We assume that the neutral countries do not change tariffs.[26]

Before we formally define the problem of a sanctioning country, let τ_{nR} be the vector of sectoral tariffs that country n imposes on Russia. Let τ_{-nR} be all global tariffs except what n imposes on Russia. Use $G_n(\tau_{nR}, \tau_{-nR})$ to denote the equilibrium welfare in country n under tariff policy (τ_{nR}, τ_{-nR}):

$$G_n(\tau_{nR}, \tau_{-nR}) = \frac{I_n(\tau_{nR}, \tau_{-nR})}{P_n^C(\tau_{nR}, \tau_{-nR})}, \tag{3.12}$$

where $I_n(\tau_{nR}, \tau_{-nR})$ denotes household income (Equation 3.9) and $P_n^C(\tau_{nR}, \tau_{-nR})$ denotes the consumer price index (Equation 3.4).

Conditional on τ_{-nR}, the objective of sanctioning country n is:

$$g_n(\tau_{-nR}) \in argmax_{\{\tau_{nR}\}} \rho G_n(\tau_{nR}, \tau_{-nR}) - (1-\rho) G_R(\tau_{nR}, \tau_{-nR}), \tag{3.13}$$

s.t. Equilibrium Conditions 3.5-3.11,

where ρ is the willingness to pay for sanctions against Russia. In other words, the domestic government is willing to pay $\$\frac{1-\rho}{\rho}$ for every US$1 of consumption forgone in Russia. This specification nests two special cases. When $\rho = 1$, country n maximizes its own real income, and when $\rho = 0$, country n minimizes Russia's real income without consideration for its own welfare.[27]

Russia, the sanctioned country, trades off maximizing its own welfare and retaliating against the countries imposing the sanctions. Use S to denote the set of sanctioning countries. Russia's problem is as follows:

$$g_R(\tau_{-RS}) \in argmax_{\{\tau_{RS}\}} \rho G_R(\tau_{RS}, \tau_{-RS}) - (1-\rho) \sum_{n \in S} \frac{G_n(\tau_{RS}, \tau_{-RS})}{N_S} \tag{3.14}$$

s.t. Equilibrium Conditions 3.5-3.11,

where $G_R(\tau_{RS}, \tau_{-RS})$ is the equilibrium welfare in Russia and $\sum_{n \in S} \frac{G_n(\tau_{RS}, \tau_{-RS})}{N_S}$ is the average real income of the sanctioning countries (N_S denotes the number of sanctioning countries, τ_{RS} denotes the set of tariffs that Russia imposes on the sanctioning countries, and τ_{-RS} denotes all global tariffs except what Russia imposes on the

[26] In Section 3.5.3, we study the case in which neutral countries join the sanctioning allies. In Section 3.5.5, we also consider the case in which Russia keeps its tariffs constant.

[27] In Section A.3, we consider an alternative cost-efficient sanction problem whereby the sanctioning countries minimize Russia's welfare but require that their own welfare does not decrease.

sanctioning countries). As with sanctioning countries, ρ captures the willingness to pay for tariff retaliation against sanctioning countries.[28] We call the equilibrium tariffs that are a solution to Problems 3.13 and 3.14 cost efficient sanctions.

Equilibrium with Sanctions *Given* $\{\{\tau_{ni}^j\}_{j,n\in S,i\neq R}, \{\tau_{Ri}^j\}_{j,i\notin S}, \{\tau_{ni}^j\}_{j,n\notin S,i\neq R}\}$, *an equilibrium with optimal sanctions is given by tariffs imposed on Russia by sanctioning countries,* $\{\tau_{nR}\}_{n\in S}$, *tariffs imposed on sanctioning countries by Russia,* $\{\tau_{Rn}\}_{n\in S}$, *a set of sectoral prices,* $\{P_n^j\}_{n,j}$, *and wages,* $\{w_n\}_n$, *such that*

1. *given tariffs* $\{\tau_{ni}^j\}_{j,n,i}$, $\{\{P_n^j\}_{n,j}, \{w_n\}_n\}$ *is an equilibrium;*

2. *sanctioning countries and Russia optimally choose their tariffs:*

$$\tau_{nR} = g_n(\tau_{-nR}), \forall n \in S;$$
$$\tau_{RS} = g_R(\tau_{-RS}).$$

To solve a counterfactual equilibrium, we rewrite the model in changes. In this way, we eliminate the fundamentals that are invariant to tariff changes and are difficult to calibrate (for example, non-tariff trade barriers $\{k_{ni}^j\}_{j,n,i}$). We present the sanction equilibrium in changes in Appendix Section A.2.

3.4 Calibration

To calibrate our model, we rely on two main data sources: 1) the OECD ICIO Database and 2) our estimates of the trade elasticities. We calibrate the baseline global economy to their levels in 2018, the latest year for which a world input-output table is available. We let each sector $j \in \{1,2,...,22\}$ denote the 22 goods sectors considered in OECD ICIO and $j = 23$ denotes a merged service sector.[29] Countries $i,n \in \{$EUN,OSA,ROW,RUS,USA$\}$ denote the European Union, other sanc-

[28] In the baseline scenario in Section 3.5, we assume that Russia has the same ρ as the sanctioning countries. In Section 3.5.5, we also consider that Russia retaliates by always maximizing its own welfare $\rho_{RUS} \equiv 1$ and by always minimizing the sanctioning countries' welfare $\rho_{RUS} \equiv 0$. We show that sanctioning countries' strategies and their real income changes are not significantly affected by Russia's retaliation strategy.

[29] See Appendix Table C.7 for the list of OECD ICIO sectors and their correspondence with the International Standard Industrial Classification (ISIC) Rev. 4 sectors. We merge all service sectors into one single sector.

tioning countries, rest of the world, Russia, and the United States.[30] The EU and the US are the two largest economies that are sanctioning Russia. Other sanctioning countries include Australia, Canada, Israel, Japan, South Korea, New Zealand, Norway, Singapore, Switzerland, Taiwan, and the United Kingdom (UK), which are the economies that had joined sanctions on Russia by March 31, 2022.[31] We combine these other sanctioning economies because of the collaborative nature of the sanctions, and we reduce the number of countries for which we have to show the optimal sanctioning tariffs. ROW includes all other economies that are covered by OECD ICIO. These countries have not imposed sanctions on Russia and will thus not change their tariffs throughout our analysis. Therefore, we combine them into one economy.[32]

We calibrate country-bilateral and sector-level expenditure shares, π_{ni}^{j}, country-level input-output coefficients, $\gamma_{n}^{k,j}$, country-level value added, $w_n L_n$, and country-level trade deficit, D_n, directly to their data counterparts in OECD ICIO.

3.5 Results

3.5.1 Cost-Efficient Sanctions

In this section, we discuss the cost-efficient sanctions imposed by the EU. Figure 3.3 shows the statistics relating to the optimal sanctions imposed by the EU according to the different levels of willingness to pay for sanctions, ρ. The left panel plots the cost-efficient sanctions for selected sectors. The right panel plots the change in imports in the EU implied by different sanctioning schemes.

The EU should increase tariffs and decrease trade with Russia, even if the willingness to pay for sanctions is zero ($\rho = 1$), as shown in Figure 3.3. This is because higher tariffs on Russia lead to a decrease in the price of imported goods relative to

[30] The EU countries that are covered by OECD ICIO are as follows: Austria, Belgium, Bulgaria, Croatia, Cyprus, Czech Republic, Denmark, Estonia, Finland, France, Germany, Greece, Hungary, Ireland, Italy, Latvia, Lithuania, Luxembourg, Malta, Morocco, Netherlands, Poland, Portugal, Romania, Slovakia, Spain, and Sweden.

[31] See https://graphics.reuters.com/UKRAINE-CRISIS/SANCTIONS/byvrjenzmve/ for the evolving list of countries that have sanctioned Russia.

[32] Section A.3 in the Appendix discusses the statistics of Russian trade. We show that the EU depends on Russia for mining and energy imports, while Russia views the EU as a significant sales market. Russia relies on sanctioning countries for input imports, but is not a crucial sales destination for them. We explore the implications of these trade patterns for cost-efficient sanctions.

exported ones, resulting in an increase in the EU's real income.[33] This result suggests that, to a certain degree, sanctioning countries can improve their own welfare and harm the Russian economy simultaneously.

Even when there is low willingness to pay for sanctions, imports from Russia should drop by more than 80%. When the EU's willingness to pay for sanctions is positive, it decreases trade with Russia by more than 60%. When there is a willingness to pay only \$0.40 per \$1 decline in Russian income, i.e., $\rho = 0.7$, the EU imposes tariffs that decrease imports from Russia by 95%.

Cost-efficient sanctions are small and uniform across sectors when there is low willingness to pay for sanctions, as shown in to Figure 3.3. If the EU is willing to pay \$0.10 for each \$1 decline in Russian income, i.e., $\rho = 0.9$, tariffs should average about 20% for all sectors. Tariffs increase with a higher willingness to pay, but the dispersion across sectors is small.[34]

If the EU is willing to pay over \$0.70 dollars for each \$1 decline in Russian income, i.e., ρ is below 0.6, an EU embargo of Russian mining and energy products is optimal. Figure 3.4 extends the horizontal axis of Figure 3.3 to $\rho = 0.4$, according to which the EU is willing to pay \$1.50 for each \$1 decline in Russian income, and shows the optimal tariffs and trade flow changes accordingly. If the EU pays \$0.70 dollars to reduce Russian real income by \$1, tariffs on mining and energy products are especially high, as shown in Figure 3.5. The tariff on energy extraction sector products, including crude oil and natural gas, is above 300%, and the tariff on petroleum is above 200%. In this case, an embargo on Russian oil and gas combined with high tariffs on other sectors is the most cost-efficient policy. When the willingness to pay rises to \$1.50, tariffs on all sectors are above 80% and an embargo on all sectors is optimal.

Conditional on the willingness to pay for sanctions, trade elasticities and initial import share are important determinants of tariffs. If the sanctioning country's main goal is to maximize domestic welfare, tariffs should target products with a low trade elasticity and a low import share from Russia. In this case, countries use tariffs to

[33] This is the traditional terms-of-trade effect discussed in, for example, Bagwell and Staiger (1990).

[34] In Section A.3, we solve the alternative cost-efficient sanction problem where the sanctioning countries minimize Russia's welfare while not decreasing their own welfare. We find that those cost-efficient sanction tariffs resemble the optimal tariffs under low willingness to pay for sanctions.

Figure 3.3: Cost-Efficient Sanctions in the EU for Different ρs, $\rho \in [0.7, 1.0]$

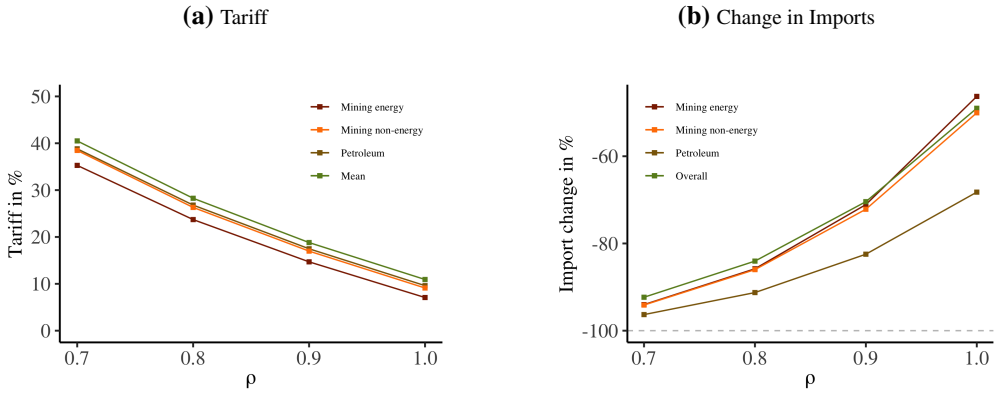

Description: This figure shows the statistics for the EU under cost-efficient sanctions against Russia that vary by the level of willingness to pay for them. ρ ranges from 0.7 to 1.0. Figure 3.3a plots the cost-efficient sanctions on mining energy, mining non-energy, petroleum, and the average tariff across sectors by different levels of willingness to pay for sanctions, ρ. Figure 3.3b plots the percentage change in imports in the EU for different sectors by different levels of willingness to pay for sanctions, ρ.

Figure 3.4: Cost-Efficient Sanctions in the EU for Different ρs, $\rho \in [0.4, 1.0]$

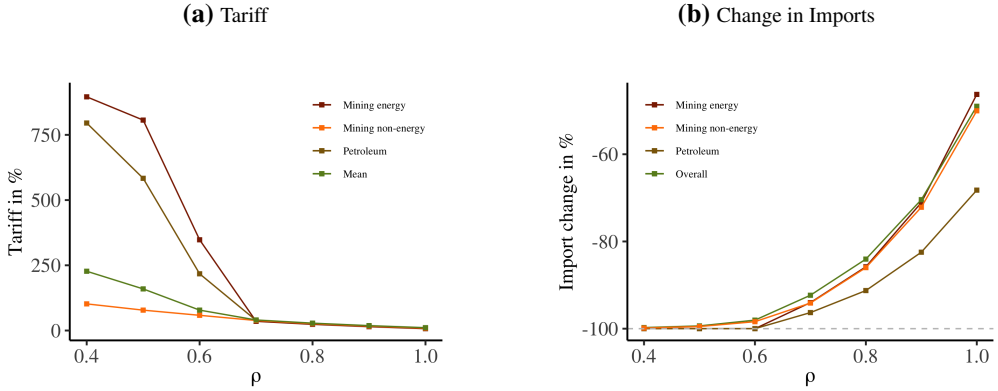

Description: This figure shows the statistics for the EU under cost-efficient sanctions against Russia that vary by the level of willingness to pay for them. ρ ranges from 0.4 to 1.0. Figure 3.3a plots the cost-efficient sanctions on mining energy, mining non-energy, petroleum, and the average tariff across sectors by different levels of willingness to pay for sanctions, ρ. Figure 3.3b plots the percentage change in imports in the EU for different sectors by different levels of willingness to pay for sanctions, ρ.

manipulate the terms of trade, i.e., to raise the export price relative to the import price.[35] The products in which the terms of trade are more affected by tariffs are the ones with lower demand elasticity and lower import share.[36]

When there is a high enough willingness to pay for sanctions, tariffs should target sectors with a large import share from Russia and with a high trade elasticity. Sanctioning these sectors can divert more Russian exports to other countries, reduce Russian output further, and cause more economic damage in Russia. Appendix A.3

[35] See, for example, Bagwell and Staiger (1990).

[36] For a formal proof, see Gros (1987), Broda et al. (2008), Opp (2010), Costinot et al. (2015), and Lashkaripour and Lugovskyy (2023), who derive theories that link optimal tariffs to market shares and trade elasticities.

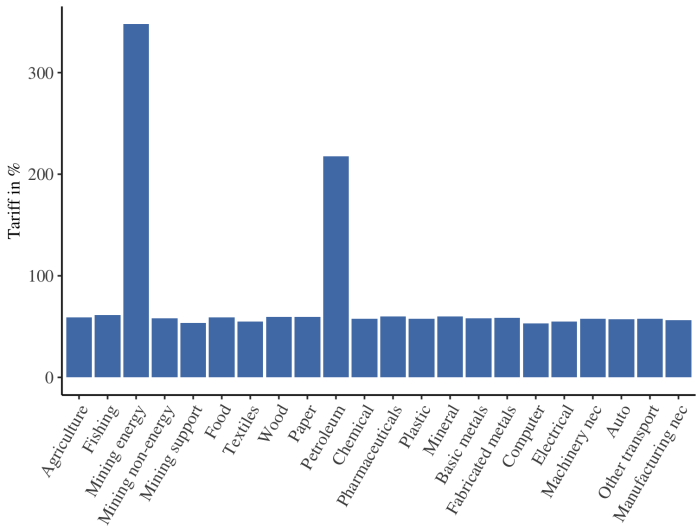

Figure 3.5: Cost-Efficient Sanctions in the EU for $\rho = 0.6$

Description: This figure shows the cost-efficient sectoral tariffs that the EU imposes on Russia at $\rho = 0.6$ – the EU is willing to pay \$0.70 dollars for \$1 real income loss in Russia.

discusses these intuitions in detail.

Cost-efficient sanctions in the US and OSA exhibit a similar pattern, which varies according to each country's willingness to pay for sanctions, as shown in Figures 3.6 and 3.7. In both cases, cost-efficient sanctions are small and uniform across sectors for low willingness to pay for sanctions, but they still cause a large drop in trade with Russia. Figure C.13 shows that as the willingness to pay increases, US optimal tariffs increase uniformly across sectors. The reason is that, as Figure C.8a shows, the share of US expenditure on Russia is small and similar across sectors. Figure C.14 shows that for other sanctioning countries, an embargo on mining and energy sectors is optimal if they would like to pay \$1 to reduce Russia's income by \$1. If the willingness to pay rises to \$1.50, an embargo by all sanctioning countries on all Russian products is optimal.

3.5.2 The Welfare Cost of Sanctions

The Welfare Cost of Sanctions for Russia

How much welfare loss can sanctions cause in Russia? To answer this question, Figure 3.8 shows the welfare changes for Russia and the sanctioning countries under two scenarios: with and without Russian retaliation. In the case with retaliation, similar to the sanctioning countries, Russia chooses tariffs based on Problem 3.14.

Figure 3.6: Cost-Efficient Sanctions in the US for Different ρs, $\rho \in [0.7, 1.0]$

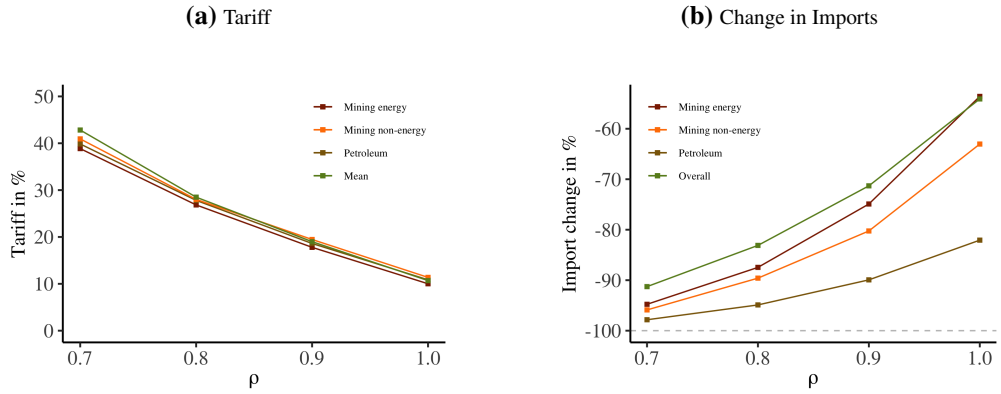

Description: This figure shows the statistics of the US under cost-efficient sanctions with different levels of willingness to pay. Figure 3.6a plots the cost-efficient sanctions on mining energy, mining non-energy, petroleum, and the average tariff across sectors for different levels of willingness to pay for sanctions, ρ. Figure 3.6b plots the percentage change in imports in the US for different sectors.

Figure 3.7: Cost-Efficient Sanctions in the OSA for Different ρs, $\rho \in [0.7, 1.0]$

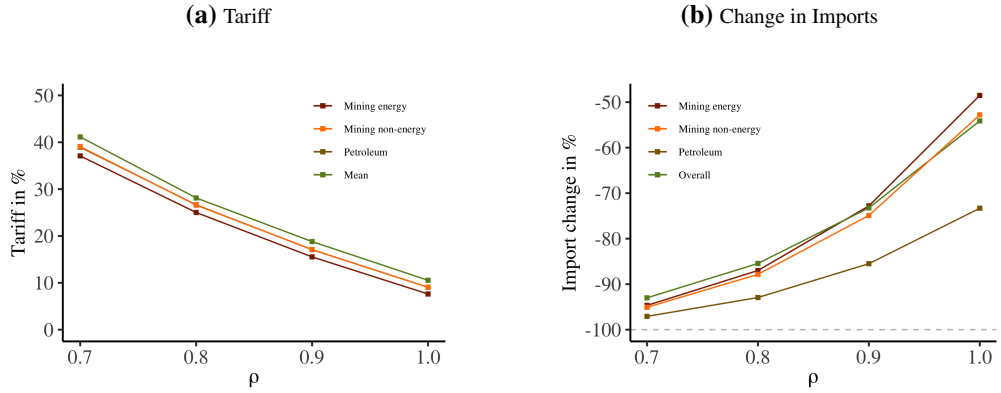

Description: This figure shows the statistics for the OSA under cost-efficient sanctions with different levels of willingness to pay. Figure 3.7a plots the cost-efficient sanctions on mining energy, mining non-energy, petroleum, and the average tariff across sectors for different levels of willingness to pay for sanctions, ρ. Figure 3.7b plots the percentage change in imports in the OSA at different sectors.

In the case without Russian retaliation (3.8b), Russian tariffs are constant at the calibrated value.

As shown in Figure 3.8, sanctions can decrease Russian welfare by between 0.5% and 3%. Without Russian retaliation, i.e., if Russian tariffs are constant at the calibrated values, the welfare loss in Russia ranges from 0.5% to 1.2%, depending on the willingness to pay of the sanctioning countries. If Russia retaliates, the welfare cost of sanctions can be as large as 3% due to the the economic size difference between Russia and the sanctioning countries. The sanctioning countries are an important sourcing origin for Russia, whereas Russia is not an important exporting destination for the sanctioning countries.[37] Because of this, restricting imports

[37]Russia spends 5.2% of their total expenditures on the sanctioning countries. The sanctioning

from the sanctioning countries can have little impact on the sanctioning countries' income, but it induces a large price increase and real income loss in Russia.[38]

Figure 3.8: Welfare Changes with and without Russian Retaliation

(a) With Russian Retaliation **(b)** Without Russian Retaliation

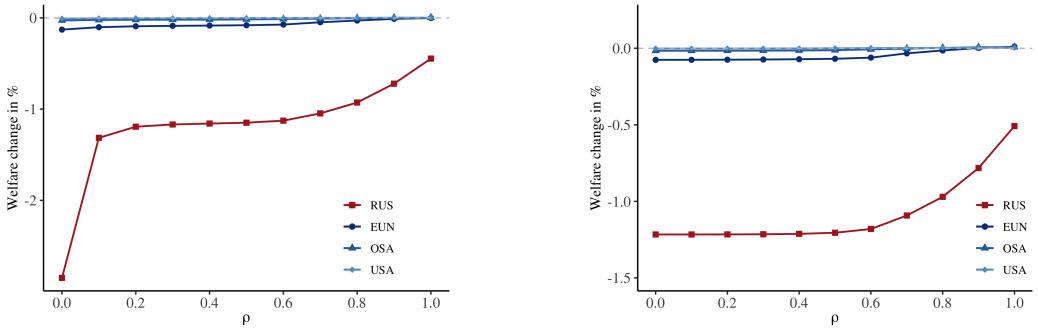

Description: This figure shows the welfare change by the different levels of willingness to pay for sanctions, ρ, under two variations of the model discussed in Section 3.3. Figure 3.8a displays the welfare changes for Russia, the EU, the OSA, and the US when Russia also changes its tariffs to affect the welfare of the sanctioning countries. Figure 3.8b displays the welfare change in Russia, the EU, the OSA, and the US under the assumption that Russia keeps its tariffs constant. Welfare refers to the equilibrium real income. Changes are calculated by comparing the resulting equilibrium from the new tariffs to the equilibrium with initial, pre-sanction tariffs.

The Welfare Cost of Sanctions on Sanctioning Countries

How much do sanctions cost the sanctioning countries? As shown in Figure 3.8, the welfare cost of sanctions is small. The sanctioning countries face a welfare loss ranging from 0.1% to 0.2%, depending on Russia's response to the sanctions. Additionally, Figure 3.8 highlights that imposing sanctions on Russia can benefit the sanctioning allies. If the sanctioning allies are not willing to pay for sanctions but choose tariffs on Russia to maximize their own welfare, i.e., $\rho = 1$, their welfare increases by 0.01%, 0.003%, and 0.003% in the EU, US, and OSA, respectively. Given the sanctioning allies' significant size and wealth advantage over Russia, they can alter the terms of trade in their favor, which harms Russia's economy while benefiting the sanctioning countries.

This finding is especially significant because it emphasizes the impact of revoking Russia's MFN status, which was one of the initial sanction measures imposed

countries sell 0.2% of their output to Russia. See Figures C.8c and C.8d.

[38]This finding also indicates that, as long as Russia cares about domestic welfare ($\rho_{RUS} \geq 0.1$), Russia should not impose high retaliatory tariffs on the sanctioning countries, and the consequences of sanctions are similar both with and without Russian retaliation. In Section 3.5.5, we elaborate on this point further. We show that the sanctioning countries' optimal tariffs are not significantly affected by Russia's retaliation strategies.

Figure 3.9: Welfare Changes with Individual Sanctions

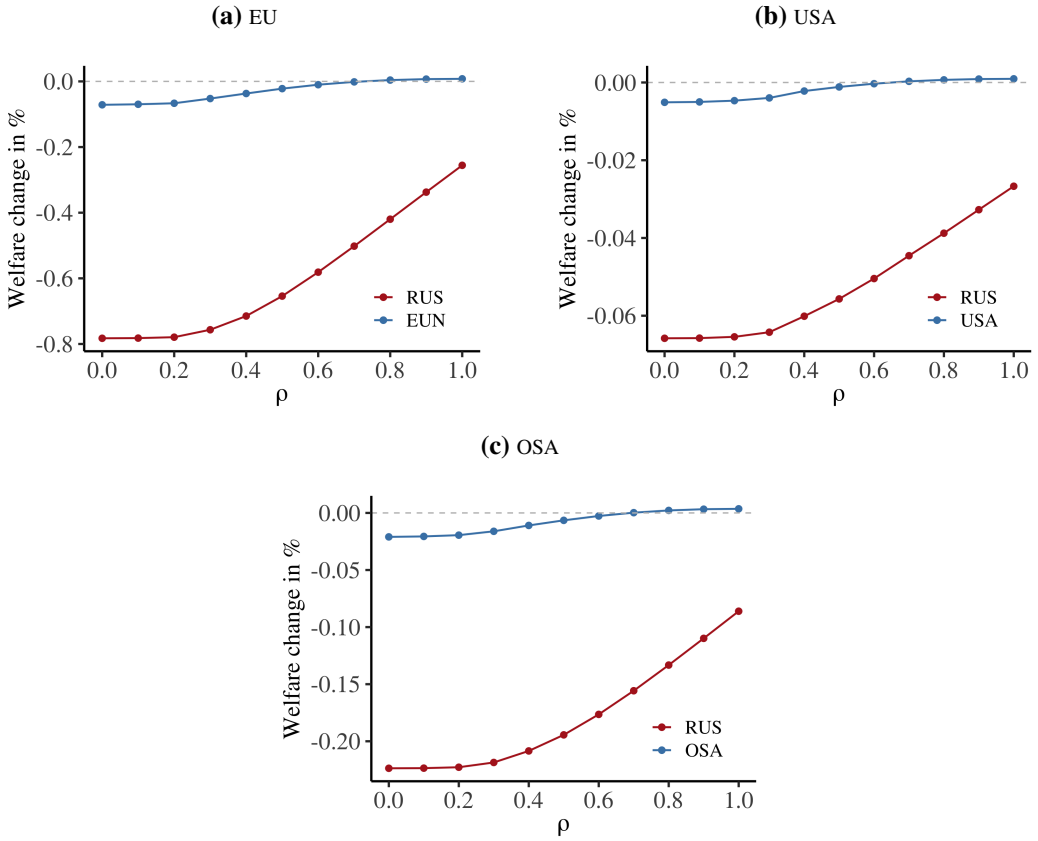

Description: This figure shows the welfare change for different willingness to pay for sanctions, ρ, under the equilibrium tariffs of the model with individual sanctions. Figure 3.9a shows the welfare change if the EU chooses tariffs on Russia to maximize 3.13 while all the other countries hold tariffs constant. Figure 3.9b shows the welfare change if the US chooses tariffs on Russia to maximize 3.13 while all the other countries hold tariffs constant. Figure 3.9c shows the welfare change if the OSA chooses tariffs on Russia to maximize 3.3 while all the other countries hold tariffs constant. Welfare refers to the equilibrium real income. Changes are calculated comparing the equilibrium to the current tariffs.

on Russia. With the implementation of this new regime, countries that are part of the WTO have the freedom to impose arbitrary tariffs on Russia. Therefore, even if these countries do not intend to harm Russia's economy, they can still inflict severe losses on Russia by selecting tariffs that enhance their own welfare (consistent with the theoretical predictions in Sturm 2022 and Sturm 2023).

To understand which of the sanctioning countries can have a greater impact on Russia, we consider the case where the EU, the US, and the OSA individually set tariffs to target Russia's real income. For simplicity, we assume that Russia keeps its tariffs constant. Figure 3.9 shows the welfare changes for Russia and the sanctioning countries under unilateral sanctions. Each of the three sub-figures plots the counterfactual equilibrium in which one country chooses tariffs on Russian imports based on Problem 3.13, while Russia and all the other countries keep their tariffs constant.

According to Figure 3.9, the EU is the sanctioning group most affected by sanctions against Russia. If $\rho = 0$, i.e., tariffs against Russia are chosen to minimize Russian welfare, the EU has a welfare loss of 0.1%. Since the US and OSA trade much less with Russia than EU, they suffer a welfare loss of only 0.01% and 0.02%.

The EU is also the trade partner that can cause the largest welfare damage to Russia. The EU alone can reduce welfare in Russia from 0.26% to 0.78%, whereas US sanctions can only reduce Russian welfare by no more than 0.1%.

3.5.3 Sanctions and the Rest of the World

In this section, we study how the ROW is affected and, in turn, affects the cost-efficient sanctions against Russia. First, we show that countries not imposing sanctions benefit from lower priced goods from Russia and higher priced goods sold to the sanctioning allies. Furthermore, if the ROW joined the allies in imposing sanctions, even a low willingness to pay for sanctions would result in an embargo on Russia's oil and energy sectors.

Effect of Sanctions on Non-Sanctioning Countries

Figure 3.10a shows that the ROW boosts its exports in reaction to sanctions placed on Russia. As sanctioning countries raise tariffs against Russia, sanctioning countries substitute imports from Russia with those from the ROW. This pattern, referred to as the trade diversion effect, leads to an increase in ROW exports to the sanctioning countries and overall.[39]

The relationship between ROW's exports to Russia and the willingness to pay for sanctions is non-monotonic, influenced by two key forces: the income effect and the trade diversion effect. Russia experiences a significant income loss even at low levels of willingness to pay for sanctions, causing its imports from the ROW to initially decrease. The trade diversion effect, which occurs when Russia imposes high tariffs against sanctioning countries reduces imports from them, and increases imports from the ROW, only becomes dominant when $\rho = 0$ and Russia closes its border for trade with allied nations.

[39] As the demand for ROW's exports from Russia hikes at the highest willingness to pay for sanctions, ROW's exports initially destined for the sanctioning countries are redirected to Russia. Consequently, when the willingness to pay for sanctions is high, the increase in ROW's exports to the sanctioning countries is not as substantial.

Figure 3.10b shows that sanctions against Russia increase imports by the ROW. As the sanctioning allies and Russia impose tariffs on each other, the prices of exported goods in both countries decrease, which motivates the ROW to import more of these goods. However, this effect is not monotone. High willingness to pay for sanctions causes tariffs to raise the marginal cost of production in Russia, leading to lower imports by the ROW from Russia when trade sanctions are intensified.

Trade sanctions increase welfare for the ROW, as shown in Figure 3.10c. The ROW benefits from the sanctions because it positively impacts their terms of trade. The trade diversion effect results in an increase in the price of exported goods, while the price of imported goods decreases. This leads to an overall increase in welfare for the ROW.

Figure 3.10: Effect of Cost-Efficient Sanctions in the ROW

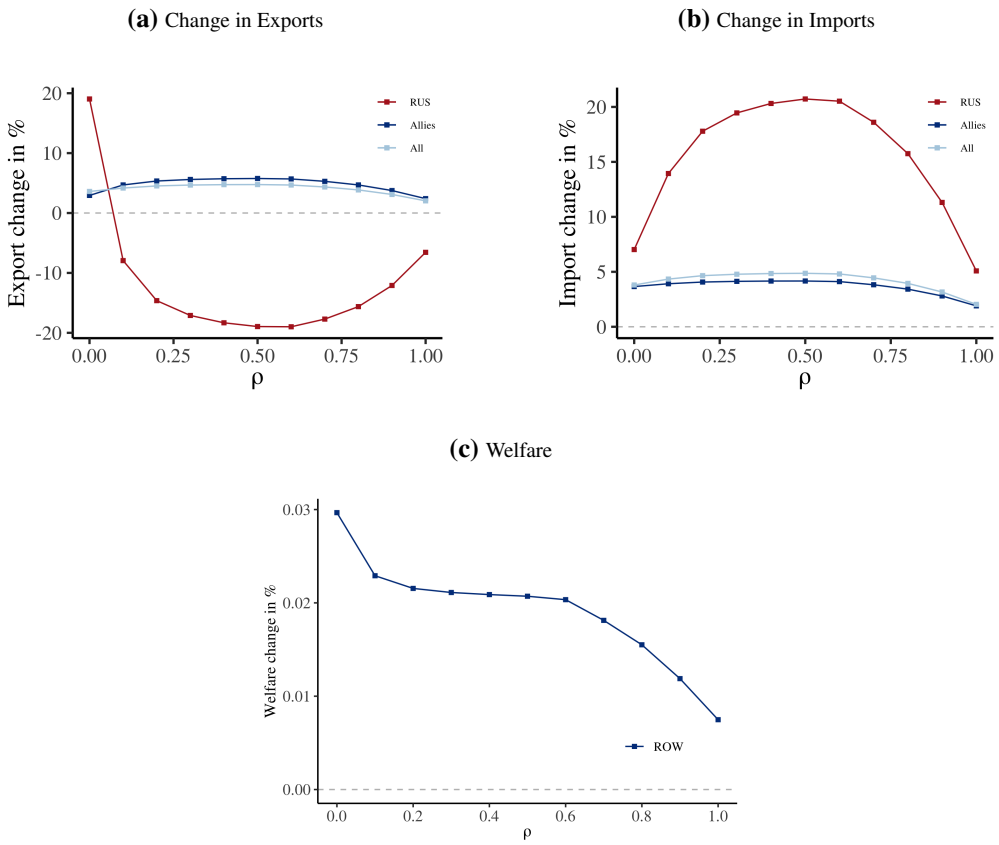

Description: This figure shows the statistics for the ROW under cost-efficient sanctions against Russia that vary by the level of willingness to pay for sanctions. We assume that the ROW keeps all its tariffs constant. Figure 3.10a plots the percentage change in exports from the ROW to the sanctioning countries, to Russia, and in total. Figure 3.10b plots the percentage change in imports by the ROW from the sanctioning, from Russia, and in total. Figure 3.10c plots the percentage change in welfare in the ROW.

A Larger Coalition

What would happen to the cost-efficient sanctions if a larger coalition of countries joined the current group of sanctioning countries? To answer this question, in this section, we calculate the cost-efficient sanctions when the ROW joins the sanctioning allies. Our findings reveal that if the ROW were to join the sanctions, the EU and other sanctioning allies could impose an embargo on Russia even with low willingness to pay for sanctions. Additionally, the welfare effects of these sanctions on Russia would increase significantly.

If the ROW joined the sanctioning allies, the EU could impose even higher tariffs on Russia for any willingness to pay for sanctions, as shown in Figure 3.11. When Russia still has the ROW to trade with, the impact of each individual sanctioning country on Russia's welfare is limited because Russia can redirect its trade to other countries that have not imposed sanctions. This reduces the benefits of imposing higher sanctions on Russia. However, if other countries are already imposing high tariffs on Russia, each individual country that joins the sanctions will have a significant impact on Russia's remaining trade. This increases the potential benefits of imposing sanctions on Russia and leads to an overall increase in the level of sanctions.

Figure 3.11: Cost-Efficient Sanctions in the EU for Different ρs if the ROW Joins the Sanctioning Allies, $\rho \in [0.6, 1.0]$

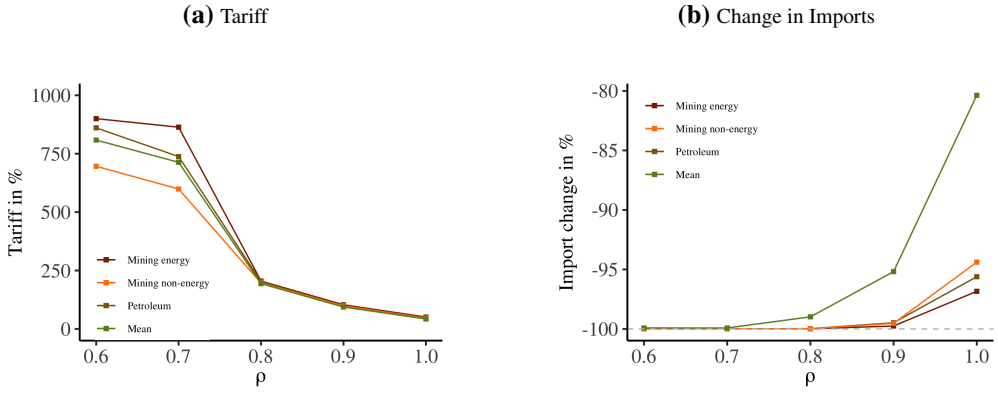

Description: This figure shows the statistics for the EU under cost-efficient sanctions against Russia that vary by the level of willingness to pay for sanctions. We assume that all countries join the sanctions against Russia and that Russia retaliates according to the same willingness to pay for sanctions. ρ ranges from 0.6 to 1.0. Figure 3.11a plots the cost-efficient tariffs on mining energy, mining non-energy, petroleum, and the average tariff across sectors by different levels of willingness to pay for sanctions, ρ. Figure 3.11b plots the percentage change in imports in the EU for different sectors by different levels of willingness to pay for sanctions.

According to Figure 3.12, sanctions would have a much greater impact on the

Russian economy if the ROW joined the sanctioning allies. The welfare cost of sanctions for Russia would go from 2% up to 6%, depending on the willingness to pay for sanctions. Two forces cause the increase in the welfare effect of sanctions. First, when all countries impose sanctions against Russia, all of Russia's exports are disrupted. Second, because Russia also retaliates against all countries in the world, Russian imports are also substantially more affected. Together, these two forces dramatically amplify the impact of sanctions against Russia.

Figure 3.12 also shows that if countries were allowed to set their tariffs on Russia to maximize their own welfare, Russian welfare would decrease by 2.5%. This is because countries would manipulate the terms of trade jointly, leading to a significant drop in the price of Russia's exported goods. This demonstrates that, to some extent, countries can increase their own welfare while reducing Russia's welfare. Therefore, policies that permit countries to impose arbitrary tariffs on Russia, such as revoking Russia's MFN status, can have significant welfare implications for Russia.

Figure 3.12: Welfare Changes if the ROW Joins the Sanctioning Allies with Russian Retaliation

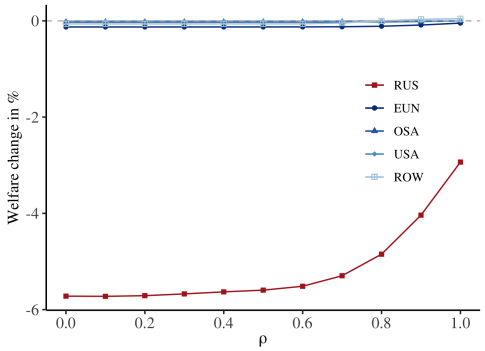

Description: This figure shows the welfare change in different countries for different levels of willingness to pay for sanctions, ρ. In this specification, the ROW joins the sanctioning countries in imposing sanctions against Russia, and Russia, the sanctioning countries, as well as the ROW have the same willingness to pay for sanctions. Welfare refers to the equilibrium real income. Changes are calculated comparing the equilibrium to current tariffs.

3.5.4 Political Weights

In this section, we calculate cost-efficient sanctions if the sanctioning countries target politically relevant sectors instead of the Russian economy as a whole. We show that an embargo on the Russian mining and energy sectors is optimal, even when there is a low willingness to pay for sanctions.

Government's Problem We assume now that the sanctioning countries want to target particular sectors in Russia according to their political relevance. Let $G_R^{pol}(\tau)$ be the politically weighted welfare in Russia and τ the vector of tariffs imposed by all countries. Formally, the politically weighted welfare is given by

$$G_R^{pol}(\tau_{nR}, \tau_{-nR}) = \sum_{j=1}^{J} \lambda_R^j \frac{I_R^j(\tau_{\mathbf{nR}}, \tau_{-\mathbf{nR}})}{P_R^C(\tau_{\mathbf{nR}}, \tau_{-\mathbf{nR}})}, \tag{3.15}$$

where λ_R^j is the political weight of sector j in Russia and $\frac{I_R^j(\tau_{\mathbf{nR}}, \tau_{-\mathbf{nR}})}{P_R^C(\tau_{\mathbf{nR}}, \tau_{-\mathbf{nR}})}$ is real income in sector j.[40]

The best response of sanctioning country n can now be formulated as the following:

$$g_n^{pol}(\tau_{-nR}) \in argmax_{\{\tau_{nR}\}} \rho G_n(\tau_{nR}, \tau_{-nR}) - (1-\rho) G_R^{pol}(\tau_{nR}, \tau_{-nR}), \tag{3.16}$$

s.t. Equilibrium Conditions 3.5-3.11,

where ρ is the willingness to pay for sanctions targeting politically relevant sectors.

Calibration We calibrate political weights to reflect the revenue share of companies owned by individuals sanctioned by the EU, UK, or US. First, we collect the names of the Russian individuals who had been sanctioned by the EU, UK, and US by March 10, 2022.[41]. Those are part of the Russian political elites, called oligarchs, which are believed to support the current regime. From the same source, we also acquire the names of the companies that they own. Second, we collect the names, sales, and industries of the top 100 Russian companies by revenue from RBC 500, a website that publishes ratings for Russian companies, and match them to the list of sanctioned people.[42] Third, we connect the industry names used in RBC 500 to OECD ICIO sectors. In the last step, we calculate, for each OECD ICIO sector, the

[40] Real income in sector j is measured with $\frac{L_R^j(\tau_{nR}, \tau_{-nR})}{L_R} \frac{I_R(\tau_{\mathbf{nR}}, \tau_{-\mathbf{nR}})}{P_R^C(\tau_{\mathbf{nR}}, \tau_{-\mathbf{nR}})}$, where $\frac{L_R^j(\tau_{nR}, \tau_{-nR})}{L_R}$ is Russia's employment share in sector j, and $\frac{I_R(\tau_{\mathbf{nR}}, \tau_{-\mathbf{nR}})}{P_R^C(\tau_{\mathbf{nR}}, \tau_{-\mathbf{nR}})}$ is real income. In this model, sector j's employment share is also the sector's share in Russian GDP. In Appendix Section A.2, we rewrite this optimal sanction problem in changes.

[41] The source is an article by the Guardian: https://www.theguardian.com/world/2022/mar/04/russia-oligarchs-business-figures-west-sanction-lists-us-eu-uk-ukraine

[42] The RBC 500 rating has been published since 2015. The rating identifies the largest Russian companies in terms of net revenue. The rating involves companies owned by Russian individuals and legal entities, regardless of their registration in Russia or abroad. The main source of the financial indicator comes from consolidated financial statements. In the case of no available consolidated financial statements, indicators are estimated.

share of sales by major Russian companies owned by oligarchs in the sector's total sales (output). We use these shares as our political weights, λ_R^j.

Table 3.3: Summary Statistics for Political Weights

Sector	# Firms owned by Oligarchs	Oligarch Share (λ_R^j)
Agriculture	2	4.89%
Mining energy	11	47.56%
Mining non-energy	6	57.57%
Petroleum	7	57.84%
Chemical	5	41.47%
Basic metals	7	12.79%
Machinery n.e.c.	1	14.31%
Manufacturing n.e.c.	1	9.75%
Service	32	8.82%

Description: This table presents the summary statistics for the political weights. The table shows, in each sector, the number of top 500 Russian firms owned by Russian oligarchs and the revenue share generated by these firms. We omit the sectors without major oligarch-owned firms.

Table 3.3 shows the summary statistics of political weights computed using the Russian oligarchs' share of revenue in each sector. Nine out of 23 sectors have oligarch-owned firms, of which the petroleum sector has the highest political weight at 57.84%, indicating that over half of the revenue in this sector is generated by firms associated with oligarchs.

Figure 3.13: Cost-Efficient Sanctions with Political Weights in the EU for Different ρs, $\rho \in [0.7, 1.0]$

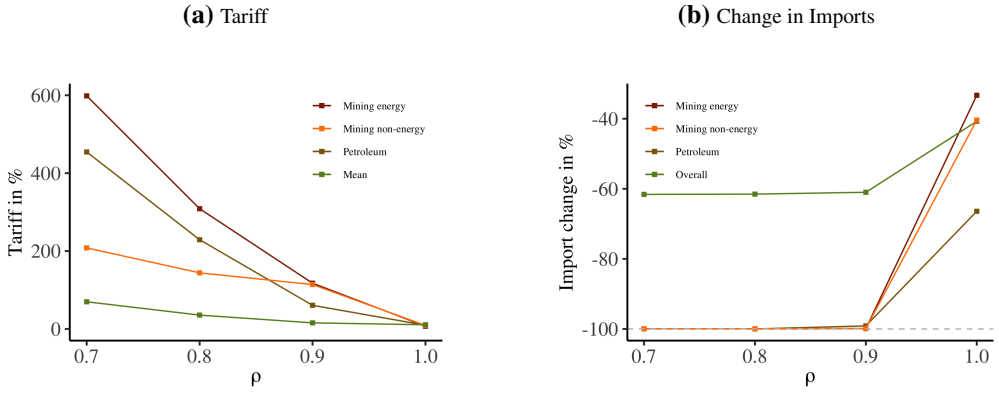

Description: This figure shows the statistics for the EU under cost-efficient sanctions with different levels of willingness to pay when the EU uses the political weights described in 3.3. Figure 3.4a plots the cost-efficient tariffs on mining energy, mining non-energy, petroleum, and the average tariff across sectors for different levels of willingness to pay for sanctions, ρ. Figure 3.4b plots the percentage change in imports in the EU for the different sectors.

Results The results presented in Figure 3.13 indicate that targeting politically connected sectors, such as the Russian mining and energy industries, with an embargo

is the most cost-efficient sanction strategy, even for countries exhibiting a low willingness to pay for sanctions. If the EU is willing to pay at least \$0.10 for each \$1 drop in Russian income, i.e., $\rho = 0.9$, tariffs should be concentrated in the mining and energy sectors. This is because these are the sectors with the highest shares of firms associated with Russian oligarchs. Moreover, such tariffs would be high enough to decrease imports of mining and energy products from Russia by almost 100%.

Figures C.15 and C.16 show the optimal sanction tariffs and resulting import changes by the US and the OSA. Similar to the EU, for a low willingness to pay for sanctions, i.e., \$0.10 to reduce Russian real income by \$1, an embargo on mining and energy sector imports from Russia would be optimal. This suggests that if sanctioning countries would like to target Russian oligarchs, a global embargo on Russia's mining and energy products is optimal.[43]

3.5.5 Robustness

In this section, we show that the cost-efficient sanctions that we derive are robust to four alternative model specifications. First, we replace the trade elasticities that we estimated with those of Caliendo and Parro (2015). Second, we consider alternative retaliation strategies by Russia. Third, we calibrate the model using estimates of the long-run trade elasticity. Fourth, we consider alternative production functions, allowing for a very high complementarity between inputs. In all these scenarios, we still find that cost-efficient sanctions are homogeneous across sectors, around 30% for small willingness to pay for sanctions and that an embargo in oil and gas should be imposed for a large enough willingness to pay that is higher than \$0.7 for \$1 income loss in Russia.

[43] Interesting, Figures C.15 and C.16 also show that if the US and the OSA only target politically relevant sectors in Russia, total imports will increase. The reason is that they have incentives to lower tariffs on the products from Russia that are not politically relevant, such that Russian employment and output can be reallocated from the politically relevant sectors to these other sectors. As the mining and energy sectors do not account for a major share of these countries' imports from Russia, a combination of high tariffs on mining and energy sectors and low tariffs on other sectors can lead to an increase in total imports.

Caliendo and Parro (2015) Trade Elasticities

We show that the cost-efficient sanctions are robust if we replace the sectoral trade elasticities that we estimated using the difference-in-differences strategy with the estimates of Caliendo and Parro (2015). This is because, as we show in Figure C.7a, these two sets of elasticities are positively correlated.[44]

Figures C.17 to C.20 show the sanctioning countries' optimal strategies under these elasticities. If they would like to pay \$0.10 for a \$1 decline in Russia's welfare, the optimal tariffs should equal, on average, about 15%. Compared to the our estimated trade elasticities, lower willingness to pay for sanctions can justify a mining and energy sector embargo under Caliendo and Parro (2015) trade elasticities. A petroleum sector embargo by the EU is optimal if the willingness to pay is as low as \$0.10 to reduce Russian real income by \$1. If the EU's willingness to pay rises to \$0.70, an embargo on all mining and energy sectors is optimal. As Figure C.7a shows, Caliendo and Parro (2015) trade elasticities are higher than ours on average, and especially so for the energy sectors. Given the willingness to pay for sanctions, higher trade elasticities provide the sanctioning countries with incentive to impose higher tariffs because they can divert more exports away from Russia and harm its income more.

Similar to Figure 3.4, if the sanctioning countries are willing to pay \$1.50 for a \$1 reduction in Russia's welfare, an embargo on Russian imports in all sectors is optimal.

Russian Retaliation Strategies

The cost-efficient sanctions are also robust to Russian retaliation strategies. The reason is that, as Russia is a relatively small export destination for the sanctioning countries (see Figure C.8c), Russia's retaliation on the sanctioning countries' exports should not strongly affect the latter group's output, income, or incentive to impose sanctions.[45] In this section, we consider two alternative strategies of Russian retaliation: in solving Problem 3.14, Russia always sets its retaliation tariff to

[44] The correlation is 0.57.

[45] This is also corroborated by Figure 3.8, which shows that the sanctioning countries' real income is not significantly affected by ρ – the willingness to pay to minimize the opponent's real income in both the the sanctioning countries and Russia.

maximize its own real income ($\rho_{RUS} \equiv 1$) and to minimize the sanctioning countries' real income ($\rho_{RUS} \equiv 0$).

Figures C.21 to C.26 show the sanctioning countries' optimal tariffs and the associated import changes, with $\rho_{RUS} \equiv 1$. Figures C.27 to C.32 show the same set of variables for $\rho_{RUS} \equiv 0$. Similar to Section 3.5 where ρ_{RUS} is equal to that of the sanctioning countries, for low willingness to pay to sanction Russia ($0.10 for a $1 real income drop in Russia), the sanctioning countries should optimally impose tariffs of about 20% on all sectors. If the sanctioning countries would like to pay $0.7 of their real income to reduce Russian real income by $1, an embargo on mining and energy sectors would be optimal for the EU. For willingness to pay higher than $1.50, a embargo on all Russian products by all sanctioning countries would be optimal.

Long-Run Trade Elasticity

Sanctions, like other trade policies, typically last for an extended period. Therefore, the relevant trade elasticity for calibrating the model is the long-run trade elasticity. In Appendix A.3, we estimate the long-run trade elasticity using a difference-in-differences method building on Section 3.2.4 and re-calibrate the model. We find that, as expected, the short-run trade elasticity is much smaller than the long-run counterpart. Furthermore, the trade elasticity obtained in Section 3.2.4 does not differ statistically from the long-run trade elasticity. Using the long-run trade elasticities, we demonstrate that it would still be optimal for the EU to impose an embargo on Russian mining and energy sectors with a sufficiently high willingness to pay for sanctions. Moreover, the results are not quantitatively different from the baseline calibration because the elasticity estimated in Section 3.2.4 is close to the long-run trade elasticity.

CES Production Function

The elasticity of substitution between inputs plays a crucial role in the impact of sanctions. For example, if petroleum can be readily substituted for other inputs or labor, imposing sanctions on Russia would have a limited impact on domestic production. In this section, we demonstrate that our main findings remain valid for

a range of elasticities of substitution across inputs.

For this section, we assume that production is given by

$$Y_n^j = A_n^j \left((e_n^j)^{\frac{1}{\rho}} (L_n^s)^{\frac{\rho-1}{\rho}} + \sum_{k=1}^{J} (f^{j,k})^{\frac{1}{\rho}} (M_n^{j,k})^{\frac{\rho-1}{\rho}} \right)^{\frac{\rho}{\rho-1}} \tag{3.17}$$

where A_n^j is the TFP of sector j in country n, L_n^s is the labor demand by sector s, and $M_n^{j,k}$ is the quantity of sector k output used by sector j. ρ denotes the elasticity of substitution across inputs. e_n^j and $f^{j,k}$ are labor- and input-augmenting technology parameters.

Figure 3.14 shows the results of the model using the production function given by equation 3.17 and a calibrated elasticity of substitution of 0.66, as estimated by de Souza and Li (2021).[46] Overall, the patterns of cost-efficient tariffs are still the same. Even for low willingness to pay for sanctions, the EU should reduce trade with Russia through a tariff ranging from 20% to 30%, depending on the willingness to pay for sanctions. If ρ is below 0.6, i.e., the EU is willing to pay \$0.70 dollars for each \$1 drop in Russian income, the EU should impose an embargo on the Russian petroleum and mining energy sectors.

In the Appendix, Figure C.34 explores the cost-efficient sanctions with an even lower elasticity of substitution between inputs of 0.1. The qualitative results remain consistent, with an optimal embargo on the Russian petroleum and mining energy sectors for ρ below 0.6. When willingness to pay for sanctions is low, the cost-efficient sanctions are homogeneous across sectors and effectively decrease trade with Russia.

3.6 Conclusion

In this paper, we study how countries should optimally impose import sanctions. We investigate how these sanctions depend on countries' willingness to pay for sanctions, trade shares, and trade elasticities. We develop a model of tariff competition that features multiple countries, multiple sectors, and input-output linkages. Countries weigh the objectives of maximizing their own income and diminishing their opponent's income, and respond optimally to other countries' tariff strategies.

[46] Oberfield and Raval (2021) finds similar elasticity of substitution across inputs.

Figure 3.14: Cost-Efficient Sanctions in the EU for Different ρs with CES Production Function

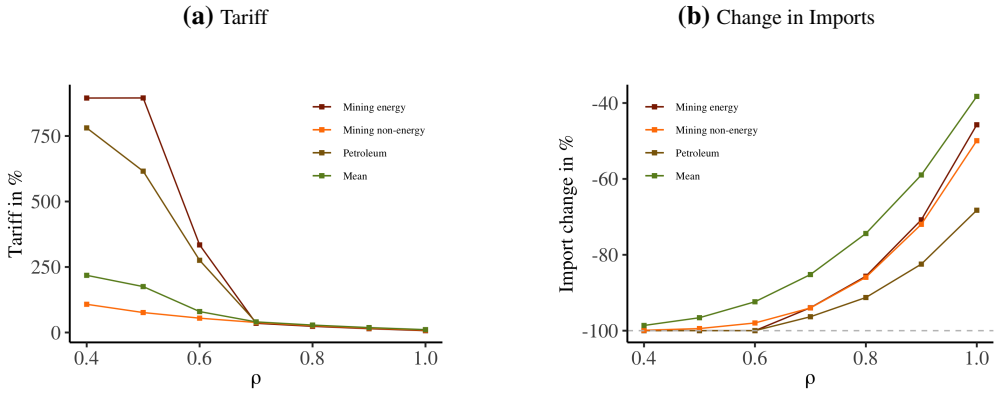

Description: This figure shows the statistics for the EU under cost-efficient sanctions with different levels of willingness to pay for sanctions. The production function is as described in 3.17 and the elasticity of substitution between labor and materials is calibrated to 0.66, as in de Souza and Li (2021). Figure 3.14a plots the cost-efficient tariff on mining energy, mining non-energy, petroleum, and the average tariff across sectors for different levels of willingness to pay for sanctions, ρ. Figure 3.14b plots the percentage change in imports in the EU for different sectors.

The Russian invasion of Ukraine has caused significant casualties and economic damage, and threatened global stability and economic prosperity. We apply the model to study the cost-efficient sanctions on Russia. Using the difference-in-differences empirical strategy developed in de Souza and Li (2021) and drawing on global AD investigations and tariffs from the Global Anti-dumping Database (Bown 2005), we first document that tariffs on imports from Russia strongly decrease Russian total exports and the sanctioning countries' total imports of the targeted products. Using the same empirical strategy, we estimate the model's trade elasticities for each sector.

We find that if the sanctioning countries would like to pay \$0.10 of real income to diminish Russian real income by \$1, the sanctioning tariffs should be about 20% and be similar across sanctioning countries and across sectors. If the sanctioning countries' willingness to pay rises to \$0.7, the EU should impose an embargo on the Russian energy and mining sectors. If the willingness to pay increases to \$1.50, an embargo on all sectors is close to optimal.

We also find that sanctions by the EU can lead to larger real income loss in Russia, compared to those by the US and other sanctioning allies. Russian retaliation slightly increases the welfare loss in the sanctioning countries. However, it leads to substantially larger welfare loss in Russia.

Furthermore, if sanctions target the sectors that are politically relevant, a global

embargo on Russia's mining and energy sectors is optimal even when willingness to pay for sanctions is low.

Many countries have implemented trade sanctions against Russia. With these analyses, we propose a rationale as to why the observed sanctions have differed across countries and sectors. We provide a toolbox that helps policy makers to optimally impose sanctions and restore peace in the region, as they trade off between undermining Russia's capacity to continue its war and the cost to domestic welfare.

Chapter 4

Conclusion

In conclusion, this dissertation explores crucial aspects of spatial economics and international trade through three comprehensive papers. The first paper addresses spatial inequalities in educational resources, highlighting the significance of geographic distribution in shaping individual educational decisions and long-term skill composition. By analyzing the context of China, it reveals that equitable distribution of colleges can enhance overall welfare and mitigate spatial inequalities. The second paper investigates the U.S.–China trade war, demonstrating that maintaining trade war tariffs can potentially improve U.S. welfare post-negotiation, regardless of the relative bargaining power. Finally, the third paper provides insights into the strategic implementation of trade sanctions, particularly against Russia, identifying the most cost-efficient approaches under varying objectives and willingness to pay. Together, these studies offer valuable policy implications for addressing spatial disparities, navigating international trade disputes, and effectively employing trade sanctions, contributing to the broader field of spatial economics and international trade policy. Future research could extend the quantitative models developed in these studies in several interesting directions. First, examining the government's role in the allocation of educational resources would be valuable, particularly in identifying optimal investment decisions made by local governement. Second, the dynamic spatial model could be employed to study other important life decisions, such as fertility and marriage, providing a more comprehensive understanding of how spatial factors influence these choices over a lifetime.

Appendix A

Appendix for Chapter 2

A.1 Steady State in Levels

The steady state of the equilibrium is described by the following system of equations:

$$p^s_{ni} = \tau_{ni}\frac{1}{A^s_i}\left[{A^s_i}^{-\omega(\eta-1)}\chi^s {w^l_{it}}^{1-\eta} + {A^s}_i^{\omega(\eta-1)}(1-\chi){w^h_{it}}^{1-\eta}\right]^{\frac{1}{1-\eta}}$$

$$\alpha^s_{ni} = \frac{{p^s_{ni}}^{1-\sigma}}{\sum_o {p^s}_{no}^{1-\sigma}}$$

$$P_n = \left(\frac{P^{s1}_n}{\zeta}\right)^{\zeta}\left(\frac{P^{s2}_n}{1-\zeta}\right)^{1-\zeta}$$

$$\mathbb{L}(n,h)w^h_n + \mathbb{L}(n,l)w^l_n = \sum_s\sum_o \alpha^s_{on}\left(\mathbb{L}^s(o,h)w^h_o + \mathbb{L}^s(o,l)w^l_o\right)$$

$$V^j(n,e) = U^j(n,e) + \kappa\log\sum_{o\in\mathscr{N}}\exp\left(\beta V^{j+1}(o,e) - D^{j+1}_{on}\right)^{1/\kappa}$$

$$V^J(n,e) = U^J(n,e)$$

$$V^0(n,e) = \kappa\log\sum_{o\in\mathscr{N}}\exp\left(V^1(o,e) - D^1_{o,n} - 1_{e=h}F_o\right)^{1/\kappa}$$

$$\pi^j(n'|n,e) = \frac{\exp(\beta V^{j+1}(n',e) - D^{j+1}_{n'n})^{1/\kappa}}{\sum_{o\in\mathscr{N}}\exp(\beta V^{j+1}(o,e) - D_{on})^{1/\kappa}}$$

$$\pi^0(n',e|n) = \frac{\exp\left(U^1(n',e) - D^1_{n'n} - 1_{e=h}F_{n'}\right)^{1/\kappa}}{\sum_{o\in\mathscr{N}}\exp(U^1(o,e) - D^1_{on} - 1_{e=h}F_o)^{1/\kappa}} \times \frac{\exp(V^0(n,e))^{1/\psi}}{\sum_{e'}\exp\left(V^0(n,e')\right)^{1/\psi}}$$

$$L^0_n = L^J_n$$

$$L^1(n',e') = \sum_n L^0_n\pi(n',e'|n)$$

$$L^j(n',e) = \sum_n L^{j-1}(n,e)\pi^{j-1}(n'|e,n) \quad j = 2,...,J$$

$$\mathbb{L}(n,e) = \mathbb{L}_{n,h} + \mathbb{L}_{n,l}$$

A.2 Algorithm to solve for the path

The economy evolves according to the law of motion of labor distribution. The following algorithm describe the process.

1. Guess $\{L_t^j(n,e)\}$ for a long enough period.
2. Solve for $\{w_{nt}^h, w_{nt}^l\}$ using the market clearing condition along with the relationship between w_{nt}^h and w_{nt}^l.
3. Compute recursively the value functions $\{V_t^j(n,e)\}$ at each location and time period for each individual type using equation 1.8.
4. Compute migration probability $\{\pi_t n', e'|n\}$ and $\{\pi_t^j(n'|n,e)\}$ using equation 1.10 and equation 1.9.
5. Update $\{L^j(n,e)\}$ using the law of motion, repeat until converge.

A.3 Additional figures

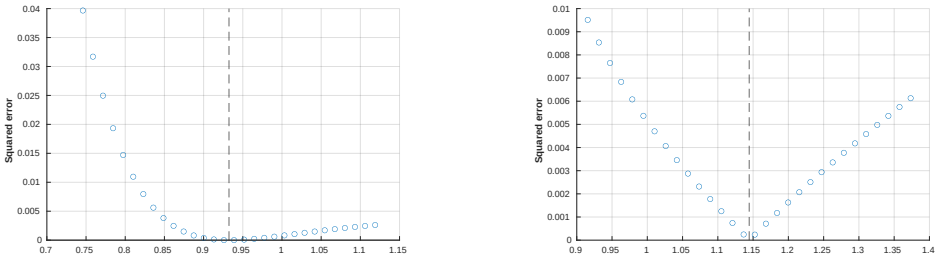

(a) $\bar{D}$ **(b)** ψ

Figure A.1: Local plot for Nested NLS Estimation

Note:The panels in this figure displays the objective function for estimating $\bar{D}$ and ψ with each parameter varying while keeping the other parameters at their estimated values. The dashed line indicates the estimated value for $\bar{D}$ andψ.

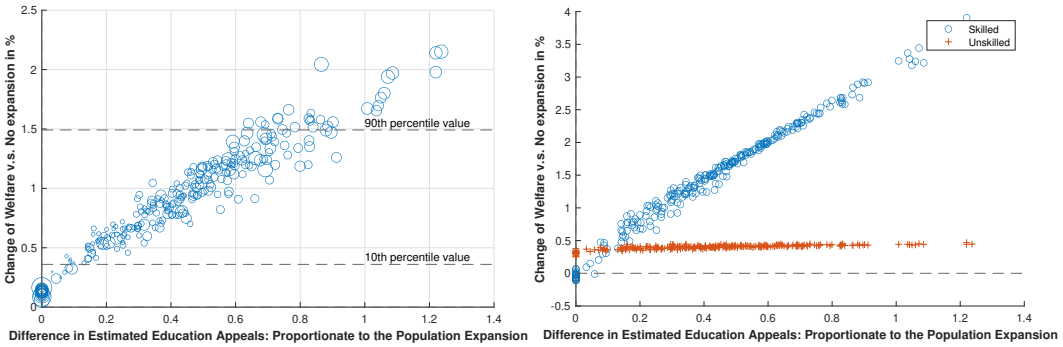

(a) Change in Welfare **(b)** Change in Welfare by skill type

Figure A.2: Proportionate to the Population Expansion

Note: Figure A.2a shows the welfare change by locations. Figure A.2b shows the welfare change of skilled and unskilled by locations. All changes are compared against the scenario without college expansion. Each dot represents a location.

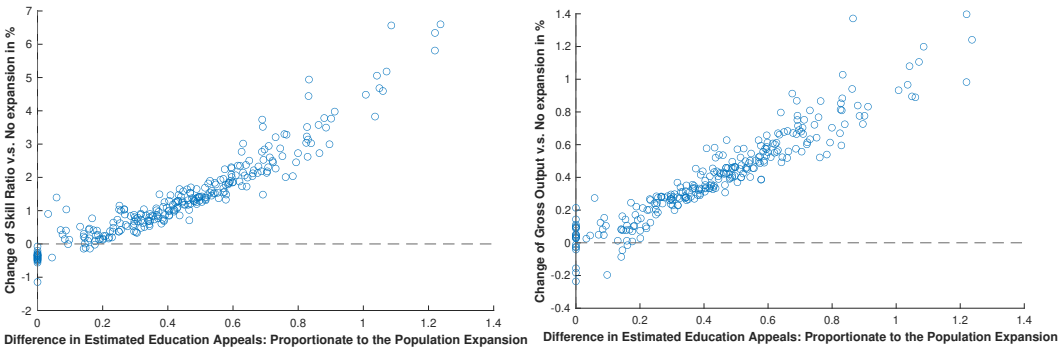

(a) Change in Skill Ratios **(b)** Change in Output

Figure A.3: Proportionate to the Population Expansion

Note: Figure A.3a shows the skill ratio change by locations. Figure A.3b shows the gross output change by locations. All changes are compared against the scenario without college expansion. Each dot represents a location.

Appendix B

Appendix for Chapter 3

A.1 Equilibrium conditions in relative changes

To solve the competitive general equilibrium, we adopt the hat-algebra approach, as in Dekle et al. (2007), to avoid calibrating unchanged underlying parameters. The equivalent hat-algebra equilibrium is stated as follows. For given tariff changes, an equilibrium is a set of $\{\hat{\omega}_n, \hat{x}_n^j, \hat{L}_n, X_n^{j\prime}\}$ such that:

Input bundle:

$$\hat{x}_n^j = (\hat{\omega}_n)^{\gamma_n^j} \prod_{k=1}^{J} \left(\hat{P}_n^k\right)^{\gamma_n^{jk}}$$

Labor mobility condition:

$$\hat{L}_n = \frac{\left(\frac{\hat{\omega}_n}{\varphi_n \hat{P}_n \hat{U} + (1-\varphi_n)\hat{b}_n}\right)^{1/\beta_n}}{\sum_i L_i \left(\frac{\hat{\omega}_i}{\varphi_i \hat{P}_i \hat{U} + (1-\varphi_i)\hat{b}_i}\right)^{1/\beta_i}} L$$

Regional market clearing in final goods:

$$X_n^{j\prime} = \sum_{k=1}^{J} \gamma_n^{k,j} \left(\sum_{i=1}^{N+M} \frac{\pi_{in}^{k\prime}}{\tau_{in}^{k\prime}} X_i^{k\prime} \right) + \alpha^j I_n' L_n'$$

for $n \in \mathscr{U}\mathscr{S}$, $I_n' L_n' = \left(\hat{\omega}_n \left(\hat{L}_n\right)^{1-\beta_n} (I_n L_n + \Upsilon_n + S_n - \Lambda_n) + \sum_{j=1}^{J} \sum_{i=1}^{N+M} t_{ni}^{j'} \frac{\pi_{ni}^{j'}}{\tau_{ni}^{j'}} X_n^{j'} - S_n' - \Upsilon_n' \right)$

for $n \in \overline{\mathscr{U}\mathscr{S}}$, $I_n' L_n' = \hat{\omega}_n \omega_n L_n + \sum_{j=1}^{J} \sum_{i=1}^{N+M} t_{ni}^{j'} \frac{\pi_{ni}^{j'}}{\tau_{ni}^{j'}} X_n^{j'} - S_n$

Labor market clearing:

$$VA' = \sum_j \gamma_n^j \sum_i \frac{\pi_{in}^{j\prime}}{\tau_{in}^{j\prime}} X_i^{j\prime}$$

for $n \in \mathscr{US}$, $VA_n' = \hat{\omega}_n \left(\hat{L}_n\right)^{1-\beta_n} (L_n I_n + \Upsilon_n + S_n - \Lambda_n)$

for $n \in \overline{\mathscr{US}}$, $VA_n' = \hat{\omega}_n \omega_n L_n$

Price index:

$$\hat{P}_n^j = \left(\sum_{i=1}^{N+M} \pi_{ni}^j \left[\hat{\kappa}_{ni}^j \hat{x}_i^j \right]^{-\theta^j} \right)^{-1/\theta^j}$$

Expenditure shares:

$$\pi_{ni}^{j'} = \pi_{ni}^j \left(\frac{\hat{x}_i^j}{\hat{P}_n^j} \hat{\kappa}_{ni}^j \right)^{-\theta^j}$$

Aggregate price index:

$$\hat{P}_n = \prod_{j=1}^{J} \left(\hat{P}_n^j\right)^{\alpha^j}$$

Utility level within the U.S.:

$$\hat{U} = \frac{1}{L} \sum_n L_n \left(\frac{1}{\varphi_n} \frac{\hat{\omega}_n}{\hat{P}_n} \left(\hat{L}_n\right)^{1-\beta_n} - \frac{1-\varphi_n}{\varphi_n} \frac{\hat{L}_n \hat{b}_n}{\hat{P}_n} \right)$$

$$\hat{b}_n = \frac{u_n' + s_n' - \lambda_n'}{u_n + s_n - \lambda_n}, \ \varphi_n = \frac{1}{1 + \frac{\Upsilon_n + S_n - \Lambda_n}{L_n I_n}}$$

Utility level outside of the U.S.:

$$\hat{U}_n = \frac{\hat{I}_n}{\hat{P}_n} = \frac{I_n'}{I_n \hat{P}_n}$$

The derivation is as follows. For regions in the U.S., using the equilibrium condition $r_n H_n = \frac{\beta_n}{1-\beta_n} w_n L_n$ and the definition of $\omega_n = (r_n/\beta_n)^{\beta_n} (\omega_n/(1-\beta_n))^{1-\beta_n}$, we can express wages as $\frac{\omega_n}{1-\beta_n} = \omega_n \left(\frac{H_n}{L_n}\right)^{\beta_n}$. Therefore, U can be expressed as

$$U = \left(\frac{H_n}{L_n}\right)^{\beta_n} \frac{\omega_n}{P_n} - \frac{u_n}{P_n} - \frac{s_n}{P_n} + \frac{\lambda_n}{P_n},$$

where $u_n = \Upsilon_n / L_n = (\iota r_n H_n - \chi L_n)$, $s_n = S_n / L_n$, and $\lambda_n = \Lambda_n / L_n = \sum_j^J \sum_{i=1}^{N+M} t_{ni}^j \frac{\pi_{ni}^j}{\tau_{ni}^j} X_n^j / L_n$. After solving for L_n and using the labor market clearing condition $\sum_n^N L_n = L$, we can get

$$U = \frac{1}{L} \sum_{n=1}^{N} \left(\frac{\omega_n}{P_n} (H_n)^{\beta_n} L_n^{1-\beta_n} - \frac{\Upsilon_n}{P_n} - \frac{S_n}{P_n} + \frac{\Lambda_n}{P_n} \right),$$

and labor in each location n can be expressed as

$$L_n = \frac{H_n \left[\frac{\omega_n}{P_n U + u_n + s_n - \lambda_n}\right]^{1/\beta_n}}{\sum_{i=1}^{N} H_i \left[\frac{\omega_i}{P_i U + u_i + s_i - \lambda_i}\right]^{1/\beta_i}} L.$$

A.2 Cooperative tariff bargaining in hat-algebra

We use the hat-algebra approach to solve the cooperative tariff bargaining problem (2.8) stated in the main text to avoid calibrating unchanged underlying parameters. The equivalent hat-algebra version of the cooperative tariff bargaining problem is as follows:

$$\max_{\left\{\hat{\omega}_n, \hat{x}_n^j, X_n^{j,}, \hat{L}_n, \hat{\tau}_{US,chn}\right\}} \left(\hat{U}_{US} - 1\right)^{\psi} \left(\hat{U}_{chn} - 1\right)^{1-\psi},$$

subject to competitive equilibrium conditions in relative changes,

as in A.1, and $\hat{U}_{US} \geq 1,\ \hat{U}_{chn} \geq 1.$

A.3 Cooperative tariff bargaining in hat-algebra with political weights

We rewrite the cooperative tariff bargaining problem in changes if governments now maximize their politically weighted welfare defined in (2.9). All the equilibrium conditions in A.2 remain the same, except for the change in welfare levels within and outside of the U.S. which are equal to the following:

Utility level within the U.S.:

$$\hat{U} = \frac{1}{L} \sum_{n=1}^{N} \sum_{j=1}^{J} \frac{\sigma^j TVA^{j\prime}}{\sum_{j=1}^{J} \sigma^j TVA^j} \frac{\sum_{j=1}^{J} TVA^j}{\sum_{j=1}^{J} TVA^{j\prime}} L_n \left(\frac{1}{\varphi_n} \frac{\hat{\omega}_n}{\hat{P}_n} \left(\hat{L}_n\right)^{1-\beta_n} - \frac{1-\varphi_n}{\varphi_n} \frac{\hat{L}_n \hat{b}_n}{\hat{P}_n} \right)$$

$$TVA^j = \sum_{n=1}^{N} X_n^j \gamma_n^j, TVA^{j\prime} = \sum_{n=1}^{N} \hat{X}_n^j X_n^j \gamma_n^j, \hat{b}_n = \frac{u_n' + s_n' - \lambda_n'}{u_n + s_n - \lambda_n}, \varphi_n = \frac{1}{1 + \frac{\Upsilon_n + S_n - \Lambda_n}{L_n I_n}}$$

Utility level outside of the U.S.:

$$\hat{U}_n = \sum_{j=1}^{J} \frac{\sigma^j VA^{j\prime}}{\sum_{j=1}^{J} \sigma^j VA^j} \frac{\sum_{j=1}^{J} VA^j}{\sum_{j=1}^{J} VA^{j\prime}} \frac{I_n'}{I_n \hat{P}_n}$$

$$VA^j = X^j \gamma^j, VA_j' = \hat{X}^j X^j \gamma^j$$

A.4 Figure appendix

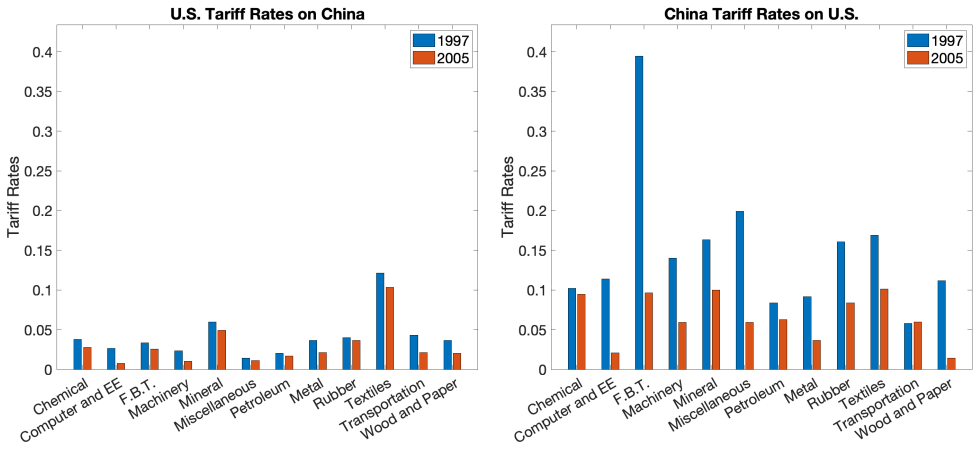

Figure B.1: Applied Tariff Rates of the U.S. and China

Note: This figure displays the applied tariff rates between the U.S. and China in 1997 (before China's accession to the WTO) and in 2005 (after China's accession to the WTO). Tariff data are aggregated into sectors based on trade volume. Sectors are arranged in alphabetical order.

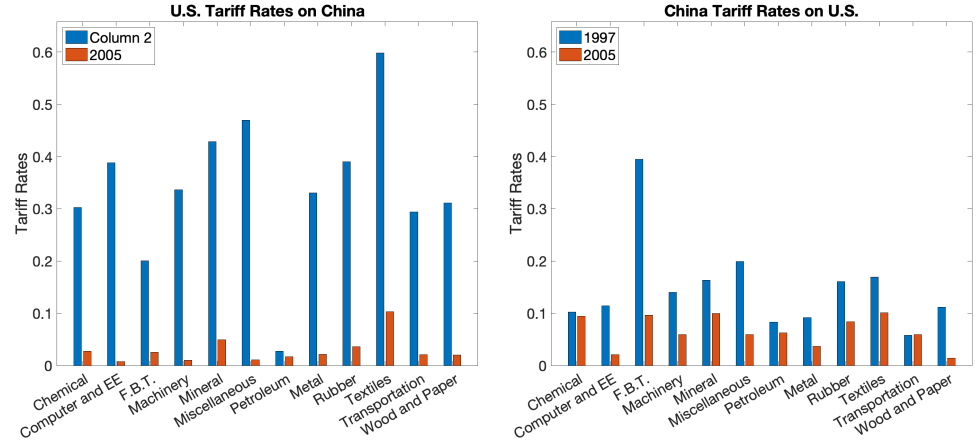

Figure B.2: Applied Tariff Rates versus U.S. Column 2 Tariff Rates

Note: The left panel displays U.S. column 2 tariff rates and the 2005 applied rates. The right panel is the same as the right panel of Figure B.1 and is shown for comparison purposes. Tariff data are aggregated into sectors based on trade volume. Sectors are arranged in alphabetical order.

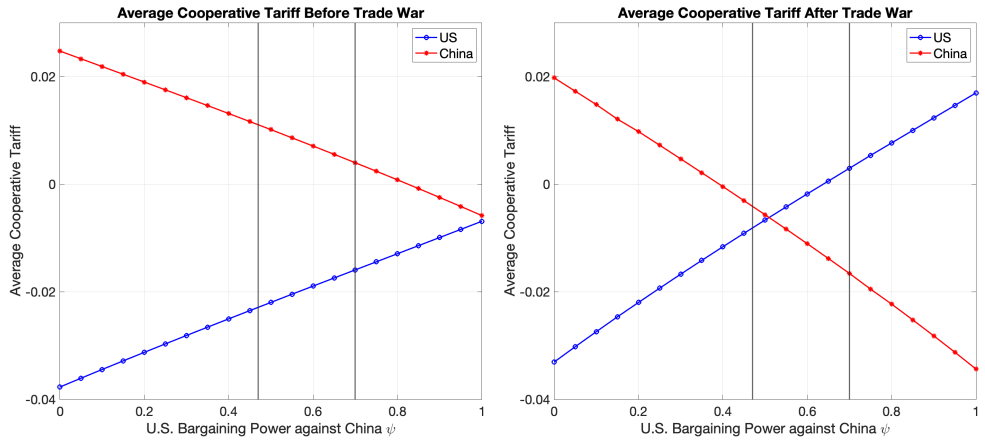

Figure B.3: Average Post-Negotiation Tariffs of the U.S. and China (Negative Tariffs Allowed)

Note: This figure plots the the simple average of post-negotiation tariffs across sectors for the U.S. and China as in Figure 2.2, but allows for negative tariff rates.

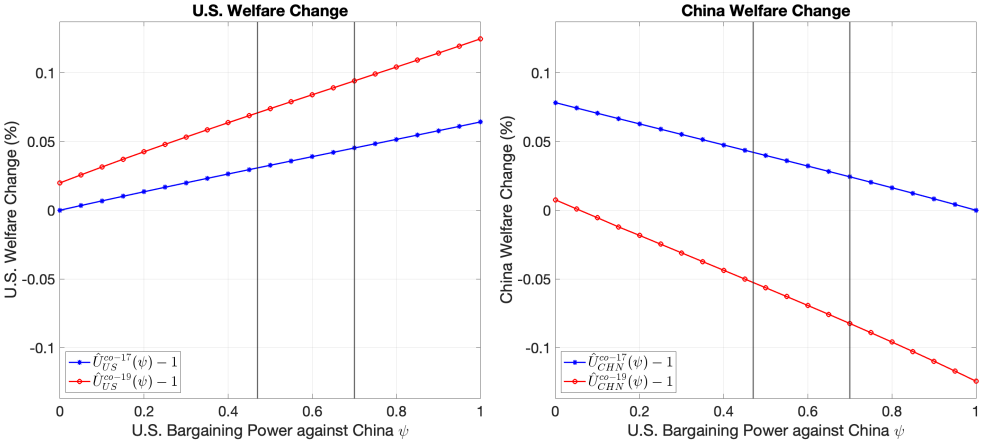

Figure B.4: Post-Negotiation Welfare Change (Negative Tariffs Allowed)

Note: This figure illustrates the post-negotiation welfare change (relative to the 2017 baseline) of the two scenarios for the U.S. and China as in Figure 2.3, but allows for negative tariff rates.

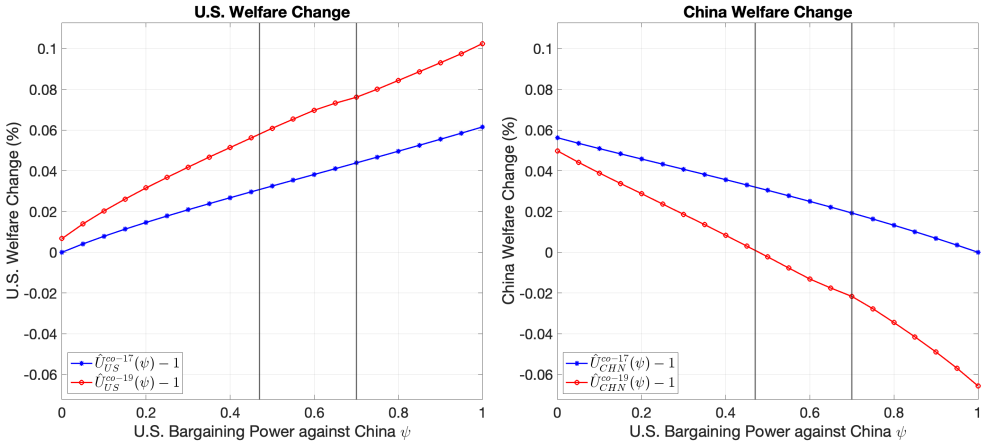

Figure B.5: Post-Negotiation Welfare Change (ROW Fixed)

Note: This figure illustrates the post-negotiation welfare change (relative to the 2017 baseline) of the two scenarios for the U.S. and China as in Figure 2.3, but keeps the U.S. and Chinese tariffs on goods from ROW unchanged.

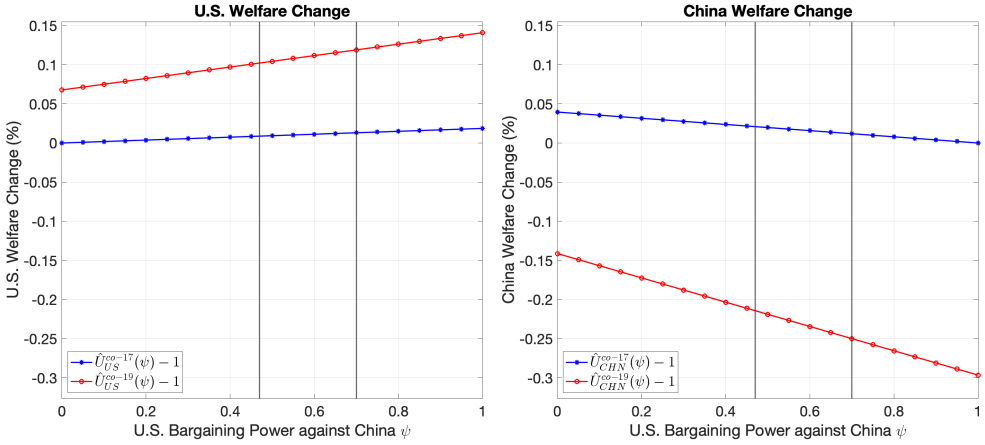

Figure B.6: Post-Negotiation Welfare Change (Fixed Trade Balances)

Note: This figure illustrates the post-negotiation welfare change (relative to the 2017 baseline) of the two scenarios for the U.S. and China as in Figure 2.3, but fixes the trade balance between the U.S. and China at 2017 level.

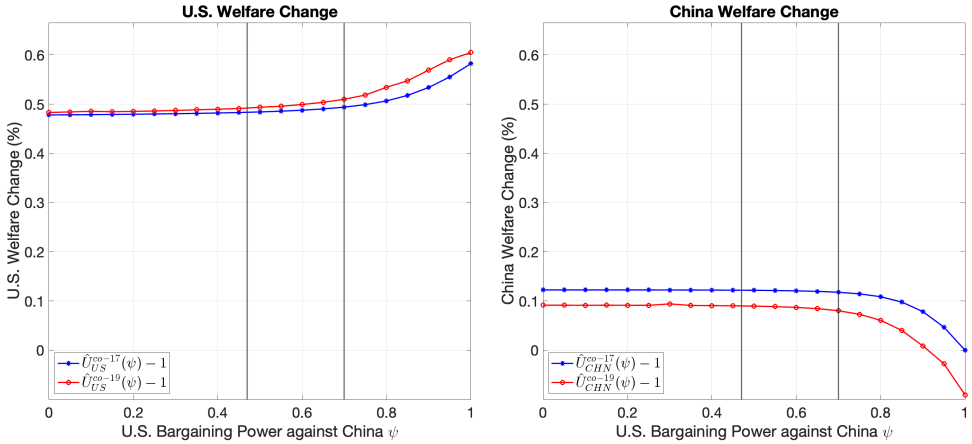

Figure B.7: Post-Negotiation Welfare Change (Elasticities from Caliendo and Parro (2015))

Note: This figure illustrates the post-negotiation welfare change (relative to the 2017 baseline) of the two scenarios for the U.S. and China as in Figure 2.3, but uses the elasticities of substitution from Caliendo and Parro (2015).

Appendix C

Appendix for Chapter 4

A.1 Empirics

Summary Statistics

Table C.1 shows the summary statistics for AD investigations targeting Russia. During the sample period (1995-2020), Russia faced 393 AD investigations, of which 298 (75%) concluded with an affirmative ruling. 150 products that Russia exported faced AD investigations, of which 112 were subject to tariff increases.[1] Twenty countries imposed AD tariffs on Russia. Conditional on an investigation that led to an AD tariff increase, the average tariff was 123% and the median tariff was 43%. Figure C.1a shows the number of AD investigations and affirmative investigations by year. Figure C.1b shows that, conditional on an investigation with an affirmative ruling, the average AD tariff was the highest on the metal and machinery sectors.

Table C.2 shows the summary statistics, by country, for the AD investigations targeting Russia. The US conducted the most AD investigations, followed by the EU, Canada, and Ukraine. Conditional on an affirmative investigation, the AD tariff rate imposed by the US was the highest (497%).

Table C.3 shows the summary statistics for AD investigations that all countries imposed on their trade partners. There were a total of 15,131 AD investigations, of which 10,370 (68%) concluded with an affirmative ruling; 1,585 products faced AD investigations, of which 1,298 were subject to tariff increases. Conditional on

[1] A product refers to an HS 6-digit code.

an investigation that led to an AD tariff increase, the average tariff was 128% and the median tariff was 55%. Figure C.2a shows the number of global AD investigations and affirmative investigations by year. Figure C.2b shows that, on the world level, conditional on an investigation with an affirmative ruling, the average AD tariff was the highest on the mining (non-energy), mining support, and automobile sectors. Tables C.4 and C.5 show the summary statistics for global AD investigations by the investigating country and the exporting country.

Table C.1: Statistics for AD Investigations Targeting Russia

	Tariff Increase	No Tariff Chg	All
# Investigations	298	105	393
# Products	112	74	150
# Countries	20	11	20
Avg. Tariff	1.23	0	0.90
Med. Tariff	0.43	0	0.33

Notes: This table presents the statistics for the AD investigations targeting Russia between 1995 and 2020. Each investigation was conducted on a product from Russia. The average and median tariffs are the simple average and the median across investigations. The investigation-level tariff is computed in ad-valorem terms.

Table C.2: AD Investigations Targeting Russia by Country

	Investigations		Treated		All	
Country	**# Investigations**	**% Treated**	**Avg. Tariff**	**Med. Tariff**	**Avg. Tariff**	**Med. Tariff**
United States	76	52.63%	4.97	3.13	2.62	1.57
European Union	68	82.35%	0.54	0.35	0.45	0.33
Canada	43	79.07%	1.44	0.87	1.14	0.86
Ukraine	32	90.63%	0.39	0.34	0.36	0.32
India	25	48.00%	0.71	0.68	0.34	0.00
Argentina	22	63.64%	0.82	0.60	0.52	0.60
China	22	100.00%	0.26	0.18	0.26	0.18
Philippines	21	42.86%	0.15	0.15	0.06	0.00
Venezuela	15	100.00%	0.64	0.64	0.64	0.64
Mexico	12	83.33%	0.49	0.34	0.41	0.30
Indonesia	11	100.00%	0.35	0.29	0.35	0.29
Pakistan	9	100.00%	0.29	0.28	0.29	0.28
Turkey	9	44.44%	0.17	0.10	0.08	0.00
Colombia	7	100.00%	1.35	0.50	1.35	0.50
Brazil	6	66.67%	0.24	0.29	0.16	0.16
South Korea	5	100.00%	0.25	0.30	0.25	0.30
South Africa	5	100.00%	0.78	0.78	0.78	0.78
Taiwan	3	33.33%	0.39	0.39	0.13	0.00
Australia	1	100.00%	0.29	0.29	0.29	0.29
Peru	1	100.00%	0.07	0.07	0.07	0.07

Description: This table presents summary statistics for the AD investigations targeting Russia by the country that initiated the investigation. The table shows the number of investigations, the fraction of the investigations that led to a tariff increase, the average tariff rate conditional on an affirmative investigation, and the average tariff rate of all investigations. The AD data are from the Global Anti-dumping Database (Bown 2005). The sample runs from 1995 to 2020.

Table C.3: Statistics for Global AD Investigations

	Tariff Increase	No Tariff Chg	All
# Investigations	10370	4761	15131
# Products	1298	808	1585
# Countries inv	31	31	31
# Countries exp	95	89	106
Avg. Tariff	1.28	0	0.88
Med. Tariff	0.55	0	0.29

Notes: This table presents the statistics for the AD investigations targeting Russia between 1995 and 2020. Each investigation was conducted on a product from Russia. The average and median tariffs are the simple average and the median across investigations. The investigation-level tariff is computed in ad-valorem terms.

Figure C.1: Summary Statistics for AD Investigations Targeting Russia

(a) Number of AD Investigations by Year

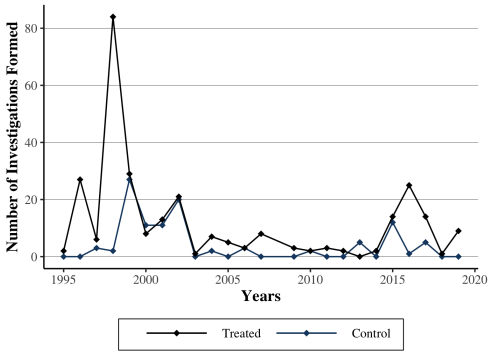

(b) Ave. AD Tariff Rate by Sector

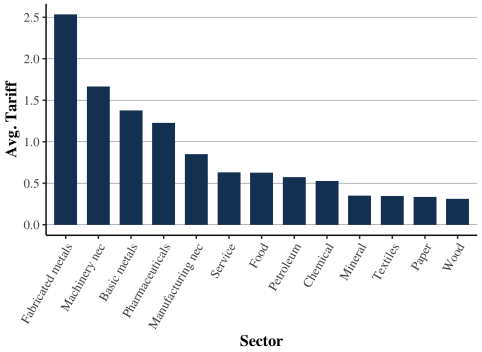

Description: This figure shows the summary statistics for the AD investigations and AD tariffs targeting Russia. The left panel shows the number of AD investigations with affirmative and negative rulings by year. The right panel shows, by sector, the average tariff rate across AD investigations conditional on an affirmative ruling. The same sector classification is used as in the 2018 OECD Inter-country Input-output Database (OECD ICIO 2018). The AD data are from the Global Anti-dumping Database (Bown 2005). The sample runs from 1995 to 2020.

Figure C.2: Summary Statistics for Global AD Investigations

(a) Number of AD Investigations by Year

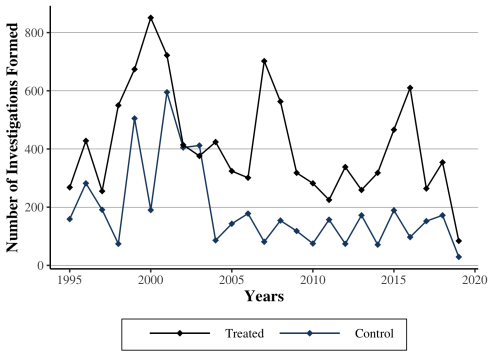

(b) Ave. AD Tariff Rate by Sector

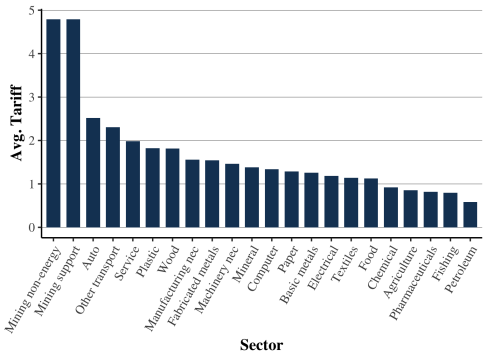

Description: This figure shows the summary statistics for the AD investigations and AD tariffs that all countries imposed on their trade partners. The left panel shows the number of AD investigations with affirmative and negative rulings by year. The right panel shows, by sector, the average tariff rate across AD investigations conditional on an affirmative ruling. The same sector classification is used as in the 2018 OECD ICIO. The AD data are from the Global Anti-dumping Database (Bown 2005). The sample runs from 1995 to 2020.

Table C.4: Global AD Investigations by Investigating Country

	Investigations		Treated		All	
Country	**# Investigations**	**% Treated**	**Avg. Tariff**	**Med. Tariff**	**Avg. Tariff**	**Med. Tariff**
United States	3611	66.46%	2.17	0.90	1.44	0.37
India	1997	81.47%	0.80	0.51	0.65	0.50
European Union	1875	60.27%	0.92	0.56	0.56	0.23
Canada	1250	63.76%	1.91	1.09	1.22	0.49
Argentina	885	71.75%	1.24	0.62	0.89	0.50
Brazil	681	48.31%	1.42	0.76	0.69	0.00
Turkey	652	75.31%	1.59	0.45	1.20	0.29
China	624	98.40%	0.44	0.29	0.43	0.29
Australia	544	64.34%	0.28	0.15	0.18	0.07
Sourh Africa	383	63.71%	0.54	0.45	0.34	0.28
South Korea	366	68.03%	0.32	0.28	0.22	0.15
Indonesia	320	65.63%	0.27	0.21	0.18	0.11
Peru	310	64.19%	2.35	0.44	1.51	0.29
Mexico	275	83.64%	1.41	0.81	1.18	0.75
Pakistan	259	81.08%	0.39	0.28	0.32	0.22
Russia	164	59.76%	0.34	0.23	0.20	0.15
Malaysia	150	55.33%	0.19	0.13	0.11	0.06
Colombia	132	52.27%	1.93	0.77	1.01	0.10
Venezuela	120	84.17%	1.42	2.04	1.19	0.95
New Zealand	102	33.33%	1.05	0.58	0.35	0.00
Taiwan	96	51.04%	0.44	0.22	0.22	0.14
Ukraine	91	91.21%	0.89	0.45	0.81	0.41
Israel	83	46.99%	2.24	1.18	1.05	0.00
Philippines	44	40.91%	0.31	0.15	0.13	0.00
Trinidad and Tobago	28	82.14%	1.76	1.92	1.44	1.92
Chile	26	57.69%	0.31	0.23	0.18	0.10
Japan	19	89.47%	0.38	0.40	0.34	0.29
Jamaica	16	93.75%	0.51	0.22	0.48	0.22
Uruguay	10	30.00%	0.63	0.55	0.19	0.00
Costa Rica	9	77.78%	0.98	0.13	0.76	0.13
Ecuador	9	11.11%	0.30	0.30	0.03	0.00

Description: This table presents summary statistics for global AD investigations by the country that initiated the investigation. The table shows the number of investigations, the fraction of the investigations that led to a tariff increase, the average tariff rate conditional on an affirmative investigation, and the average tariff rate of all investigations. The AD data are from the Global Anti-dumping Database (Bown 2005). The sample runs from 1995 to 2020.

Table C.5: Global AD Investigations by Exporting Country

	Investigations		Treated		All	
Country	**# Investigations**	**% Treated**	**Avg. Tariff**	**Med. Tariff**	**Avg. Tariff**	**Med. Tariff**
China	3791	79.87%	2.01	0.99	1.60	0.61
South Korea	1258	62.80%	0.50	0.24	0.32	0.08
Taiwan	837	71.92%	0.97	0.37	0.70	0.24
Japan	689	64.01%	0.98	0.60	0.63	0.29
India	628	63.85%	1.80	0.40	1.15	0.15
United States	522	72.22%	0.84	0.47	0.61	0.36
Indonesia	498	69.48%	0.67	0.50	0.46	0.20
Thailand	442	72.85%	0.57	0.33	0.41	0.20
Brazil	407	69.78%	1.04	0.73	0.73	0.37
Russia	393	73.54%	1.23	0.43	0.90	0.33
Viet Nam	349	65.04%	2.82	0.76	1.84	0.26
Malaysia	327	64.83%	0.49	0.29	0.32	0.15
Germany	307	65.80%	0.65	0.39	0.43	0.21
Ukraine	295	83.39%	1.17	0.68	0.98	0.47
France	266	45.49%	0.97	0.60	0.44	0.00
South Africa	255	73.33%	1.07	0.79	0.79	0.38
Turkey	239	45.61%	1.04	0.46	0.47	0.00
European Union	224	78.57%	0.65	0.40	0.51	0.35
Italy	180	68.89%	0.89	0.45	0.61	0.18
Spain	171	51.46%	0.81	0.46	0.42	0.07
United Kingdom	165	73.33%	1.14	0.77	0.84	0.49
Mexico	162	75.31%	0.93	0.56	0.70	0.37
Romania	149	79.87%	1.13	0.66	0.91	0.43
Hong Kong	134	48.51%	0.88	0.63	0.42	0.00
Canada	130	49.23%	0.40	0.28	0.20	0.00
Pakistan	127	66.93%	0.31	0.33	0.21	0.12
Singapore	119	66.39%	0.59	0.36	0.39	0.17
Argentina	116	44.83%	0.92	0.85	0.41	0.00
Kazakhstan	104	84.62%	1.90	0.81	1.61	0.77
Belgium	101	63.37%	0.54	0.41	0.34	0.24
Slovakia	97	61.86%	1.03	0.62	0.64	0.24
Australia	96	51.04%	1.43	0.70	0.73	0.29
Netherlands	94	62.77%	0.47	0.12	0.30	0.05
Egypt	83	20.48%	0.20	0.20	0.04	0.00
New Zealand	74	8.11%	0.14	0.11	0.01	0.00
Saudi Arabia	73	28.77%	0.53	0.30	0.15	0.00
Chile	71	73.24%	0.56	0.28	0.41	0.14
United Arab Emirates	70	77.14%	0.85	0.56	0.66	0.37
Peru	60	48.33%	0.49	0.50	0.23	0.00
Austria	57	66.67%	1.01	0.54	0.67	0.54
Bulgaria	57	94.74%	1.65	0.63	1.57	0.63
Poland	57	75.44%	0.69	0.51	0.52	0.43
Iran	54	55.56%	0.41	0.29	0.23	0.15
Macao	53	5.66%	0.23	0.23	0.01	0.00
Sweden	43	39.53%	0.44	0.27	0.17	0.00
Venezuela	40	20.00%	2.07	1.44	0.41	0.00
Belarus	39	66.67%	2.44	1.09	1.63	0.49
Israel	37	54.05%	0.47	0.53	0.26	0.34
Macedonia	36	69.44%	2.38	1.26	1.65	0.63
Hungary	34	50.00%	1.14	1.57	0.57	0.07
Philippines	33	69.70%	1.05	0.45	0.73	0.45
Finland	30	53.33%	1.10	0.41	0.59	0.12
Czechia	28	82.14%	1.71	0.91	1.40	0.78
Oman	22	59.09%	0.58	0.46	0.34	0.09
Greece	21	80.95%	0.89	0.55	0.72	0.45
Uruguay	21	42.86%	0.44	0.34	0.19	0.00
Switzerland	20	35.00%	1.37	0.72	0.48	0.00
Luxembourg	20	0.00%			0.00	0.00
Lithuania	18	33.33%	0.13	0.11	0.04	0.00
Colombia	15	66.67%	0.38	0.28	0.25	0.28
Moldova	14	50.00%	9.48	11.07	4.74	0.20
Sri Lanka	13	76.92%	0.30	0.25	0.23	0.25
Portugal	13	76.92%	0.98	1.03	0.76	0.59
Denmark	12	83.33%	2.27	1.67	1.89	0.76
Malawi	12	100.00%	1.10	1.10	1.10	1.10
Croatia	11	90.91%	0.69	0.53	0.63	0.46
Trinidad and Tobago	11	45.45%	0.43	0.56	0.20	0.00
Bahrain	10	0.00%			0.00	0.00
Libya	10	20.00%	1.03	1.03	0.21	0.00
Norway	10	80.00%	0.33	0.38	0.27	0.32
Dominican Republic	9	88.89%	0.22	0.22	0.20	0.22
Ireland	9	88.89%	0.13	0.08	0.11	0.08
Paraguay	9	100.00%	0.28	0.28	0.28	0.28
Bangladesh	6	100.00%	0.27	0.31	0.27	0.31
Estonia	6	66.67%	0.40	0.40	0.27	0.06
Faroe Islands	6	50.00%	0.55	0.55	0.27	0.27
Liechtenstein	6	0.00%			0.00	0.00
Guatemala	5	20.00%	0.52	0.52	0.10	0.00
Latvia	5	100.00%	0.14	0.17	0.14	0.17
Bosnia and Herzegovina	4	75.00%	0.34	0.28	0.25	0.28
Nepal	4	100.00%	0.18	0.18	0.18	0.18
North Korea	4	0.00%			0.00	0.00
Qatar	4	100.00%	0.45	0.45	0.45	0.45
Cuba	3	66.67%	0.21	0.21	0.14	0.21
Slovenia	3	33.33%	0.46	0.46	0.15	0.00
Uzbekistan	3	33.33%	0.13	0.13	0.04	0.00
Algeria	2	100.00%	0.13	0.13	0.13	0.13
Georgia	2	100.00%	0.38	0.38	0.38	0.38
Kyrgyzstan	2	100.00%	0.26	0.26	0.26	0.26
Kuwait	2	100.00%	0.20	0.20	0.20	0.20
Laos	2	0.00%			0.00	0.00
Nigeria	2	100.00%	0.40	0.40	0.40	0.40
Serbia	2	100.00%	0.29	0.29	0.29	0.29
Armenia	1	100.00%	0.37	0.37	0.37	0.37
Costa Rica	1	0.00%			0.00	0.00
Ecuador	1	100.00%	0.04	0.04	0.04	0.04
Jordan	1	100.00%	0.34	0.34	0.34	0.34

Description: This table presents summary statistics for the global AD investigations by the exporting country. The table shows the number of investigations, the fraction of the investigations that led to a tariff increase, the average tariff rate conditional on an affirmative investigation, and the average tariff rate of all investigations. The AD data are from the Global Anti-dumping Database. The sample runs from 1995 to 2020.

Table C.6: Summary Statistics of Diff-in-Diff Regression by Sector

Sector	No. Obs	No. Prods	No. Importer	No. Exporter	Mean Ave Tariff	Mean Log Value	Sd. Ave Tariff	Sd. Mean Log Value
Agriculture	1959	10	6	7	0.03	8.68	0.07	6.70
Fishing	304	5	2	3	0.01	4.66	0.05	9.12
Mining non-energy	124	3	2	2	0.03	5.98	0.07	3.52
Mining support	72	3	2	2	0.03	6.35	0.08	3.43
Food	6048	87	21	37	0.03	4.95	0.07	7.46
Textiles	22568	212	18	30	0.03	-2.96	0.07	10.24
Wood	3629	64	15	25	0.03	2.08	0.07	9.53
Paper	8738	97	20	38	0.03	2.60	0.07	9.01
Petroleum	10041	140	19	45	0.04	2.86	0.08	9.00
Chemical	25126	259	23	61	0.04	3.04	0.07	8.79
Pharmaceuticals	784	21	11	12	0.05	6.38	0.09	5.81
Plastic	8502	100	22	32	0.03	4.42	0.07	8.19
Mineral	4415	69	22	29	0.04	3.18	0.08	8.27
Basic metals	100308	203	21	58	0.03	-0.48	0.07	10.15
Fabricated metals	5039	90	22	31	0.04	5.24	0.08	7.56
Computer	11945	111	21	38	0.03	4.30	0.07	8.15
Electrical	7533	95	22	33	0.03	4.25	0.07	8.61
Machinery n.e.c.	13712	229	24	44	0.04	5.37	0.08	7.60
Auto	1148	29	13	14	0.04	6.18	0.08	7.73
Other transport	1986	40	13	13	0.04	5.85	0.08	7.70
Manufacturing n.e.c.	35834	353	27	52	0.03	4.88	0.07	7.90
Service	1559	29	8	19	0.04	1.62	0.08	9.96

Description: This table presents summary statistics for the variables used in the difference-in-differences regressions used to estimated sectoral trade elasticities (Model 3.3). The AD data are from the Global Anti-dumping Database. The sample runs from 1995 to 2020.

Table C.7: OECD ICIO Sectors and International Standard Industrial Classification (ISIC) Revision 4 Sectors

Sector	OECD ICIO	ISIC Rev. 4
Agriculture	Agriculture, hunting, forestry	1-2
Fishing	Fishing and aquaculture	3
Mining energy	Mining and quarrying, energy producing products	5-6
Mining non-energy	Mining and quarrying, non-energy producing products	7-8
Mining support	Mining support service activities	9
Food	Food products, beverages and tobacco	10-12
Textiles	Textiles, textile products, leather and footwear	13-15
Wood	Wood and products of wood and cork	16
Paper	Paper products and printing	17-18
Petroleum	Coke and refined petroleum products	19
Chemical	Chemical and chemical products	20
Pharmaceuticals	Pharmaceuticals, medicinal chemical and botanical products	21
Plastic	Rubber and plastics products	22
Mineral	Other non-metallic mineral products	23
Basic metals	Basic metals	24
Fabricated metals	Fabricated metal products	25
Computer	Computer, electronic and optical equipment	26
Electrical	Electrical equipment	27
Machinery n.e.c.	Machinery and equipment, nec	28
Auto	Motor vehicles, trailers and semi-trailers	29
Other transport	Other transport equipment	30
Manufacturing n.e.c.	Manufacturing nec; repair and installation of machinery and equipment	31-33
Service	Electricity, gas, steam and air conditioning supply	35
	Water supply, sewerage, waste management and remediation activities	36-39
	Construction	41-43
	Wholesale and retail trade; repair of motor vehicles	45-47
	Land transport and transport via pipelines	49
	Water transport	50
	Air transport	51
	Warehousing and support activities for transportation	52
	Postal and courier activities	53
	Accommodation and food service activities	55-56
	Publishing, audiovisual and broadcasting activities	58-60
	Telecommunications	61
	IT and other information services	62-63
	Financial and insurance activities	64-66
	Real estate activities	68
	Professional, scientific and technical activities	69-75
	Administrative and support services	77-82
	Public administration and defence; compulsory social security	84
	Education	85
	Human health and social work activities	86-88
	Arts, entertainment and recreation	90-93
	Other service activities	94-96
	Activities of households as employers; undifferentiated goods- and services-producing activities of households for own use	97-98

Description: This table shows the relationship between the OECD ICIO sectors that we consider and the International Standard Industrial Classification (ISIC) Rev. 4 sectors.

Additional Figures and Tables

Figure C.3: Impact of AD Tariffs on Quantity and Prices

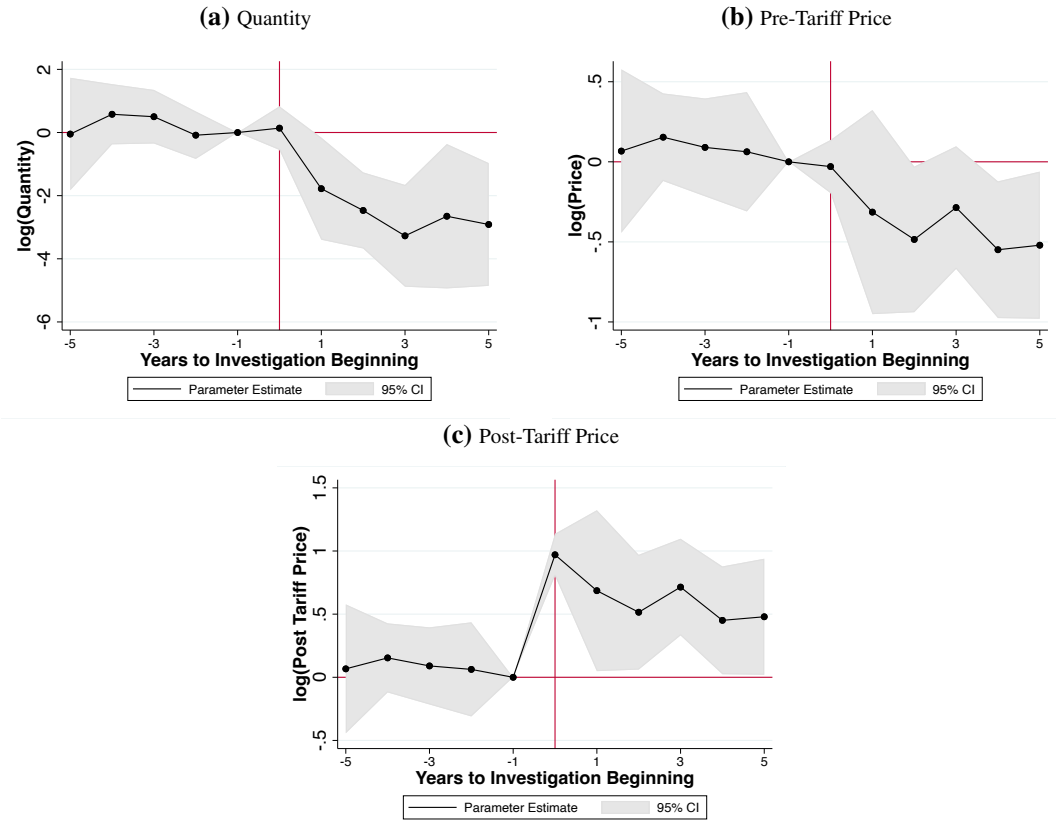

Description: This figure shows the dynamic impact of AD tariffs on the quantity, pre-tariff price, and post-tariff price of imports using Model 3.2. The impact on yearly import quantity and price is plotted on the y-axis. The number of years to the beginning of the investigation is plotted on the x-axis. The import quantity is measured with HS 6-digit level metric tons imported from Russia by the country that initiated the AD investigation. HS 6-digit level price is measured with the value per metric ton. The import data are from the United Nations Comtrade Database, acquired through the BACI Database of CEPII (Gaulier and Zignago 2010). The AD data are from the Global Anti-dumping Database (Bown 2005). The sample runs from 1995 to 2020. The sample includes the product-origins that faced at least one AD investigation. The shaded area contains the 95% confidence interval. Standard errors are clustered at the product-country level.

Figure C.4: Distribution of the Number of Countries Investigating the Same Product from Russia in the Same Year

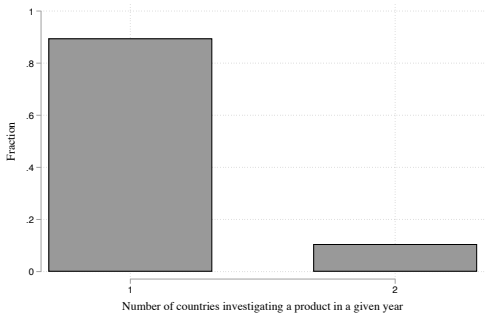

Description: This figure illustrates the distribution of the number of countries involved in an AD investigation against Russia. An investigation is defined as a product being investigated in a year.

Table C.8: Effect of AD Tariffs on Trade Diversion

	(1)	(2)	(3)
VARIABLES	Log Exports to Other Destinations	Log Imports from Other Origins	Log Imports of Other Products
AD Tariff	0.202	0.112	-0.214
	(0.525)	(0.372)	(0.344)
Observations	1,063	1,062	1,064
R-squared	0.888	0.908	0.901
Fixed Effects	Product X Importer, Importer X Year, Number of AD committees, After AD investigation		
Cluster	Product X Importer		
Robust standard errors in parentheses			
*** p<0.01, ** p<0.05, * p<0.1			

Description: This table presents the impact of AD tariffs imposed on Russia by other countries on the trade diversion to other destinations, origins, and products, estimated with Model 3.1. *Log Exports to Other Destinations* denotes the log of exports of HS 6-digit level products by Russia to all destinations except the country that imposed the AD tariff on the same 6-digit product from Russia (for which an AD investigation was initiated). *Log Imports from Other Origins* denotes the log of HS 6-digit level imports by the country that imposed the AD tariff on the same 6-digit product from Russia (for which an AD investigation was initiated). *Log Imports of Other Products* denotes the imports from Russia of all HS 6-digit level products within the same HS 2-digit category except the HS 6-digit product that faces an AD investigation by another country. The import data are from the United Nations Comtrade Database, acquired through the BACI Database of CEPII (Gaulier and Zignago 2010). The AD data are from the Global Anti-dumping Database (Bown 2005). The sample runs from 1995 to 2020.

Table C.9: Robustness Test: Effect of AD Tariffs on Russian Trade

	(1)	(2)	(3)	(4)	(5)	(6)	(7)	(8)	(9)
	Log Value	Log Value	Log Value	Log Value	Log Value	Log Value	Value	Value	Arsinh(Value)
AD Tariff	-4.306**	-4.306**	-4.479**	-3.976**	-3.571*	-5.057**	-3.020***	-1.631***	-4.394*
	(1.895)	(1.921)	(1.997)	(1.907)	(1.793)	(2.136)	(0.801)	(0.137)	(2.297)
Observations	1534	1534	1534	1638	1300	312	1302	250	1404
R^2	0.807	0.807	0.804	0.688	0.931	0.907	NA	NA	0.884
Product X Importer FE	X	X	X		X	X	X	X	X
Importer X Year FE	X	X	X		X		X		X
Product X Year FE						X		X	
4-digit X Year FE					X				X
Product FE				X					
Importer FE				X					
Year FE				X					
PPML							X	X	
Number of AD committees	X	X		X	X	X	X	X	X
Dummy for AD committee			X						
After AD investigation	X	X	X	X	X	X	X	X	X
Cluster	Product X Importer	4-digit X Importer	Product X Importer	Product X Importer	Product X Importer	Product X Importer	Product X Importer	Product X Importer	Product X Importer
Standard errors in parentheses									
* p<0.10, ** p<0.05, *** p<0.010									

Description: This table presents the impact of AD tariffs imposed on Russia by other countries on the log of imports from Russia by the country that initiated the AD investigation. We study HS 6-digit level imports. Imports are measured in FOB, current dollar value terms. The coefficients are estimated with Model 3.1. Different columns include different combinations of fixed effects and controls. The import data are from the United Nations Comtrade Database, acquired through the BACI Database of CEPII (Gaulier and Zignago 2010). The AD data are from the Global Anti-dumping Database (Bown 2005). The sample runs from 1995 to 2020.

Table C.10: Robustness Test: Effect of AD Tariffs on Total Exports

	(1)	(2)	(3)	(4)	(5)	(6)	(7)
	Log Total Exports	Log Total Exports	Log Total Exports	Log Total Exports	Log Total Exports	Total Exports	Arsinh(Value)
AD Tariff	-1.577**	-1.577*	-1.445*	-1.013	-0.992	-1.182**	-1.863
	(0.726)	(0.796)	(0.741)	(0.989)	(0.765)	(0.540)	(2.030)
Observations	1534	1534	1534	1638	1300	1302	1404
R^2	0.804	0.804	0.803	0.657	0.913	NA	0.819
Product X Importer FE	X	X	X		X	X	X
Importer X Year FE	X	X	X		X	X	X
4-digit X Year FE					X		X
Product FE				X			
Importer FE				X			
Year FE				X			
Number of AD committees	X	X		X	X	X	X
Dummy for AD committee			X				
After AD investigation	X	X	X	X	X	X	X
PPML						X	
Cluster	Product X Importer	4-digit X Importer	Product X Importer	Product X Importer	Product X Importer	Product X Importer	Product X Importer
Standard errors in parentheses							
* p<0.10, ** p<0.05, *** p<0.010							

Description: This table presents the impact of AD tariffs imposed on Russia by other countries on the log of HS 6-digit level total exports by Russia to all destinations. The coefficients are estimated with Model 3.1. Total exports refers to total exports of the HS 6-digit level product by Russia to all destinations; these exports are of the same 6-digit products for which other countries initiated an AD investigation on Russia. Different columns include different combinations of fixed effects and controls. The import data are from the United Nations Comtrade Database, acquired through the BACI Database of CEPII (Gaulier and Zignago 2010). The AD data are from the Global Anti-dumping Database (Bown 2005). The sample runs from 1995 to 2020.

Table C.11: Robustness Test: Effect of AD Tariffs on Total Imports

	(1)	(2)	(3)	(4)	(5)	(6)	(7)	(8)
	Log Total Imports	Log Total Imports	Log Total Imports	Log Total Imports	Log Total Imports	Log Total Imports	Total Imports	Arsinh(Value)
AD Tariff	-1.867**	-1.867**	-1.890**	-1.499*	-1.708	-1.233	-0.974**	-2.445
	(0.743)	(0.764)	(0.826)	(0.871)	(1.074)	(0.741)	(0.396)	(2.318)
Observations	1534	1534	1534	1638	1300	312	1302	1404
R^2	0.839	0.839	0.837	0.738	0.922	0.910	NA	0.847
Product X Importer FE	X	X	X		X	X	X	X
Importer X Year FE	X	X	X		X	X	X	X
Product X Year FE								
4-digit X Year FE					X			X
Product FE				X				
Importer FE				X				
Year FE				X				
Number of AD committees	X	X		X	X		X	X
Dummy for AD committee			X			X		
After AD investigation	X	X	X	X	X	X	X	X
PPML							X	
Cluster	Product X Importer	4-digit X Importer	Product X Importer	Product X Importer	Product X Importer	Product X Importer	Product X Importer	Product X Importer
Standard errors in parentheses								
* p<0.10, ** p<0.05, *** p<0.010								

Description: This table presents the impact of AD tariffs imposed on Russia Russia by other countries on the log of HS 6-digit level total imports by another country from all origins. The coefficients are estimated with Model 3.1. Total imports refers to the total imports of the HS 6-digit level product from all origins by the country that initiated an AD investigation on Russia; these imports are of the same 6-digit products on which the AD tariffs have been imposed. Different columns include different combinations of fixed effects and controls. The import data are from the United Nations Comtrade Database, acquired through the BACI Database of CEPII (Gaulier and Zignago 2010). The AD data are from the Global Anti-dumping Database (Bown 2005). The sample runs from 1995 to 2020.

Table C.12: Robustness Test: Alternative Specifications

	(1) Log Value	(2) Log Value	(3) Log Value	(4) Value	(5) Arsinh(Value)
AD Tariff	-6.094***	-4.359***	-4.365***	-3.547***	-3.595***
	(0.862)	(0.903)	(0.900)	(0.426)	(0.408)
Observations	269950	268938	268938	236927	269950
R^2	0.834	0.865	0.866	NA	0.875
Product X Year FE	X	X	X	X	X
Product X Exporter FE	X	X		X	X
Product X Importer FE	X	X		X	X
Exporter X Year FE	X			X	X
Importer X Year FE	X			X	X
Exporter X Importer X Year FE		X	X		
Product X Exporter X Importer FE			X		
PPML				X	
Number of AD committees	X	X	X	X	X
After AD investigation	X	X	X	X	X
Cluster	Product X Exporter X Importer	Product X Exporter X Importer	Product X Exporter X Importer	Product X Exporter X Importer	Product X Exporter X Importer

Standard errors in parentheses
*** p<0.01, ** p<0.05, * p<0.1

Description: This table presents the average trade elasticity across sectors estimated using the difference-in-differences method and different fixed effect combinations and estimation strategies. The import data are from the United Nations Comtrade Database, acquired through the BACI Database of CEPII (Gaulier and Zignago 2010). The AD data are from the Global Antidumping Database (Bown 2005). The sample runs from 1995 to 2020. Standard errors are clustered at origin-destination-product level.

Figure C.5: Robustness Test: Sectoral Trade Elasticities Estimated with Different Specifications

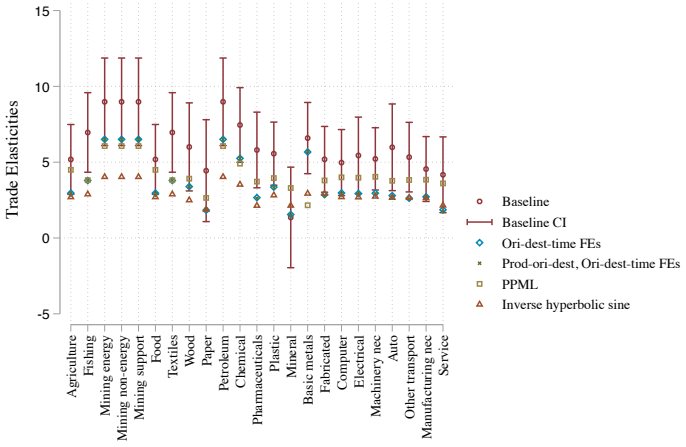

Description: This figure displays the sector-level trade elasticities estimated using Model 3.3 and alternative empirical specifications. These specifications correspond to the different columns in Table C.12. The import data are from the United Nations Comtrade Database, acquired through the BACI Database of CEPII (Gaulier and Zignago 2010). The AD data are from the Global Antidumping Database (Bown 2005). The sample runs from 1995 to 2020. Standard errors are clustered at origin-destination-product level.

Figure C.6: Distribution of the Number of Countries that Investigate the Same Product from the Same Country in the Same Year

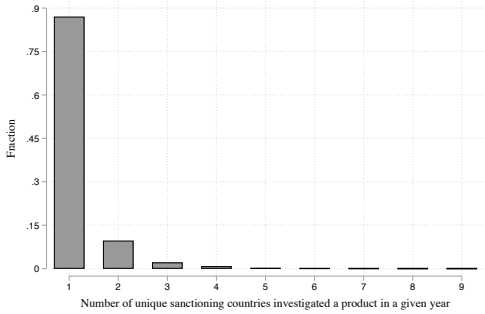

Description: This figure illustrates the distribution of the number of countries involved in an AD investigation. An investigation is characterized by a specific product from a certain country being examined in a year.

Figure C.7: Correlation between Trade Elasticities Estimated with Diff-in-Diff and the Estimated Values (1) in Caliendo and Parro (2015) and (2) using the Feenstra (1994) Method

(a) Correlation with Caliendo and Parro (2015) elasticities

(b) Correlation with the elasticities that we estimate with the Feenstra (1994)

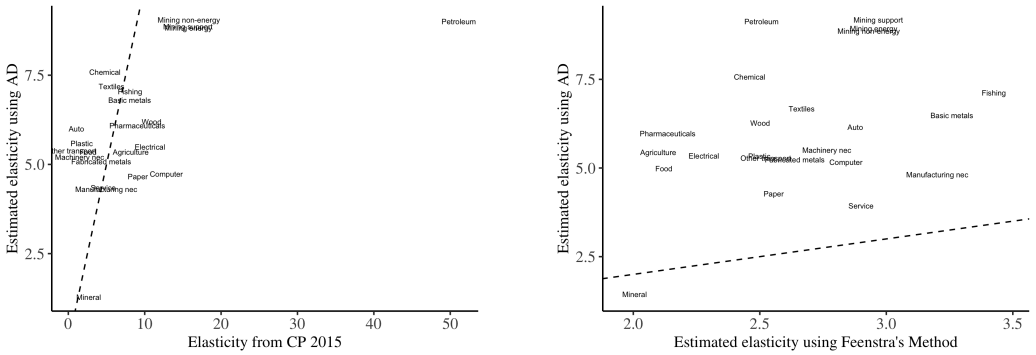

Description: This figure shows the sector-level trade elasticities that we estimate with the difference-in-differences method and those estimated in the literature. The left panel shows the correlation between our elasticities and those that Caliendo and Parro (2015) find. The right panel shows the correlation between our elasticities and those we estimate using the Feenstra (1994) method at the same level of sectors.

Table C.13: Robustness Test: Unique Investigating Country

	(1) Log Value	(2) Log Value	(3) Log Value	(4) Value	(5) Arsinh(Value)
AD Tariff	-4.633***	-2.539*	-2.541*	-3.885***	-2.691***
	(1.221)	(1.347)	(1.327)	(0.479)	(0.563)
Observations	126287	124668	124644	110378	126287
R^2	0.859	0.888	0.888	NA	0.899
Product X Year FE	X	X	X	X	X
Product X Exporter FE	X	X		X	X
Product X Importer FE	X	X		X	X
Exporter X Year FE	X			X	X
Importer X Year FE	X			X	X
Exporter X Importer X Year FE		X	X		
Product X Exporter X Importer FE			X		
PPML				X	
Number of AD committees	X	X	X	X	X
After AD investigation	X	X	X	X	X
Cluster	Product X Exporter X Importer	Product X Exporter X Importer	Product X Exporter X Importer	Product X Exporter X Importer	Product X Exporter X Importer
Standard errors in parentheses					
*** p<0.01, ** p<0.05, * p<0.1					

Description: This table presents the average trade elasticity across sectors, estimated using the difference-in-differences method and different estimation strategies. The sample is composed of the investigations that involve a unique investigating country. The import data are from the United Nations Comtrade Database, acquired through the BACI Database of CEPII (Gaulier and Zignago 2010). The AD data are from the Global Antidumping Database (Bown 2005). The sample runs from 1995 to 2020. Standard errors are clustered at origin-destination-product level.

Table C.14: Heterogeneity Analysis: Pre-investigation Trade Flows

	(1) Log Value	(2) Log Value	(3) Log Value	(4) Value	(5) Value	(6) Value
AD Tariff	-13.06***	-11.81***	-7.900***	-7.615***	-6.688***	-3.761***
	(1.841)	(2.152)	(2.655)	(0.991)	(0.879)	(1.178)
AD Tariff x Log Value 1-yr before Investigation	0.939***			0.392***		
	(0.184)			(0.107)		
AD Tariff x Log Value 5-yr before Investigation		0.757***			0.294***	
		(0.221)			(0.102)	
AD Tariff x Log Value 10-yr before Investigation			0.550**			0.143
			(0.264)			(0.124)
Observations	218420	158629	86769	213092	154172	83935
R^2	0.776	0.803	0.854	NA	NA	NA
Product X Year FE	X	X	X	X	X	X
Product X Exporter FE	X	X	X	X	X	X
Product X Importer FE	X	X	X	X	X	X
Exporter X Year FE	X	X	X	X	X	X
Importer X Year FE	X	X	X	X	X	X
PPML				X	X	X
Number of AD committees	X	X	X	X	X	X
After AD investigation	X	X	X	X	X	X
Cluster	Product X Exporter X Importer	Product X Exporter X Importer	Product X Exporter X Importer	Product X Exporter X Importer	Product X Exporter X Importer	Product X Exporter X Importer
Standard errors in parentheses						
*** p<0.01, ** p<0.05, * p<0.1						

Description: This table presents how the impact of AD tariffs depends on pre-investigation trade flow values, estimated with the difference-in-differences method. The import data are from the United Nations Comtrade Database, acquired through the BACI Database of CEPII (Gaulier and Zignago 2010). The AD data are from the Global Antidumping Database (Bown 2005). The sample runs from 1995 to 2020. Standard errors are clustered at origin-destination-product level.

Table C.15: Heterogeneity Analysis: Large Tariffs

	(1)	(2)	(3)	(4)	(5)	(6)
	Log Value	Log Value	Log Value	Value	Value	Value
AD Tariff	-5.518***	-5.390***	-5.116***	-4.034***	-4.175***	-4.225***
	(1.025)	(1.040)	(1.081)	(0.496)	(0.514)	(0.553)
AD Tariff X Top 5%	-8.282***			-2.232***		
	(1.833)			(0.719)		
AD Tariff X Top 10%		-5.097***			-0.271	
		(1.407)			(0.558)	
AD Tariff X Top 25%			-3.331***			0.0490
			(1.249)			(0.474)
Observations	208059	208059	208059	180651	180651	180651
R^2	0.832	0.832	0.832	NA	NA	NA
Product X Year FE	X	X	X	X	X	X
Product X Exporter FE	X	X	X	X	X	X
Product X Importer FE	X	X	X	X	X	X
Exporter X Year FE	X	X	X	X	X	X
Importer X Year FE	X	X	X	X	X	X
PPML				X	X	X
Number of AD committees	X	X	X	X	X	X
After AD investigation	X	X	X	X	X	X
Cluster	Product X Exporter X Importer	Product X Exporter X Importer	Product X Exporter X Importer	Product X Exporter X Importer	Product X Exporter X Importer	Product X Exporter X Importer

Standard errors in parentheses

*** p<0.01, ** p<0.05, * p<0.1

Description: This table presents how the impact of AD tariffs depends on the tariffs' magnitudes, estimated with the difference-in-differences method. The import data are from the United Nations Comtrade Database, acquired through the BACI Database of CEPII (Gaulier and Zignago 2010). The AD data are from the Global Antidumping Database (Bown 2005). The sample runs from 1995 to 2020. Standard errors are clustered at origin-destination-product level.

A.2 Model

Equilibrium in Changes

Using the "exact hat algebra" technique popularized by **?**, we can express the equilibrium conditions in terms of changes from the baseline equilibrium, given changes in tariffs $\left\{\hat{t}_{ni}^{j}\right\}_{j,n,i}$ ($\hat{t}_{ni}^{j} = (1+\tau_{ni}^{j'})/(1+\tau_{ni}^{j})$):

$$\hat{c}_n^j = (\hat{w}_n)^{\gamma_n^j} \prod_{k=1}^{J} (\hat{P}_n^k)^{\gamma_n^{k,j}} \tag{C.1}$$

$$\hat{P}_n^j = \left[\sum_{i=1}^{N} \pi_{ni}^j (\hat{t}_{ni}^j \hat{c}_i^j)^{-\theta^j} \right]^{-1/\theta^j} \tag{C.2}$$

$$\hat{\pi}_{ni}^j = \left(\frac{\hat{c}_i^j \hat{t}_{ni}^j}{\hat{P}_n^j} \right)^{-\theta^j} \tag{C.3}$$

$$X_n^{j'} = \sum_{k=1}^{J} \gamma_n^{j,k} \sum_{i=1}^{N} \frac{\pi_{in}^{k'}}{t_{in}^{k'}} X_i^{k'} + \alpha_n^j I_n' \tag{C.4}$$

$$I_n' = \hat{w}_n w_n L_n + D_n' + \sum_{j=1}^{J} \sum_{i=1}^{N} \tau_{ni}^{j'} \frac{X_n^{j'} \pi_{ni}^{j'}}{t_{ni}^{j'}} \tag{C.5}$$

$$\hat{w}_n = \sum_{j=1}^{J} \gamma_n^j \sum_{i=1}^{N} X_i^{j'} \frac{\pi_{in}^{j'}}{t_{in}^{j'} w_n L_n}, \tag{C.6}$$

To compute the counterfactuals, we only need data on bilateral trade shares π_{ni}^j, the share of value added in production γ_n^j, value added $w_n L_n$, incumbent tariffs τ_{ni}^j, the share of intermediate consumption $\gamma_n^{k,j}$, and sectoral trade elasticity θ^j.

We follow Ossa (2014) and Caliendo and Parro (2015) to construct a trade flow matrix without trade imbalance using the approach introduced in **?**. All later calculations of welfare changes given counterfactual tariffs will treat this purged trade flow data as the factual equilibrium.

Equilibrium in Changes Given Tariff Changes *Given changes in tariffs* $\left\{\hat{t}_{ni}^{j}\right\}_{j,n,i}$, *an equilibrium is defined as changes in sectoral prices,* $\{\hat{P}_n^j\}_{n,j}$, *and wages,* $\{\hat{w}_n\}_n$, *such that*

1. *Firms maximize profit (Equation C.1);*
2. *The price index satisfies Equations C.2 and C.3;*
3. *The goods markets clear, satisfying Equations C.4 and C.5;*

4. The labor market clears, satisfying Equation C.6;

Tariff Competition with Equilibrium in Changes Following the notations in Section 3.3.6, we denote changes in the sectoral tariffs that country n imposes on Russia with $\hat{\mathbf{t}}_{\mathbf{nR}}$, and all other tariffs – changes in tariffs imposed on Russia by all countries except country n and those that country n imposes on all other countries except Russia – with $\hat{\mathbf{t}}_{-\mathbf{nR}}$.

The change in country n's welfare equals the following:

$$\hat{G}_n(\hat{\mathbf{t}}_{\mathbf{nR}}, \hat{\mathbf{t}}_{-\mathbf{nR}}) = \frac{\hat{I}_n(\hat{\mathbf{t}}_{\mathbf{nR}}, \hat{\mathbf{t}}_{-\mathbf{nR}})}{\hat{P}_n^C(\hat{\mathbf{t}}_{\mathbf{nR}}, \hat{\mathbf{t}}_{-\mathbf{nR}})}, \tag{C.7}$$

where $\hat{I}_n(\hat{\mathbf{t}}_{\mathbf{nR}}, \hat{\mathbf{t}}_{-\mathbf{nR}})$ denotes the change in country n's income and $\hat{P}_n^C(\hat{\mathbf{t}}_{\mathbf{nR}}, \hat{\mathbf{t}}_{-\mathbf{nR}})$ denotes the change in country n's consumer price index.

Conditional on $\hat{\mathbf{t}}_{-\mathbf{nR}}$, the objective of sanctioning country n is to both maximize its own welfare (real income, or GNI) and minimize Russian welfare in the counterfactual equilibrium:

$$g_n(\hat{\mathbf{t}}_{-\mathbf{nR}}) \in argmax_{\{\hat{\mathbf{t}}_{\mathbf{nR}}\}} \rho G_n \hat{G}_n(\hat{\mathbf{t}}_{\mathbf{nR}}, \hat{\mathbf{t}}_{-\mathbf{nR}}) - (1-\rho) G_R \hat{G}_R(\hat{\mathbf{t}}_{\mathbf{nR}}, \hat{\mathbf{t}}_{-\mathbf{nR}}), \tag{C.8}$$

s.t. Equilibrium Conditions C.1-C.6,

where G_n and G_R denote country n's and Russia's real income in the baseline equilibrium. We calibrate them to the country's purchasing power parity (PPP) adjusted GNI in 2018, the same year as the OECD ICIO data.[2]

Russia, when it retaliates, maximizes a weighted average of its own welfare and minimizing the allies' welfare, both in the counterfactual equilibrium:

$$g_R(\hat{\mathbf{t}}_{-\mathbf{RS}}) \in argmax_{\{\hat{\mathbf{t}}_{\mathbf{RS}}\}} \rho G_R \hat{G}_R(\hat{\mathbf{t}}_{\mathbf{RS}}, \hat{\mathbf{t}}_{-\mathbf{RS}}) - (1-\rho) \sum_{n \in S} \frac{G_n \hat{G}_n(\hat{\mathbf{t}}_{\mathbf{RS}}, \hat{\mathbf{t}}_{-\mathbf{RS}})}{N_S} \tag{C.9}$$

s.t. Equilibrium Conditions C.1-C.6

Equilibrium in Changes with Sanctions *Given changes in all tariffs except what the sanctioning countries impose on Russia and Russia imposes on sanctioning countries,* $\{\hat{t}_{ni}^j\}_{j,n,i} \setminus \{\hat{\mathbf{t}}_{\mathbf{nR}}, \hat{\mathbf{t}}_{\mathbf{Rn}}\}_{n \in \mathbf{S}}$*, an equilibrium with optimal sanctions is given by tariffs imposed on Russia by sanctioning countries,* $\{\hat{\mathbf{t}}_{\mathbf{nR}}\}_{n \in \mathbf{S}}$*, tariffs imposed on*

[2]The data source is the World Bank. See https://data.worldbank.org/indicator/NY.GNP.MKTP.PP.CD?locations=1W-EU-RU-US.

the sanctioning countries by Russia, $\{\hat{\mathbf{t}}_{\mathbf{Rn}}\}_{n\in\mathbf{S}}$*, a set of sectoral prices,* $\{\hat{P}_n^j\}_{n,j}$*, and wages,* $\{\hat{w}_n\}_n$*, such that*

1. *Given tariffs* $\{\hat{t}_{ni}^j\}_{j,n,i}$*,* $\{\{\hat{P}_n^j\}_{n,j},\{\hat{w}_n\}_n\}$ *is an equilibrium;*

2. *Sanctioning countries and Russia optimally choose changes in their tariffs:*

$$\hat{\mathbf{t}}_{\mathbf{nR}} = g_n(\hat{\mathbf{t}}_{-\mathbf{nR}}), \forall n \in \mathbf{S}$$
$$\hat{\mathbf{t}}_{\mathbf{RS}} = g_R(\hat{\mathbf{t}}_{-\mathbf{RS}})$$

Equilibrium in Changes with Political Weights

Here, we rewrite the sanctioning countries' problem in changes if they target the politically relevant sectors in Russia. The change in Russia's politically weighted welfare is equal to the following:

$$\hat{G}_R^{pol}(\hat{\mathbf{t}}_{\mathbf{nR}},\hat{\mathbf{t}}_{-\mathbf{nR}}) = \sum_{j=1}^{J} \frac{\lambda_R^j L_R^j}{\sum_{s=1}^{S}\lambda_R^s L_R^s}\hat{L}_R^s(\hat{\mathbf{t}}_{\mathbf{nR}},\hat{\mathbf{t}}_{-\mathbf{nR}})\frac{\hat{I}_R(\hat{\mathbf{t}}_{\mathbf{nR}},\hat{\mathbf{t}}_{-\mathbf{nR}})}{\hat{P}_R^C(\hat{\mathbf{t}}_{\mathbf{nR}},\hat{\mathbf{t}}_{-\mathbf{nR}})}, \tag{C.10}$$

where $\frac{\lambda_R^j L_R^j}{\sum_{s=1}^{S}\lambda_R^s L_R^s}$ denotes the politically weighted initial employment share of sector j in Russia. The politically weighted welfare increases if the whole economy's real income, $\frac{\hat{I}_R(\hat{\mathbf{t}}_{\mathbf{nR}},\hat{\mathbf{t}}_{-\mathbf{nR}})}{\hat{P}_R^C(\hat{\mathbf{t}}_{\mathbf{nR}},\hat{\mathbf{t}}_{-\mathbf{nR}})}$, increases and if employment/value added increases more in the sectors that have higher political weights. As a result, if other countries would like to target the politically related sectors, on top of reducing the whole economy's real income, they can also set tariffs to reduce employment/value added in the politically related sectors.

Similar to Problem C.8, the objective of sanctioning country n is to both maximize its own welfare and minimize Russia's real income in the politically connected sectors:

$$g_n^{pol}(\hat{\mathbf{t}}_{-\mathbf{nR}}) \in argmax_{\{\hat{\mathbf{t}}_{\mathbf{nR}}\}}\rho G_n\hat{G}_n(\hat{\mathbf{t}}_{\mathbf{nR}},\hat{\mathbf{t}}_{-\mathbf{nR}}) - (1-\rho)G_R^{pol}\hat{G}_R^{pol}(\hat{\mathbf{t}}_{\mathbf{nR}},\hat{\mathbf{t}}_{-\mathbf{nR}}), \tag{C.11}$$

s.t. Equilibrium Conditions C.1-C.6,

where $G_R^{pol} = \sum_{j=1}^{J}\lambda^j\frac{L_R^j}{L_R}G_R$ represents Russia's politically weighted real income in the initial equilibrium. We calibrate λ^j to Russia's political weights, $\frac{L_R^j}{L_R}$ to Russia's sectoral employment shares, and G_R to Russia's GNI.

Just as for Problem C.9, we assume that Russia retaliates by maximizing the weighted average of its own welfare and negative impact on the sanctioning countries' welfare.

A.3 Quantitative

Sectoral Trade Statistics with Russia

In Figure C.8, we highlight two findings from analyzing the sanctioning countries' trade statistics with Russia. First, Russia's exports of mining and energy products to the EU are important for both the EU's consumption and Russia's production. Mining and energy sector products from Russia account for about 20% of the EU's total expenditure on these products (Figure C.8a), and exports of these products to the EU account for more than a quarter of Russia's total output (Figure C.8b). This suggests that among all sanctioning countries, the EU plays a pivotal role.[3] If the EU sanctions mining and energy products from Russia, it may cause significant economic losses in Russia, but it may also hurt the EU's welfare.

Second, the sanctioning countries are a major importing origin for Russia. However, Russia is not a major exporting destination for the sanctioning countries. Figure C.8d shows that when it comes to imports from sanctioning countries, Russia allocates approximately 50% of its total expenditure on machinery and pharmaceutical products, and over a quarter of its spending on electrical equipment and chemicals. However, the share of exports to Russia in the sanctioning countries' sectoral output never exceeds 5% (Figure C.8c). This suggests that tariff retaliation by Russia may not cause substantial harm to the income of sanctioning countries. Rather, it can significantly reduce Russia's welfare. If Russia cares about its own welfare, it is optimal to not impose high retaliatory tariffs.

[3]The EU accounts for 36% of Russia's total exports (5% of Russia's total output) and 39% of Russia's total imports (4% of Russia's total expenditure). The US accounts for 4% of Russia's total exports (1% of Russia's total output) and 5% of Russia's total imports (0.5% of Russia's total expenditure). Other sanctioning countries account for 12% of Russia's total exports (2% of Russia's total output) and 11% of Russia's total imports (1% of Russia's total expenditure).

Figure C.8: Trade Statistics with Russia by Sector

(a) Other Countries' Expenditure Share

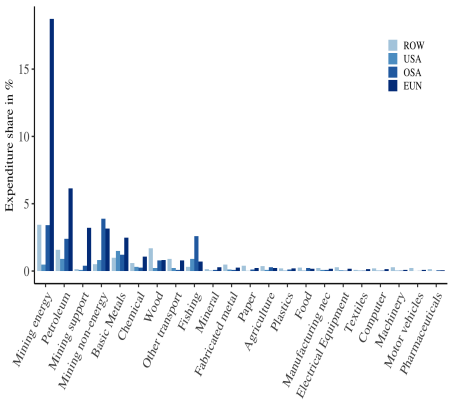

(b) Russia's Share of Output

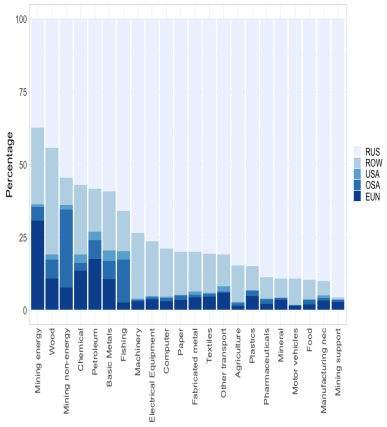

(c) Other Countries' Share of Output

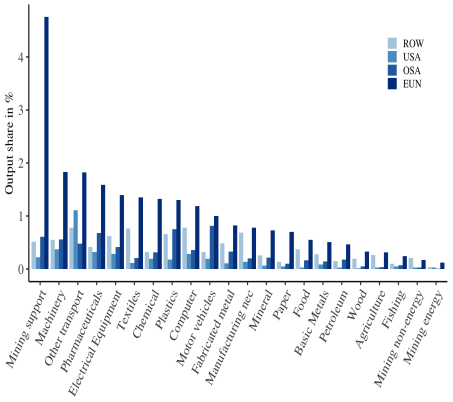

(d) Russia's Expenditure Share

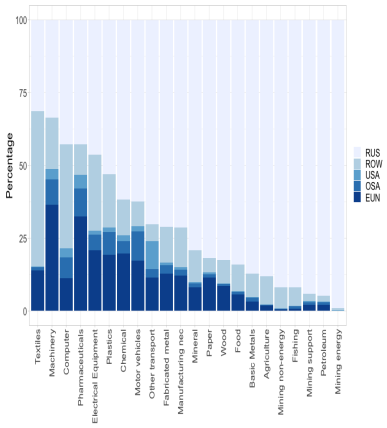

Description: This figure shows, by country and sector, the trade statistics with Russia. Figure C.8a shows Russia's share of total expenditure on the sector's products. Figure C.8b shows the share of output sold to each country in Russia's sectoral total output. Figure C.8c shows the share of output sold to Russia in other countries' sectoral total output. Figure C.8d show other countries' shares in Russia's total expenditure on the sector's product.

Cost-Efficient Sanctions and Fundamentals

To study the relationship between optimal sectoral tariffs imposed on Russia and sectoral characteristics, we use the following regression:

$$\tau_{s,\rho} = \beta_{imp,\rho} ImpShr_s + \beta_{\sigma,\rho}\sigma_s + \beta_{ups,\rho} upstreamness_s + \varepsilon_{s,\rho}, \tag{C.12}$$

where $\tau_{s,\rho}$ is the optimal tariff imposed by the EU on sector s imports from Russia when EU's willingness to pay is governed by ρ. σ_s is the trade elasticity of sector s. $upstreamness_s$ measures sector s's upstreamness (Antràs et al. 2012) – the average number of sectors one dollar of sector s output goes through until it reaches the final consumer. $ImpShr_s$ is the share of imports from Russia in total sector s's imports by the EU in the baseline economy. To make each variable comparable, they are

Figure C.9: Correlations between Sectoral Cost-Efficient Sanction Tariffs and Fundamentals: Sectoral Import Shares from Russia, Trade Elasticities, and Sector Upstreamness

(a) Tariffs and Initial Import Share, $\rho = 1$

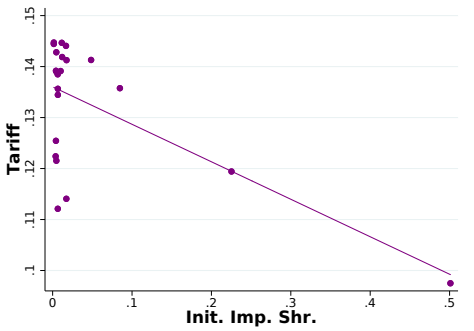

(b) Tariffs and Initial Import Share, $\rho = 0.6$

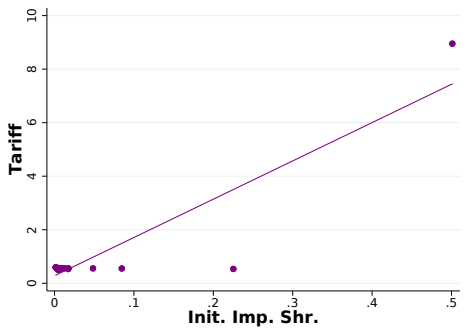

(c) Tariffs and Trade Elasticity, $\rho = 1$

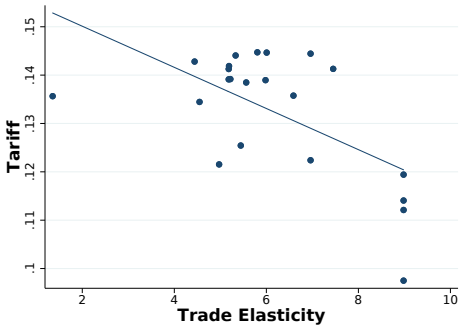

(d) Tariffs and Trade Elasticity, $\rho = 0.6$

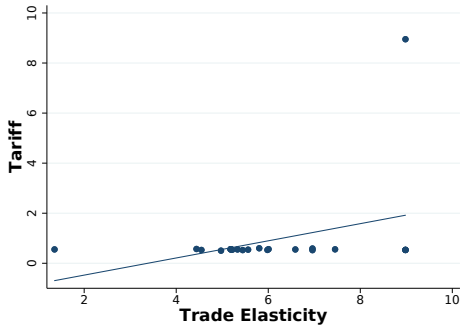

(e) Tariffs and Upstreamness, $\rho = 1$

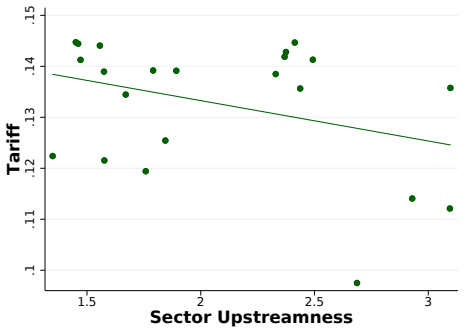

(f) Tariffs and Upstreamness, $\rho = 0.6$

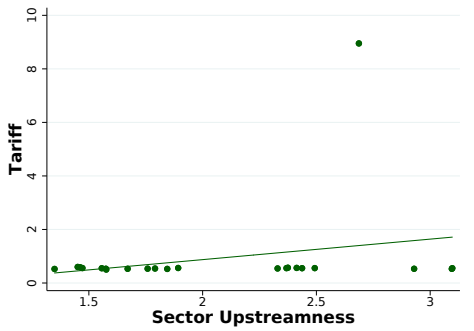

Description: This figure shows the correlations between the optimal sectoral tariffs imposed on Russia by the EU and different sector-level fundamentals under $\rho = 0$ and $\rho = 0.6$.

normalized to have a mean of 0 and a variance of 1.

In Figure C.9, we plot the raw correlations between optimal sectoral tariffs by the EU and individual sector characteristics for $\rho = 1$ and $\rho = 0.6$. In Figure C.10, we plot how the partial correlations change with ρ. For low willingness to pay for sanctions, i.e., when ρ is large, higher tariffs should be set on sectors that have small import shares, have lower trade elasticities, and are more downstream. For example, when $\rho = 1$, a sector whose import share is 1 standard deviation smaller should be

targeted by a tariff that is 0.5 standard deviation higher. Similarly, a sector whose trade elasticity is 1 standard deviation larger should face a tariff that is 0.4 standard deviation lower. These relationships change when ρ falls below 0.7, i.e., when the EU places greater weight on punishing Russia. When there is higher willingness to pay, sectors with larger import shares and higher trade elasticities are targeted with higher tariffs.

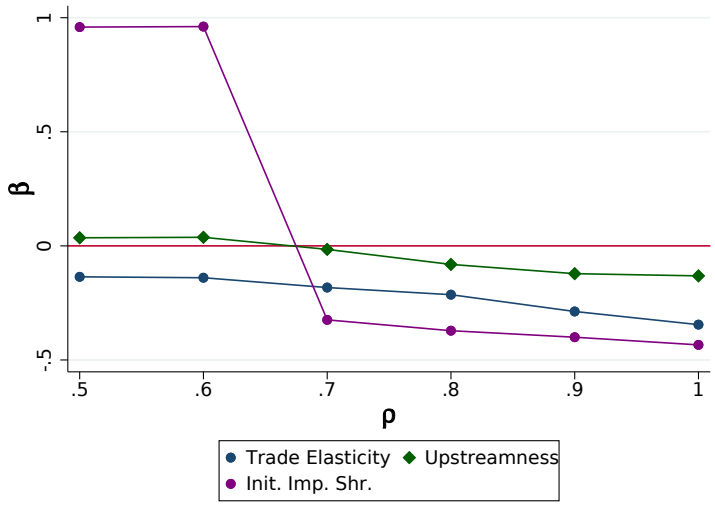

Figure C.10: Correlations between Tariffs with Different Fundamentals for Different ρs

Description: This figure shows the partial correlations between the optimal sectoral tariffs imposed on Russia by the EU and different sector-level fundamentals under different ρs (estimated with Equation C.12).

Short- and Long-Run Trade Elasticity

In this section, we show that our results are robust to calibrating the model to the long-run trade elasticities.

Calibration We modify Equation 3.3 to allow for different trade elasticities in the short and long run and by sector. Specifically, we estimate the equation:

$$\begin{aligned}\log(y_{p,d,o,t}) = \sum_{j=1}^{J} \Big[& \theta^{j}_{\text{Before}} \mathbf{1}(p \in j) \tau_{p,d,o,t} \mathbb{I}_{p,d,o,t} \{u \text{ Yrs. to AD}, u < 0\} \\ & + \theta^{j}_{\text{Short Run}} \mathbf{1}(p \in j) \tau_{p,d,o,t} \mathbb{I}_{p,d,o,t} \{u \text{ Yrs. to AD}, 0 \leq u \leq 2\} \\ & + \theta^{j}_{\text{Long Run}} \mathbf{1}(p \in j) \tau_{p,d,o,t} \mathbb{I}_{p,d,o,t} \{u \text{ Yrs. to AD}, u > 2\} \Big] \\ & + \gamma \mathbb{N}_{p,d,o,t} \{\text{Committee}\} + \eta_{p,t} + \eta_{p,d} + \eta_{p,o} + \eta_{d,t} + \eta_{o,t} + \varepsilon_{p,d,o,t}.\end{aligned}$$

As in Equation (3.3), we utilize within-sector, cross product-country-pair-time tariff variations to identify sectoral trade elasticities in the short and long run (by comparing affirmative and negative investigations). p denotes an investigated product, d denotes a destination, o denotes an origin, and t denotes a year. $y_{p,d,o,t}$ denotes the imports of product p from country o to country d in year t. $\tau_{p,d,o,t}$ denotes the AD tariff that d imposes on o in year t on the product p. On the right hand side, j represents a sector, and $\mathbf{1}(p \in j)$ is activated if product p belongs to sector j. $\mathbb{N}_{p,d,o,t}\{\text{Committee}\}$ controls for the number of investigation committees formed at the same product-country-bilateral-year level. $\eta_{p,t}$, $\eta_{p,d}$, $\eta_{p,o}$, $\eta_{d,t}$, and $\eta_{o,t}$ denote product-year, product–destination, product–origin, destination–year, and origin–year fixed effects, respectively.

We interact the AD tariffs with time dummies indicating whether year t is before, in the short run after, or in the long run after the AD investigation.
$\mathbb{I}_{p,d,o,t}\{u \text{ Yrs. to AD}, u < 0\}$ is a dummy variable that is turned on if time t is before the first AD investigation on product p from country o by country d.
$\mathbb{I}_{p,d,o,t}\{u \text{ Yrs. to AD}, 0 \leq u \leq 2\}$ takes the value 1 up to two years after the first AD investigation on product p from country o by country d. $\mathbb{I}_{p,d,o,t}\{u \text{ Yrs. to AD}, u > 2\}$ takes the value 1 three years after the AD tariff is imposed. The parameters of interest are $\theta^{j}_{\text{Short Run}}$, which captures the short-term effect of tariffs after they are imposed, and $\theta^{j}_{\text{Long Run}}$, which captures the long-term effect of tariffs.

Figure C.11 shows the estimates of the short- and long-run trade elasticities, along with the sectoral trade elasticities in an average year after imposition that we estimated in Section 3.2.4. As anticipated, the short-run trade elasticity is smaller than the long-run trade elasticity. In general, the average trade elasticity we estimated in Section 3.2.4 is close to the long-run trade elasticity.

Results Using long-run trade elasticities, an embargo on the Russian mining and energy sectors is still the cost-efficient policy when there is high enough willingness to pay for sanctions, according to the results shown in Figure C.12. Overall, the cost-efficient sanctions are similar to the baseline results.[4]

[4]Figure C.33 in the Appendix displays the cost-efficient tariffs using short-run trade elasticities.

Figure C.11: Estimates of the Long- and Short-Run Trade Elasticities

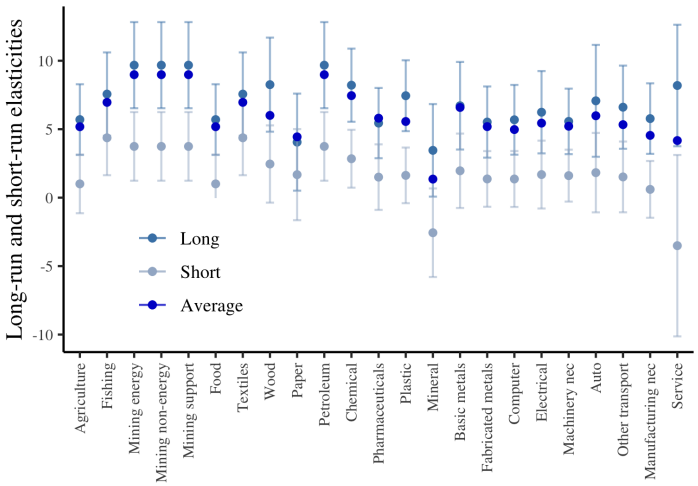

Description: This figure shows sectoral trade elasticities in the short run (from year 0 to year 2), in the long run (from year 3 to year 5), and the average.

Figure C.12: Cost-Efficient Sanctions in the EU with Long-Run Elasticities for Different ρs, $\rho \in [0.4, 1.0]$

(a) Tariff

(b) Change in Imports

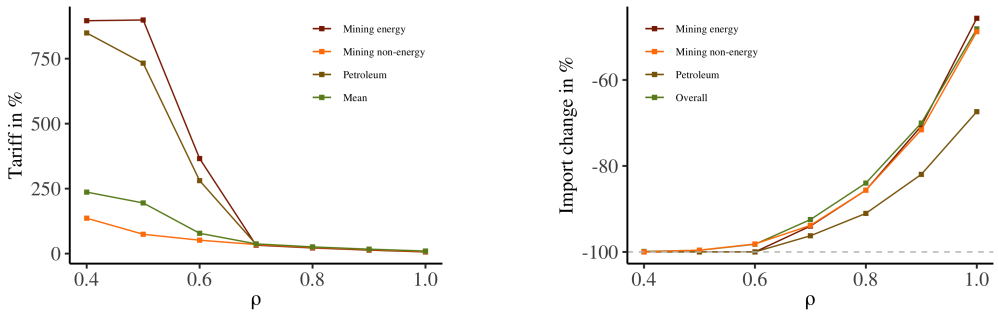

Description: This figure shows the statistics for the EU under cost-efficient sanctions with different levels of willingness to pay with long-run elasticities, as described in Section C.11. Figure C.12a plots the cost-efficient tariffs on mining energy, mining non-energy, petroleum, and the average tariff across sectors for different levels of willingness to pay for sanctions, ρ. Figure C.12b plots the percentage change in imports in the EU for different sectors.

Other Figures and Tables

Figure C.13: Cost-Efficient Sanctions for Different Levels of Willingness to Pay in the US, $\rho \in [0.4, 1]$

(a) Tariff

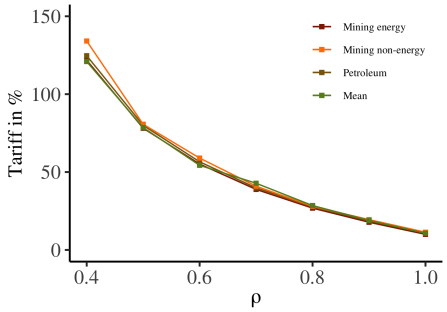

(b) Change in Imports

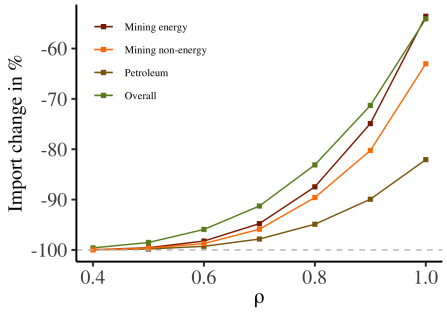

Description: This figure shows the statistics for the US under cost-efficient sanctions with different levels of willingness to pay. Figure C.13a plots the cost-efficient tariffs on mining energy, mining non-energy, petroleum, and the average tariff across sectors for different levels of willingness to pay for sanctions, ρ. Figure C.13b plots the percentage change in imports in the US at different sectors.

Figure C.14: Cost-Efficient Sanctions for Different Levels of Willingness to Pay in the OSA, $\rho \in [0.4, 1]$

(a) Tariff

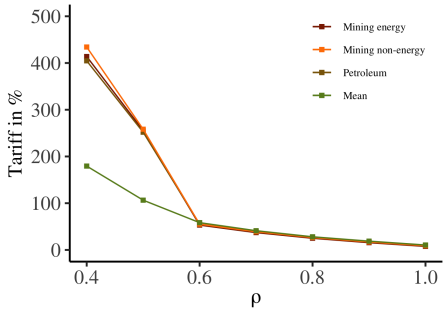

(b) Change in Imports

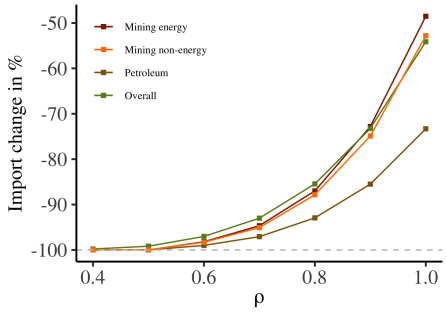

Description: This figure shows the statistics for the OSA under cost-efficient sanctions with different levels of willingness to pay. Figure C.14a plots the cost-efficient tariffs on mining energy, mining non-energy, petroleum, and the average tariffs across sectors for different willingness to pay for sanctions, ρ. Figure C.14b plots the percentage change in imports in the OSA for different sectors.

Figure C.15: Cost-Efficient Sanctions with Political Weights for Different Levels of Willingness to Pay in the US, $\rho \in [0.7, 1]$

(a) Tariff

(b) Change in Imports

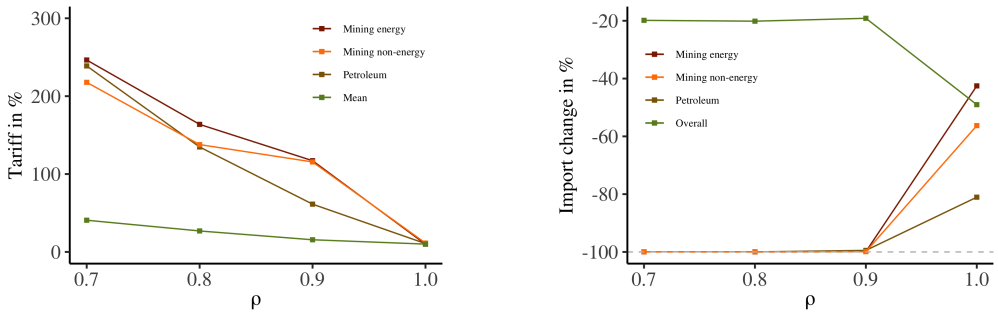

Description: This figure shows the statistics for the US under cost-efficient sanctions with different levels of willingness to pay when the US targets the politically relevant sectors, as described in Table 3.3. Figure C.15a plots the cost-efficient tariffs on mining energy, mining non-energy, petroleum, and the average tariff across sectors for different levels of willingness to pay for sanctions, ρ. Figure C.15b plots the percentage change in imports in the US for different sectors.

Figure C.16: Cost-Efficient Sanctions with Political Weights for Different Levels of Willingness to Pay in the OSA, $\rho \in [0.7, 1]$

(a) Tariff

(b) Change in Imports

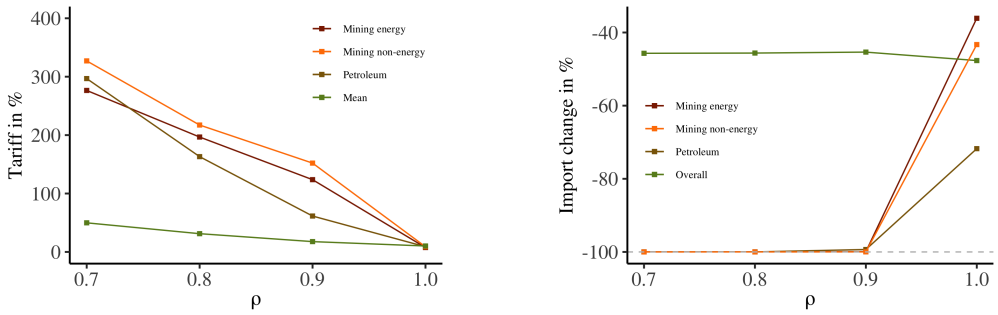

Description: This figure shows statistics for the OSA under cost-efficient sanctions with different levels of willingness to pay when the OSA targets the politically relevant sectors, as described in Table 3.3. Figure C.16a plots the cost-efficient tariffs on mining energy, mining non-energy, petroleum, and the average tariff across sectors for different levels of willingness to pay for sanctions, ρ. Figure C.16b plots the percentage change in imports in the OSA for different sectors.

Figure C.17: Cost-Efficient Sanctions for Different Levels of Willingness to Pay in the EU, $\rho \in [0.7, 1]$ and Caliendo and Parro (2015) trade elasticities

(a) Tariff

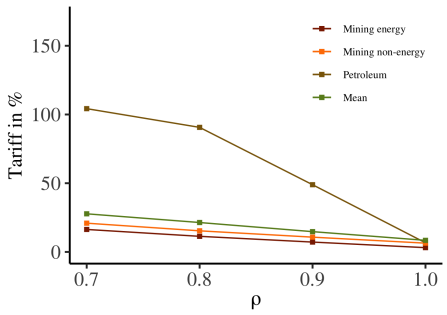

(b) Change in Imports

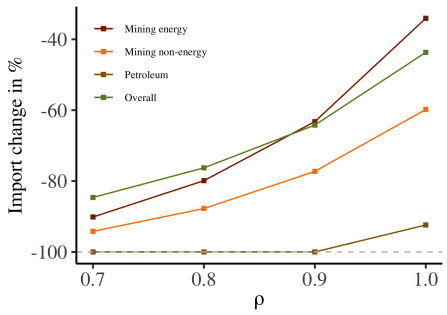

Description: This figure shows the statistics for the EU under cost-efficient sanctions with different levels of willingness to pay. Figure C.17a plots the cost-efficient tariffs on mining energy, mining non-energy, petroleum, and the average tariff across sectors for different levels of willingness to pay for sanctions, ρ. Figure C.17b plots the percentage change in imports in the EU for different sectors.

Figure C.18: Cost-Efficient Sanctions for Different Levels of Willingness to Pay in the EU, $\rho \in [0.4, 1]$ and Caliendo and Parro (2015) trade elasticities

(a) Tariff

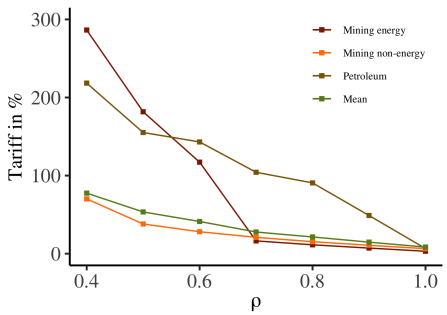

(b) Change in Imports

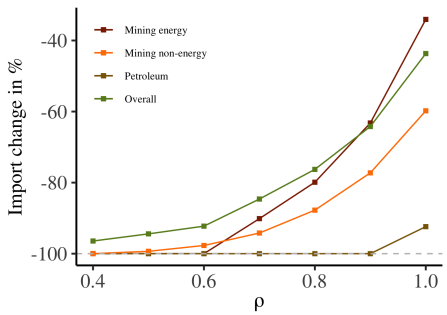

Description: This figure shows the statistics of the EU under cost-efficient sanctions with different levels of willingness to pay. Figure C.18a plots the cost-efficient tariffs on mining energy, mining non-energy, petroleum, and the average tariff across sectors for different levels of willingness to pay for sanctions, ρ. Figure C.18b plots the percentage change in imports in the EU for different sectors.

Figure C.19: Cost-Efficient Sanctions for Different Levels of Willingness to Pay in the OSA, $\rho \in [0.7, 1]$ and Caliendo and Parro (2015) trade elasticities

(a) Tariff **(b)** Change in Imports

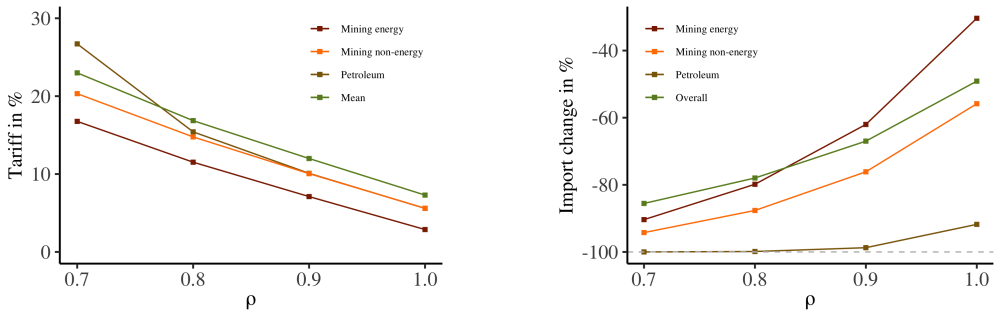

Description: This figure shows the statistics for the OSA under cost-efficient sanctions with different levels of willingness to pay. Figure C.19a plots the cost-efficient tariffs on mining energy, mining non-energy, petroleum, and the average tariff across sectors for different levels of willingness to pay for sanctions, ρ. Figure C.19b plots the percentage change in imports in the OSA for different sectors.

Figure C.20: Cost-Efficient Sanctions for Different Levels of Willingness to Pay in the US, $\rho \in [0.7, 1]$ and Caliendo and Parro (2015) trade elasticities

(a) Tariff **(b)** Change in Imports

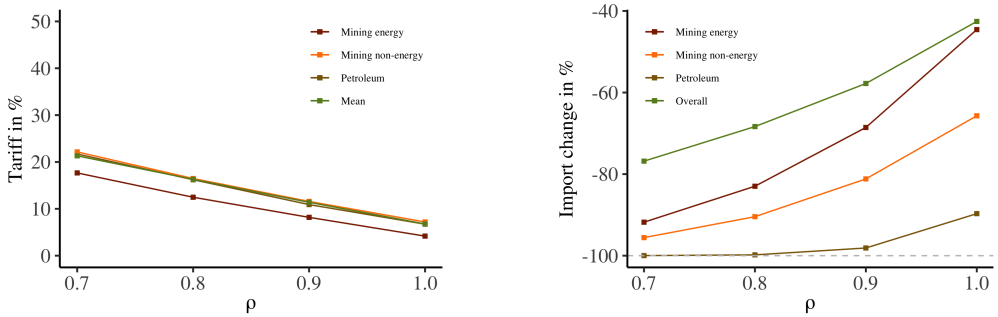

Description: This figure shows the statistics for the US under cost-efficient sanctions with different levels of willingness to pay. Figure C.20a plots the cost-efficient tariffs on mining energy, mining non-energy, petroleum, and the average tariff across sectors for different levels of willingness to pay for sanctions, ρ. Figure C.20b plots the percentage change in imports in the US for different sectors.

Figure C.21: Cost-Efficient Sanctions for Different Levels of Willingness to Pay in the EU, $\rho_{\text{Sanction}} \in [0.7, 1]$ and $\rho_{RUS} \equiv 1$

(a) Tariff **(b)** Change in Imports

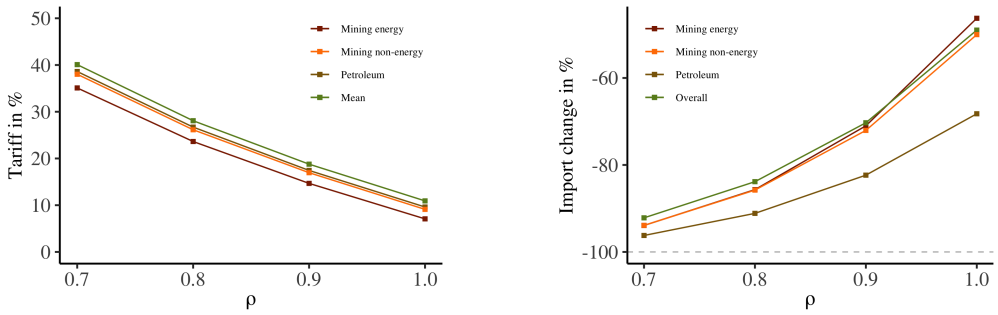

Description: This figure shows the statistics for the EU under cost-efficient sanctions with different levels of willingness to pay. Figure C.21a plots the cost-efficient tariffs on mining energy, mining non-energy, petroleum, and the average tariff across sectors for different levels of willingness to pay for sanctions, ρ. Figure C.21b plots the percentage change in imports in the EU for different sectors.

Figure C.22: Cost-Efficient Sanctions for Different Levels of Willingness to Pay in the EU, $\rho_{\text{Sanction}} \in [0.4, 1]$ and $\rho_{RUS} \equiv 1$

(a) Tariff **(b)** Change in Imports

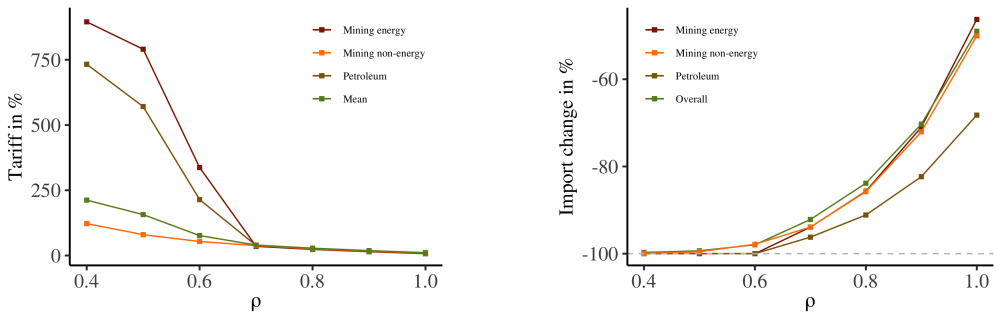

Description: This figure shows the statistics for the EU under cost-efficient sanctions with different levels of willingness to pay. Figure C.22a plots the cost-efficient tariffs on mining energy, mining non-energy, petroleum, and the average tariff across sectors for different levels of willingness to pay for sanctions, ρ. Figure C.22b plots the percentage change in imports in the EU for different sectors.

Figure C.23: Cost-Efficient Sanctions for Different Levels of Willingness to Pay in the US, $\rho_{\text{Sanction}} \in [0.7, 1]$ and $\rho_{RUS} \equiv 1$

(a) Tariff **(b)** Change in Imports

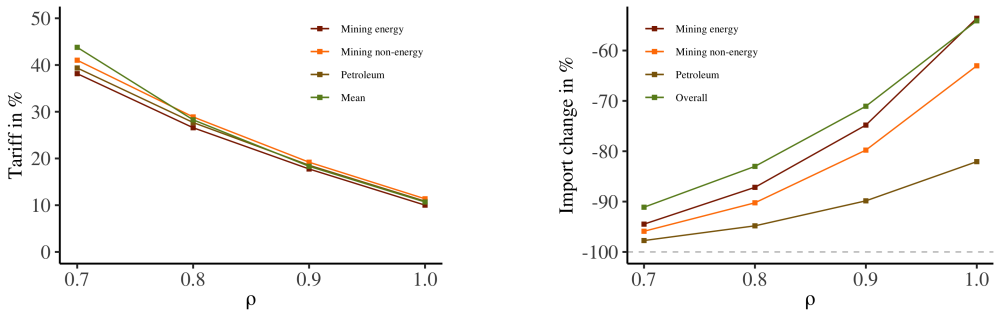

Description: This figure shows the statistics for the US under cost-efficient sanctions with different levels of willingness to pay. Figure C.23a plots the cost-efficient tariffs on mining energy, mining non-energy, petroleum, and the average tariff across sectors for different levels of willingness to pay for sanctions, ρ. Figure C.23b plots the percentage change in imports in the US for different sectors.

Figure C.24: Cost-Efficient Sanctions for Different Levels of Willingness to Pay in the US, $\rho_{\text{Sanction}} \in [0.4, 1]$ and $\rho_{RUS} \equiv 1$

(a) Tariff **(b)** Change in Imports

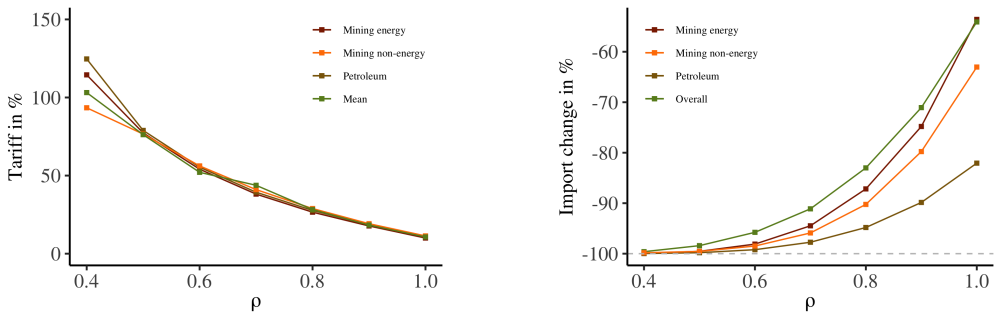

Description: This figure shows the statistics of the US under cost-efficient sanctions with different levels of willingness to pay. Figure C.24a plots the cost-efficient tariffs on mining energy, mining non-energy, petroleum, and the average tariff across sectors for different levels of willingness to pay for sanctions, ρ. Figure C.24b plots the percentage change in imports in the US for different sectors.

Figure C.25: Cost-Efficient Sanctions for Different Levels of Willingness to Pay in the OSA, $\rho_{\text{Sanction}} \in [0.7, 1]$ and $\rho_{RUS} \equiv 1$

(a) Tariff

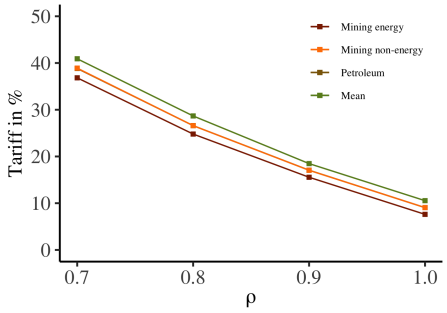

(b) Change in Imports

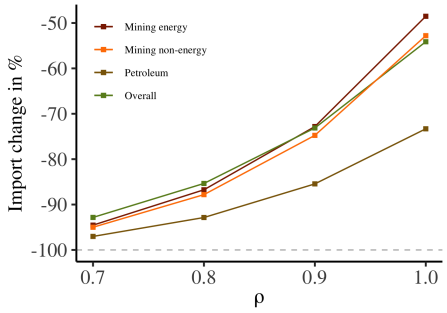

Description: This figure shows the statistics of the OSA under cost-efficient sanctions with different levels of willingness to pay. Figure C.25a plots the cost-efficient tariffs on mining energy, mining non-energy, petroleum, and the average tariff across sectors for different levels of willingness to pay for sanctions, ρ. Figure C.25b plots the percentage change in imports in the OSA for different sectors.

Figure C.26: Cost-Efficient Sanctions for Different Levels of Willingness to Pay in the OSA, $\rho_{\text{Sanction}} \in [0.4, 1]$ and $\rho_{RUS} \equiv 1$

(a) Tariff

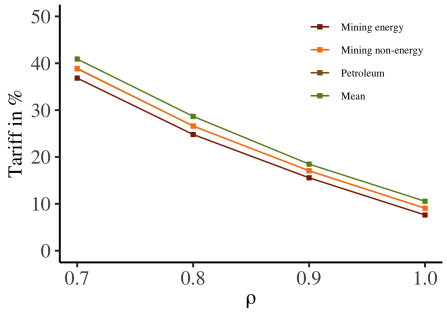

(b) Change in Imports

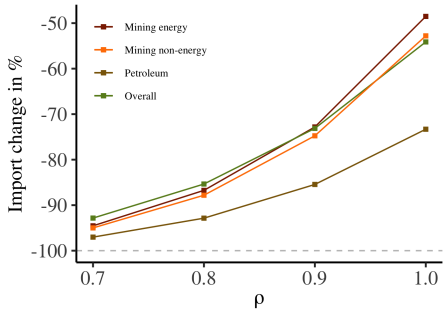

Description: This figure shows the statistics for the OSA under cost-efficient sanctions with different levels of willingness to pay. Figure C.26a plots the cost-efficient tariffs on mining energy, mining non-energy, petroleum, and the average tariff across sectors for different levels of willingness to pay for sanctions, ρ. Figure C.26b plots the percentage change in imports in the OSA for different sectors.

Figure C.27: Cost-Efficient Sanctions for Different Levels of Willingness to Pay in the EU, $\rho_{\text{Sanction}} \in [0.7, 1]$ and $\rho_{RUS} \equiv 0$

(a) Tariff **(b)** Change in Imports

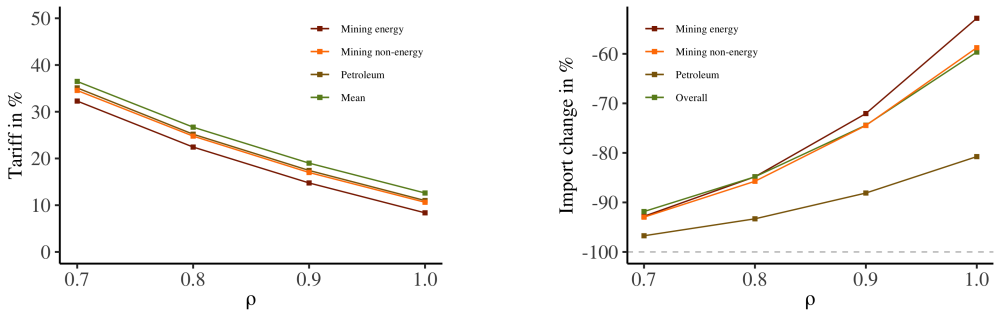

Description: This figure shows the statistics for the EU under cost-efficient sanctions with different levels of willingness to pay. Figure C.27a plots the cost-efficient tariffs on mining energy, mining non-energy, petroleum, and the average tariff across sectors for different levels of willingness to pay for sanctions, ρ. Figure C.27b plots the percentage change in imports in the EU for different sectors.

Figure C.28: Cost-Efficient Sanctions for Different Levels of Willingness to Pay in the EU, $\rho_{\text{Sanction}} \in [0.4, 1]$ and $\rho_{RUS} \equiv 0$

(a) Tariff **(b)** Change in Imports

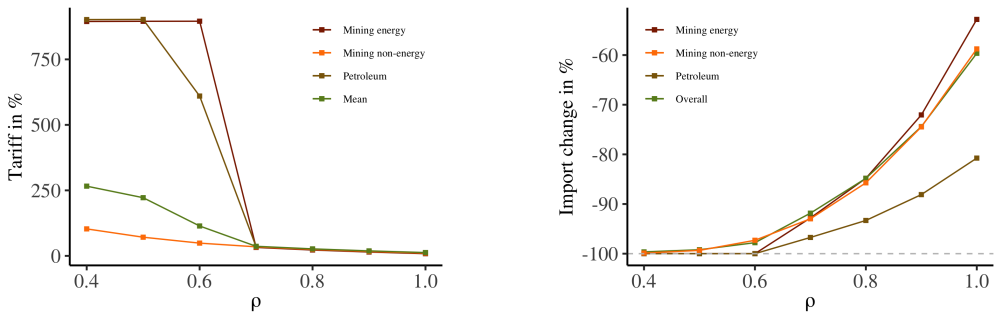

Description: This figure shows the statistics for the EU under cost-efficient sanctions with different levels of willingness to pay. Figure C.28a plots the cost-efficient tariffs on mining energy, mining non-energy, petroleum, and the average tariff across sectors for different levels of willingness to pay for sanctions, ρ. Figure C.28b plots the percentage change in imports in the EU for different sectors.

Figure C.29: Cost-Efficient Sanctions for Different Levels of Willingness to Pay in the US, $\rho_{\text{Sanction}} \in [0.7, 1]$ and $\rho_{RUS} \equiv 0$

(a) Tariff **(b)** Change in Imports

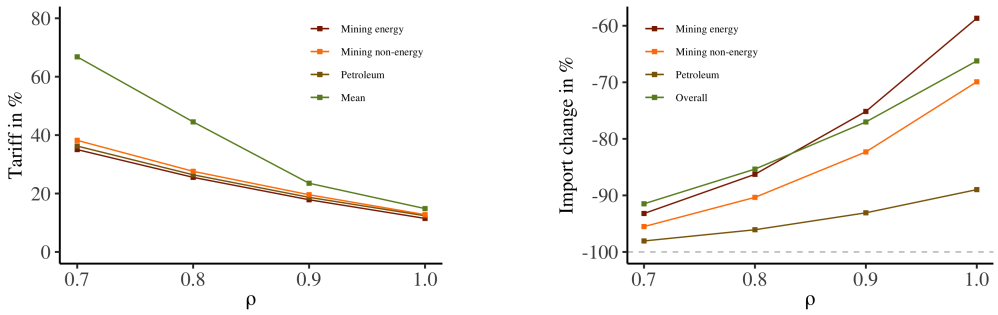

Description: This figure shows the statistics for the US under cost-efficient sanctions with different levels of willingness to pay. Figure C.29a plots the cost-efficient tariffs on mining energy, mining non-energy, petroleum, and the average tariff across sectors for different levels of willingness to pay for sanctions, ρ. Figure C.29b plots the percentage change in imports in the US for different sectors.

Figure C.30: Cost-Efficient Sanctions for Different Levels of Willingness to Pay in the US, $\rho_{\text{Sanction}} \in [0.4, 1]$ and $\rho_{RUS} \equiv 0$

(a) Tariff **(b)** Change in Imports

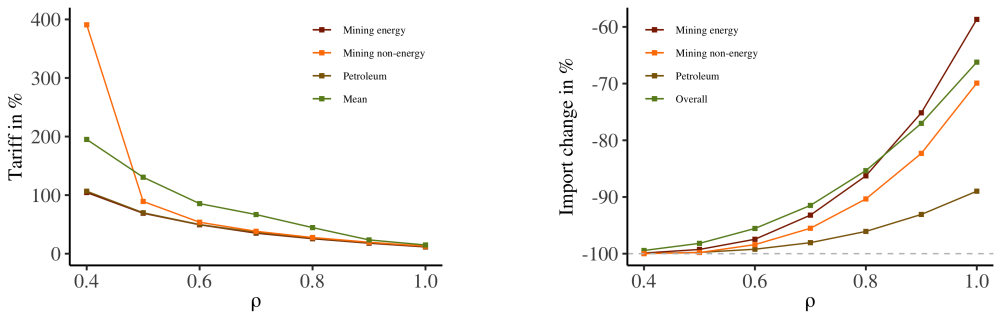

Description: This figure shows the statistics of the US under cost-efficient sanctions with different levels of willingness to pay. Figure C.30a plots the cost-efficient tariffs on mining energy, mining non-energy, petroleum, and the average tariff across sectors for different levels of willingness to pay for sanctions, ρ. Figure C.30b plots the percentage change in imports in the US for different sectors.

Figure C.31: Cost-Efficient Sanctions for Different Levels of Willingness to Pay in the OSA, $\rho_{\text{Sanction}} \in [0.7, 1]$ and $\rho_{RUS} \equiv 0$

(a) Tariff

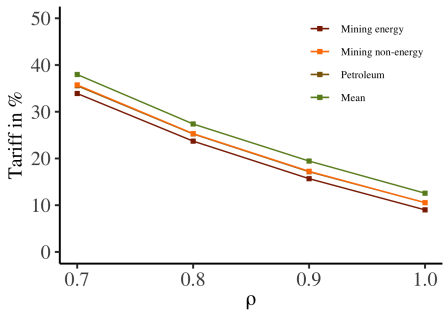

(b) Change in Imports

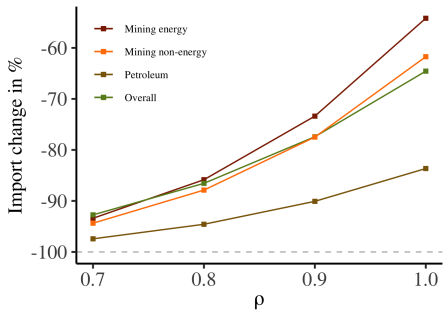

Description: This figure shows the statistics of the OSA under cost-efficient sanctions with different levels of willingness to pay. Figure C.31a plots the cost-efficient tariffs on mining energy, mining non-energy, petroleum, and the average tariff across sectors for different levels of willingness to pay for sanctions, ρ. Figure C.31b plots the percentage change in imports in the OSA for different sectors.

Figure C.32: Cost-Efficient Sanctions for Different Levels of Willingness to Pay in the OSA, $\rho_{\text{Sanction}} \in [0.4, 1]$ and $\rho_{RUS} \equiv 0$

(a) Tariff

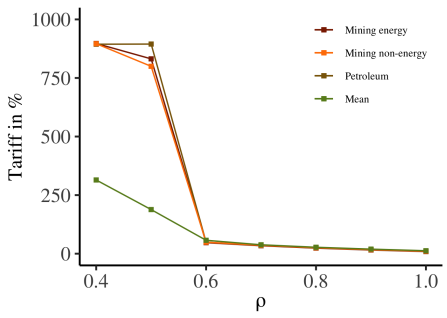

(b) Change in Imports

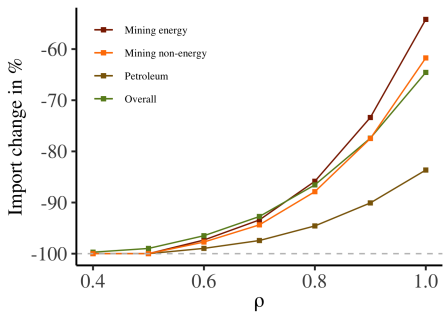

Description: This figure shows the statistics of the OSA under cost-efficient sanctions with different willingness to pay. Figure C.32a plots the cost-efficient tariffs on mining energy, mining non-energy, petroleum, and the average tariff across sectors for different levels of willingness to pay for sanctions, ρ. Figure C.32b plots the percentage change in imports in the OSA for different sectors.

Figure C.33: Cost-Efficient Sanctions with Short-Run Elasticities in the EU for Different ρs, $\rho \in [0.4, 1.0]$

(a) Tariff

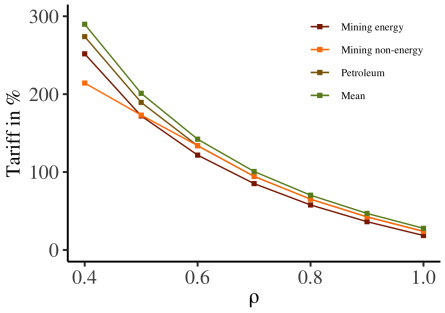

(b) Change in Imports

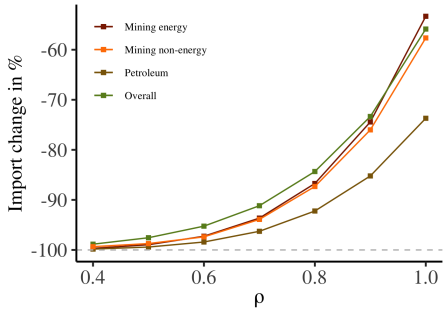

Description: This figure shows the statistics for the EU under cost-efficient sanctions with different levels of willingness to pay with short-run elasticities described in Section C.11. Figure C.33a plots the cost-efficient tariffs on mining energy, mining non-energy, petroleum, and the average tariff across sectors for different levels of willingness to pay for sanctions, ρ. Figure C.33b plots the percentage change in imports in the EU for different sectors.

Figure C.34: Cost-Efficient Sanctions in the EU for Different ρ's with CES Production Function and Low Elasticity of Substitution

(a) Tariff

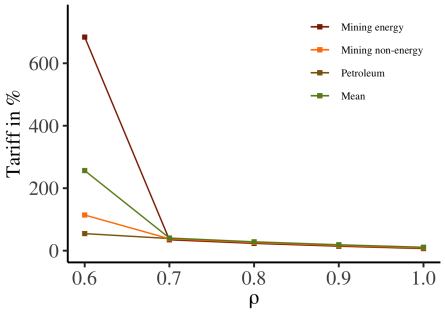

(b) Change in Imports

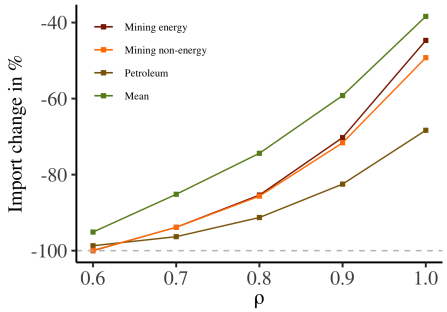

Description: This figure shows the statistics for the EU under cost-efficient sanctions with different levels of willingness to pay for sanctions. The production function is described in Equation 3.17 and the elasticity of substitution between labor and materials is calibrated to 0.1. Figure C.34a plots the cost-efficient tariffs on mining energy, mining non-energy, petroleum, and the average tariff across sectors for different levels of willingness to pay for sanctions, ρ. Figure C.34b plots the percentage change in imports in the EU for different sectors.

Sanctioning Countries' Real Income Does not Decrease

In this section, we study the cost-efficient sanctions that do not decrease the sanctioning countries' real income but minimize the real income in Russia. The sanctioning country n's problem (in changes) is the following. Conditional on all other tariffs except those country n imposes on Russia, $\hat{\mathbf{t}}_{-\mathbf{nR}}$, country n solves:[5]

$$g_n(\hat{\mathbf{t}}_{-\mathbf{nR}}) \in argmin_{\{\tau_{n,R}\}} G_R \hat{G}_R(\hat{\mathbf{t}}_{\mathbf{nR}}, \hat{\mathbf{t}}_{-\mathbf{nR}}), \tag{C.13}$$

$$\text{s.t. Equilibrium Conditions C.1-C.6,}$$

$$\hat{G}_n(\tau_{nR}, \tau_{-nR}) \geq 1$$

Figure C.35 shows cost-efficient sanctions by the EU that satisfy Problem C.13. These tariffs are similar to those when the sanctioning country has low willingness to pay to sanction Russia. The tariffs are low (about 10%) on average and similar across sectors. As the EU does not want to decrease its own real income, lower tariffs should be imposed on energy extraction and petroleum sectors.

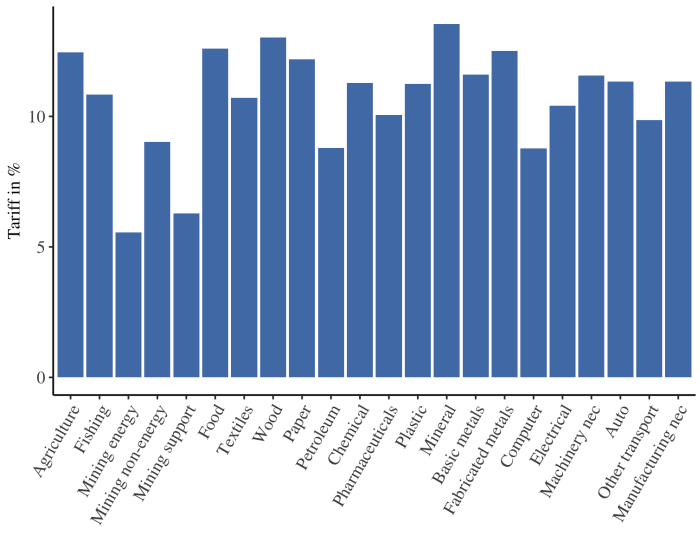

Figure C.35: Cost-Efficient Sanctions with No Decrease in EU Welfare

Description: This figure shows the cost-efficient sectoral tariffs that the EU imposes on Russia when the EU solves Problem C.13: the EU minimizes Russian welfare but requires that its own welfare does not decrease.

[5] We assume that Russia's retaliation strategy is to set tariffs on the sanctioning countries to maximize Russia's welfare; it follows Problem 3.14 where we set $\rho_{RUS} = 1$.

Bibliography

Ahlfeldt, G. M., Redding, S. J., Sturm, D. M., and Wolf, N. (2015). The economics of density: Evidence from the berlin wall. *Econometrica*, 83(6):2127–2189.

Ahn, D. P. and Ludema, R. D. (2020). The sword and the shield: The economics of targeted sanctions. *European Economic Review*, 130:103587.

Alessandria, G., Khan, S. Y., and Khederlarian, A. (2023). Taking stock of Trade Policy Uncertainty: Evidence from China's Pre-WTO Accession.

Allen, T. and Arkolakis, C. (2014). Trade and the topography of the spatial economy. *The Quarterly Journal of Economics*, 129(3):1085–1140.

Allen, T. and Donaldson, D. (2022). Persistence and path dependence: A primer. *Regional Science and Urban Economics*, 94:103724.

Amiti, M., Redding, S. J., and Weinstein, D. E. (2019). The Impact of the 2018 Tariffs on Prices and Welfare. *Journal of Economic Perspectives*, 33(4):187–210.

Amiti, M., Redding, S. J., and Weinstein, D. E. (2020). Who's Paying for the US Tariffs? A Longer-Term Perspective. *AEA Papers and Proceedings*, 110:541–546.

Antràs, P., Chor, D., Fally, T., and Hillberry, R. (2012). Measuring the upstreamness of production and trade flows. *American Economic Review*, 102(3):412–16.

Armington, P. S. (1969). A theory of demand for products distinguished by place of production (une théorie de la demande de produits différenciés d'après leur origine)(una teoría de la demanda de productos distinguiéndolos según el lugar de producción). *Staff Papers-International Monetary Fund*, pages 159–178.

Artuç, E., Chaudhuri, S., and McLaren, J. (2010). Trade shocks and labor adjustment: A structural empirical approach. *American economic review*, 100(3):1008–1045.

Bachmann, R., Baqaee, D., Bayer, C., Kuhn, M., Löschel, A., Moll, B., Peichl, A., Pittel, K., and Schularick, M. (2022). What if? the economic effects for germany of a stop of energy imports from russia. EconPol Policy Report 36, ifo Institute.

Bagwell, K. and Staiger, R. W. (1990). A theory of managed trade. *American Economic Review*, 80(4):779–795.

Bagwell, K. and Staiger, R. W. (1999). An Economic Theory of GATT. *American Economic Review*, 89(1):215–248.

Bagwell, K. and Staiger, R. W. (2004). Multilateral trade negotiations, bilateral opportunism and the rules of GATT/WTO. *Journal of International Economics*, 63(1):1–29.

Bagwell, K. and Staiger, R. W. (2018). Multilateral trade bargaining and dominant stragies. *International Economic Review*, 59(4):1785–1824.

Bagwell, K., Staiger, R. W., and Yurukoglu, A. (2020). "Nash-in-Nash" tariff bargaining. *Journal of International Economics*, 122:103263.

Bagwell, K., Staiger, R. W., and Yurukoglu, A. (2021). Quantitative analysis of multiparty tariff negotiations. *Econometrica*, 89(4):1595–1631.

Baliga, S. and Sjöström, T. (2022). Optimal sanctions. Working Paper.

Bartelme, D., Costinot, A., Donaldson, D., and Rodríguez-Clare, A. (2021). The textbook case for industrial policy: Theory meets data. Working Paper.

Bellemare, M. F. and Wichman, C. J. (2020). Elasticities and the inverse hyperbolic sine transformation. *Oxford Bulletin of Economics and Statistics*, 82(1):50–61.

Benguria, F., Choi, J., Swenson, D. L., and Xu, M. J. (2022). Anxiety or pain? The impact of tariffs and uncertainty on Chinese firms in the trade war. *Journal of International Economics*, 137:103608.

Besedeš, T. and Prusa, T. J. (2017). The hazardous effects of antidumping. *Economic Inquiry*, 55(1):9–30.

Besedeš, T., Goldbach, S., and Nitsch, V. (2021). Cheap talk? financial sanctions and non-financial firms. *European Economic Review*, 134:103688.

Beshkar, M., Chang, P.-L., and Song, S. (2022). Balance of Concessions in the World Trade Organization.

Beshkar, M. and Lashkaripour, A. (2020). Interdependence of Trade Policies in General Equilibrium.

Beshkar, M. and Lee, R. (2022). How does import market power matter for trade agreements? *Journal of International Economics*, 137:103580.

Blanchard, E. J., Bown, C. P., and Chor, D. (2024). Did Trump's trade war impact the 2018 election? *Journal of International Economics*, 148:103891.

Bown, C. P. (2005). Global antidumping database version 1.0. *World Bank Policy Research Working Paper*, (3737).

Bown, C. P. (2021). The US–China trade war and Phase One agreement. *Journal of Policy Modeling*, 43(4):805–843.

Bown, C. P., Caliendo, L., Parro, F., Staiger, R. W., and Sykes, A. O. (2023). Reciprocity and the China Shock.

Broda, C., Limao, N., and Weinstein, D. E. (2008). Optimal tariffs and market power: the evidence. *American Economic Review*, 98(5):2032–65.

Burstein, A. and Vogel, J. (2017). International trade, technology, and the skill premium. *Journal of Political Economy*, 125(5):1356–1412.

Caliendo, L., Dvorkin, M., and Parro, F. (2019). Trade and labor market dynamics: General equilibrium analysis of the china trade shock. *Econometrica*, 87(3):741–835.

Caliendo, L., Opromolla, L. D., Parro, F., and Sforza, A. (2021). Goods and factor market integration: A quantitative assessment of the eu enlargement. *Journal of Political Economy*, 129(12):3491–3545.

Caliendo, L. and Parro, F. (2015). Estimates of the trade and welfare effects of nafta. *The Review of Economic Studies*, 82(1):1–44.

Caliendo, L., Parro, F., Rossi-Hansberg, E., and Sarte, P.-D. (2017). The impact of regional and sectoral productivity changes on the U.S. economy. *The Review of Economic Studies*, 85(4):2042–2096.

Cavallo, A., Gopinath, G., Neiman, B., and Tang, J. (2021). Tariff Pass-Through at the Border and at the Store: Evidence from US Trade Policy. *American Economic Review: Insights*, 3(1):19–34.

Che, Y., Lu, Y., Pierce, J. R., Schott, P. K., and Tao, Z. (2022). Did trade liberalization with China influence US elections? *Journal of International Economics*, 139:103652.

Che, Y. and Zhang, L. (2018). Human capital, technology adoption and firm performance: Impacts of china's higher education expansion in the late 1990s. *The Economic Journal*, 128(614):2282–2320.

Choi, J. and Lim, S. (2023). Tariffs, agricultural subsidies, and the 2020 US presidential election. *American Journal of Agricultural Economics*, 105(4):1149–1175.

Chor, D. and Li, B. (2021). Illuminating the Effects of the US-China Tariff War on China's Economy.

Costinot, A., Donaldson, D., Vogel, J., and Werning, I. (2015). Comparative ddvantage and optimal trade policy. *The Quarterly Journal of Economics*, 130(2):659–702.

Costinot, A. and Werning, I. (2019). Lerner symmetry: A modern treatment. *American Economic Review: Insights*, 1(1):13–26.

Crozet, M. and Hinz, J. (2020). Friendly fire: the trade impact of the russia sanctions and counter-sanctions. *Economic Policy*, 35(101):97–146.

Crozet, M., Hinz, J., Stammann, A., and Wanner, J. (2021). Worth the pain? firms' exporting behaviour to countries under sanctions. *European Economic Review*, 134:103683.

de Souza, G., Hu, N., Li, H., and Mei, Y. (2022). (Trade) War and Peace: How to Impose International Trade Sanctions.

de Souza, G. and Li, H. (2021). The employment consequences of anti-dumping tariffs: Lessons from brazil.

Dekle, R., Eaton, J., and Kortum, S. (2007). Unbalanced trade. *American Economic Review*, 97(2):351–355.

Dixit, A. and Bewley, T. F. (1987). Strategic aspects of trade policy. In *Advances in Economic Theory: Fifth World Congress*, pages 329–362. Cambridge University Press, New York, NY.

Dorsey, T. W. (2003). *China Competing in the Global Economy*. International Monetary Fund.

Draca, M., Garred, J., Stickland, L., and Warrinnier, N. (forthcoming). On target? sanctions and the economicinterests of elite policymakers in iran. *Economic Journal*.

Dustmann, C. and Glitz, A. (2011). Migration and education. In *Handbook of the Economics of Education*, volume 4, pages 327–439. Elsevier.

Eaton, J. and Engers, M. (1992). Sanctions. *Journal of Political Economy*, 100(5):899–928.

Eaton, J. and Kortum, S. (2002). Technology, geography, and trade. *Econometrica*, 70(5):1741–1779.

Eckert, F. and Peters, M. (2022). Spatial structural change.

Elliott, K. A. and Hufbauer, G. C. (1999). Same song, same refrain? economic sanctions in the 1990's. *American Economic Review*, 89(2):403–408.

Evenett, S. J. and Muendler, M.-A. (2022a). Isolating the russian economy: The overlooked role of international shipping costs. https://www.globaltradealert.org/reports/download/91. Accessed: 2022-07-10.

Evenett, S. J. and Muendler, M.-A. (2022b). Making moscow pay: How much extra bite will g7 & eu trade sanctions have? https://www.wita.org/atp-research/making-moscow-pay/. Accessed: 2022-07-10.

Fajgelbaum, P., Goldberg, P. K., Kennedy, P. J., Khandelwal, A., and Taglioni, D. (2021). The US-China Trade War and Global Reallocations.

Fajgelbaum, P. D., Goldberg, P. K., Kennedy, P. J., and Khandelwal, A. K. (2020). The return to protectionism. *The Quarterly Journal of Economics*, 135(1):1–55.

Fajgelbaum, P. D. and Khandelwal, A. K. (2022). The Economic Impacts of the US–China Trade War. *Annual Review of Economics*, 14(1):205–228.

Fan, J. (2019). Internal geography, labor mobility, and the distributional impacts of trade. *American Economic Journal: Macroeconomics*, 11(3):252–88.

Feenstra, R. C. (1994). New product varieties and the measurement of international prices. *American Economic Review*, pages 157–177.

Feenstra, R. C. (2010). *Product Variety and the Gains from International Trade*. MIT Press Cambridge, MA.

Felbermayr, G., Kirilakha, A., Syropoulos, C., Yalcin, E., and Yotov, Y. V. (2020a). The global sanctions data base. *European Economic Review*, 129:103561.

Felbermayr, G., Morgan, T. C., Syropoulos, C., and Yotov, Y. V. (2021). Understanding economic sanctions: Interdisciplinary perspectives on theory and evidence. *European Economic Review*, 135:103720.

Felbermayr, G., Syropoulos, C., Yalcin, E., and Yotov, Y. V. (2020b). On the heterogeneous effects of sanctions on trade and welfare: Evidence from the sanctions on iran and a new database. *School of Economics Working Paper Series 2020-04, Drexel University.*

Gaulier, G. and Zignago, S. (2010). Baci: International trade database at the product-level (the 1994-2007 version).

Gros, D. (1987). A note on the optimal tariff, retaliation and the welfare loss from tariff wars in a framework with intra-industry trade. *Journal of international Economics*, 23(3-4):357–367.

Gullstrand, J. (2020). What goes around comes around: The effects of sanctions on swedish firms in the wake of the ukraine crisis. *World Economy*, 43(9):2315–2342.

Handley, K., Kamal, F., and Monarch, R. (2020). Rising Import Tariffs, Falling Export Growth: When Modern Supply Chains Meet Old-Style Protectionism.

Handley, K. and Limão, N. (2017). Policy Uncertainty, Trade, and Welfare: Theory and Evidence for China and the United States. *American Economic Review*, 107(9):2731–2783.

He, C., Mau, K., and Xu, M. (2021). Trade Shocks and Firms Hiring Decisions: Evidence from Vacancy Postings of Chinese Firms in the Trade War. *Labour Economics*, 71:102021.

Hinz, J. and Monastyrenko, E. (2022). Bearing the cost of politics: Consumer prices and welfare in russia. *Journal of International Economics*, 137:103581.

Itskhoki, O. and Mukhin, D. (2022). Sanctions and the exchange rate. Technical report, National Bureau of Economic Research.

Jiang, L., Lu, Y., Song, H., and Zhang, G. (2023). Responses of exporters to trade protectionism: Inferences from the US-China trade war. *Journal of International Economics*, 140:103687.

Jiao, Y., Liu, Z., Tian, Z., and Wang, X. (2022). The impacts of the US trade war on Chinese exporters. *Review of Economics and Statistics*, pages 1–34.

Kleinman, B., Liu, E., and Redding, S. J. (2023). Dynamic spatial general equilibrium. *Econometrica*, 91(2):385–424.

Klimenko, M., Ramey, G., and Watson, J. (2008). Recurrent trade agreements and the value of external enforcement. *Journal of International Economics*, 74(2):475–499.

Komissarova, K. (2022). Location choices over the life cycle: The role of relocation for retirement.

Krugman, P. (1980). Scale economies, product differentiation, and the pattern of trade. *The American Economic Review*, 70(5):950–959.

Kwon, O., Syropoulos, C., and Yotov, Y. V. (2022). The extraterritorial effects of sanctions. Working Paper.

Lacy, D. and Niou, E. M. S. (2004). A theory of economic sanctions and issue linkage: The roles of preferences, information, and threats. *The Journal of Politics*, 66(1):25–42.

Lashkaripour, A. (2021). The cost of a global tariff war: A sufficient statistics approach. *Journal of International Economics*, 131:103419–103419.

Lashkaripour, A. and Lugovskyy, V. (2023). Profits, Scale Economies, and the Gains from Trade and Industrial Policy. *American Economic Review*, 113(10):2759–2808.

Lee, Y. S. (2018). International isolation and regional inequality: Evidence from sanctions on north korea. *Journal of Urban Economics*, 103:34–51.

Lerner, A. P. (1936). The symmetry between import and export taxes. *Economica*, 3(11):306–313.

Li, J., Liu, S., and Wu, Y. (2020). Identifying knowledge spillovers from universities: Quasi-experimental evidence from urban china. *Available at SSRN 3621422*.

Limao, N. and Saggi, K. (2008). Tariff retaliation versus financial compensation in the enforcement of international trade agreements. *Journal of International Economics*, 76(1):48–60.

Lorenzoni, G. and Werning, I. (2022). A minimalist model for the ruble during the russian invasion of ukraine. *National Bureau of Economic Research Working Paper Series*, No. 29929.

Lu, Y., Tao, Z., and Zhang, Y. (2013). How do exporters respond to antidumping investigations? *Journal of International Economics*, 91(2):290–300.

Ma, H., Ning, J., and Xu, M. J. (2021). An eye for an eye? The trade and price effects of China's retaliatory tariffs on U.S. exports. *China Economic Review*, 69:101685.

Ma, L. and Tang, Y. (2020). Geography, trade, and internal migration in china. *Journal of Urban Economics*, 115:103181.

Ma, L. and Tang, Y. (2024). The distributional impacts of transportation networks in china. *Journal of International Economics*, page 103873.

Ma, X. (2023). College expansion, trade and innovation: Evidence from china. *International Economic Review*.

Maggi, G. (1999). The role of multilateral institutions in international trade cooperation. *American Economic Review*, 89(1):190–214.

Mei, Y. (2020). Sustainable cooperation in international trade: A quantitative analysis. *Journal of International Economics*, 123:103305.

Mei, Y. (2021). Regulatory protection and the role of international cooperation.

Mei, Y. (forthcoming). Regulatory Protection and the Role of International Cooperation. *International Economic Review*.

Miromanova, A. (2021a). The effectiveness of embargoes: Evidence from russia. Working Paper.

Miromanova, A. (2021b). Quantifying the trade reducing effect of embargoes: Firm level evidence from russia. Working Paper.

Oberfield, E. and Raval, D. (2021). Micro data and macro technology. *Econometrica*, 89(2):703–732.

Opp, M. M. (2010). Tariff wars in the ricardian model with a continuum of goods. *Journal of International Economics*, 80(2):212–225.

Ossa, R. (2011). A "New Trade" Theory of GATT/WTO Negotiations. *Journal of Political Economy*, 119(1):122–152.

Ossa, R. (2014). Trade wars and trade talks with data. *American Economic Review*, 104(12):4104–46.

Ossa, R. (2016). Quantitative models of commercial policy. In *Handbook of Commercial Policy*, volume 1, pages 207–259. Elsevier.

Park, J.-H. (2000). International trade agreements between countries of asymmetric size. *Journal of International Economics*, 50(2):473–495.

Prusa, T. J. (2001). On the spread and impact of anti-dumping. *Canadian Journal of Economics*, pages 591–611.

Redding, S. J. and Rossi-Hansberg, E. (2017). Quantitative spatial economics. *Annual Review of Economics*, 9:21–58.

Ritel, M. (2022). A Quantitative Analysis of Trade Cooperation Over Three Decades.

Silva, J. S. and Tenreyro, S. (2006). The log of gravity. *The Review of Economics and statistics*, 88(4):641–658.

Sonali Chowdhry, Julian Hinz, K. K. and Wanner, J. (2022). Brothers in arms: The value of coalitions in sanctions regimes. Technical Report 2234, Kiel Institute for the World Economy.

Staiger, R. W. and Wolak, F. A. (1994). Measuring industry specific protection: Antidumping in the united states. *NBER Working Papers*, 4696.

Sturm, J. (2022). A theory of economic sanctions as terms-of-trade manipulation. Working Paper.

Sturm, J. (2023). How should sanctions account for bystander countries? Working Paper.

Su, C.-L. and Judd, K. L. (2012). Constrained Optimization Approaches to Estimation of Structural Models. *Econometrica*, 80(5):2213–2230.

Suzuki, Y. (2023). Local shocks and regional dynamics in an aging economy. *Available at SSRN 4360965*.

Takeda, K. (2022). The geography of structural transformation: Effects on inequality and mobility.

Tombe, T. and Zhu, X. (2019). Trade, migration, and productivity: A quantitative analysis of china. *American Economic Review*, 109(5):1843–1872.

van Bergeijk, P. A. (2022). Sanctions and the russian-ukraine conflict: a critical appraisal. Working Paper.

Waugh, M. E. (2019). The Consumption Response to Trade Shocks: Evidence from the US-China Trade War.

Whang, T., McLean, E. V., and Kuberski, D. W. (2013). Coercion, information, and the success of sanction threats. *American Journal of Political Science*, 57(1):65–81.